Understanding and Optimising Binding Mechanisms to Enhance Process Sustainability Within Food Granulation

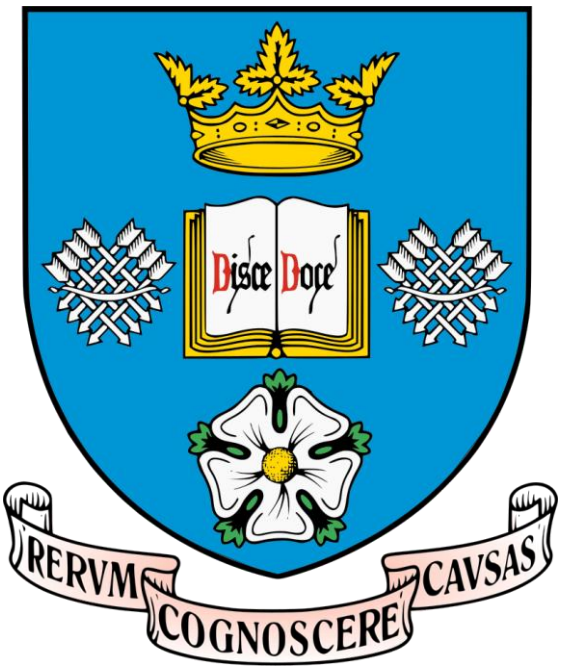

Yashodh Karunanayake

School of Chemical, Materials and Biological Engineering

The University of Sheffield

A thesis submitted in partial fulfilment of the requirements of the degree of Doctor of Philosophy

September 2025

Abstract

Granulation is a well-established size enlargement process in which small particles agglomerate to form larger structures called granules. Enhancing sustainability within granulation is a key focus for the food industry, particularly when processing amorphous powders. These powders are sensitive to moisture and heat due to their Glass Transition Temperature, making controlled agglomeration difficult and often leading to material waste.

Despite its significance, the sustainability of competing granulation technologies remains underexplored. This study addresses this gap by screening the sustainability of four major granulators based on material, energy, and time efficiency. The findings highlight the energy efficiency of dry granulation due to the elimination of the drying step and the high material efficiency of wet granulation, attributed to its cyclic bonding mechanism.

Among the screened technologies, the High Shear Granulator emerged as a strong candidate for further development. A novel regime map was constructed using the parameters ‘Temperature – Glass Transition Temperature’ and ‘Liquid/Solid Ratio divided by a viscosity based constant’ to define an optimal operating region where controlled agglomeration can occur, minimizing caking and material waste.

High Shear Granulation was also used to create layered granule microstructures. Compared to standard granules with randomly distributed components, these layered granules demonstrated greater resistance to humidity-induced caking, colour change, and shrinkage during storage.

Additionally, this study evaluated Dry Twin Screw Granulation for the agglomeration of amorphous food powders. This led to the development of the first-ever regime map for the process, which captured key operational behaviours including granulation, barrel blocking, and extrusion. Dry Twin Screw Granulation exhibited strong potential based on sustainability metrics, positioning it as a viable future alternative to the more established techniques.

Ultimately, this study takes a multifaceted approach to advancing sustainable granulation by identifying key factors contributing to efficiency, process optimisation to minimize material waste, and developing next-generation granulation technologies.

Acknowledgement

First and foremost, I would like to thank my academic supervisor Prof Agba Salman for his years of support. Initially as my Research Project Supervisor and then as my PhD Supervisor, he challenged me to deliver the best science I could. I will always be indebted to the guidance and support he gave me. I also want to voice my deep appreciation to my industrial supervisor's Dr Vincent Meunier and Dr Linda Brutsch. Thank you for the care you showed during my trips to NR Lausanne and ensuring that I had all the support needed for my work.

I would also like to thank my family for their motivation and encouragement. They were a constant pillar that I could always lean on and my PhD would not have been possible without them. This is especially true of my grandfather Marcus, whose unwavering support meant so much to me, and who I wish had been able to read this. Lastly a massive shout out to all the friends who kept me going. To the PPG group – I cannot imagine a better group of people to have done my PhD alongside. Thank you to Harry, Owen, Francesca, Eleni and Shengda for motivating each other and all the support. Thank you to Luc for being my PhD partner in crime and Jeanina for being an excellent desk neighbour. Thank you to Jack and Alex for helping me up my pool game and making lunchtime such a highlight of the day. Thank you to all the friends outside of Sheffield who made their support felt despite the distance. Special thank you to Danny for sticking around, being an excellent housemate and keeping me company in Sheffield all these years.

One last huge thank you to all the people I could not mention here that have made my 9 years as a student in Sheffield so incredible. Sheffield - you will always have a special place in my heart.

Publications

The following publications and awards are a result from this thesis

Journal Papers

- Y.H. Karunanayake, L. Brütsch, V. Meunier, A.D. Salman (2024). Sustainability vs suitability in granulation. Chemical Engineering Research and Design, Volume 202. pp 272–283
- Y.H. Karunanayake, L. Brütsch, V. Meunier, G. Niederreiter, A.D. Salman (2025). Development of a high shear wet granulation regime map for the controlled agglomeration of heat sensitive amorphous food powders. Powder Technology, Volume 466, 121470
- Y.H. Karunanayake, L. Brütsch, V. Meunier, A.D. Salman (2025). Layered granulation to enhance the shelf life of granular food systems. Chemical Engineering Research and Design, Volume 223. pp 425-438

Conference Papers

- Y.H. Karunanayake, L. Brütsch, V. Meunier, A.D. Salman (2023). Evaluating Affordable Granulation Technologies. Oral presentation, poster and paper at the 10th International Granulation Workshop, Sheffield, UK 21-23rd June. Paper 112

- Y.H. Karunanayake, L. Brütsch, V. Meunier, A.D. Salman (2023). Modelling Sustainability in Granulation. Oral presentation, poster and paper at the International Congress on Particle Technology (PARTEC), Nuremberg, Germany 26-28th September.

- Y.H. Karunanayake, L. Brütsch, V. Meunier, A.D. Salman (2024). Evaluating the sustainability of competing granulation technologies. Oral presentation and paper at the 27th International Congress of Chemical and Process Engineering (CHISA), Prague, Czech Republic, 25-29th August.

- Y.H. Karunanayake, L. Brütsch, V. Meunier, A.D. Salman (2024). Future of Granulation. Oral presentation and paper at the 11th International Conference on Conveying and Handling of Particulate Solids (CHOPS), Edinburgh, UK, 2-4th September.

Awards

- Best Poster Award Winner by Glatt. Poster Title: Evaluating Affordable Granulation Technologies. 10th International Granulation Workshop, Sheffield, UK 21-23rd June 2023
- PTSIG Early Career Researcher of the Year Award 2nd Place. 11th International Conference on Conveying and Handling of Particulate Solids (CHOPS), Edinburgh, UK, 2-4th September 2024.

Table of Contents

1 Introduction 1
1.1 What is Granulation? 1
1.2 Wet Granulation 1
1.2.1 Wetting and Nucleation 2
1.2.2 Consolidation and Coalescence 3
1.2.3 Attrition and Breakage 4
1.2.4 Drying 4
1.2.5 Typical Wet Granulators 4
1.3 Dry Granulation 7
1.4 Sustainability in Granulation 7
1.5 Aims and Objectives of the Thesis 8
1.5.1 Aims 8
1.5.2 Thesis Overview 8
2 Literature Review 11
2.1 Understanding Amorphous Powders 11
2.1.1 Glass Transition Temperature 12
2.1.2 Maltodextrin DE number and the Glass Transition phenomena 14
2.1.3 Maltodextrin DE number and viscosity 15
2.1.4 Amorphous powder binding mechanism 16
2.2 High Shear Granulation 17
2.2.1 High Shear Granulation Regime Maps 17
2.2.2 Sustainability in High Shear Granulation 20
2.3 Twin Screw Granulation 21
2.3.1 Twin Screw Granulation Regime Map 22
2.3.2 Sustainability in Wet Twin Screw Granulation 25
2.3.3 Dry Twin Screw Granulation 25
2.4 Fluidised Bed Granulation 27
2.4.1 Fluidised Bed Granulation Regime Map 27
2.4.2 Sustainability in Fluidised Bed Granulation 30
2.5 Roller Compaction 30
2.5.1 Roller Compaction Regime Map 31
2.6 Caking of Amorphous Powders 32
2.6.1 Glass Transition Driven Caking in Granulation 33
2.6.2 Glass Transition Driven Caking During Storage 33
2.7 Summary and Knowledge Gaps 34

3 Materials and Methods 36
3.1 Materials 36
3.1.1 Maltodextrin 36
3.1.2 Coffee 37
3.2 Methods 38
3.2.1 High Shear Granulator 38
3.2.2 Twin Screw Granulation 39
3.2.3 Fluidised Bed Granulator 41
3.2.4 Roller Compactor 43
3.2.5 Sieving 45
3.2.6 Flowability 46
3.2.7 Dissolution Time 47
3.2.8 Dynamic Image Analysis 47
3.2.9 X-Ray Tomography and ImageJ 48
3.2.10 Differential Scanning Calorimetry 49
3.2.11 Thermo-Gravimetric Analysis 50
3.2.12 Viscometry 50
3.2.13 Jet Mill 51
3.2.14 Direct Vapour Sorption 52
4 Selecting the Optimal Granulation Pathway by Considering Sustainability and Suitability 53
4.1 Introduction 54
4.2 Materials and Methods 55
4.2.1 Materials 55
4.2.2 Equipment and Methods 55
4.3 Sustainability in granulation 60
4.3.1 Fluidised Bed Granulator (FBG) 60
4.3.2 High Shear Granulator (HSG) 61
4.3.3 Roller Compactor (RC) 63
4.3.4 Twin Screw Granulator (TSG) 64
4.3.5 Comparing granulation pathways 65
4.4 Granule suitability 72
4.4.1 Granule Flowability 74
4.4.2 Granule Friability 76
4.4.3 Granule Dissolution 77
4.5 Choosing the optimum granulation pathway 78
4.6 Conclusion 83
5 Development of a High Shear Wet Granulation Regime Map to Avoid Caking in Heat Sensitive Amorphous Food Powders 85

5.1 Introduction 86
5.2 Materials and Methods 87
5.2.1 Materials 87
5.2.2 Granulation Experiments 88
5.2.3 Granule Size Characterisation 89
5.2.4 Measuring Moisture Content 90
5.2.5 Developing the Gordon and Taylor Model 90
5.2.6 Measuring Viscosity 91
5.2.7 Powder Stickiness 91
5.2.8 Particle Image Velocimetry 92
5.3 Results: The role of Temperature within the granulation process 93
5.3.1 Glass Transition behavior of Maltodextrins 94
5.3.2 Caking behavior of Maltodextrins 95
5.3.3 Effect of process parameters on powder bed temperature 95
5.3.4 Effect of process parameters on granular yield and caking 99
5.3.5 Modelling temperature interactions with Maltodextrin 103
5.4 Results: The role of water binder within the granulation process 106
5.4.1 Interaction between water and Maltodextrin grade 107
5.4.2 Theory development for the interactions of water and Maltodextrin during granulation 108
5.4.3 Viscosity measurement 113
5.4.4 Selection of a suitable shear rate 116
5.4.5 Linking Viscosity to Granular Yield 117
5.5 Regime Map 119
5.6 Conclusion 123
6 Layered Granulation to Enhance the Shelf Life of Granular Food Systems 124
6.1 Introduction 125
6.2 Materials and Methods 126
6.2.1 Materials 126
6.2.2 Sieving and Micronisation of Maltodextrin DE6 for Layered Granulation 127
6.2.3 Production of Pure Maltodextrin granules 128
6.2.4 Production of pure Coffee granules 128
6.2.5 Theory for Layered Granulation 128
6.2.6 Production of the Standard Coffee-Maltodextrin Granule Structure 130
6.2.7 Production of the Layered Coffee-Maltodextrin Granule Structure 130
6.2.8 Determining layer thickness 135
6.2.9 Evaluating Caking Index 136
6.2.10 Evaluating changing granule morphology during storage 137

6.2.11 Dynamic vapor sorption 137
6.2.12 Production of Gordon Taylor Model and GAB Model 137
6.2.13 Granule shape and size 139
6.2.14 Internal granule structure evaluation 139
6.2.15 Tabletting 139
6.3 Simple size enlargement to prevent caking 139
6.3.1 Comparing the caking tendency between granules and raw powder 140
6.4 Evaluation of the Layered Granule 147
6.4.1 Granule Size 147
6.4.2 Granule Shape 148
6.4.3 Granule layer Thickness 149
6.4.4 Caking tendency of the Standard Versus Layered Granule structures 151
6.4.5 Change in colour of the Standard Versus Layered Granule structures 154
6.4.6 Granule deformation of the Standard Versus Layered Granule structures 157
6.5 Layered structure to prevent moisture migration into granule core 161
6.6 Conclusion 165
7 Dry Twin Screw Granulation: The future of amorphous food granulation? 166
7.1 Introduction 167
7.2 Materials and Methods 169
7.2.1 Materials 169
7.2.2 Dry Twin Screw Granulator Set-up 169
7.2.3 Granulation Compartment (C6) Temperature Measurement 174
7.2.4 Yield 174
7.2.5 Granule Size and Sphericity Characterisation 174
7.2.6 ANOVA analysis 175
7.2.7 Barrel Fill Level 175
7.2.8 Peak Shear Rate 176
7.3 Results and Discussion 176
7.3.1 Process Stability 176
7.3.2 Granule Size 180
7.3.3 Total Process Yield 183
7.3.4 Granule Shape 185
7.3.5 Granule Porosity 188
7.3.6 Regime Map Development 192
7.4 Comparison with existing technologies 195
7.4.1 Material Efficiency 196
7.4.2 Energy Efficiency 197

7.4.3 Time Efficiency 198
7.5 Conclusion 199
8 Conclusion and Future Work 201
8.1 Understanding the sustainability of existing granulation technologies 201
8.2 Reducing material waste by preventing unwanted over agglomeration 202
8.3 Reducing material waste during storage by developing humidity resistant granules 203
8.4 Developing more sustainable granulation technologies for the future 203
References 205
Appendix 216

List of Figures

Figure 1.1: The three main stages of wet granulation [1]. 2
Figure 1.2: Showing the dependence between binder droplet size and nucleation mechanism [1]. 3
Figure 1.3: Common wet granulators with differing sources of agitation [7] 6
Figure 1.4: Schematic overview of the Roller Compaction process [9] 7
Figure 1.5: Visualises the relationship between Experimental Chapters 4 – 7 10
Figure 2.1: Example molecular structures of crystalline and amorphous substances [10] 12
Figure 2.2: Temperature and humidity dependent state change of amorphous powders [12] 13
Figure 2.3: Glass Transition Temperature of Maltodextrin powders [14] 14
Figure 2.4: DE grade dependent viscosity behaviour of Maltodextrins [15]. 15
Figure 2.5: Solid concentration dependent viscosity behaviour of Maltodextrins [14] 16
Figure 2.6: Possible binding mechanisms for amorphous powders [17]. 17
Figure 2.7: Iveson and Litster (1998) High Shear Granulation Regime Map [18] 19
Figure 2.8: Santomaso et al (2017) High Shear Granulation Regime Map [24]. 20
Figure 2.9: Possible Twin Screw Granulation Screw Elements [31]. 22
Figure 2.10: Dhenge et al (2013) Twin Screw Granulation Regime Map [34]. 23
Figure 2.11: Tu et al (2013) Regime Map Development Matrix [35]. 24
Figure 2.12: Tu et al (2013) Twin Screw Granulation Regime Map [35]. 25
Figure 2.13: Aviles-Aviles et al (2015) Fluidised Bed Granulation Regime Map [46] 29
Figure 2.14: Palzer (2005) Fluidised Bed Granulation Regime Map [17] 29
Figure 2.15: Fries et al (2019) Roller Compaction Regime Map [54]. 32
Figure 3.1: Image of the Eirich EL1 High Shear Granulator. 39
Figure 3.2: Schematic of the Eirich EL1 High Shear Granulator. 39
Figure 3.3: Image of the ThermoFisher Euro Lab 16 mm Twin Screw Granulator 40
Figure 3.4: Schematic of the ThermoFisher Euro Lab 16 mm Twin Screw Granulator 41
Figure 3.5: Image of the Glatt GPCG3 Fluidised Bed 42
Figure 3.6: Schematic of the Glatt GPCG3 Fluidised Bed Granulator. 42
Figure 3.7: Image of the Alexanderwerk WP120 Roller Compactor. 44
Figure 3.8: Schematic of the Alexanderwerk WP120 Roller Compactor. 44
Figure 3.9: Measurement principle for the Sieve Shaker 45
Figure 3.10: Measurement principle for the Shear Cell 46
Figure 3.11: Image of the dissolution apparatus used 47
Figure 3.12: Measurement principal for the Camsizer [66] 48
Figure 3.13: Image analysis procedure to evaluate porosity using ImageJ 49
Figure 3.14: Measurement principle for the Differential Scanning Calorimetry 50
Figure 3.15: Measurement principle for the Malvern Kinexus Pro rheometer 51
Figure 3.16: Schematic of a Spiral Jet Mill. 52
Figure 4.1: Schematic of the power measurement technique. 58
Figure 4.2: The different granulation pathways for the evaluated technologies. 58
Figure 4.3: Energy Consumption, Yield and Specific Energy in the Fluidised Bed Granulator. 61
Figure 4.4: Energy Consumption, Yield and Specific Energy in the High Shear Granulator 63
Figure 4.5: Energy Consumption, Yield and Specific Energy in the Roller Compactor. 64
Figure 4.6: Energy Consumption, Yield and Specific Energy in the Twin Screw Granulator 65
Figure 4.7: Comparing Yield of the different granulation pathways 67
Figure 4.8: Comparing the Specific Energy of the different granulation pathways. 69
Figure 4.9: Energy consumption distribution of the different granulation pathways 70
Figure 4.10: Comparing Specific Time of the different granulation pathways 72
Figure 4.11: X-Ray Scans of granules from the different granulation technologies 74
Figure 4.12: Comparing the granule flowability between the different technologies 76

Figure 4.13: Comparing the granule friability between the different technologies 77
Figure 4.14: Comparing the granule dissolution time between the different technologies. 78
Figure 4.15: Use of Parallel Co-ordinate Graphs to select optimum technologies 80
Figure 4.16: Use of Radar Charts to select optimum technologies 81
Figure 5.1: Schematic diagram of the Eirich EL1 Granulator with the thermal camera 89
Figure 5.2: Measurement procedure to measure stickiness. 92
Figure 5.3: Image of the bed area evaluated by the PIV modelling. 93
Figure 5.4: Fitted Gordon and Taylor model for the different Maltodextrin powders 94
Figure 5.5: Caking of Maltodextrin in the High Shear Granulator. 95
Figure 5.6: Thermal images of the DE6 powder bed when granulated at 200 g and 1800 rpm 96
Figure 5.7: Increase in bed temperature at varying batch sizes, impeller speeds and L/S ratios. 98
Figure 5.8: Change in granular yield with increasing L/S, impeller speed and batch size 102
Figure 5.9: Change in moisture content of fines and granule factions during granulation 104
Figure 5.10: Calculated distribution of the water binder in the granule and fine fraction 105
Figure 5.11: Varying rate at which Maltodextrin was granulated with water 107
Figure 5.12: Effect of Maltodextrin Grade on the Granulation Efficiency 108
Figure 5.13: Visualisation of the spreading of a binder droplet during wetting 110
Figure 5.14: Bridge developed between the DE29 coated bead and mixtures at varying M/W ratios 112
Figure 5.15: Maximum Tensile Force at different M/W ratios for different Maltodextrins 112
Figure 5.16: Effect of shear rate on the viscosity of the Maltodextrin-water mixture 115
Figure 5.17: Surface powder bed velocity and shear rate in the High Shear Granulator 117
Figure 5.18: Modelling Maltodextrin viscosity increase with M/W ratio 118
Figure 5.19: Correlating Granulation Efficiency with $1/k_{\mu}$ 119
Figure 5.20: Effect of changing L/S ratio and $T\text{-}T_{g,Bed}$ on granular yield 121
Figure 5.21: Completed Regime Map indicating the normal operation and caking regions 123
Figure 6.1: Illustration of the Standard Granule and Layered Granule cross section 130
Figure 6.2: Process pathway to produce the Layered Coffee – DE6 Granule 134
Figure 6.3: Schematic showing the Eirich granulator in its original and new configuration. 135
Figure 6.4. Example methodology for measuring granule thickness 136
Figure 6.5: Caking behaviour of granules compared with powder 143
Figure 6.6: Moisture uptake between the different materials at 20˚C and 80% relative humidity 144
Figure 6.7: Fitted GAB model (A) and Gordon Taylor model (B) 145
Figure 6.8: Changing characteristics of Coffee stored at 20˚C and 60% relative humidity 146
Figure 6.9: Changing granule size distribution through the Layered Granule production process 148
Figure 6.10: Changing granule sphericity through the Layered Granule production process 149
Figure 6.11: Changing DE6 layer thickness through the Layered Granule production process. 150
Figure 6.12: Visual representation of the granule layer characteristics. 151
Figure 6.13: Caking Index of the Layered Granules compared to Standard Granules 153
Figure 6.14: Caking Index after 16 days of storage at 20˚C and 60% RH 153
Figure 6.15: Changing characteristics of bulk Layered and Standard Granules 156
Figure 6.16: Changing greyscale value of the bulk Layered and Standard Granules 157
Figure 6.17: Changing characteristics of 5 random Standard Granules 159
Figure 6.18: Changing characteristics of 5 random Layered Granules 160
Figure 6.19: Granule deformation during storage 161
Figure 6.20: X-RAY scan of a layered granule composing of 50% DE6 162
Figure 6.21: Proposal of an ideal 3-component layered granule structure to extend shelf life 162
Figure 6.22: Change in colour profile of the layered tablet formulations over time. 164
Figure 7.1: Schematic diagram of the Dry Twin Screw Granulation Configuration 171
Figure 7.2: The two main screw configurations evaluated in the Dry Twin Screw Granulator. 173
Figure 7.3: Modelling the barrel and screw geometries used in the Dry Twin Screw Granulator 176
Figure 7.4: Process Stability of the Dry Granulation Process. 179

Figure 7.5: ANOVA analysis of key parameters affecting Process Stability 180
Figure 7.6: Change in Granule Size at varying screw speeds and throughputs. 182
Figure 7.7: ANOVA analysis of key parameters affecting Granule Size 183
Figure 7.8: Granule Yield at varying screw speeds and throughputs. 184
Figure 7.9: ANOVA analysis of key parameters affecting Granule Yield 185
Figure 7.10: Change in Granule Sphericity at varying screw speeds and throughputs. 187
Figure 7.11: ANOVA analysis of key parameters affecting Granule Sphericity 188
Figure 7.12: Change in Granule Porosity at varying screw speeds and throughputs. 190
Figure 7.13: X-Ray images of the most and least porous Dry Twin Screw Granulation granules 191
Figure 7.14: ANOVA analysis of key parameters affecting Granule Porosity 191
Figure 7.15: Dry Twin Screw Granulation Process Regime Map 195
Figure 7.16: Evaluating Material Efficiency of the Dry Twin Screw Granulation Process 196
Figure 7.17: Evaluating Specific Energy of the Dry Twin Screw Granulation Process 198
Figure 7.18 Evaluating Time Efficiency of the Dry Twin Screw Granulation Process 199

List of Tables

Table 1.1: Granulators studied in this thesis alongside the source of agitation in each 5
Table 3.1: Particle size distribution of the raw Maltodextrins used in this study 36
Table 3.2: Particle size distribution of the raw Instant Coffee used in this study 38
Table 3.3: Flow descriptors based on ffc value 46
Table 4.1: Priority based score rating system to select optimum granulation pathways. 83
Table 5.1: Particle size distribution of the raw powders used in Chapter 5 88
Table 5.2: Binder addition times for example L/S ratios at different batch sizes 88
Table 6.1: Particle size distribution of the raw powders used in Chapter 6 127
Table 6.2: Particle size distribution of the Raw, Fine and Micronized DE6 powder variants 127

Nomenclature

A	Particle Projected Area
a_w	Water Activity
C	GAB Model (Energy of Absorbance)
Ca*	Capillary Viscous Number
D	Diameter
k	Gordon Taylor Constant
k_μ	Viscosity-M/W Ratio Growth Rate Constant
N	Screw Speed
P	Particle Projected Perimeter
S_{max}	Maximum Pore Saturation
St_{def}	Deformation Number
T	Temperature
T_g	Glass Transition Temperature
U_c	Granule Collision Velocity
u_r	Relative Velocity
W_a	Work of Adhesion
W_b	Moisture Content (Wet Basis)
W_m	GAB Model (Monolayer Moisture Value)
Y_g	Granule Dynamic Yield Strength
X_A	Fraction of Component A
X_B	Fraction of Component B

Greek Letters

β	Deformation Value
γ	Shear Rate
ε_{min}	Minimum Porosity
η_L	Binder Viscosity
ρ_g	Granule Density
ρ_l	Liquid Density
ρ_s	Particle Density
τ	Shear Stress
Φ	Ribbon Porosity

Abbreviations

DE	Dextrose Equivalent
FBG	Fluidised Bed Granulator
HSG	High Shear Granulator
HSWG	High Shear Wet Granulation
L/S	Liquid to Solid
MgSt	Magnesium Stearate
M/W	Maltodextrin/Water
PIV	Particle Image Velocimetry
TSG	Twin Screw Granulator
RC	Roller Compactor
BET	Brunauer-Emmett-Teller

1 Introduction

1.1 What is Granulation?

The work presented in this thesis centres on the powder technology known as Granulation and how current granulation practices can be adapted to enhance sustainability within the field. Therefore, a suitable starting point to delve into this topic is to answer the question: **What is Granulation?** Granulation is a size enlargement process where fine, powder particulates are agglomerated together to form larger structures known as granules. This agglomeration commonly occurs with the aid of liquid binders, high mechanical stresses or applied heat.

The next relevant question is: **Why is Granulation important?** Granulation is a prevalent powder process across a diverse range of industries from food to pharmaceuticals to fertilizer. This thesis focuses on the application of Granulation processes within the food industry where Granulation is carried out for the following reasons:

- Improved handling properties - Granulation can be used to increase particle size and sphericity, both of which, improve particle flowability and make materials easier to handle
- Improved homogeneity - during granulation different components are physically adhered together, preventing any downstream segregation and improving formulation homogeneity.
- Consumer acceptance - the change in particle size and surface morphology results in changes to product colour and texture which enhances its appeal to consumers.

There are countless additional reasons why granulation is carried out such as improving product shelf life and enabling special functionalities (for instance, optimizing the dissolution rate for controlled release products) which highlights the importance of granulation to the food industry.

To complete the overview into granulation, the reader will now be introduced to: **How is Granulation carried out?** While there are a wide variety of granulation technologies, the majority can be classed as either wet granulation or dry granulation. In wet granulation, the driving force for agglomeration is the liquid binder, while in dry granulation, the driving force is typically a strong compressive force. These two different pathways for agglomeration will be discussed further is subsequent sections.

1.2 Wet Granulation

Wet Granulation describes a process where a liquid binder is added to an agitated powder bed. This liquid forms interparticle bridges causing powder particles to adhere to each other. The process is generally divided into three distinct stages which can happen sequentially or simultaneously to each

other depending on the granulator. The first stage is Wetting & Nucleation which describes the instance where a liquid drop is first introduced into the powder bed. This liquid drop mixes with primary particles to form a liquid rich nuclei granule. The next stage is Consolidation & Coalescence. During this stage the granules experience densification which squeezes liquid to the granule surface. This makes the granule surface stickier causing coalescence of separate granules and leading to a growth in granule size. The final stage is Attrition & Breakage which describes the breakup of granules into fragments due to destructive forces inside the granulator. These stages are visually illustrated by Figure 1.1 [1].

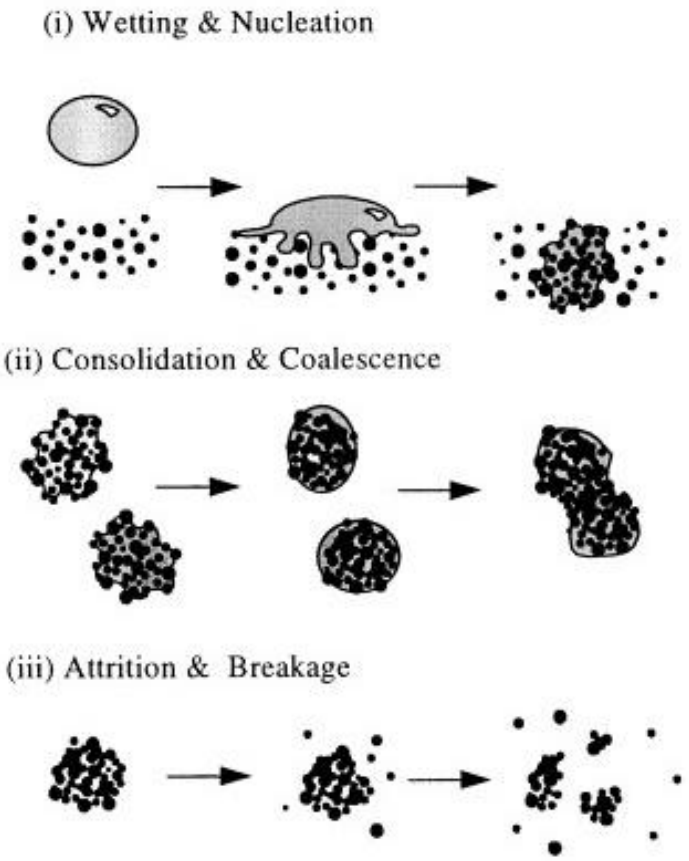

Figure 1.1: The three main stages of wet granulation. The Wetting and Nucleation stage describes the first contact between the liquid droplet and the powder to form a nuclei granule. The Consolidation and Coalescence stage describes the densification and growth of these nuclei granules through coalescence. The Attrition and Breakage stage describes the breakage experienced by the granule due to impact with other granules or granulator surfaces [1].

1.2.1 Wetting and Nucleation

During wetting, the binder droplet first contacts primary particles in an area of the powder bed known as the wetting zone. The binder then penetrates into the powder bed and spreads leading to the formation of weak, porous, binder rich nuclei granules. The degree to which wetting occurs depends on the affinity between the binder and the powder which is a unique property of each system. There are two different mechanisms under which the formation of these nuclei granules can occur: Distribution or Immersion.

The primary factor that determines the nucleation mechanism is binder droplet size. Distribution nucleation occurs when the binder droplet size is similar in size or smaller than the primary particles. In this scenario binder droplets gradually accumulate on the surface of primary particles. When the surfaces of these particles are sufficiently wet, they coalesce to form a nuclei granule. Meanwhile, Immersion nucleation occurs when the binder droplets are much larger than the primary particles. In this case, the binder droplet immerses and absorbs primary particles into itself to form the nuclei granules [1,2]. The dependence between binder droplet size and nucleation mechanism is shown in Figure 1.2 [1].

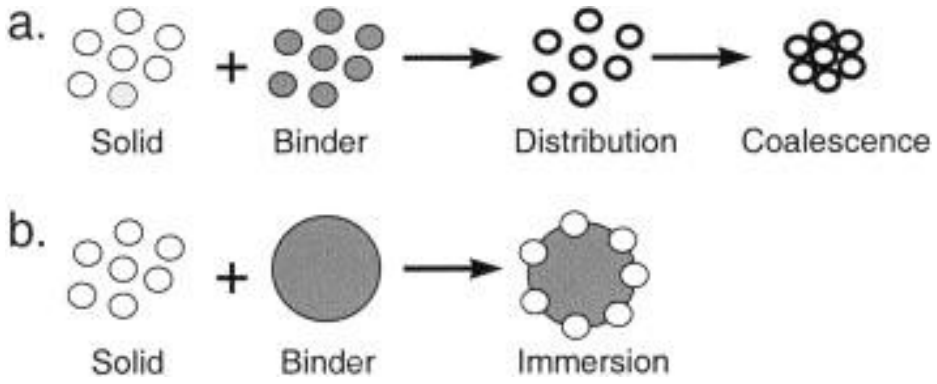

Figure 1.2: Shows the dependence between binder droplet size and nucleation mechanism. Distribution nucleation (a) occurs when the binder droplet size is similar in size or smaller than the primary particles. Immersion nucleation (b) occurs when the binder droplet in much larger than the primary particles [1].

Alternatively, nucleation can be described as either droplet controlled, or dispersion controlled. Droplet controlled nucleation occurs when the spray flux is low, and the droplet penetrates fast into the powder bed. Under these conditions one binder droplet goes on to form one nuclei granule and the nuclei size distribution reflects the droplet size distribution. Dispersion controlled nucleation occurs at high spray fluxes and when droplet penetration is slow. Under these conditions, binder droplets amalgamate together on the powder bed surface. The mixing conditions present within the granulator will then dominate the dispersion of this binder and will decide the characteristics of the nuclei granule. The ideal nucleation mechanism is droplet controlled because it leads to a more controllable granule size [3].

1.2.2 Consolidation and Coalescence

Once created, the nuclei granule starts to experience compressive forces acting on it. These compressive forces can come from a multitude of sources including collisions with other granules, impact with granulator internals and compression under the powder bed weight. This compression causes powder particles in the granule to move inwards which squeezes the more mobile, liquid binder outwards to the

surface. This densification process is known as Consolidation [4]. The outward movement of liquid results in the granule surface becoming wetter and stickier. Granule growth occurs when two particles collide resulting in adhesion and the formation of a larger agglomerate. For a collision to be successful, the liquid layer on the granule surface must be capable of dissipating the energy of the collision. The thicker the liquid layer, the better it dissipates this energy [5]. Therefore, Consolidation allows the granule to best utilise its binder to promote adhesion by acting to renew the liquid layer on the granule surface. A successful collision between two similar sized granules to form a larger agglomerate is known as coalescence while the successful collision between a granule and a much smaller particle is known as layering. As these stages repeatedly cycle, the formed agglomerates become less deformable, and consolidation happens to less and less an extent. This results in the availability of binder on the granule surface dropping below the critical amount needed for coalescence. At this stage there is insufficient binder available to promote growth and no further increase in size is observed [1].

1.2.3 Attrition and Breakage

As a granule experiences growth due to coalescence, the stresses acting on it increase. These stresses are a result of the agitative forces in the granulator which result in inter-granular collision and equipment-granule collisions. If the bonding within the granule is not strong enough to withstand these forces, then breakage occurs. This results in the reduction in granule size and the formation of granule fragments [1].

Furthermore, depending on the granulator and the process conditions chosen, there is the possibility of granules undergoing drying alongside granulation (such as in the Fluidised Bed Granulator). This drying results in the decrease in liquid binder within the granule. A decreasing binder content makes the granule less deformable and weaker, therefore meaning it is more susceptible to breakage by destructive forces in the granulator [1].

1.2.4 Drying

After the granulation step, the granules are typically dried to remove the liquid binder [6]. As evaporation occurs from the liquid bridges, the solid components precipitate out and develop into solid bridges between particles. This drying step is crucial because the presence of liquid make the granules stickier, which worsens their handling properties in downstream process. If water was used as the binder, as it commonly is, it can also result in granule degradation and a reduced shelf life due to microbial growth unless the water is removed.

1.2.5 Typical Wet Granulators

All wet granulators utilise a liquid binder to drive the agglomeration process and undergo the general wet granulation pathway presented in Section 1.2. The main difference between them is the source of the agitation that is used to mix the powder bed and disperse the binder. Table 1.1 presents the wet granulators represented in this study and the agitation type associated with each, while Figure 1.3 [7] presents a schematic diagram of each wet granulator. The High Shear and Twin-Screw Granulators utilise mechanical agitation to achieve mixing. In the case of the High Shear Granulator, it is a rotating impeller while in the case of the Twin Screw Granulator, it's a pair of co-rotating screws. Meanwhile, the Fluidised Bed Granulator uses an upwards flow of air to fluidise the powder particles with variations in local air velocity and rebound effects from collisions ensuring a multidirectional movement of particles.

Table 1.1: Granulators studied in this thesis alongside the source of agitation in each

Wet Granulator Unit	Agitation Type
High Shear Granulator	Impeller
Twin Screw Granulator	Co-Rotating Screws
Fluidised Bed Granulator	Fluidising Air

High Shear Granulator

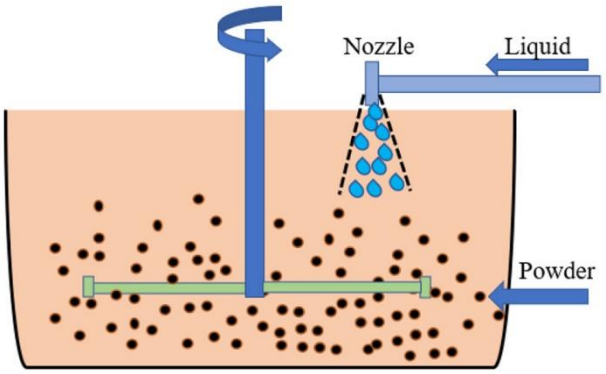

Twin Screw Granulator

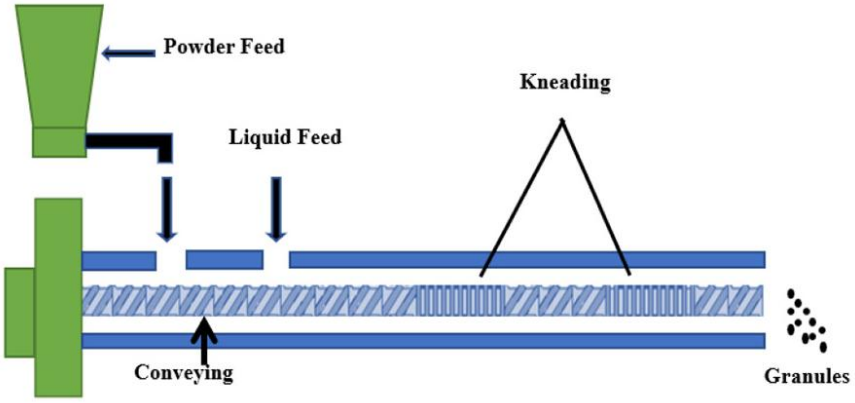

Fluidised Bed Granulator

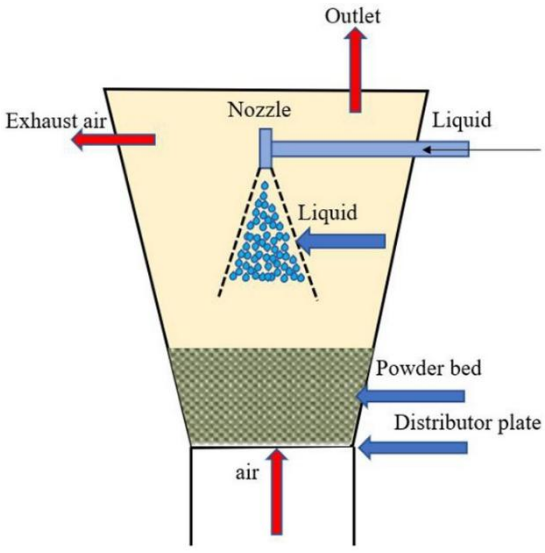

Figure 1.3: Common wet granulators with differing sources of agitation [7]

1.3 Dry Granulation

In contrast to wet granulation, dry granulation does not involve the use of liquid binder to drive the adhesion process. Instead, strong mechanical forces are typically used to compact the primary powder particles. This densification pushes the particles so close together that the increase in Van der Waal forces and the mechanical interlocking between particles result in bonding. Slugging is one form of batch, dry granulation where slugs or tablets are produced by the compaction of the powder. The compact that is formed then undergoes milling to produce granules of the desired size [8]. Comparatively, Roller Compaction is by far the most popular form of dry granulation due to its continuous nature. A schematic diagram of Roller Compaction is presented in Figure 1.4 [9]. In Roller Compaction, the powder is fed between two counter rotating rollers which applies a sufficiently high compressive force to produce a ribbon compact. This ribbon is then broken into smaller flake fragments by a flake crusher. These fragments then enter a mill which breaks them down to produce granules. Granule size is strongly determined by the mesh size used in the milling system.

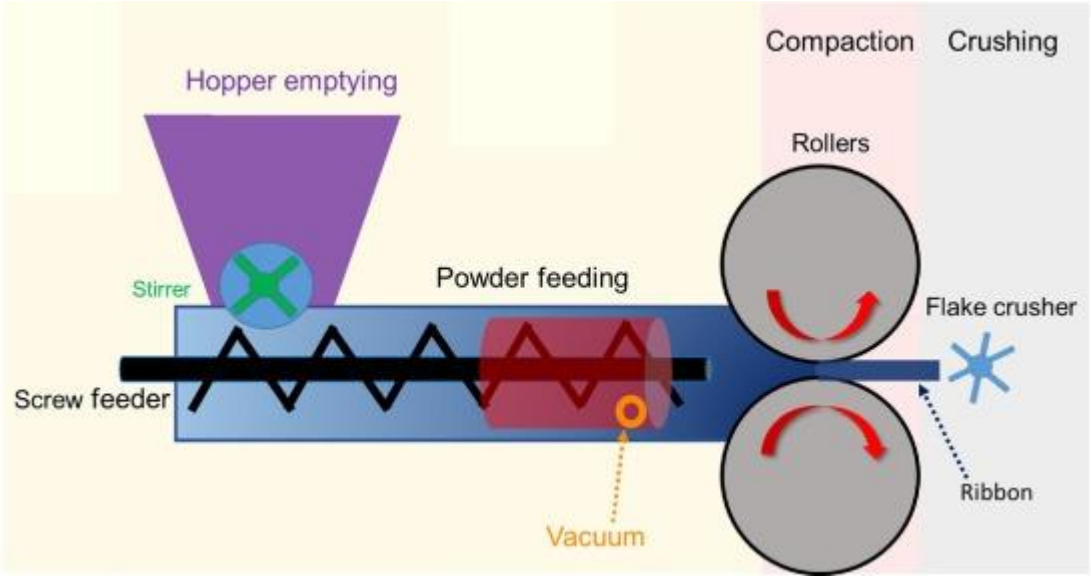

Figure 1.4: Schematic overview of the Roller Compaction process. The key stages involve Compaction of the primary powder particles to form a ribbon. This is followed by Crushing of the ribbon to form flakes. While not presented in the figure, the final stage involves Milling of these flakes to form granules [9].

1.4 Sustainability in Granulation

Sustainability is an aspect of food production that has been under intense scrutiny lately. This is driven by increased social awareness by the public and food manufacturers about the importance of fair governance of natural resources as well as reducing carbon emissions to fight climate change. Sustainability is a multi-faceted topic and there are many ways to judge it. The most popular metric is energy consumption with a higher energy consumption linked to a greater carbon footprint and higher

production costs. Another relevant metric is material wastage where more wastage is linked to overuse of natural resources, pollution due to waste generation and increased costs. Food production can be made more sustainable by combatting material waste by increasing granule yields during the production stage. Granulation can also be used to better optimise the product granule structure to prevent degradation during storage and reduce material waste postproduction. The rate at which technologies produce granules is the final metric by which sustainability can be evaluated. Technologies that produce granules faster result in the more efficient use of production sites and lower production costs.

1.5 Aims and Objectives of the Thesis

1.5.1 Aims

The overall aim of this thesis is to enhance sustainability within the field of granulation by considering both the process and the product. This will be achieved by meeting the below objectives.

- Comprehensively evaluate the sustainability of four established granulation technologies when applied to heat and moisture sensitive amorphous powders. Determining which technologies are the most sustainable will help food manufacturers to make informed decisions when choosing production pathways.
- Develop knowledge of how uncontrolled agglomeration can be avoided in wet granulation. Uncontrolled agglomeration (known as caking) is a phenomenon that heat and moisture sensitive amorphous powders are prone to during wet granulation, which results in low yield and high levels of material waste.
- Propose novel granule microstructures that are more resistant to humidity induced degradation during storage. This is aimed at preventing material waste postproduction and the creation of more sustainable granular products with a longer shelf life.
- Evaluate a newly proposed granulation technology as an alternative, sustainable manufacturing route for amorphous food powders. This evaluation will be carried out by judging the feasibility of the process with amorphous food powders and comparing process sustainability with the established granulation technologies.

1.5.2 Thesis Overview

This section presents an outline of the thesis which covers the content and delineates how each chapter contributes towards enhanced sustainability in the food industry. Please note that each chapter has been written in paper format. Figure 1.5 visualises how the different experimental chapters relate to each other.

Chapter 2 will present the literature review for this work. It will begin by introducing the properties of amorphous powders, specifically, it will highlight the importance of the Glass Transition Temperature

which is a key consideration in this study. Subsequently the principles behind the granulation technologies will be presented in depth by discussing the existing regime maps for each. The limited, sustainability literature covering each granulation technology will also be presented here. The literature review will then conclude by identifying the gaps in the literature that this study will address in Chapter 4 – 7.

Chapter 3 will present the working principles behind the main granulation equipment and characterising equipment used throughout the thesis.

Chapter 4 will present the work carried out evaluating the sustainability of the four established granulation technologies by considering their energy, material and time efficiencies alongside key product attributes such as flowability, dissolution time and friability. Chapter 4 concludes by recommending several tools to help food manufacturers select the optimum production pathway based on process sustainability and granule functionality. **Sustainability Aim: Identify sustainable granulation technologies for food production**

Chapter 5 will present the development of the first High Shear Granulation regime map which includes the Glass Transition Temperature (T_g) parameter. This regime map is aimed at delineating an operational region where controlled agglomeration can occur and caking (which is a key cause of material waste) can be avoided. **Sustainability Aim: Prevent material waste due to uncontrolled agglomeration during granulation**

Chapter 6 developed a novel method to produce a multicomponent, layered granule microstructure. The benefits of this layered granule microstructure in extending the shelf life of granules during storage and preventing humidity driven degradation was evaluated. **Sustainability Aim: Development of more humidity resistant granule structures to prevent material waste during storage**

Chapter 7 will present the application of a very recently proposed Dry Twin Screw Granulation process on amorphous food powder. The chapter will evaluate process feasibility and develop the first regime map for a Dry Twin Screw Granulation process. The regime map will delineate possible mix behaviours and an 'ideal' operable region for the production of good granules. It will conclude by evaluating the sustainability of this process in relation to the established technologies. **Sustainability Aim: Evaluation of new, sustainable granulation technologies for the future**

Chapter 8 will conclude the findings and summarise the highlights of this thesis.

Chapter 9 will suggest future avenues of research that can be explored to further build upon the findings and theories presented in this work.

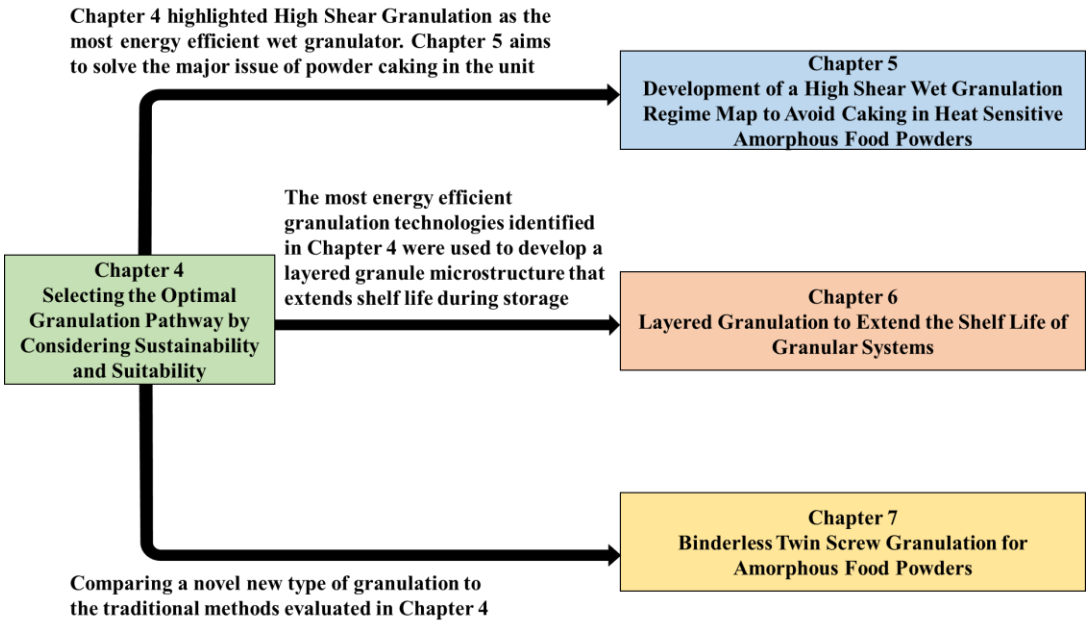

Figure 1.5: Visualises the relationship between Experimental Chapters 4 – 7

2 Literature Review

A suitable starting point for the literature review is to introduce the concept of amorphous powders, specifically focusing on Maltodextrins, which are the primary powders used in this thesis. Therefore, this section will outline the key properties of amorphous powders, referring specifically to Maltodextrins, which can impact the granulation process. The subsequent sections will introduce the principle and regime maps associated with each evaluated granulation technology. The most common metric used to evaluate process sustainability is the energy consumption. Therefore, this literature review will also cover the existing literature evaluating the energy consumption of the granulation technologies. Finally, the literature review will conclude by identifying the existing gaps in literature and state in which chapter they are addressed.

2.1 Understanding Amorphous Powders

There are two main categories that are used to describe powder particles: Crystalline or Amorphous. As shown in Figure 2.1, a crystalline powder possesses a well ordered, repeating lattice structure. This ordered structure maximises the attractive intermolecular forces meaning that large amounts of energy are required to disrupt it. This gives Crystalline powders a high and well-defined melting point making them temperature insensitive until that point is reached. The tight packing of the molecular lattice also reduces the solubility and hygroscopicity of the material as it makes it more difficult for foreign small molecules such as water to penetrate. Meanwhile, Amorphous powders have a random molecular arrangement. This leads to a weaker and less efficient bonding in the material structure. Compared to Crystalline powders which have a well-defined melting point, the random structure of Amorphous powders means that they gradually soften as temperature increases. Eventually this softening causes them to transition from a glassy, brittle state to a viscous, rubbery state. The temperature where this transition occurs is known as the Glass Transition Temperature (T_g). The random structure of Amorphous powder also allows small, foreign molecules like water to penetrate into the molecular structure which leads to a quick dissolution time and high hygroscopicity. This hygroscopicity is important because as water penetrates into Amorphous powders, it weakens existing intermolecular bonds and reduces the material's Glass Transition Temperature [10–12]. This makes the initial storage conditions very important when determining the properties and behaviour of Amorphous powders during granulation. As shown by Figure 2.1, a mixed form is also possible where a material has both Crystalline and Amorphous components.

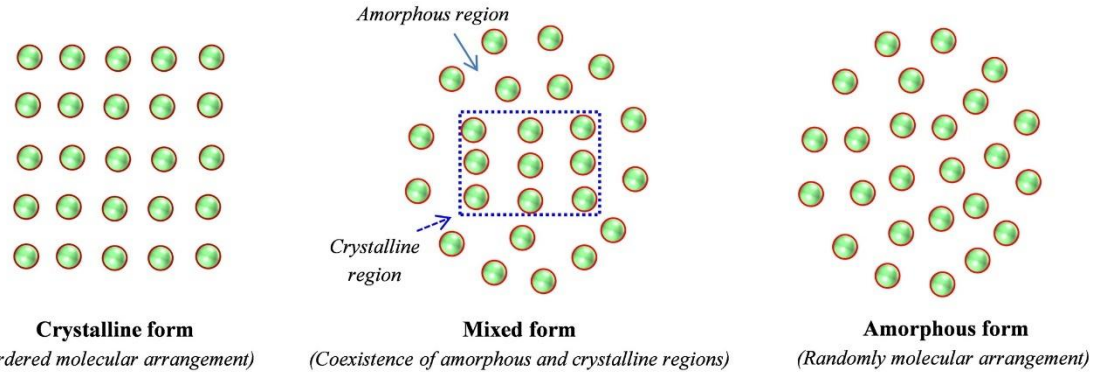

Figure 2.1: Example molecular structures of crystalline, amorphous and mixed form substances. The Crystalline form shows a regular, well-ordered lattice while the Amorphous form shows a disordered, random arrangement [10].

Maltodextrin is the generic umbrella name given to a group of amorphous powders which are formed from either the acid or enzymatic controlled hydrolysis of starch. They are composed of d-glucose units which are connected by (1-4) glucosidic linkage to give d-glucose polymers of varying length and molecular weight. The DE (Dextrose Equivalent) number represents the reducing sugar content of the Maltodextrin. Pure Starch has a DE number of 0 while Glucose has a DE number of 100, and Maltodextrins are placed in between this range [13]. As the DE number increases, the average molecular weight decreases as the polymer chains become shorter. This was confirmed by the work of Castro et al [13], who looked at the composition of several Maltodextrins (such as DE6, 12, 17 and 19) and found that the composition of high molecular weight oligosaccharides was found to increase as the DE number decreased.

2.1.1 Glass Transition Temperature

The most important characteristic of amorphous powders is their ability to change state depending on the process temperature and water content. This behaviour is highlighted in Figure 2.2. At low temperatures and low moisture contents, the material exists in a glassy, rigid state. Under these conditions the material is not sticky and experiences no viscous material flow. As temperature is increased, the molecules gain sufficient energy to overcome the weak intermolecular bonds locking them in place and begin to move. The temperature at which point this occurs is called the Glass Transition Temperature (T_g) and it results in the material transitioning to a viscous state. Higher moisture contents mean more water molecules are adsorbed into the molecular structure. These water molecules bond to the amorphous powder, and as they do so, replace and weaken the existing network of intermolecular bonds. This reduces the activation energy required to induce molecular movement in the structure. This leads to the displayed decrease in T_g with moisture content [14–16]. The greater the increase in powder temperature above its Glass Transition Temperature, the more pronounced the viscous flow becomes. This increased viscous flow can result in increased stickiness. Sometimes this increased stickiness leads to excessive and undesired agglomeration of the powder during granulation,

which is known as caking. At very high temperatures and moisture contents, the surface boundaries between particles fuse and the physical structure of the powder collapses resulting in liquid flow [14].

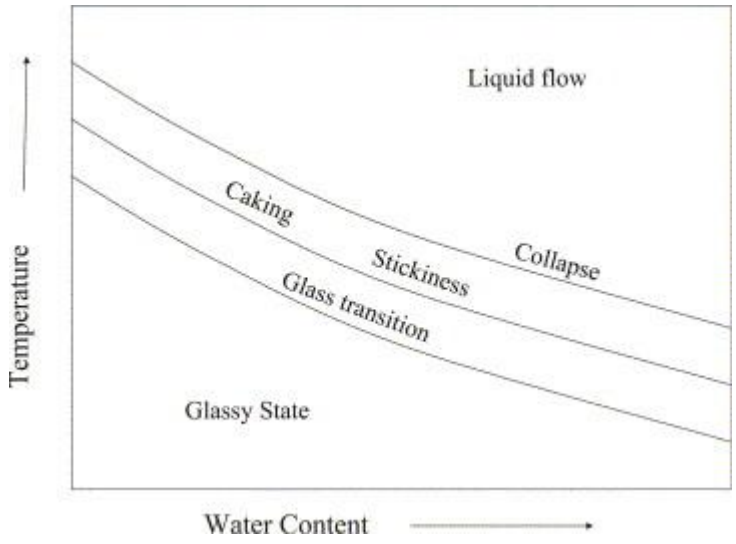

Figure 2.2: Impact of system temperature and water content on the change of state from glassy to rubbery (presented as liquid flow) in amorphous powders [14].

The relationship between the moisture content and Glass Transition Temperature is commonly modelled using the Gordon Taylor Model [17] which is presented in Equation 2.1. The model was initially developed to predict the Glass Transition Temperature of binary amorphous mixtures where $T_{g,A}$ and $T_{g,B}$ are the respective T_g's of pure components A and B while x_A and x_B are the mass factions of components A and B in the mixture. The Gordon Taylor constant (k) is used as a fitting parameter which accounts for the strength of interaction between the two pure components. While originally developed using rubber polymers, this model is widely accepted in literature and has been proven to apply well to model the change in powder Glass Transition Temperature due to changing moisture content [18–20]. In this scenario, component A represents the pure powder while component B represents water. The Glass Transition Temperature of water at ambient pressure is commonly taken as -135°C [18–21] in literature.

$$T_g = \frac{x_A T_{g,A} + k x_B T_{g,B}}{x_A + k x_B}$$

Equation 2.1

Literature credits the term 'T – T_g' rather than the actual values of T_g and T (temperature) as the dominant factor that determines the behaviour of amorphous powders. For instance, Haider et al [22] determined that the deformation behaviour of Maltodextrin particles was dependent on the difference between the system temperature (T) and T_g rather than the actual values of those parameters. Similarly Palzer [23] determined that the parameter 'T – T_g' correlated well with the compaction behaviour of

amorphous powders during tabletting, while Osborne [24] highlighted the importance of 'T – T_g' in determining amorphous powder granulation behaviour during Roller Compaction. The changing state of amorphous powders from glassy to viscous is key to understanding the behaviour of the powder in the granulation process where temperature and moisture contents are constantly in flux.

2.1.2 Maltodextrin DE number and the Glass Transition phenomena

Generally, an increasing DE number correlates with a lower Glass Transition Temperature as shown by Figure 2.3. This is because low DE number Maltodextrins are composed of longer chained polymers. These long chain polymers form a much more extensive network of hydrogen bonding compared to high DE Maltodextrins which are formed from short chain polymers. Low DE Maltodextrins also experience significant entanglement. Large amounts of energy are required to sufficiently excite longer chained polymers to cause the breakage of the bonding network and disentanglement. This results in low DE Maltodextrins having significantly higher T_g's at similar moisture content to their high DE counterparts [25,26]. The effect of DE grade on Glass Transition Temperature will become important when comparing the granulation of these powders because it means that they will behave differently to each other at the same system temperature. Generally, amorphous powders show the same trend observed here with Maltodextrins, where materials composing of shorter and more weakly bonded molecular chains possess lower Glass Transition Temperatures.

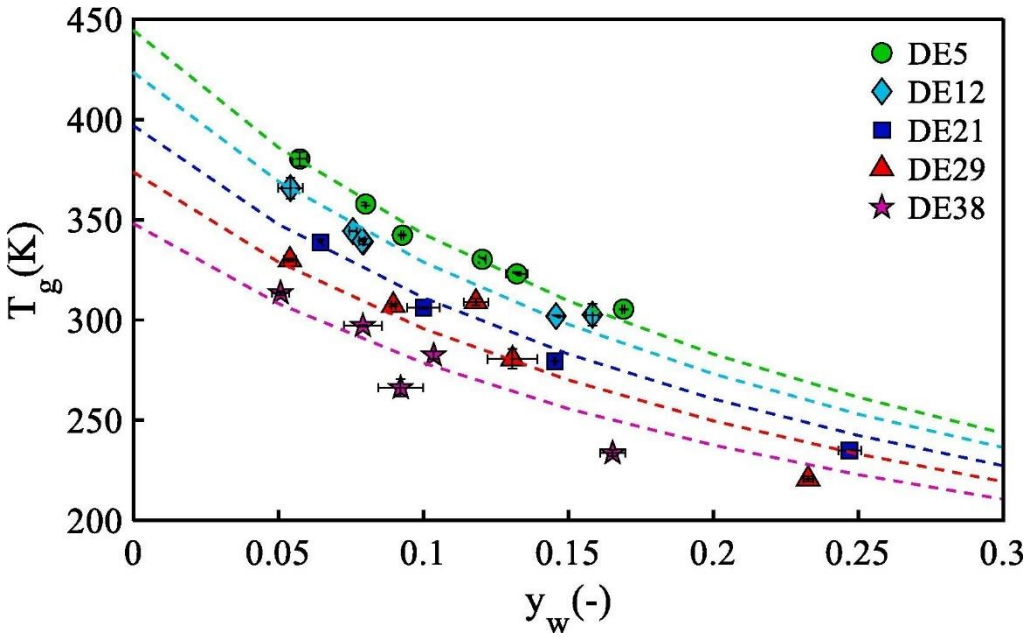

Figure 2.3: Impact of moisture content on the Glass Transition Temperature of different Maltodextrin grades. High DE Maltodextrins display lower T_g's due to their composition including shorter chained polymers which experience less entanglement and have weaker bonding [25].

2.1.3 Maltodextrin DE number and viscosity

The high solubility of Maltodextrin powder means that it easily dissolves in water to produce mixtures with varying properties based on the DE number and Maltodextrin concentration. For example, Figure 2.4 indicates that the viscosity of Maltodextrin-water mixtures is dependent on DE number. For the concentration evaluated in Figure 2.4 (500 g/dm^{-3}), viscosity appears to decrease in a linear manner with increasing DE number [27]. This again can be explained by considering the longer chained nature of low DE Maltodextrins. When added to water, these longer chained molecules form more hydrogen bonds with the water molecules and experience greater entanglement. This leads to the development of a more ordered structure which possesses a greater resistance to motion, resulting in a higher viscosity [28]. The Maltodextrin concentration in the mixture also affects viscosity as shown by Figure 2.5. Figure 2.5 displays viscosity increasing alongside Maltodextrin concentration with low DE Maltodextrins showing the steepest increase. This non-linear increase in viscosity with Maltodextrin concentration is attributed to the disproportionate increase in the extent of entanglement and network of hydrogen bonding that occurs as the Maltodextrin concentration increases. This leads to a nonlinear increase in the resistance to flow and therefore viscosity [25,27].

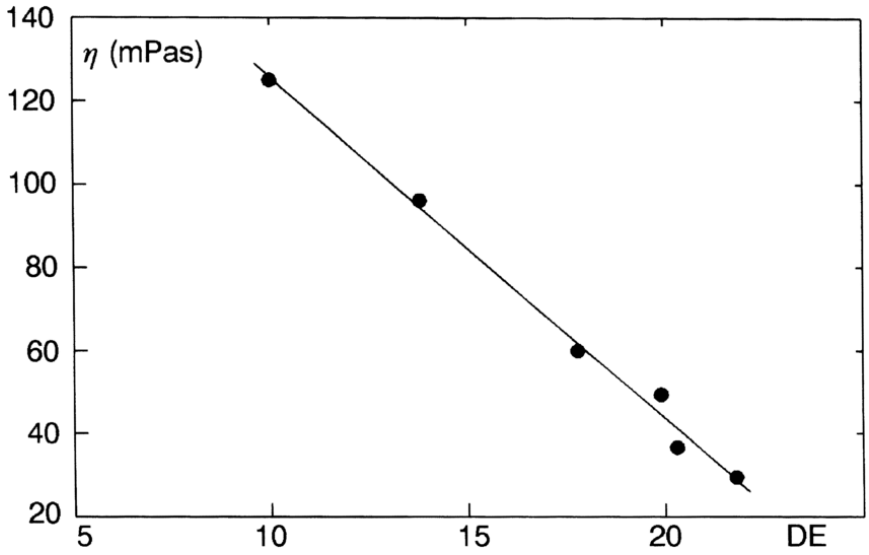

Figure 2.4: Impact of DE number on viscosity (at a Maltodextrin concentration of 500 g/dm^{-3}). Generally, there is a linear relationship between DE number and viscosity at this concentration [27].

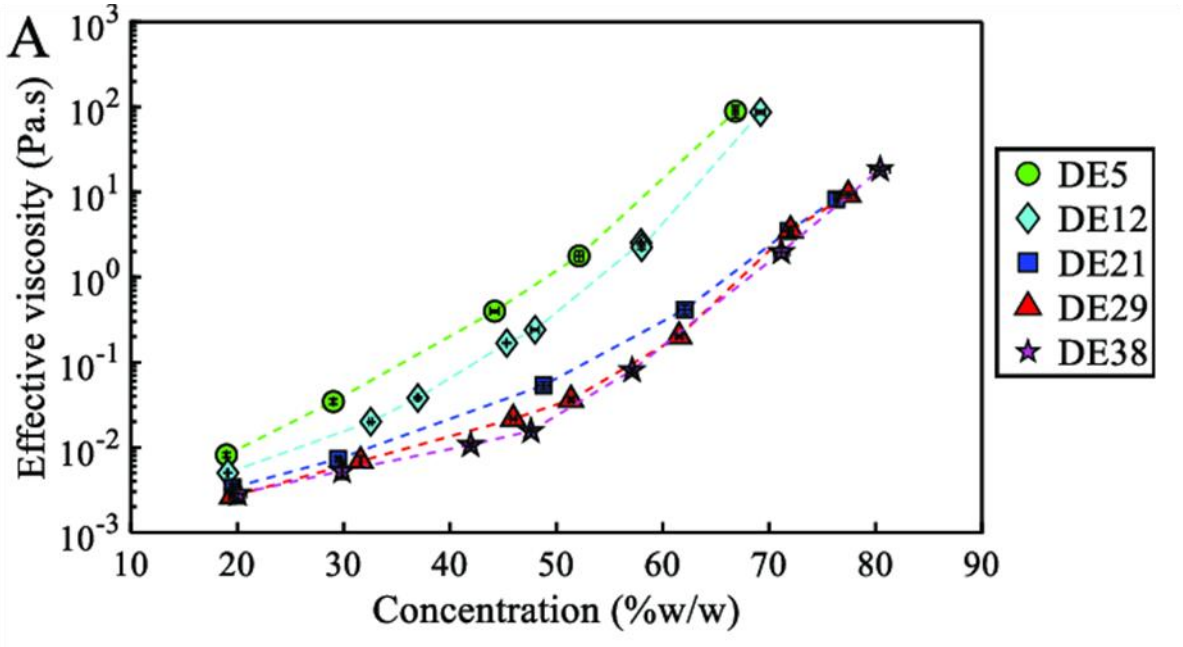

Figure 2.5: Impact of Maltodextrin concentration on effective viscosity for a range of DE grades. As concentration increases so does the effective viscosity. Low DE Maltodextrin show steeper increases compared to their high DE counterparts [25]

2.1.4 Amorphous powder binding mechanism

The unique phase changes displayed by amorphous powders allow agglomeration to occur under several different mechanisms as summarised in Figure 2.6. The first mechanism is the formation of liquid bridges during wet granulation. During drying, the water in these bridges evaporate and the dissolved solid precipitates to form solid bridges which adheres particles together. The next mechanism is the formation of sinter bridges. This occurs when the material temperature has surpassed the T_g which causes Glass Transition to occur and the material to gain mobility. The resulting viscous flow of material into the gaps between particles leads to the formation of solid bridges and bonding. The final bonding mechanism is visco-elastic deformation as particles are compressed together. This increases the contact area between particles while also reducing the distance between particles. This leads to bonding through increased Van der Waal forces of attraction and is the primary bonding mechanism observed in Roller Compaction [23,29].

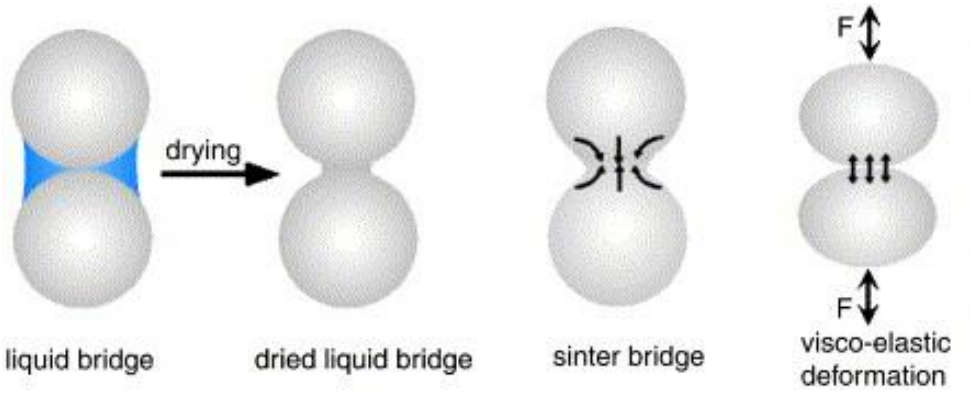

Figure 2.6: Possible binding mechanisms for amorphous powders. The first includes the formation of liquid bridges that dry to form solid bridges (which is the primary bonding mechanism for wet granulation). The second is the formation of sinter bridges due to glass transition induced viscous flow of material. The final binding mechanism is the increase in Van der Waals attractive forces due to visco-elastic deformation during compression (which is the primary bonding mechanism for dry granulation) [23].

2.2 High Shear Granulation

The High Shear Granulator (HSG) is a wet, batch granulation unit which achieves agitation using a rotating impeller. This granulator is illustrated in Figure 1.3. The typical High Shear Wet Granulation (HSWG) process first involves a dry mixing stage to ensure homogeneity of the powder mix. Then liquid binder is added, and impeller speed is altered to achieve the required growth and breakage rates. The final product is then taken and dried (usually in a Fluidised Bed Dryer) to produce the final product. This section will introduce the current regime maps for High Shear Granulation and the existing literature on the energy efficiency of the process.

2.2.1 High Shear Granulation Regime Maps

The most well adopted, comprehensive regime map for High Shear Granulation was developed by Iveson and Litster [30] and is presented in Figure 2.7. The regime map characterises the system behaviour depending on the Deformation Number and the Maximum Pore Saturation (S_{max}). The Deformation Number represents the extent of deformation experienced by the granule and is dependent on the granule density (ρ_g), granule collision velocity (U_c) and the granule dynamic yield strength (Y_g). Meanwhile, the Maximum Pore Saturation represents the liquid content of the system and depends on the L/S ratio (w), particle density (ρ_s), minimum porosity (ε_{min}) and the liquid density (ρ_l). Five key regions are evident in this map: The dry free flowing region, the nucleation only region, the crumb region, the granule growth region and the slurry region.

In the **dry free flowing region**, the S_{max} is so low that there is insufficient binder for the formation of nuclei granules. Although Iveson and Litster [30] do state that the formation of some small agglomerates

is possible in this region if the compaction stresses are high enough to sufficiently increase the Van der Waals forces of attraction to allow primary particles to bond together. In the **nucleation only region**, there is sufficient binder to form nuclei granules. However, there is insufficient liquid on the surface of the nuclei granules produced in this region to promote granule growth due to coalescence. In the **crumb** region, the stresses applied on the granule are too high compared to the granule strength (as indicated by the very high Deformation Number). This results in the breakage and destruction of any granules that exist in this region [30].

The **granule growth region** can be described as steady, induction or rapid which is dependent on the Deformation Number. If the granules have a medium Deformation Number, indicating that they deform easily, then they will experience Steady Growth. During Steady Growth, granules undergo significant deformation and consolidation during intergranular collisions. This forms large contact areas between granules and squeezes liquid to the granule surface. This increased rejuvenation of liquid on the granule surface promotes bonding and causes granule size to increase steadily with time. This type of growth is typically shown by coarse, narrow sized particles being agglomerated by low viscosity and low surface tension binder. Granules that deform less and consolidate slowly (as indicated by a lower Deformation Number) undergo Induction Growth. During Induction Growth, granules must first undergo an initial induction phase where the granule slowly becomes compacted, and the liquid is gradually squeezed out into the surface. Little growth occurs during this slow induction phase. Eventually the slow consolidation makes the granule surface wet enough for growth to occur and granule size increases quickly leading to rapid growth. As the amount of binder added increases, the duration of the induction phase decreases. This type of growth is associated with fine particles and binders with a high viscosity. As pore saturation approaches 100%, rapid growth occurs regardless of the Deformation Number as granules become surface wet very quickly, leading to a rapid increase in granule size. However, eventually a point is reached where there is too much liquid in the system. This can lead to excessive liquid bridge formation in the mix which produces large lumps rather than granules which is known as **Overwetting**. It can also result in the formation of a **Slurry** where granules become saturated in liquid and lose their structural integrity leading to collapse [30].

The Iveson and Litster [30] regime map which is presented in Figure 2.7 has been validated by multiple studies in HSG [31,32] and drum granulators [33,34]. It has also been further developed by Iveson et al [35] to better establish the boundary conditions for each regime.

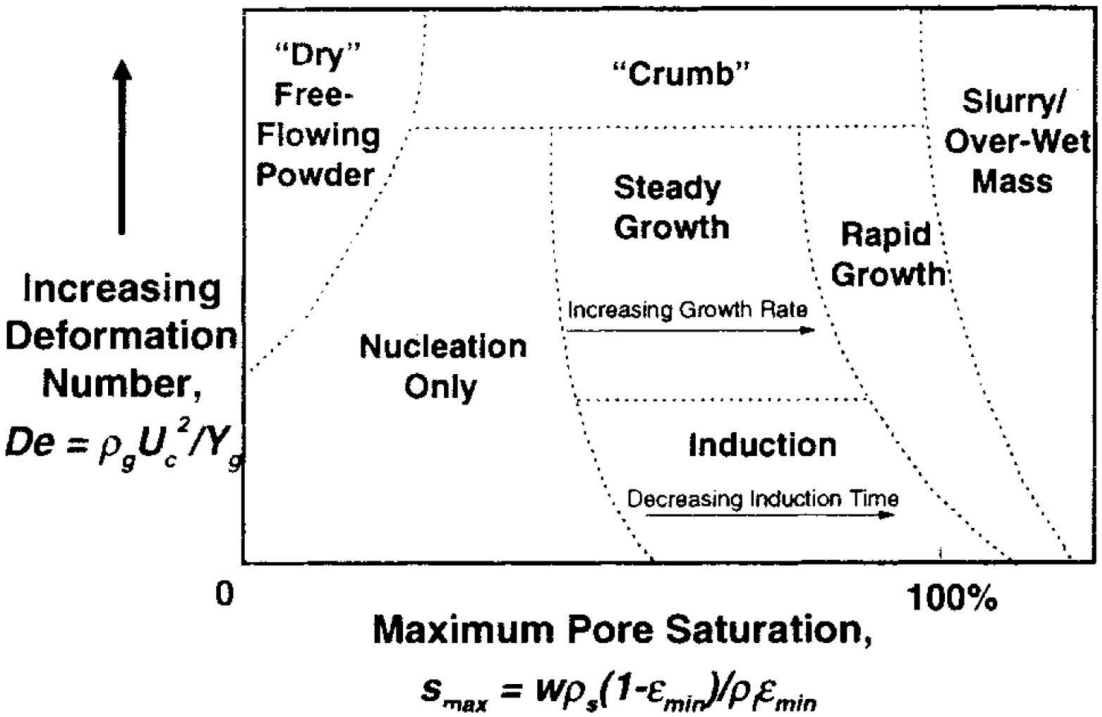

Figure 2.7: High Shear Granulation Regime Map displaying different mix behaviours based on the Deformation Number and Maximum pore saturation. Key regions highlighted include the Dry Region, Nucleation Only Region, Crumb Region, Slurry Region and Granule Growth Regions [30]

Santomaso et al [36] produced a regime map based on granulating MCC and crystalline sugar blends with water which is presented in Figure 2.8. Similarly, to the map proposed by Iveson and Litster [30], the Deformation Number (in this case presented as St_{def}) is used to represent the extent of deformation of the granules. However, in this case, the pore saturation number has been replaced by the Capillary Viscous Number (Ca*) which is defined according to Equation 2.2 where η_L is the binder viscosity, u_r is the relative velocity and W_a is the work of adhesion.

$$Ca^* = \frac{\eta_L u_r}{W_a}$$

Equation 2.2

The regime map by Santomaso et al [36] highlights that the growth mechanism was dependent on the Ca* value for the MCC-sugar mixtures. At Capillary Viscous Numbers less than 1, the granules grew via a steady growth mechanism. While at Capillary Viscous Numbers greater than 1, the granules grew via an induction growth mechanism. The results showed MCC mixes containing low thickening power sugars such as Mannitol adhered to the steady growth mechanism while those containing high thickening power sugars such as Sucrose adhered to the induction growth mechanism. This is because liquid bridges in mixes with high thickening power sugars are likely to be more viscous and stiffer, and therefore result in the formation of granules that deform and consolidate to a lesser extent. This means an induction period is needed for these granule surfaces to get sufficiently wet for growth to occur. A

Ca* value of 1 indicates the boundary condition at which the liquid bridge viscosity increases to the point where viscous forces dominate. This work highlights the importance of viscosity during granulation which is a key variable that is omitted in the map of Iveson and Litster [30].

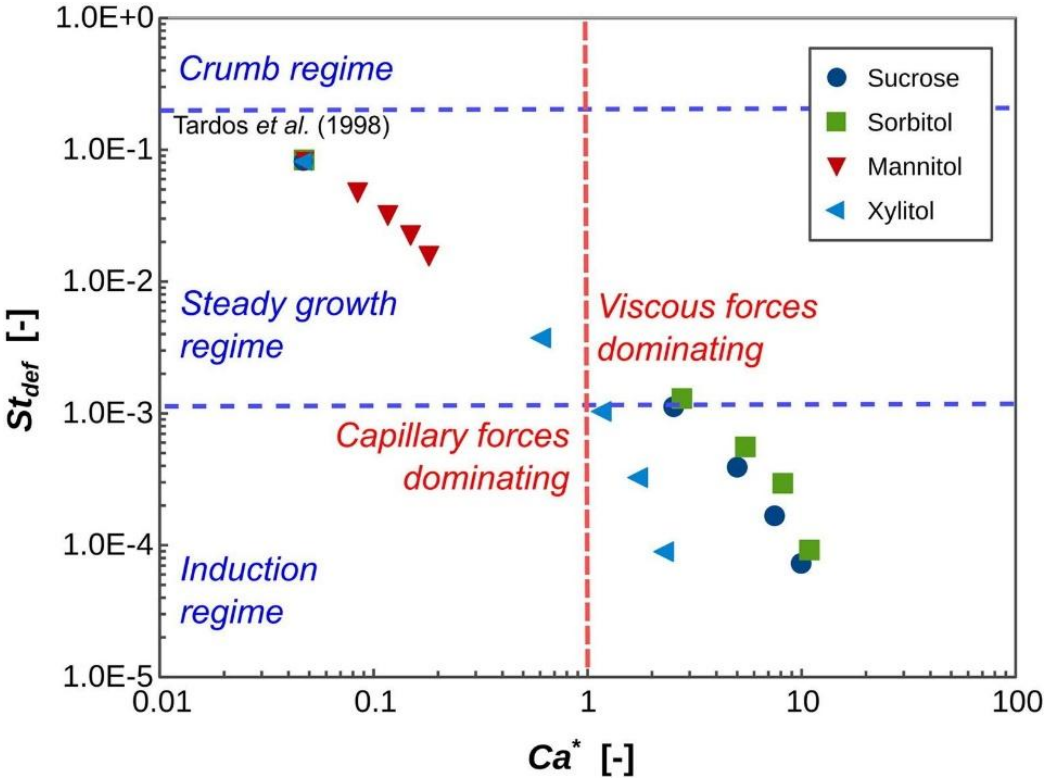

Figure 2.8: High Shear Granulation regime map highlighting the importance of viscosity in determining mix behaviour. Systems with sugars of high thickening powers (Sucrose, Sorbitol and Xylitol) produce viscous, stiff liquid bridges when granulated with water. This reduces the deformation experienced by granules during consolidation which results in induction growth. Meanwhile low thickening power sugar (Mannitol) systems produced more deformable granules which underwent quick consolidation and experienced steady growth [36].

The issue with these regime maps can be explained by considering the materials used in their development. This is because a regime map is generally only applicable to the powders that were used to produce it. These HSG regime maps were developed via experiments on heat insensitive, insoluble materials and many of the experiments in literature validating it were limited to such materials. These materials include glass ballontini as used by Iveson and Litster [30], Zirconium Hydroxide [31], Iron Ore fines and Copper Chalcopyrite [35], Crystalline Lactose Monohydrate [32] and crystalline sugars [36]. Therefore, their applicability when considering highly soluble, heat sensitive amorphous powders is in doubt.

2.2.2 Sustainability in High Shear Granulation

While the energy consumption during High Shear Granulation has been evaluated in literature, it is usually done with the aim of optimising process control rather than evaluating process sustainability. In fact the link between power consumption and process behaviour in the HSG is so strong that Jang et al

[37] states that it is the primary PAT tool for HSG. For instance, Pepin et al [38] evaluated the power consumed in the HSG with the aim of identifying the overwetting point of the mix. Meanwhile, Betz et al [39] looked at changing trends in power consumption due to changing process parameters to evaluate its suitability for an in-process control neural network. Furthermore, numerous studies have evaluated the link between power consumption and the ability to monitor key granule quality attributes [40–42]. However, none of the studies approached energy consumption within the granulator from a sustainability perspective.

2.3 Twin Screw Granulation

The Twin Screw Granulator is composed of a long barrel chamber containing two parallel co-rotating screws as illustrated in Figure 1.3. The barrel is often equipped with complicated temperature controls which enable them to heat and cool the powder mix during the granulation process. The strength of the TSG is in the versatility of the screw configurations possible. This is because there are a large variety of possible screw elements which can be included in the screw as shown by Figure 2.9, which enables a great deal of process flexibility. Out of these possible elements, Conveying Elements (A) and Kneading Elements (E) are the most common and are the only types of elements used in this thesis. As the name suggests, Conveying Elements are primarily used to transport material along the barrel and they provide less mixing on the powder compared to other types of elements. Meanwhile, Kneading Elements apply a lot of stress and generate a very strong mixing effect on the powder. These Kneading Elements are attached together to form Kneading Blocks (H) to amplify their effect. The mixing action of the kneading block increases with block length and the offset angle between the individual elements. Simultaneously, the conveying action of the kneading block decreases with block length and offset angle. This means that at one extreme, an offset angle of 90 degrees will produce a high degree of mixing but will result in little conveying power. At the other extreme, an offset angle of 30 degrees will provide a lesser mixing effect but will enhance the conveying power to aid the passage of poorly flowing materials. In between these, 60-degree offsets can be achieved to produce a better balance between mixing and conveying [43,44].

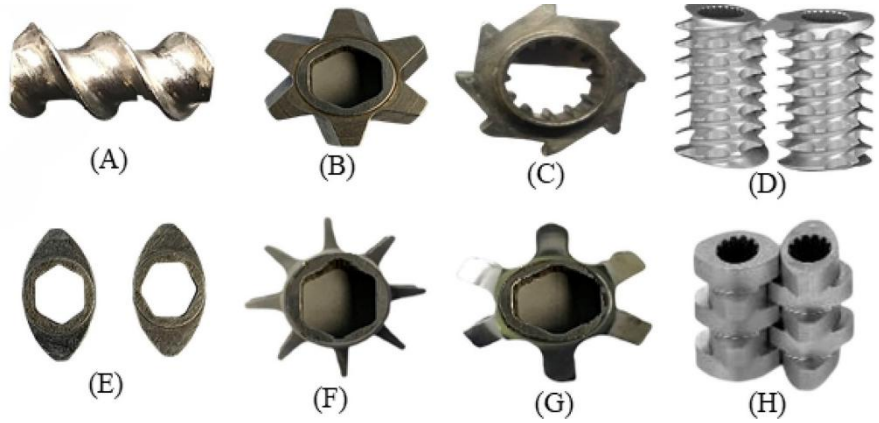

Figure 2.9: Various possible screw elements which include Conveying Elements (A), Wide Toothed Mixing Elements (B), Cutter Elements (C), Comb Mixing Elements (D), Kneading Elements (E), Narrow Toothed Mixing Elements (F), Screw Mixing Elements (G) and Kneading Blocks (H) [43].

As visualised in Figure 1.3, during the process, powder is added at one end of the barrel and conveyed along by the motion of the screw. Next liquid is added through an injection port where it mixes with the powder and initiates the wet granulation process. The shear stresses produced by the different elements configured in the screw generate the driving forces required for consolidation and breakage. Unlike in batch granulators where the granulation stages happen simultaneously, in the Twin Screw Granulator, the stages are spatially separated and can be attributed to different parts of the unit. Wetting and nucleation occurs near the liquid addition port which is usually in the pre-kneading zone inhabited by conveying elements. Granule consolidation and growth then occurs in the mixing zone inhabited by the kneading elements. Breakage and attrition are also governed by this section depending on the number of kneading elements and formulation. Another conveying section is then present to transport the granules to the exit [44].

The subsequent sub-sections will introduce the existing TSG regime maps and energy consumption literature. It will also introduce a recently developed TSG granulation process which has the potential of granulating amorphous powders in the absence of a water binder.

2.3.1 Twin Screw Granulation Regime Map

Dhenge et al [45] produced a Twin Screw Granulation Regime Map which plots the Deformation Value (β) against the multiple of L/S ratio and Binder Viscosity as shown by Figure 2.10. The term on the y axis (β) represents the deformation experienced by the granule and is defined according to Equation 2.3 as the stress acting on the granule divided by the granule strength. The stress acting on the granule is based on dividing the torque by the material volume while granule strength is obtained from compression testing. The term on the x axis was chosen because it represents the binding ability of the liquid to influence growth. This binding ability of the liquid depends on the amount of liquid and its viscosity. For instance, the more liquid in the mix (as reflected by the L/S ratio) the greater the liquid

saturation and the more liquid bridges form. Meanwhile, greater binder viscosity's produce stronger liquid bridges which results in the formation of stronger granules.

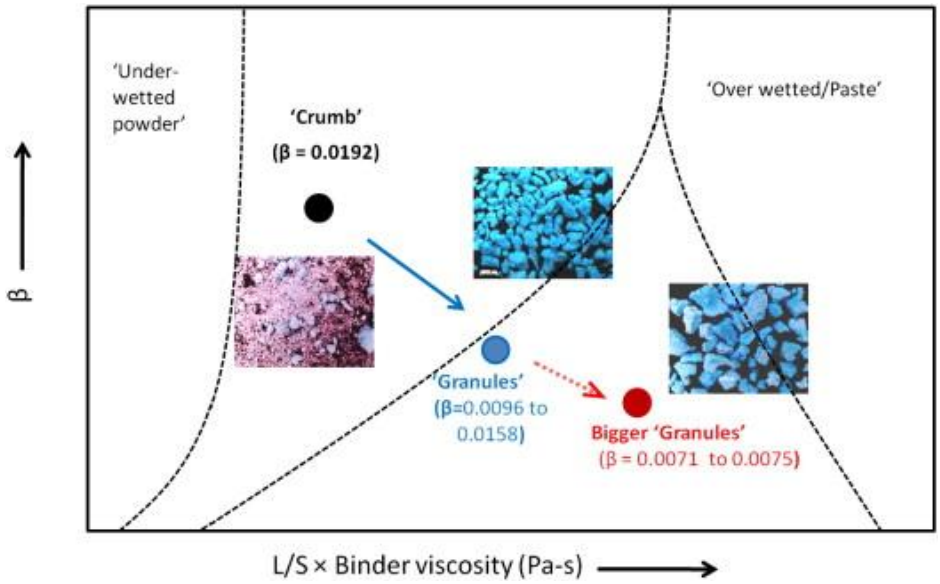

Figure 2.10: Twin Screw Granulation regime map for a two kneading block screw configuration. Highlights 4 possible mix regimes (under-wet, crumb, granule and paste) depending on the Deformation value (β) and the multiple of L/S ratio and Binder Viscosity [45].

$$\beta = \frac{Stress\ acting\ on\ granule}{Granule\ Strength}$$

Equation 2.3

The descriptors used by Dhenge et al [45] to describe the different behaviours in Figure 2.10 share many similarities with those used by Iveson and Litster [30] with both maps including an under wet (dry), crumb, granule and overwet region. At very low 'L/S x Binder Viscosity' values the mix is predominantly in the under wet region where the liquid binding ability is insufficient to result in granulation. As 'L/S x Binder Viscosity' is increased, the crumb region begins to dominate. In this region, the liquid binding ability is just sufficient to form granules. However, these granules are weak and crumble easily when exposed to stresses inside the granulator. This limits granule growth, meaning that only small granules are produced in this region. The use of intermediate 'L/S x Binder Viscosity' values facilitates the good granulation of the mix with granule size increasing as 'L/S x Binder Viscosity' increases and β decreases. Finally, the use of excessive 'L/S x Binder Viscosity' values means the liquid has too great a binding ability leading to the formation of a overwet paste. This regime map is only valid for the screw configuration used to produce it (which in this case is a screw containing two kneading blocks). This is because changes in screw configuration altered the mix behaviour to a considerable extent. For example, the inclusion of more kneading elements compared to a conveying element will alter the Deformation Number as the stresses acting on the granule will be much greater,

and the produced strength of the granule will also be greater. An example of the regime map for a conveying element only configuration which was developed by Dhenge et al [46] is presented in Figure 1A in the Appendix to highlight the importance of screw configuration in determining mix behaviour. Dhenge et al [45] states that it is the almost infinite type, number and combination of elements that can go into the design of a screw configuration, that makes the generic development of a regime map for Twin Screw Granulation very difficult.

Tu et al [47] produced another regime map for Twin Screw Granulation which identified three key zones depending on screw configuration. Figure 2.11 displays the experimental matrix used by Tu et al [47] to evaluate process behaviour based on changing screw speed and L/S ratio for a screw configuration with a long, single kneading zone. The corresponding behaviours that were observed at each combination of process parameters are presented in Figure 2.12. The three key zones include the blocked zone, the granulation zone and the extrudate zone. In the blocked zone, the torque required far exceeded the safety rating of the motor and the granulator would shut down to protect the drive system and the screws. Tu et al [47] states that for the long kneading segment configuration, this tended to occur at the low screw speed of 50 rpm due to the higher barrel fill level at this condition, which increased the required throughput force. In the granulation zone, the granule size distribution was measured which showed the distribution narrowed with increasing screw speed and shifted right with increasing L/S ratio. The last zone was the extrudate zone where the powder was so wet (typically at L/S ratio's greater than 1.5) that the mix behaved as a paste. While this map is well described in the text, Pohl and Kleinebudde [48] is highly critical of Tu et al [47] due to the incoherent nature of the figures. For instance, the use of log(x) and f(log(x)), where x is aperture size, to characterise the graph axis (as explained in Figure 2.12) makes it hard to draw conclusions between the behaviours shown and the process parameters used. This leads to a confusing experience when attempting to match the regime maps to their descriptors in the text and limits their usefulness.

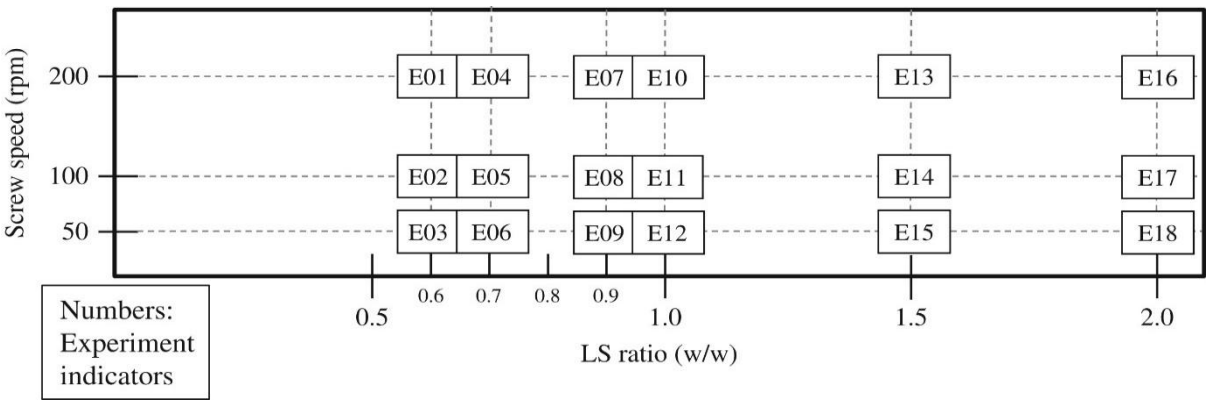

Figure 2.11: The L/S ratios and screw speeds evaluated by Tu et al [47] for a long single kneading segment screw configuration. Each entry represents an experimental condition. For instance, E01 (Experiment 01) represents an experimental run at a screw speed of 200 rpm and L/S ratio of 0.6. This above matrix corresponds to the below matrix showing the regime descriptions at each of the process conditions [47].

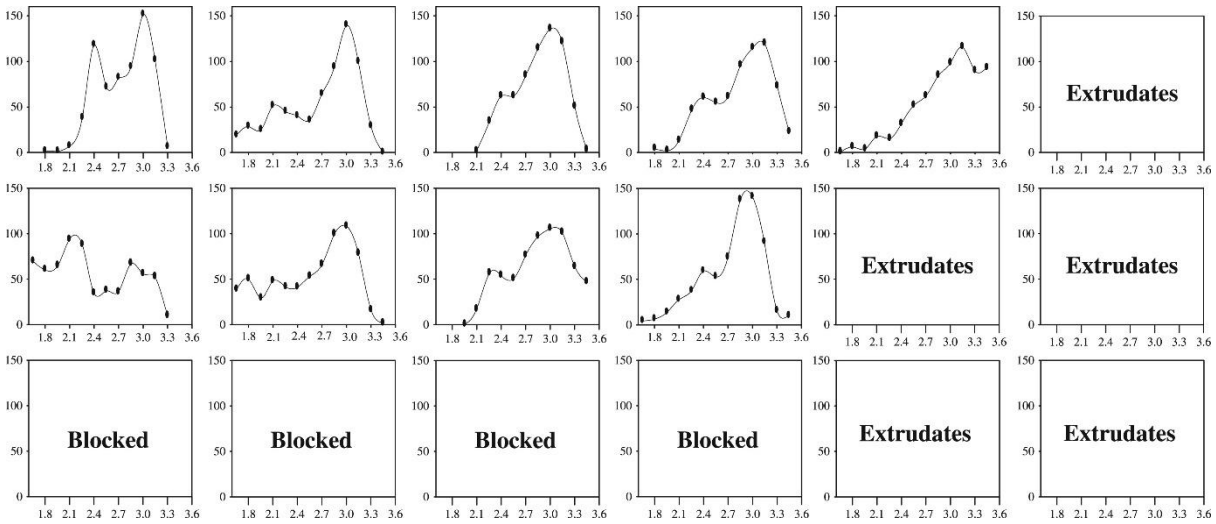

Figure 2.12: Proposed Twin Screw Granulation regime map for a screw configuration with a long, single kneading segment for the granulation of MCC PH 102 and PEG. This matrix corresponds to the process parameters highlighted by Figure 2.11 – for example, the top left graph represents Experiment E01 while the bottom right graph represents Experiment E18. The x coordinate refers to the log of the granule aperture size (in microns). The y coordinate meanwhile is described by the function $w_i/[log(x)_i - log(x)_{i-1}]$ where x is the granule aperture size, w_i is the mass faction in the i^{th} interval and x_i is the top size of interval i. The blocked region indicates the conditions where the torque requirement on the motor was too high and shutdown occurred. The extrudate region indicates the point where the mixture was too wet and formed a paste. The remaining graphs show the granulation growth region and the typical granule size distribution associated with each [47].

2.3.2 Sustainability in Wet Twin Screw Granulation

Similarly, to the High Shear Granulator, existing research in the Twin Screw Granulator has focused on evaluating power consumption as a process control aid. For instance, Rychaert et al [49] evaluated power consumption as a tool to monitor granule size and Zheng et al [50] worked on a correlation between power consumption and granule shape. Literature also commonly refers to the stabilisation point of power consumption during start up as a reliable indicator for when steady state has been achieved [51,52]. Furthermore, Twin Screw Granulation literature frequently uses auxiliary terms to describe power consumption. For example, Tan et al [53] used the term screw loading to evaluate the effect of formulation, liquid injection rate and screw speed. This screw loading term was said to be a function of torque and power consumption. Meanwhile, Meier et al [51] looked at the impact of key process parameters such as screw speed and throughput on the percentage power consumption (%) of the unit. The absence of absolute values for energy in the works of Tan et al [53] and Meier et al [51] highlights a trend in TSG literature where energy consumption is represented through substitute terms. This makes the use of such research to evaluate process sustainability difficult.

2.3.3 Dry Twin Screw Granulation

A recent, novel advancement in the field of Twin Screw Granulation was developed by the University of Mississippi. This development is outlined in a patent [54] and the works of Kallakunta et al [55] and Ye et al [56]. The technique involves the Dry Twin Screw Granulation of a pharmaceutical formulation

containing an API component and a carrier component which is capable of undergoing melting or glass transition. The process begins with the powder mix being heated as it passes through the barrel. However, care is taken to ensure the barrel temperature is below the melting or glass transition temperature of the components so no agglomeration occurs in this stage. As the mixture traverses the kneading block, the stress and energy input on the powder by the kneading elements provides sufficient energy for the carrier component to undergo melting or glass transition. The melting or glass transition process converts the carrier component into a sticky, viscous phase and allows it to function as binder which facilitates granulation in this region. Magnesium Stearate is typically added to the formulation, where it acts as a lubricant and prevents excessive grinding in the kneading block [56]. Existing literature highlights the importance of the carrier material (example evaluated carriers include Hydroxypropyl Cellulose and Ethyl Cellulose), with carrier materials that plastically deform more easily and have a better binding capacity resulting in higher yields at lower compositions. While similar to melt granulation, this technology uses far lower barrel temperatures and results in less heat degradation of sensitive API components [55,56]. Dry Twin Screw Granulation is highly novel and offers a potential rival to Roller Compaction for the dry granulation of amorphous powders.

Existing research into this new technique has mainly focused on investigating potential thermal degradation of API during the process and evaluating the performance of the produced granules during tabletting. Therefore, information on the effect of key process parameters on the granulation mechanism and key granule attributes is sparse. However, there is limited information on the effect of screw configuration, screw speed and throughput on yield and granule size.

Since this dry granulation process is driven by the kneading blocks, the screw configuration was shown to have a strong impact on the process yield. For instance, the presence of more kneading blocks was found to increase the granular yield. This was attributed to the increased shear facilitating better binder distribution and a more pronounced melting or glass transition of the carrier material. The location of the kneading block was also found to be significant because granules formed in the kneading blocks underwent crushing in the conveying elements afterwards leading to the formation of fines. Therefore, it was beneficial to place the kneading blocks nearer to the exit to mitigate this breakage and increase granular yield [55]. Meanwhile, Ye et al [56] states that the percentage of mid-sized granules decreases as the number of kneading blocks is increased due to increased breakage of existing granules as they pass through them. If the granule yield had been defined as this mid-sized granule percentage then it would have led to yield decreasing as the number of kneading blocks is increased in contrast to Kallakunta et al [55]. This highlights how the effect of process parameters on granule yield can change depending on the size classification of the yield faction.

Meanwhile, screw speed was found to decrease the granule yield. This was attributed to the reduced residence time at high screw speeds resulting in the powder passing through the kneading block quicker

and allowing less time for granulation to occur [55,56]. On the other hand, increasing throughput increased yield due to the higher compaction stresses that exist at higher barrel fill levels [55]. This is supported by the work of Ye et al [56] who similarly found that the fine content decreased with increasing barrel fill level due to more particle interactions leading to more agglomeration. Higher barrel temperatures were also found to result in a higher yield due to formation of stronger and more numerous sinter bridges at high temperatures [56].

2.4 Fluidised Bed Granulation

A Fluidised Bed Granulator is typically a conical shaped batch granulator as illustrated in Figure 1.3. Powder is first placed inside of the fluidisation chamber. Then a heated airflow is introduced into the chamber through a distributor plate at the bottom. This air flows up through the vessel, fluidizing the powder as it moves upwards and exits through a fine filter at the top. This filter allows the air to leave the vessel while containing the powder inside. Liquid binder meanwhile is introduced into the chamber through a spray system which initiates the wet granulation process. The heated nature of the airflow means that granulation and drying occurs in tandem with each other. This is a key differentiation from the HSG and TSG where granulation and drying are separate processing steps. As with the HSG and the TSG, this section will present the relevant regime maps and energy consumption literature that is associated with the Fluidised Bed technology.

2.4.1 Fluidised Bed Granulation Regime Map

The first regime map for Fluidised Bed Granulation was proposed by Walker et al [57], who modified the Iveson and Litster [30] High Shear Granulation Regime Map to fit experimental data from Fluidised Bed Granulation. Then a second regime map for Fluidised Bed granulation was proposed by Boerefijn et al [58] and it used the superficial gas velocity and the binder spray flux to define an ideal operation zone for good granulation and coating. However, the most relevant regime maps to consider in this thesis are those produced by Palzer [23] and Aviles-Aviles et al [59] which are shown by Figure 2.13 and Figure 2.14 respectively. This is because these regime maps for Fluidised Bed Granulation were produced through experiments on amorphous powders and involve the concept of Glass Transition Temperature. Both maps use product temperature and the system liquid content to describe process behaviour. The liquid content of the system is described as the dry matter % (with lower dry matter percentages representing higher moisture content) by Palzer [23] and water activity by Aviles-Aviles et al [59]. In both cases, three key regions are identified. The first is the zone labelled collapse of the powder bed [23] or liquid [59] which occurs at high temperatures and high water activity's/low dry matter percentages. In this zone the liquid content of the system is too high, and excessive agglomeration starts to occur in the powder bed leading to the formation of caked lumps and the defluidisation (collapse) of the bed. Higher liquid contents also decrease the Glass Transition

Temperature of the bed as the water acts as a plasticizer. This means lower bed temperatures are needed for Glass Transition to occur which increases the stickiness of the powder and promotes uncontrolled agglomeration leading to bed collapse. Consequently, the temperature boundary at which bed collapse occurs decreases as liquid content increases in Figure 2.13 and Figure 2.14. The middle zone represents the active zone for granulation and is contained between the Glass Transition Temperature and the collapse temperature in Figure 2.13 or sticky point temperature in Figure 2.14. In this zone, the powder particle surface is viscous enough for agglomeration to occur. The final zone is the product shelf stable region in Figure 2.13 or glassy region in Figure 2.14. This occurs at low moisture contents and low temperatures. Under these conditions, the powder is surface dry and no granule growth can occur. As indicated by the cyclic pathways highlighted in Figure 2.13 and Figure 2.14, the ideal process for an amorphous particle undergoing Fluidised Bed Granulation first involves contact between the particle and a water droplet. This increases the particle moisture content which places it within the granulation zone and the high moisture content acts to decrease material T_g making the material more likely to undergo glass transition. This produces a sticky, surface wet particle which is capable of undergoing growth via coalescence. Over time, the drying action of the FBG causes the moisture content to decrease and therefore the material T_g to increase. This brings the granule back into the glassy/shelf stable zone where it begins the cycle once again. The idea behind this constant wetting and drying cycle is to facilitate growth while ensuring the granule bed does not become overwet and collapse. While the regime maps presented in Figure 2.13 and Figure 2.14 are very useful in understanding the process mechanism, they do not directly utilize T_g as a parameter on either axis. This means that they can only be applied to the specific powders used to produce them, which is Maltodextrin DE12 [59] and Glucose syrup DE21 [23] and therefore limits their usefulness when applied to the granulation of other amorphous powders.

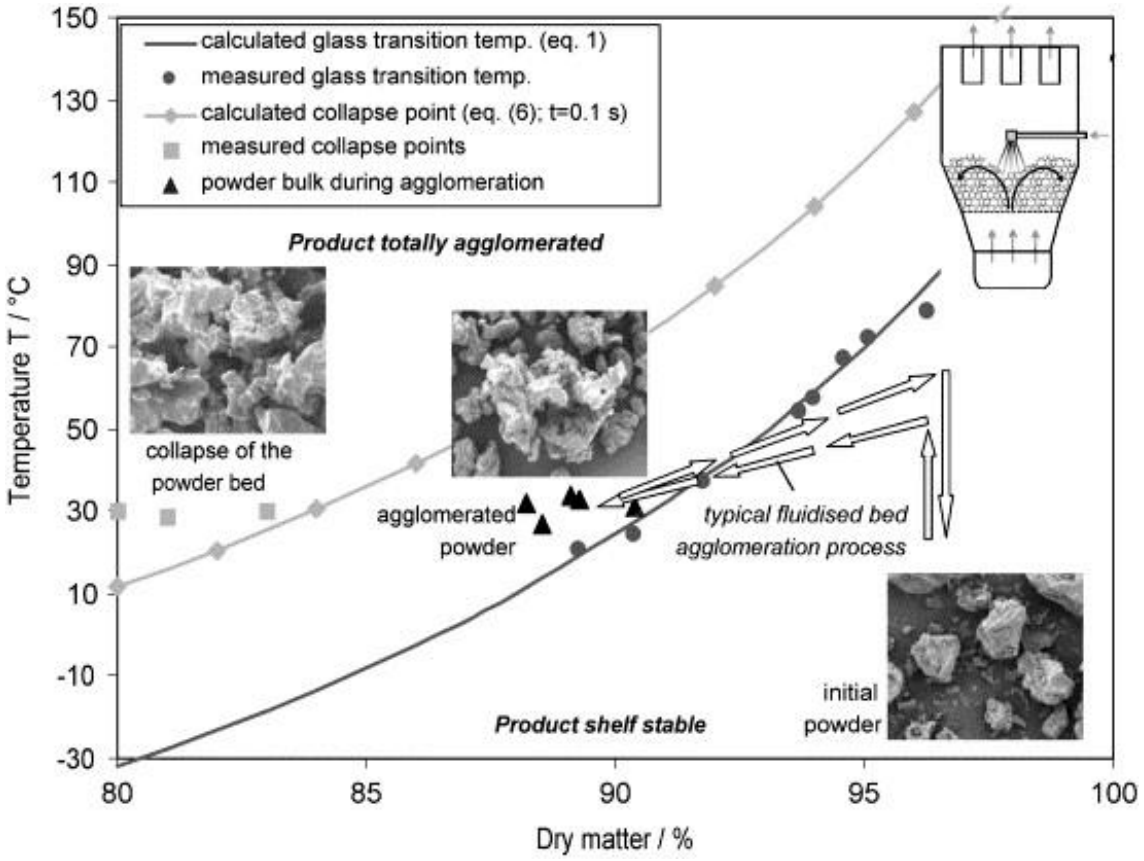

Figure 2.13: Fluidised Bed Granulation Regime Map for amorphous DE21 Glucose Syrup which is based on the system temperature and dry matter percentage in the mix. Lower dry matter percentages represent higher moisture contents [23].

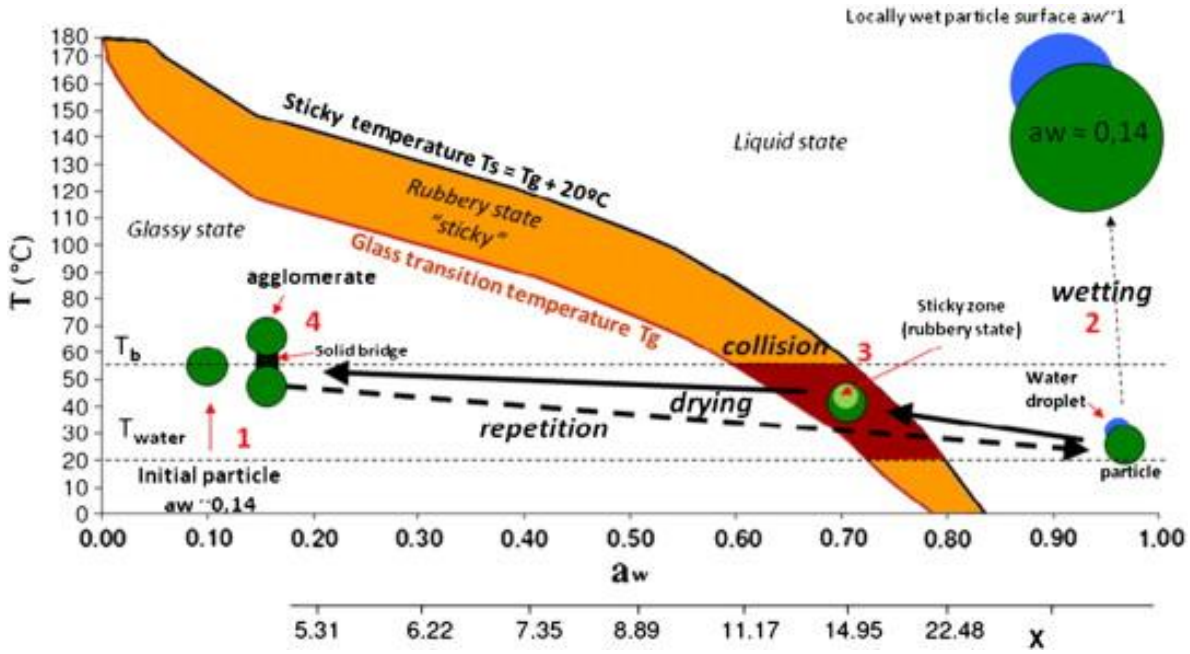

Figure 2.14: Fluidised Bed Granulation Regime Map for Maltodextrin DE12 based on the system temperature and water activity of the particles. Higher water activities represent higher moisture contents. Granulation occurs in the highlighted orange zone where the system temperature is below the sticky temperature but above the glass transition temperature [59].

2.4.2 Sustainability in Fluidised Bed Granulation

Existing literature for the Fluidised Bed Granulator investigating power consumption currently focuses on ways to reduce the energy demand on the process. For instance, Mielke et al [60] found that the energy consumption of the process could be reduced by temporally separating the granulation and drying step. First a benchmark experiment was carried out with a set spray rate and set processing time. A series of experiments were then carried out where spray rate was increased which reduced the time for liquid addition and therefore the duration in which active granulation occurs. The remainder of the processing time (compared to the benchmark experiment) was used purely for drying (no liquid sprayed in). The powder bed during this drying step was evaluated in both the fluidised or packed state. The separation of the granulation and drying stages reduced the energy required to produce good granules of a fixed moisture content considerably. Meanwhile, Takasaki et al [61] investigated the use of moisture absorbing materials during FBG to reduce the drying requirement and lower energy consumption. Literature has also investigated modifying equipment components such as nozzles to reduce the energy consumption of the process [62].

2.5 Roller Compaction

Roller Compaction describes a dry granulation mechanism which is driven by the application of high compressive pressures onto primary powder particles. These pressures are sufficient to bond the powder particles to form a ribbon. This compressive stage which forms the ribbon can be broken down into 4 phenomena which include particle rearrangement, deformation (initially elastic and then plastic), fracture and interlocking. The first stage is particle rearrangement which occurs as the powder particles are forced through a constricting volume in the feeding zone and into the rollers. This reduces the amount of space available for the particles to occupy causing them to rearrange themselves by moving closer together. The most important parameters for the particle rearrangement stage are the particle shape and size. The compaction pressure acting on the powder increases as particles moves closer to and through the rollers. This increase in the applied pressure causes deformation to occur. The deformation will be elastic initially but will become plastic as the load is increased. This elastic and plastic deformation increases the contact area between particles, which alongside the decrease in particle distance during compression, results in the development of large Van der Waal forces of attraction. Furthermore, this high applied pressure can result in particle breakage and fragmentation. This fragmentation generates new surfaces and increases the total contact area which further increases the Van der Waals forces of attraction. The fragments produced can also mechanically interlock together to further increase the strength of the compact. The ribbon produced by this process is then reduced in size to flakes by a crusher. These flakes then enter a milling process to form the product granules [63]. This section will introduce the existing Roller Compaction regime map. Unfortunately, no literature

could be found which evaluated the energy consumption in the granulator so that section is absent from this literature review.

2.5.1 Roller Compaction Regime Map

Despite being a dry granulation process, the impact of water must be considered on the Roller Compaction process when granulating amorphous powders. This is because amorphous powders absorb moisture from their environment. These varying moisture contents have been shown to alter the powder compaction properties and impact the Roller Compaction process. For example, Osborne et al [64] found that the ribbon strength increased with moisture content and that bonding mechanism changed as well depending on compaction pressure and moisture content. These changes were linked to the parameter $T - T_g$, with higher compaction pressures resulted in higher ribbon temperatures while higher moisture contents resulted in lower T_g values. Meanwhile, Omar et al [65] discussed the importance of conditioning amorphous powders under the same environment prior to Roller Compaction, to eliminate the effect of moisture content from experimental results. Increased moisture contents can also lead to severe process issues such as flowability and caking issues in the feeder [64] and rolls [66] when Roller Compacting amorphous powders. Therefore, despite being a dry granulation process, moisture content is a key variable to consider when determining the behaviour of amorphous powder in the Roller Compactor.

Osborne [24] and Fries et al [67] presented the only regime map for Roller Compaction which describes different bonding regimes through the $T_g - T$ parameter and compaction stress as shown by Figure 2.15. This inclusion of the T_g parameter which accounts for the material moisture content and lattice structure makes it particularly relevant to the granulation of amorphous powders. This map highlights the dominant bonding mechanism depending on the process conditions and uses the ribbon porosity (Φ) as an indicator to differentiate between the mechanisms. In the powder regime, the compaction stress is too low and the material too glassy to result in bonding to form a compact. However, if the compaction stress is increased further then the Van der Waals forces become significant enough to form a very porous ribbon with a porosity between 20 – 50 %. Increasing the normal stress further can result in two possibilities depending on the value of $T_g - T$. The first is when $T_g - T$ is low, where the material will consequently display a high tendency for rubbery behaviour. The application of increased stress onto the material in this state will cause it to transition into a viscous, sticky paste. In this region no ribbon as produced and roller compaction cannot occur. The second eventuality is when the value of $T_g - T$ is high and therefore glass transition becomes unlikely. At this condition, the material will display micro – sintering. The effect of this micro-sintering alongside the higher pressure will form a low porosity ribbon between 5 – 20%. Increasing the normal stress higher than this induces a significant amount of sinter flow in the material which fills in any voids to produce a very high-density sintered ribbon with a porosity less than 5%. The extent of sintering at these conditions is such that individual particles

become indistinguishable from each other. While this map is considered important as it is the only existing regime map for Roller Compaction, it has been criticised in literature for the lack of clarity in the specific process conditions used to produce it, as well as the number and identity of the materials used in its development [48].

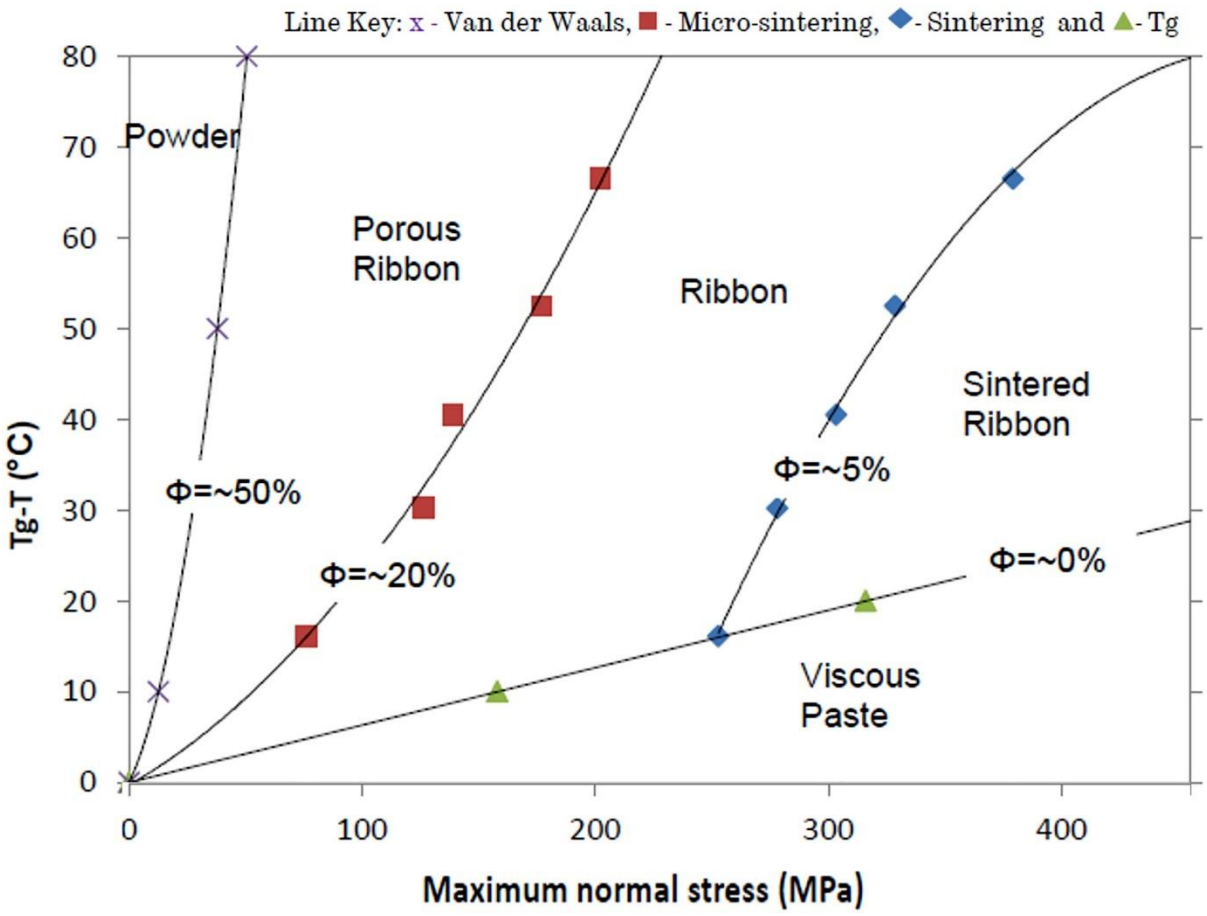

Figure 2.15: Roller Compaction Regime Map for amorphous powders based on T_g – T and the maximum normal stress. The different regimes are based on the ribbon porosity (Φ) which is correlated with 3 key modes of bonding which include Van der Waals forces, Micro-sintering, Sintering and T_g (Glass Transition induced viscous flow) [67].

2.6 Caking of Amorphous Powders

One of the biggest challenges with processing amorphous powders is their tendency to cake. This describes the scenario where uncontrolled agglomeration occurs and leads to the formation of large lumps called cake which reduces the granular yield and material efficiency of a process. It also results in material sticking to granulator internals which can lead to jamming and processing failure in serious cases. For amorphous material, this caking phenomenon can be very hard to prevent because it can be initiated by the Glass Transition process which results in the powder becoming too sticky and viscous. This increased stickiness then promotes uncontrolled agglomeration leading to caking. Caking can

occur within the granulation process and also during storage. This section will outline the existing literature studying the caking of amorphous powders in both granulation and storage environments.

2.6.1 Glass Transition Driven Caking in Granulation

Literature investigating the caking phenomenon during granulation is most extensive for the Fluidised Bed Granulator. This literature looks at the conditions that result in caking and how it can be avoided inside the FBG. For example, the work highlighted in Figure 2.13 and Figure 2.14 identifies the moisture and temperature constraints at which the collapse of the powder bed due to caking occurs. Compared to the Fluidised Bed Granulator, there is limited literature discussing the T_g related caking within Roller Compaction. The only study found was that of Mahmah et al [68] which evaluated the effect of compaction stress on roller caking across a wide range of powders which included Maltodextrin DE6. Mahmah et al [68] found that ribbon temperature increased with compaction stress. If the ribbon temperature increased to a point higher than the material T_g ($T > T_g$), then there would be a high degree of adhesion between the ribbon and roller surface leading to caking. For the Maltodextrin DE6 used in that study, this occurred at stresses of 122 MPa which caused a ribbon temperature of 80°C. Unfortunately, the T_g of this DE6 powder was not provided by the study.

There is a complete lack of literature discussing the Glass Transition driven caking process for High Shear and Twin Screw Granulation. However, there is limited available research evaluating the (non-glass transition driven) caking process for non-amorphous powders which can give insight into the caking phenomenon in these granulators. In the High Shear Granulator, Briens and Logan [69] highlighted the increased build-up of a caked layer at high impeller speeds. This is caused by the significant centrifugal forces generated at high impeller speeds which drives material to the bowl's edge and promotes material build up. As a result, a caked layer would form which affected the flow pattern in the granulator and hindered effective granulation. In the Twin Screw Granulator, Saleh et al [70] showed the importance of screw configuration on (non-glass transition driven) caking of crystalline Lactose and MCC. For instance, the inclusion of more kneading elements resulted in more caking on the barrel. This was attributed to the increased number of kneading elements causing the granules to experience more consolidation, which squeezed more liquid to the granule surface, making the granule surface stickier which promoted caking. Meanwhile, the use of a conveying element only configuration (no kneading elements utilised) meant that the use of higher binder viscosity's during granulation led to an increased likelihood of caking. This is because without the aggressive mixing effect of the kneading elements there would only be a limited spreading of high viscous binders throughout the powder mass. The limited spreading caused the build-up of binder at localised points causing caking.

2.6.2 Glass Transition Driven Caking During Storage

During storage, amorphous powders absorb moisture if stored in high humidity environments. This causes their Glass Transition Temperature to decrease. If it decreases below the storage temperature, then the material undergoes glass transition, which initiates the viscous flow of material between particles that forms solid bridges and leads to lumping over time. This lumping alters the particle attributes, making them unsuitable for use. The tendency for caking to occur during storage is often represented by the T - T_g parameter with T reflecting the storage temperature and T_g reflecting the storage humidity [71,72]. Current literature focuses on preventing the Glass Transition driven caking during storage through the use of packaging or anti-caking agents. For instance, both Zang et al [73] and Kumar and Mishra [74] evaluated different packaging materials and found that aluminium laminated polyethylene pouches provided the best protection to powders during storage. This is attributed to it forming an excellent barrier against moisture. This helps maintain a low moisture environment that limits any moisture absorption from the powder. Meanwhile, Fu et al [75] and Nurhadi and Roos [76] established how anti-caking agents like calcium silicate and calcium stearate prevent caking by reducing the hygroscopic activity of the bulk powder. These anticaking agents work by forming a thin hydrophobic coating on the surface of hydrophilic amorphous particles. This coating repels moisture and hinders amorphous powder from absorbing moisture. Other anti-caking agents work by forming physical barriers to prevent bridging or outcompeting other powders for moisture [77].

2.7 Summary and Knowledge Gaps

There are numerous gaps in the existing literature that have been identified by this literature review. The first is in the lack of research into the energy consumption of the granulation processes with the aim of evaluating process sustainability. For example, with Roller Compaction no literature investigating the energy usage of the process could be identified. Where there is research, for example in the HSG and TSG, it focuses on the use of energy consumption as a tool for process control rather than as way to evaluate sustainability. The data from these studies cannot be used to evaluate sustainability either because they often represent this energy consumption through auxillary terms or as a percentage. The resulting lack of data in terms of direct energy usage then makes comparison efforts difficult. Additionally, many of these studies approximate the energy consumption using the impeller or screw torque. While there is a correlation between energy consumption and torque, the torque does not represent the energy consumed by the unit as a whole and therefore it is not a fair variable to use to investigate energy consumption. Most importantly, there is no existing literature comparing the energy consumption of different granulation technologies. Neither are there studies comparing the sustainability of these granulation technologies based on material or time efficiency. This will be addressed in Chapter 4 of this thesis.

The second research gap is the unsuitability of the existing Wet Granulation regime maps for the granulation of amorphous powders. For instance, it is clear that the current regime maps for the High Shear Granulator and Twin Screw Granulator were produced through experiments on heat insensitive powders. Amorphous powders display several key differences to heat insensitive powders. The major difference is in the Glass Transition Temperature which can dominate process behaviour through phenomena like caking and is not accounted for by these maps. While the regime maps for Fluidised Bed Granulation considers the Glass Transition phenomenon, it has limited use outside of the same materials used to produce it. This is because these map do not include the T_g parameter as a variable on either axis and therefore the domain boundaries shown are only valid for the specific material used to develop them. This research gap will be addressed in Chapter 5 through the development of a regime map for the High Shear Wet Granulation of amorphous powders which includes the T_g parameter. As highlighted by Section 2.6.1, there is no existing literature investigating the T_g driven caking phenomenon in the High Shear Granulator. This will be addressed by focusing the development of the regime map on caking and identifying an operable region for controlled agglomeration.

Thirdly as highlighted by Section 2.6.2, current research into preventing caking during storage focuses on the use of plastic and metal packaging or anti-caking agents. This is not ideal as the food industry seeks to minimise packaging use and simplify recipes by removing ingredients. Granulation offers significant opportunities to restructure particulate systems to reduce their sensitivity to moisture. Therefore, it is surprising that no existing literature has investigated the roll that granulation can play in preventing caking during storage. Chapter 6 will address this by presenting a novel, multi-step granulation pathway to produce multi-component, layered granules that are more resistant to humidity based caking.

The final research gap identified in this literature review is the under developed nature of Dry Twin Screw Granulation. Dry Twin Screw Granulation is a process that is very attractive to the food industry as a competitor to Roller Compaction because it has the potential to produce granule structures more suited for food applications. Despite this, the process understanding of Dry Twin Screw Granulation is immature and basic. This is because research into this new technique has been led by the pharmaceutical industry which has primarily focused on evaluating thermal degradation of the API during the granulation process and tablet properties arising from the product granules [55,78]. This limited knowledge of process mechanics is highlighted by the fact that there is no regime map for Dry Twin Screw Granulation which is a hallmark of good process understanding. There is also an absence of information outlining the impact of process parameters on key granule attributes, especially when applied to food specific powders. This research gap will be address in Chapter 7.

3 Materials and Methods

3.1 Materials

3.1.1 Maltodextrin

Maltodextrin was the primary material used in this work. In the food industry, Maltodextrins are commonly added as a bulking and carrier agent due to their cheap nature and ability to significantly alter product texture and viscosity. Meanwhile in the pharmaceutical industry it is used as a stabilizer and thickener in cosmetic products and as a cheap filler in oral dosage forms. This multi-industry functionality has seen Maltodextrins establish a large global market size of $3.15 billion, which is only projected to increase, with current projections putting it at a market size of $4.5 billion by 2029 [79]. This makes the knowledge development of key processing mechanisms, such as granulation, for Maltodextrins important.

Maltodextrins are also very good model materials to represent amorphous food powders with different DE grades correlating to other common food powders. For example, DE29 has very similar properties to skimmed milk powder causing it to behave in similar manners. This makes the conclusions of this work not only applicable to Maltodextrin powders but to a wide variety of amorphous food powders.

Five grades of Maltodextrin were sourced from Roquette (France) and are used throughout this thesis. These include Glucidex IT6, IT12, IT21, IT29 and IT47. The IT grade correlates with the DE number of the Maltodextrin. For example, IT6 has a DE number of 6. In this thesis IT6, IT12, IT21, IT29 and IT47 are referred to as DE6, DE12, DE21, DE29 and DE47 as is the norm in literature. The particle size distribution of these powders, as measured by a Camsizer (Retsch,UK), is presented in Table 3.1. As evidenced by Figure 3.1, the raw Maltodextrin particles are irregular shaped with some particles appearing highly spherical while others are extremely elongated. The Maltodextrin powders also display holes of varying sizes on the particle surface indicating a porous nature.

Table 3.1: Particle size distribution of the raw Maltodextrins used in this study

	Particle Size (µm)				
	DE6	DE12	DE21	DE29	DE47
d10	144 ± 9	153 ±14	141 ± 20	143 ± 17	55 ± 2
d50	292 ± 21	271 ± 20	270 ± 15	255 ± 19	153 ± 1
d90	651 ± 30	569 ± 37	547 ± 25	455 ± 19	248 ± 9

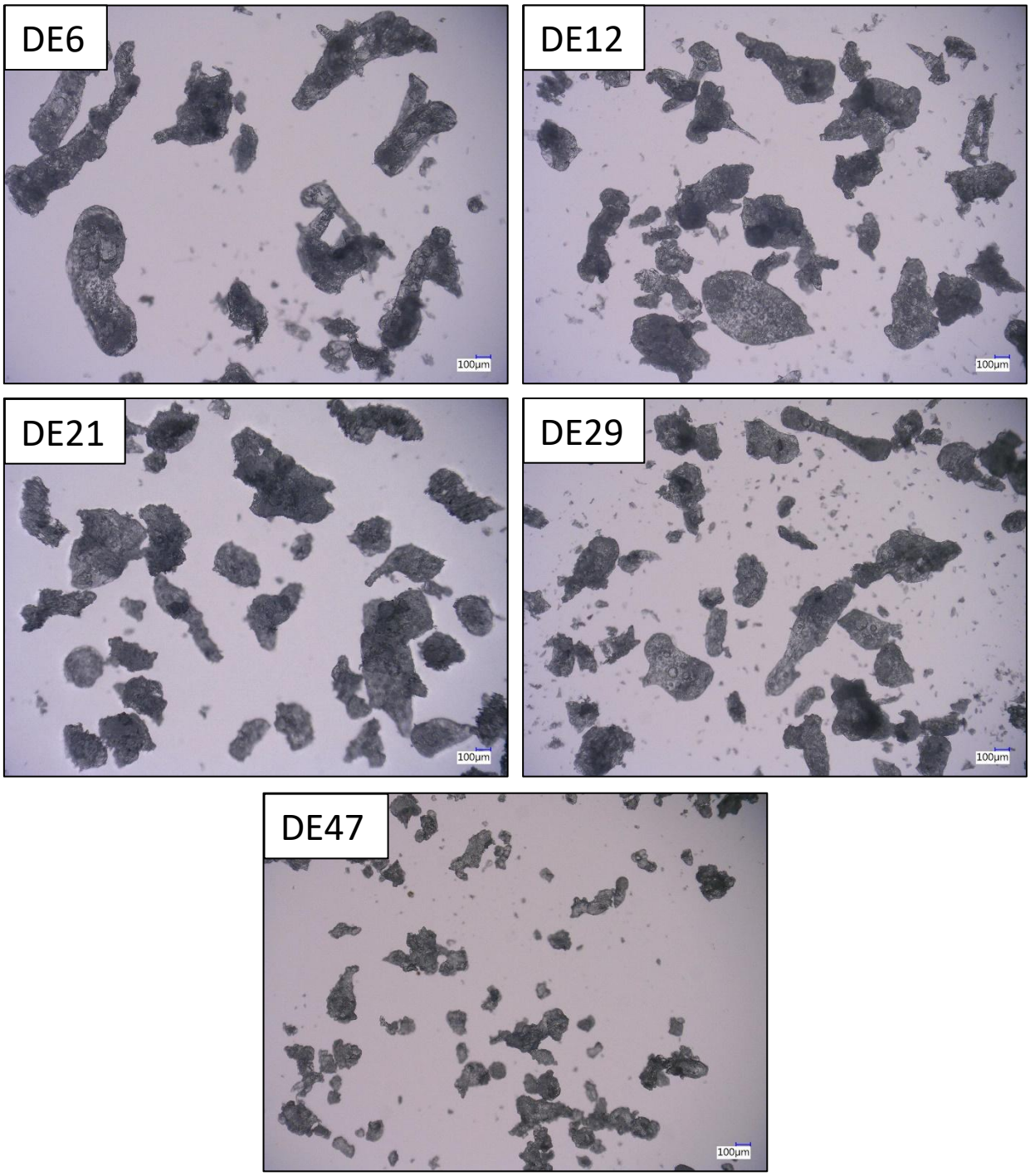

Figure 3.1: The raw Maltodextrin powders used in this study as observed under a microscope

3.1.2 Coffee

Instant Coffee was also used as a granulation powder in Chapter 6 of this thesis. Coffee is one of the most well recognized food powders, having applications in the beverage, baking, confectionary, dairy and nutraceutical industries. The Instant Coffee used in this thesis was supplied by Nestle Research (Switzerland). The particle size distribution of the Instant Coffee, as measured by a Camsizer

(Retsch,UK), is shown in Table 3.2. As shown by Figure 3.2, this powder appears as small, spherical particles which have adhered together to form aggregates.

Table 3.2: Particle size distribution of the raw Instant Coffee used in this study

	Particle Size (µm)		
	d10	**d50**	**d90**
Instant Coffee	33 ± 2	126 ± 7	287 ± 46

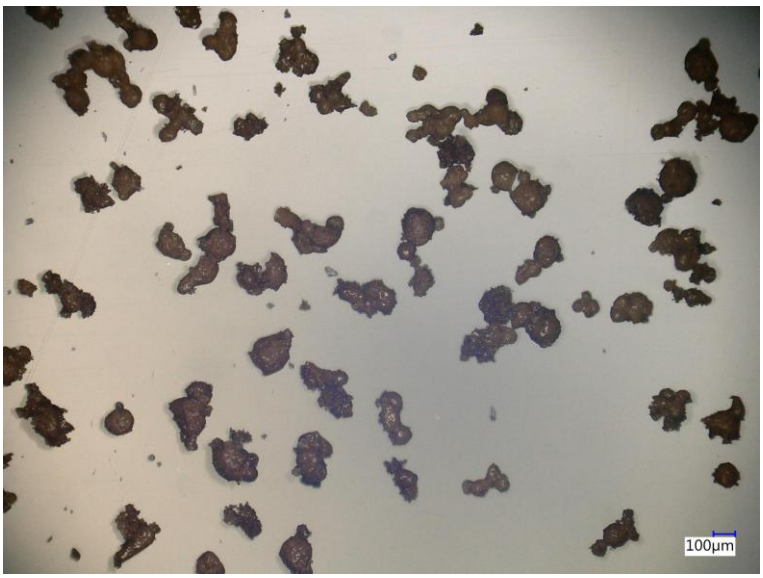

Figure 3.2: The raw Instant Coffee powder used in this study as observed under a microscope

3.2 Methods

3.2.1 High Shear Granulator

The High Shear Granulator used in this thesis was an Eirich EL1 High Shear Granulator (Eirich GmbH, Germany). This granulator is displayed visually in Figure 3.3 and schematically in Figure 3.4. The granulator consists of a spinning bowl. This bowl rotates in a clockwise motion at either 85 rpm (Slow Mode) or 170 rpm (Fast Mode). Inside the granulator there is a top mounted pin impeller which is located eccentrically to the bowl centre. The impeller consists of a 8 cm disk shaped base which has six blades equally distributed around the disk. On each of these blades there is a perpendicular small pin. This impeller can rotate at speeds between 300 rpm and 7200 rpm. There are two operating modes for the granulator: Co-Current or Counter Current. In Co-Current Mode, the impeller rotates clockwise while the bowl also rotates clockwise. Meanwhile, in Counter Current Mode, the impeller rotates anticlockwise while the bowl rotates clockwise. The changing direction in which the impeller can be rotated is highlighted by the coloured arrows shown in the top view of Figure 3.4. There is also a top

mounted scraper which scrapes any powder or granules that adheres to the bowl sides. The granulator lid possesses a viewing port which is used for the addition of liquid binder and also to observe the process within.

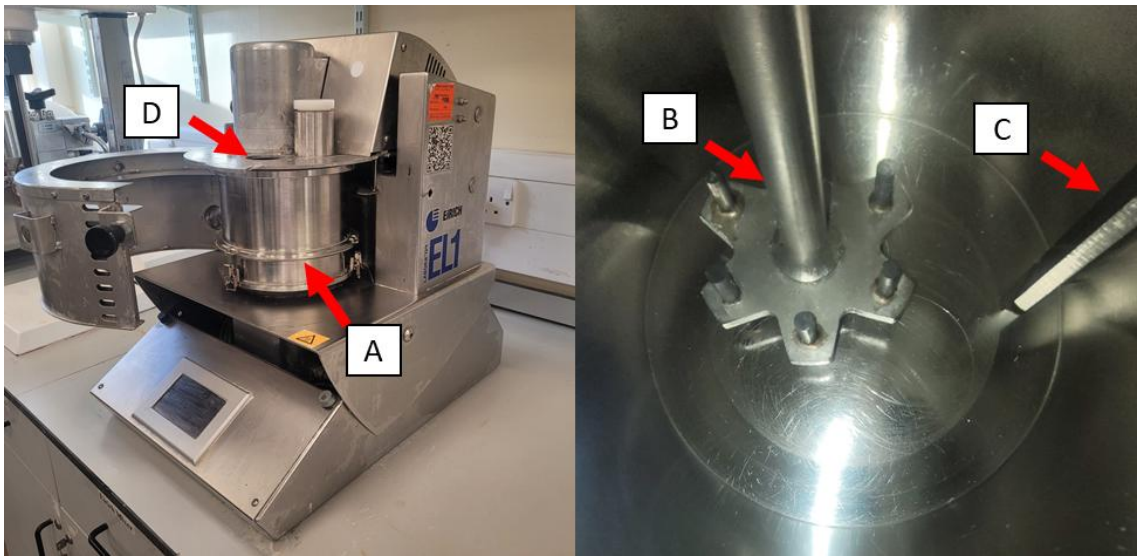

Figure 3.3: Shows an external (left) and internal (right) view of the Eirich EL1 High Shear Granulator used in this study. The granulator consists of a spinning bowl (A) which contains a rotating pin impeller (B) and top mounted scraper (C). There is a viewing port (D) which can be used to observe the process occurring inside the granulator.

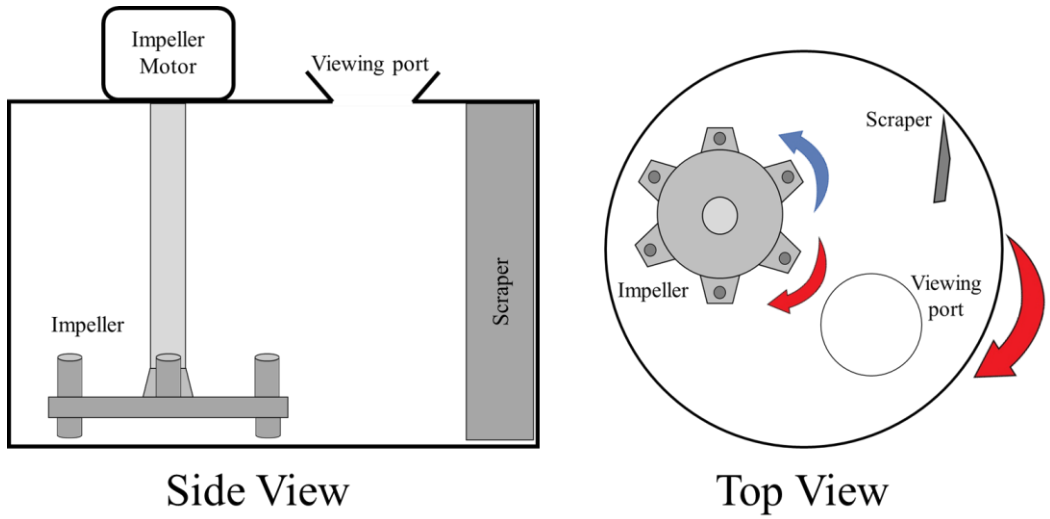

Figure 3.4: Schematic representation of the Eirich EL1 granulator as viewed from the side and from the top. The bowl rotates in a clockwise motion as shown by the large red arrow. The impeller meanwhile can rotate in either a clockwise (small red arrow) or anticlockwise motion (blue arrow).

3.2.2 Twin Screw Granulation

The Twin Screw Granulator used in this study was a ThermoFisher Euro Lab 16 mm Twin Screw (ThermoFisher Scientific, UK). The granulator has a barrel length (L) of 400 mm and a diameter (D) of 16 mm (resulting in a L/D of 25). Incorporated into the TSG system is a loss in weight Twin Screw

Powder Feeder (K-Tron Soder, Switzerland). The Twin Screw Granulator and Twin Screw Feeder are presented visually in Figure 3.5 and schematically in Figure 3.6. The Twin Screw Granulator barrel can be broken down into 6 compartments, each of which can be individually temperature controlled to different set points. The temperature control is achieved by using heating functions in the lower barrel or cooling functions in the upper barrel. The heating function in the lower barrel is provided by inbuilt heating elements which can be used to heat the compartment temperature up to 300 °C. Meanwhile, the cooling function in the upper barrel is created by a regulated flow of cooling water provided by an external IC05C Water Chiller (ICS Cool Energy, UK). The flow of this cooling water is regulated by the Twin Screw Granulator control system to reduce the compartment temperature to the set point. Powder is fed in through a powder inlet chute while the liquid is fed in through the liquid inlet nozzle. The location of this powder and liquid inlet could be changed to be in any of the barrel compartments. For the work presented in this thesis, the powder inlet zone was in Compartment 1 and the liquid inlet zone was in Compartment 2 as presented in Figure 3.5 and Figure 3.6. Two co-rotating 16 mm screws were housed inside the barrel which could be configured with different screw elements. The screw elements available for this work were conveying and kneading elements. The maximum screw conveying speed is 1000 rpm and the maximum torque allowance before the screw motor fails is 12 Nm. The screw tip to barrel wall clearance is 0.2 mm.

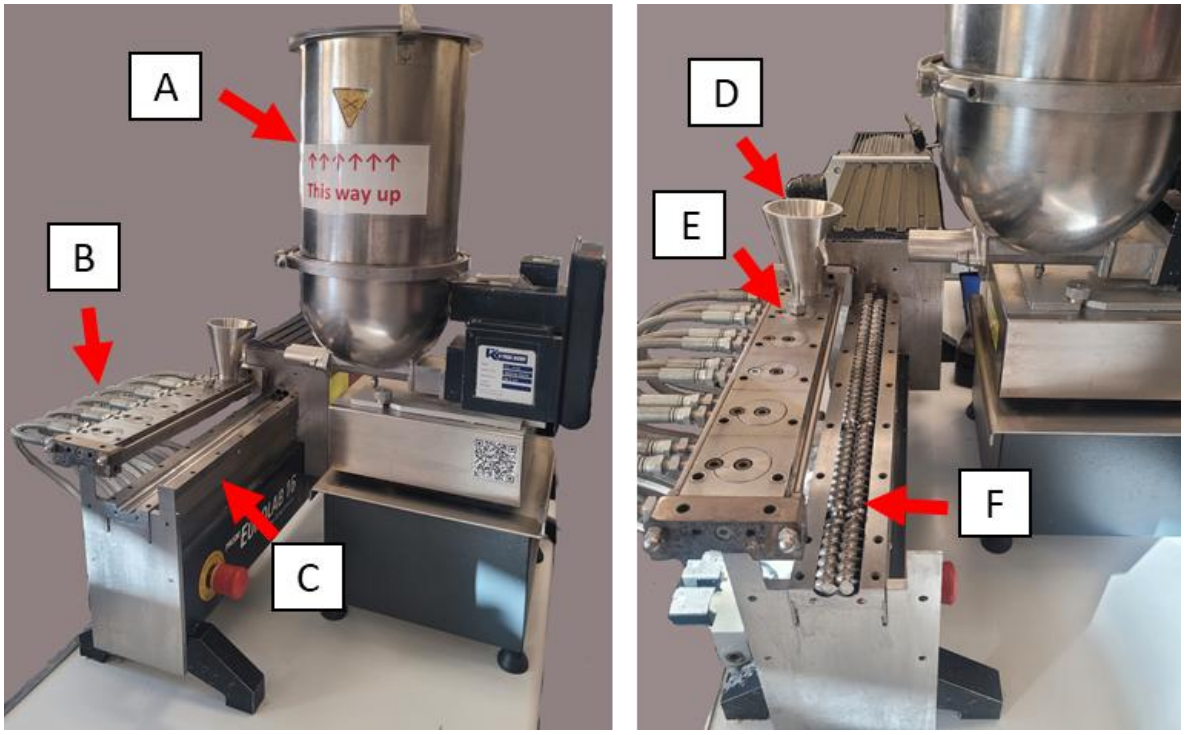

Figure 3.5: Visual depiction of the Twin Screw Granulator used in this thesis without the two screw in (left) and with the two screws in (right). The TSG system composes of a Loss in Weight Twin Screw Powder Feeder (A) and a Twin Screw Granulator which can be split into an Upper Barrel (B) and Lower Barrel (C). The Powder Entry Port (D) and the subsequent Liquid Entry Port (E) are situated on the Upper Barrel. The Screw Configuration (F) is enclosed between the Upper and Lower Barrel.

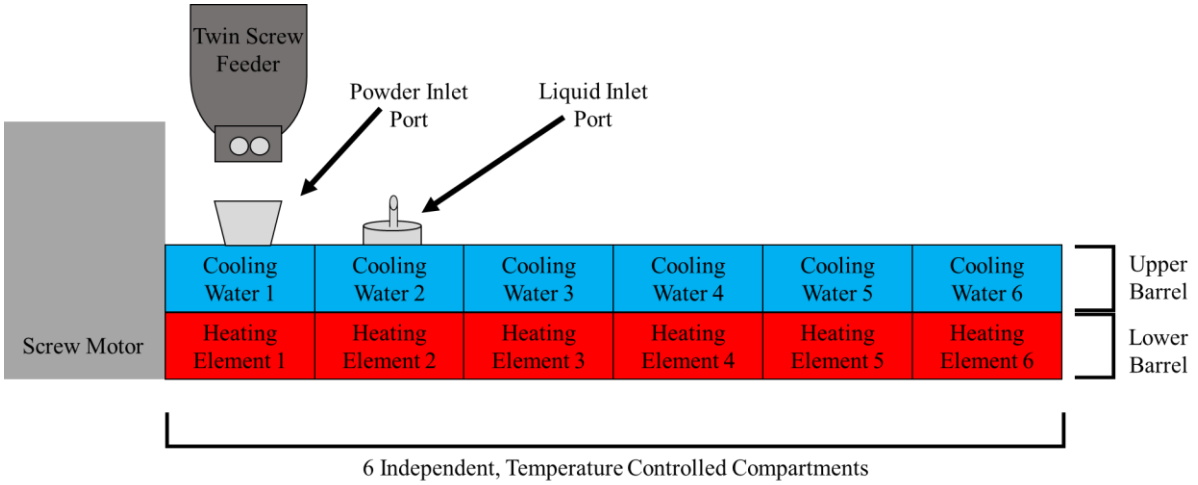

Figure 3.6: Schematic representation of the Twin Screw Granulator. The barrel is composed of an upper and lower half. The lower half contains heating elements which facilitates the heating of the barrel. The upper half contains controlled circulation devices which cool the barrel down to a given setpoint using cooling water from an external chiller. The barrel is also separated into 6 compartments. The temperature of each compartment can be individually controlled.

3.2.3 Fluidised Bed Granulator

The Fluidised Bed Granulator used in this study was a Glatt GPCG3 Fluidised Bed (Glatt, Germany). A visual representation of the granulator is shown in Figure 3.7, while a schematic representation is shown in Figure 3.8. As shown in Figure 3.8, the granulator can be broken down into three main compartments: Lower, Middle and Upper which each houses a critical component of the granulator. The Lower compartment houses the mesh distribution plate with a mesh size of 0.2 mm. It is through this distribution plate that the heated fluidizing air flows into the granulator. The air can be heated up to a temperature of 100°C. The distribution plate ensures an even distribution of air flow through the granulator. The mesh also acts as a physical barrier to stop particles from falling out. Meanwhile, the Middle compartment houses a custom built, side entry spray nozzle. During the granulation process, this nozzle sprays the binder into the chamber using an atomization pressure between 0 – 2 bar. This wets the fluidized powder and initiates the wet granulation process. Finally, the Upper compartment houses a bag filter. The bag filter allows the air to exit the granulator while containing the powder inside the chamber. The active granulation zone is within the lower and middle compartments which have heights of 200 mm and 260 mm respectively.

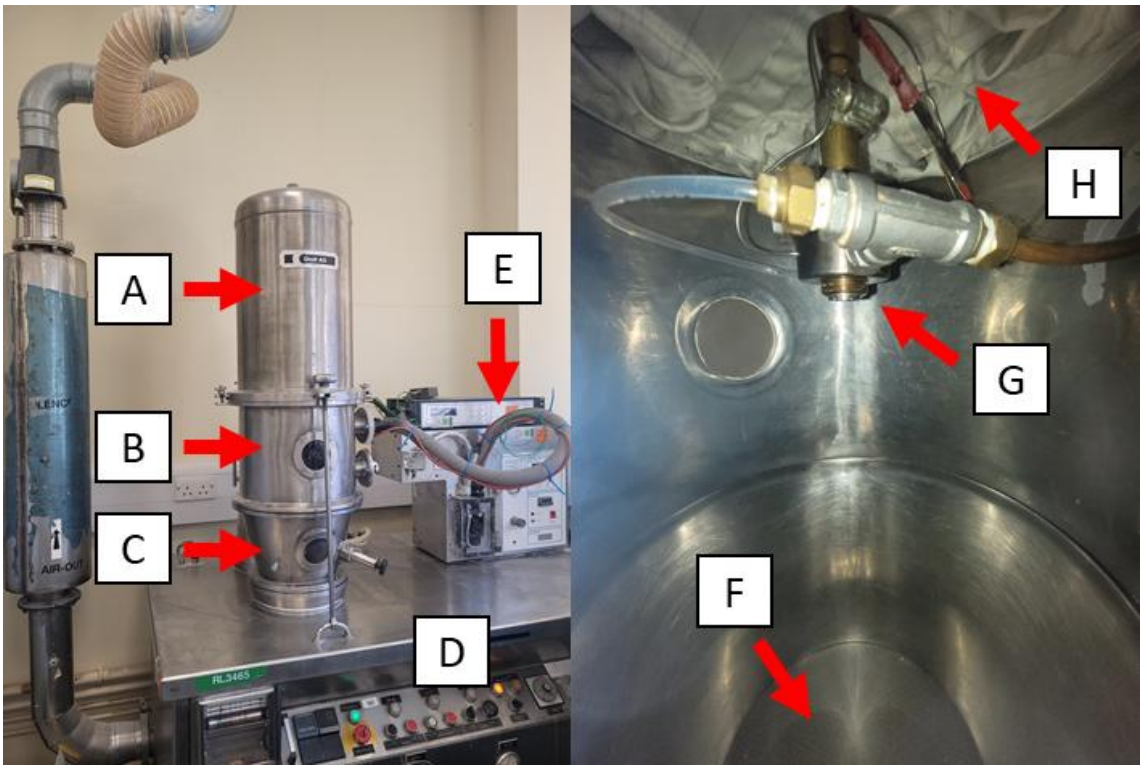

Figure 3.7: Shows the external (left) and internal (right) view of the Glatt GPCG3 Fluidised Bed used in this study. The Fluidised Bed Granulator can be split into an Upper (A), Middle (B) and Lower (C) compartment. Fluidising air is fed in through the Air Generation Unit (D) and binder is fed in using a custom built spray system (E). Inside the granulator, the Lower Compartment houses the Distributor Plate (F), the Middle Compartment houses the Spray Nozzle (G) and the Upper Compartment houses the Bag Filter (H).

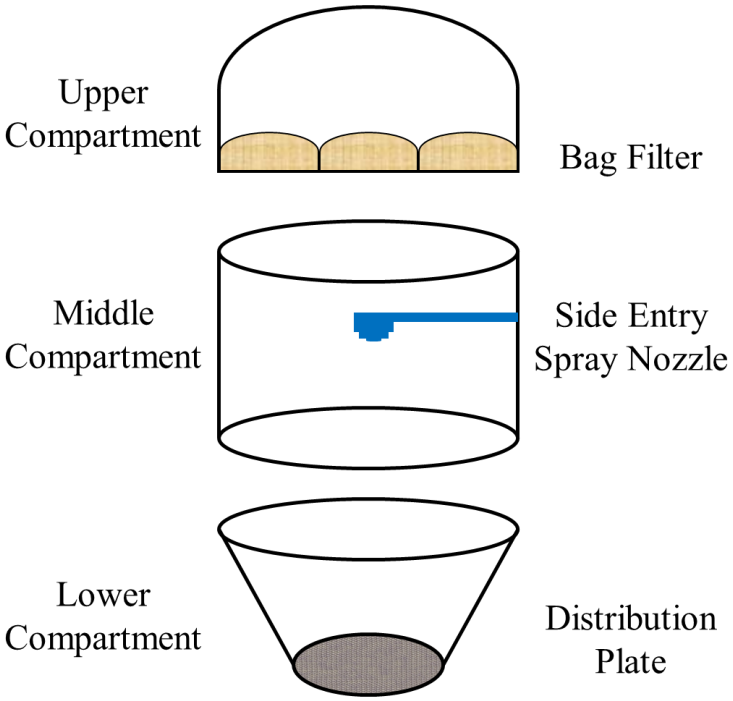

Figure 3.8: Schematic diagram of the Fluidised Bed Granulator showing the three main compartments of the granulator and the key component of each.

3.2.4 Roller Compactor

The Roller Compactor used in this project was an Alexanderwerk WP120 Pharma Roller Compactor (Alexanderwerk AG, Germany). This Roller Compactor is visually shown in Figure 3.9 and schematically shown in Figure 3.10. The Roller Compactor can be broken down into the Feeding, Compaction and Milling Sections. The Feeding Section contains a powder hopper, single screw feeder and a de-aeration unit. Powder is loaded into the feed hopper. Inside the hopper there is an inbuilt impeller which agitates the added powder. The single screw feeder transports material from the hopper to the compaction area. During this transportation, a de-aeration system removes air from the powder to improve the compactability of the powder. The Compaction Section includes the rollers and a flake crusher. The Rollers used in this work have a 12 cm diameter and a 4 cm width with a knurled surface finish. The powder throughput can be controlled in two ways – manual or automatic. In the manual mode, the screw feeder speed is specified and kept constant. In the automatic mode, the roller gap is specified. The screw feeder speed is then automatically changed by the Roller Compactor to keep roll gap constant when other parameters are changed. For example, increasing roller speed would increase the amount of material required to keep a constant roll gap. Therefore, at faster roller speeds, the screw feeder speed would increase to boost throughput to maintain a constant roller gap. In this work the machine was operated in automatic mode. The roller gap determines the resulting ribbon thickness and could be altered between 1 – 4 mm. The hydraulic pressures possible ranged from 18 bar to 230 bar while the possible roller speeds ranged from 3 rpm to 13 rpm. The ribbon produced by compaction between the two rollers was broken into flakes using a 6 bladed flake crusher. These flakes drop vertically under gravity into the milling section. The milling section is composed of two horizontally aligned rotor impact mills. These mills are enclosed by mesh screens. Once the flakes are sufficiently broken down due to impact with the mills, they pass through the mesh screens and out of the product chute as granules.

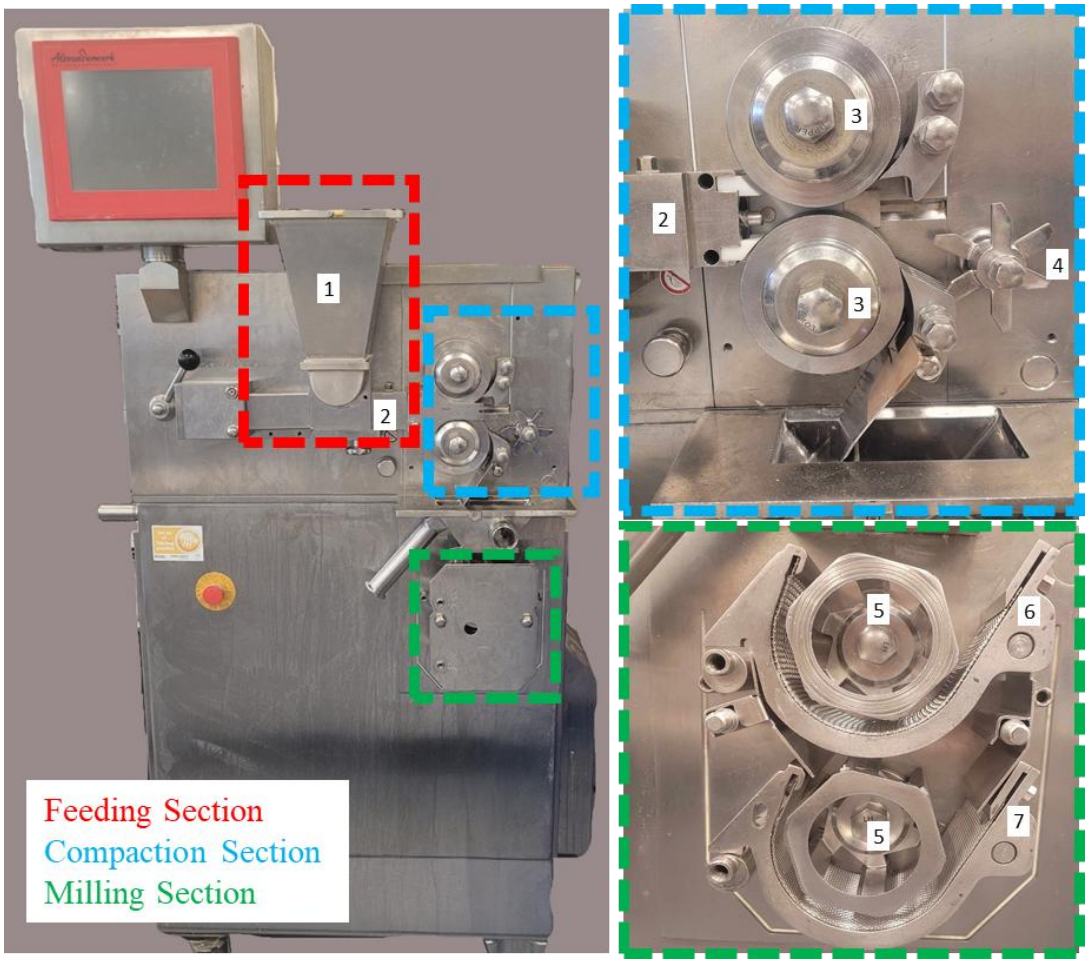

Figure 3.9: Visual depiction of the Roller Compactor highlighting the Feeding Section, Compaction Section and Milling Section. Key components include the Feed Hopper (1) and Screw Feeder (2) in the Feeding Section, Rollers (3) and Flake Crusher (4) in the Compaction Section, and Impact Mills (5) along with the Upper (6) and Lower (7) Mill Screens in the Milling Section.

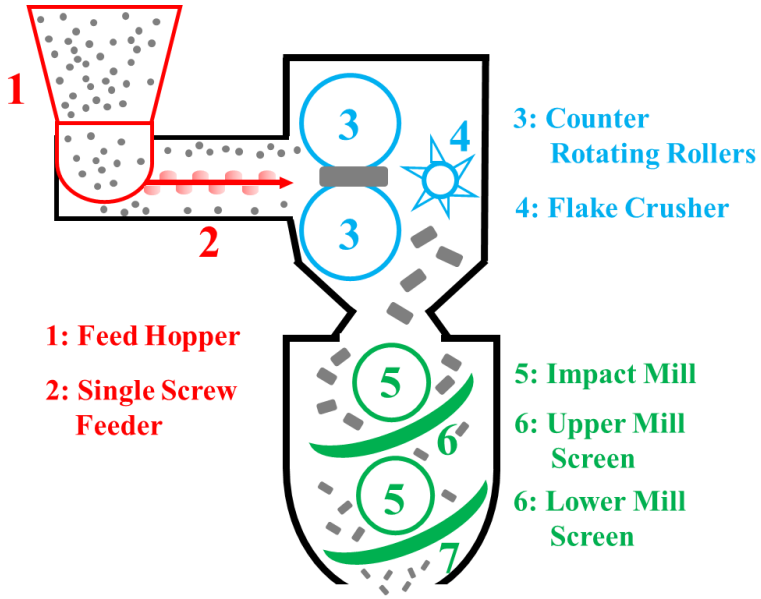

Figure 3.10: Schematic diagram of the Roller Compactor presenting the transition of material (shown in grey) through the Feeding Section, Compaction Section and Milling Section. Key components in the Feeding Section are the feed hopper and single screw feeder, while in the Compaction Section it is the rollers and flake crusher. Finally, in the Milling Section, it is the upper and lower mills.

3.2.5 Sieving

Sieving was used throughout this thesis, primarily, for size characterization. The sieve shaker used was a Retsch Sieve Shaker AS200 (Retsch, UK) as presented in Figure 3.11. Sieving is one of the oldest processes used to categorise a material's particle size distribution. In a sieve shaker, sieves are stacked on top of each other in order of decreasing mesh size (top to bottom). Each sieve has a defined mesh screen which allows particles smaller than the aperture to pass through. At the very bottom, a pan is placed to collect the finest of particles. The sieving process begins with the powder sample being place on the top mesh. The sieve shaker then applies vertical and horizontal vibration to promote the particles to pass through the mesh. For a particle to pass through, it must be smaller than the mesh aperture size. This means that as the particles pass through the sieve stack, they are size categorized by the various mesh screens. After shaking for the set period of time, the particles on each sieve is collected and their mass measured. The particle size of the sample can then be characterized by evaluating the percentage of the total mass that was found between each sieve size interval.

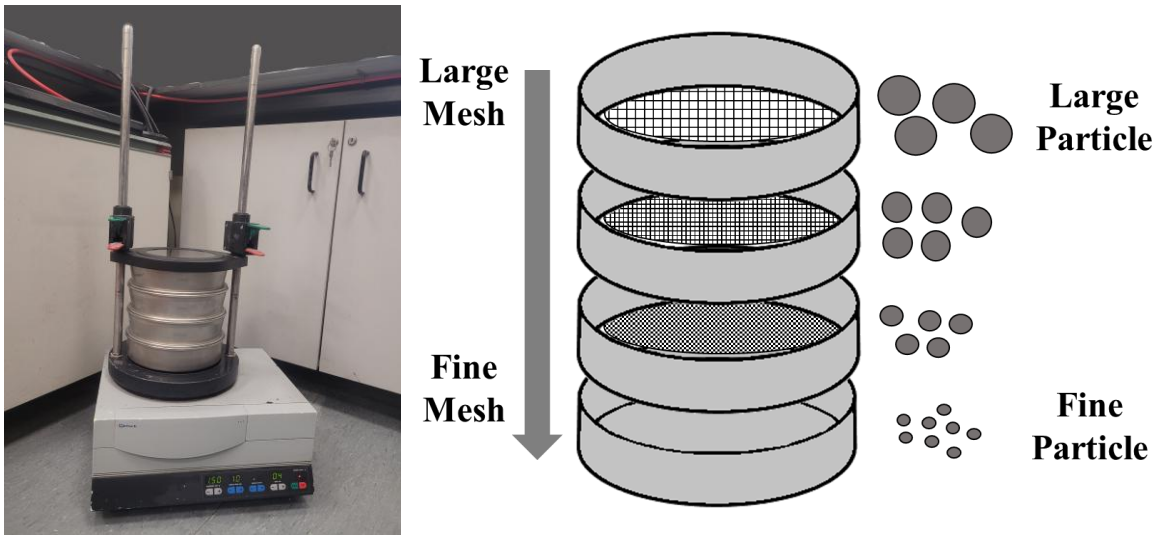

Figure 3.11: The Retsch AS200 sieve shaker used in this thesis (left) with an illustration of the principle behind sieving (right).

A sieve shaker can also be used to evaluate friability. Friability judges the particle's physical weakness. Friability can be evaluated by taking particles of a known size, placing them on a sieve mesh with an aperture size smaller than the particles and then exposing them to high intensity vibrations. This generates strong impact forces which results in breakage and attrition. This causes a reduction in particle size and allows the particles to fall through the mesh. The mass of this reduced faction can be used as an indicator of friability according to Equation 3.1.

$$Friability = \frac{Mass\ of\ Reduced\ Faction}{Total\ Mass} \times 100$$

Equation 3.1

3.2.6 Flowability

A Shear Cell RST – XS.s (Dietmar-Schulze, Germany) was used to classify flowability according to the ffc value as visualized in Figure 3.12 . The test involves filling a shear cell with the particles to be tested (A). A lid is then placed on top of the powder which connects onto the loading rod (B) and two crossbeams (C) during operation. A normal stress is then applied onto the powder bed through the loading rod (B). The two crossbeams (C) are then used to apply incrementally increasing rotational shear stress on the sample. This eventually causes one layer of powder to move against another and the shear stress required for this incipient flow is measured. The shear cell carries out this procedure for a range of normal stresses to evaluate how the shear stress required for incipient flow changes. A plot of these variables produces a line known as the yield locus. Mohr circles are then drawn onto the start and end of the yield locus which determines the major principal plane stress (σ_1) and the unconfined yield strength of the particles (σ_c) as shown in Figure 3.12. The ffc value is then determined as the ratio between the major principal plane stress and the unconfined yield strength of the particles ($ffc = \sigma_1 / \sigma_c$). Based on the ffc value, the particle flowability can be described as in Table 3.3.

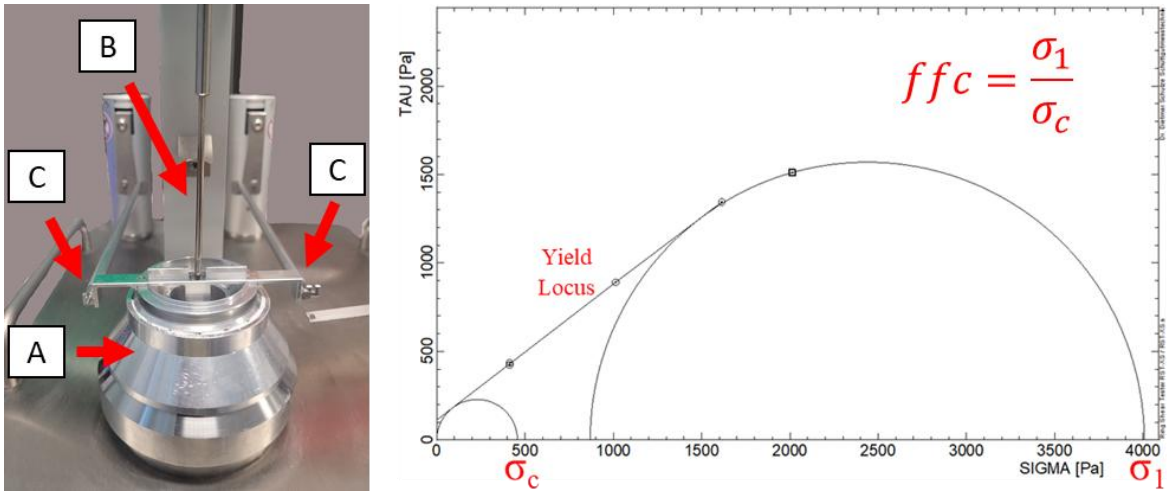

Figure 3.12: The Shear Cell RST – XS.s setup used in this thesis (left) and the measurement principle for calculating ffc (right). Left shows a loaded shear cell containing the powder sample (A). A downwards pointing Loading Rod (B) applies a normal stress onto the powder bed while side attached crossbeams (C) provide a rotational shear stress. Right shows a typical yield locus for Roller Compacted DE29 granules which highlights the σ_c and σ_1 parameters used to calculate the ffc value.

Table 3.3: Flow descriptors based on ffc value

Flow Function (ffc)	Classification
ffc<1	Non-flowing
1< ffc<2	Very Cohesive
2< ffc<4	Cohesive
4< ffc<10	Easy Flowing
10<ffc	Free Flowing

3.2.7 Dissolution Time

Dissolution testing was carried out using a Jenway 4520 Conductivity Meter (Jenway, UK) as presented in Figure 3.13. A conductivity meter measures the electrical conductivity of a solution. When materials such as Maltodextrin dissolve, they release ions into the water which increases the ability of the solution to conduct electricity. The conductivity probe, measures this increase in conductivity during the dissolution process until the plateau is reached. The plateauing point indicates that there is no further release of ions into the water which indicates complete dissolution. In this work, the dissolution time is the time taken for the conductivity to increase to 90% of the plateauing value.

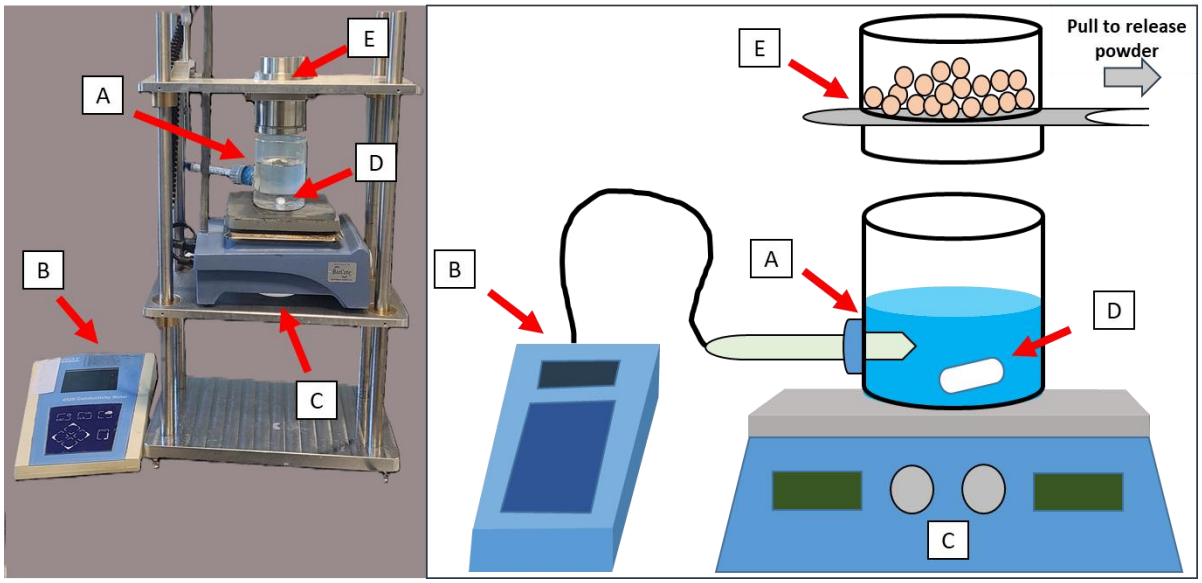

Figure 3.13: Visual (left) and schematic (right) representation of the dissolution setup used in this thesis. The Conductivity Probe (A) was fitted to the beaker using an inbuilt side entry port which ensured that the measurement location was consistent between runs. The probe was connected to a Jenway 4520 Conductivity Meter (B) which analysed and recorded the data. The solution was heated and agitated using a combined Magnetic Stirrer and Hot Plate (C). A 2.5 cm Magnetic Stir Bar (D) was inserted into the solution to activate the stirring function. Powder was added to the solution using a Guillotine Frame Device (E). This device was composed of a powder holding funnel and a trap door. Pulling the trap door out would instantly drop the powder into the solution underneath. This ensured a more standardized addition of powder to the beaker compared to spoon addition.

3.2.8 Dynamic Image Analysis

Dynamic Image Analysis in a Camsizer (Microtrac, UK) has been used throughout this thesis to evaluate particle size and shape. The measurement principal involves feeding the powder sample into a chute using a vibratory feeder. The particles are captured as they fall through the chute by a high resolution (Zoom) camera and a Basic camera as shown by Figure 3.14. The Zoom camera focuses on capturing fine particles while the Basic camera captures large particles. A light source behind the falling particles provides a high contrast image. The edges of the particles are extracted by the software and used to classify the particles. The particle diameter was classified as the shortest chord of the measured

set of maximum chords of the particle projection. This definition aligns closely with the particle size measurements obtained via sieving. Meanwhile, sphericity is defined as $4\pi A/P^2$ (ISO 9276-6) where A is the measured particle projection area and P is the measured particle projection circumference. For an ideal sphere, the sphericity is expected to be 1.

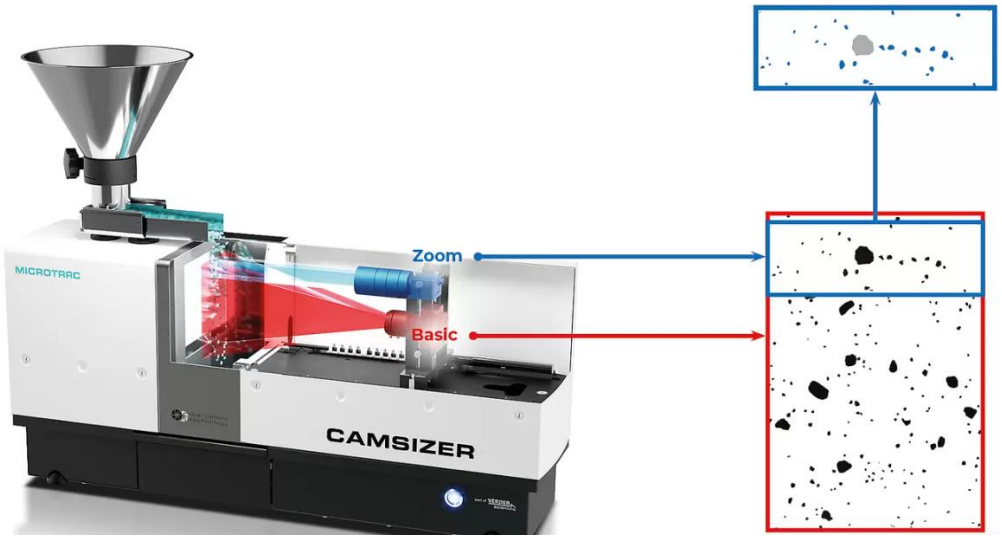

Figure 3.14: Measurement principal for the Camsizer used for particle analysis [80]

3.2.9 X-Ray Tomography and ImageJ

X-Ray tomography was used to gain an indication on granule porosity. Granules were scanned using a µCT 35 (Scanco Medical, Switzerland) XRAY scanner to generate 2D cross section images of the granules. The scan intensity was 70 kV and 114 µA throughout this work. The images were then taken and evaluated using ImageJ. This was done by selecting an envelope around the granule. This means the porosity determined by the method considers both open and closed pores. The colour threshold is then changed which quantifies the percentage of pixels which are gray (solid matter) within the enclosed space as shown by Figure 3.15. Porosity was taken as the inverse of this value. The same threshold limit was used across this work to ensure consistency.

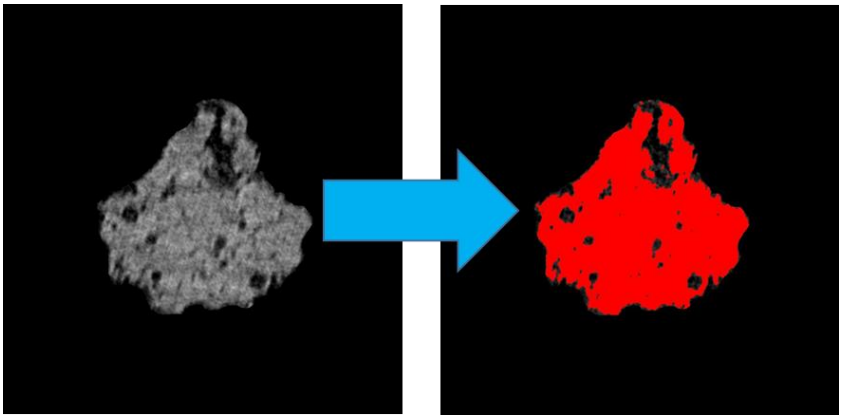

Figure 3.15: Image analysis procedure to evaluate porosity using ImageJ

3.2.10 Differential Scanning Calorimetry

Differential Scanning Calorimetry was carried out using a DSC25 (TA Instruments, Switzerland) to measure the Glass Transition Temperature of the powder. The measurement procedure involves preparing two hermetically sealed capsules. One contains a small amount of the powder. The other is an empty reference pan which is used as a control. The DSC heats both capsules at the set rate between the evaluated temperature range. While this occurs, the system measures the heat flow required to maintain the constant temperature in both pans. When a powder undergoes Glass Transition, its heat capacity increases due to the increased molecular mobility of the powder. This means more energy is required to heat the powder which causes the heat flow to shift towards the endothermic direction. The temperature at which Glass Transition occurs can be determined by detecting when this endothermic shift occurs.

Figure 3.16 shows than example curve for the heating of raw DE12 from -50°C to 160°C. The shifting of the heat flow towards the endothermic side due to the Glass Transition effect is highlighted by the red region. The Onset Glass Transition Temperature can be determined by drawing a tangent to the initial line prior to the endothermic shift and another on the slope representing the shift. The crossover point is the Onset T_g which represents the start of the Glass Transition process. These tangent lines can be automatically generated using the DSC software. The Midpoint Glass Transition Temperature is the average T_g value. This thesis has used the Onset T_g value to represent the Glass Transition Temperature of the various powders.

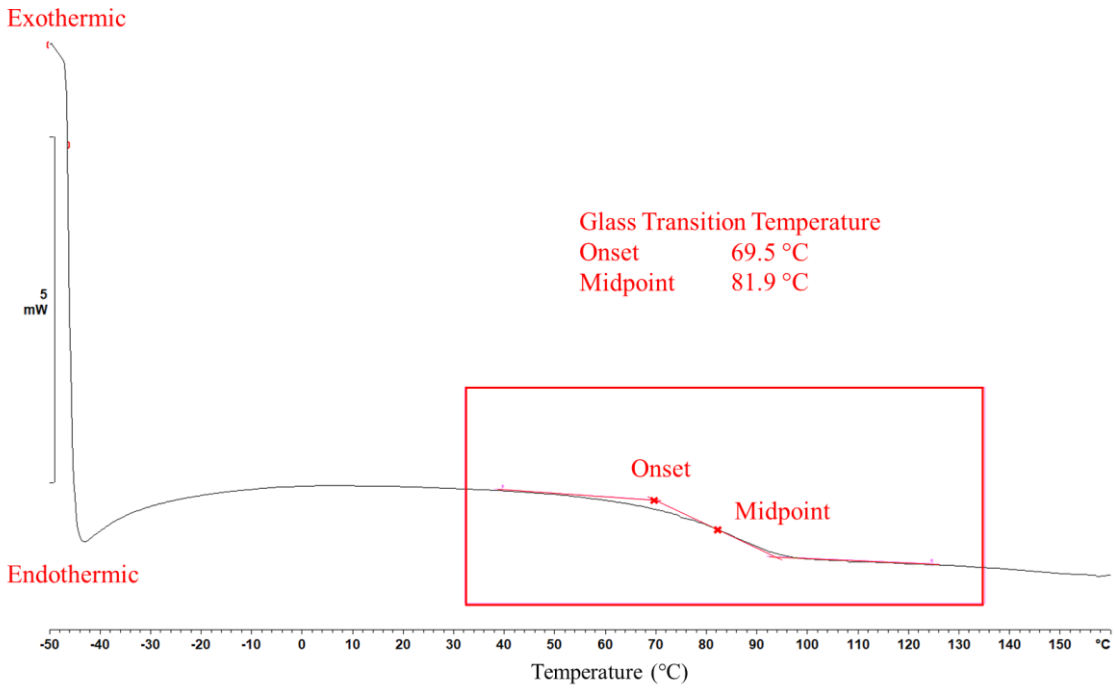

Figure 3.16: Example Glass Transition Temperature Analysis extracted from the DSC25 System for raw DE12. The Onset Glass Transition Temperature is the intersect between the tangent of the initial baseline and the tangent of the slope.

3.2.11 Thermo-Gravimetric Analysis

Thermo-Gravimetric Analysis was done using a TGA550 (TA Instruments, Switzerland) to measure the moisture content of samples. First measurement capsules are prepared containing ~25 mg of powder samples. The lids of these capsules are pierced to allow evaporated water to pass through. The samples then have their mass continuously measured while they are heated at ever increasing temperatures. Plateaus indicate temperature ranges where the powder is stable, while mass drops indicate temperature ranges where moisture loss, decomposition or oxidation occur. For the Maltodextrin powders, the first plateauing point after mass drop occurs (which is indicated by the first minimum point of the weight loss derivative curve) is taken as the temperature at which mass loss due to evaporation ends. The moisture content of the sample is then determined from the weight loss at this temperature. This helps ensure that mass loss due to other non-drying related phenomena is not counted as moisture.

3.2.12 Viscometry

Viscosity of Maltodextrin and water mixtures was measured using a Malvern Kinexus Pro rheometer (Malvern, UK). The measurement was carried out using a cup and bob system as presented in Figure 3.17. A cup was used rather than a plate because the Maltodextrin mixtures tended to slip against the plate and travel outside of the evaluation area. Around ~25 ml of the sample would be placed into the cup. The bob then moves down until the bottom clearance is 9.15 mm. Viscosity is measured using a

rotational steady shear setup. In this setup, the rheometer applies a constant shear rate (γ) onto the mixture by rotating the bob. It then measures the resulting shear stress (τ). The viscosity at this shear rate is determined by dividing the measured shear stress by the applied shear rate (τ / γ). The rheometer then repeats this across a range of ramped shear rates (0.1 – 1000 s^{-1} in this study) to evaluate how material behavior with respect to viscosity changes with shear rate.

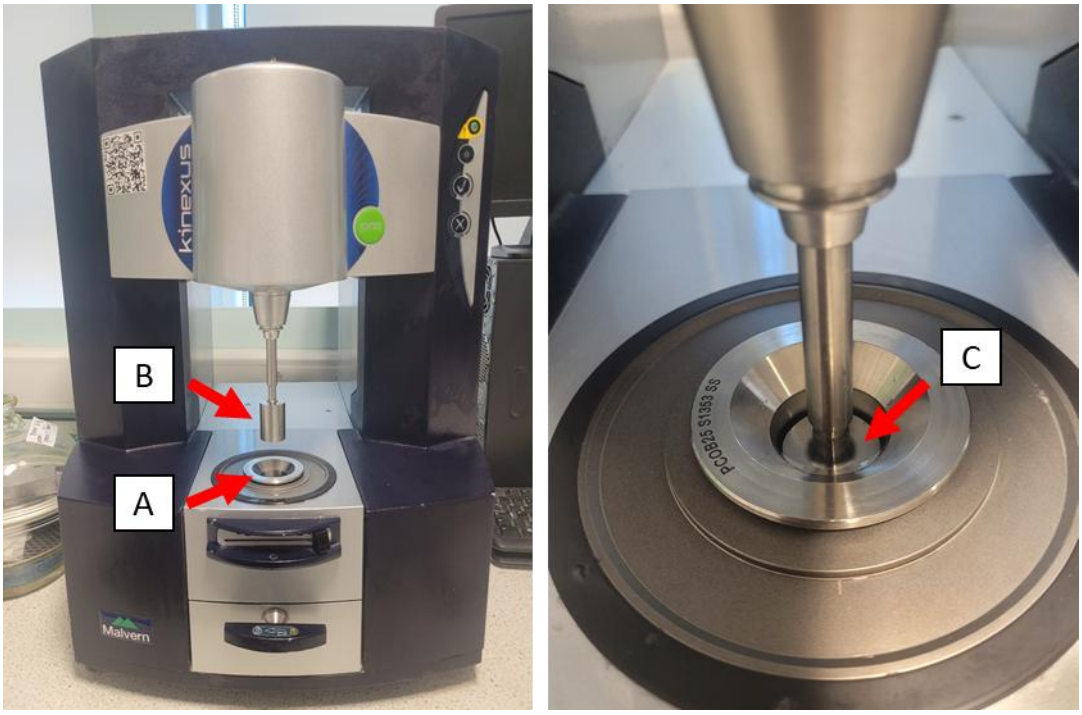

Figure 3.17: Left shows the Malvern Kinexus Pro rheometer used to measure viscosity in this study as configured with a cup (A) and bob (B) system. Right shows the completed setup (C) with the cup filled with water and the bob inserted to a bottom clearance of 9.15 mm. Subsequently, the bob will rotate at different speeds within the cup which generates varying shear rates. The resulting shear stress developed in relation to the applied shear rate is used to determine viscosity.

3.2.13 Jet Mill

Jet Milling is a popular size reduction technique that is used to produce micronized powder. The jet mill used in this study was a J-20 Fluid Jet Mill (Tecnologia Meccanica, Italy) which has a spiral design. The operating mechanism of a spiral jet mill is highlighted in Figure 3.18. In this design, particles are fed into a circular milling chamber by a suction effect. In the chamber, a high pressure compressed air stream is tangentially injected in through multiple nozzles. This injection creates a high speed spiral vortex inside the chamber which causes particles to move in a circular path. As they travel along this circular path, the particles experience high velocity inter-particle and particle-wall collisions. This leads to breakage and a reduction in particle size. The centrifugal force means that larger particles rotate at the outer edge of the vortex. This means that as particles reduce in size, they migrate towards the center where they leave the mill and are collected. This ensures that only the fine particles are allowed to exit.

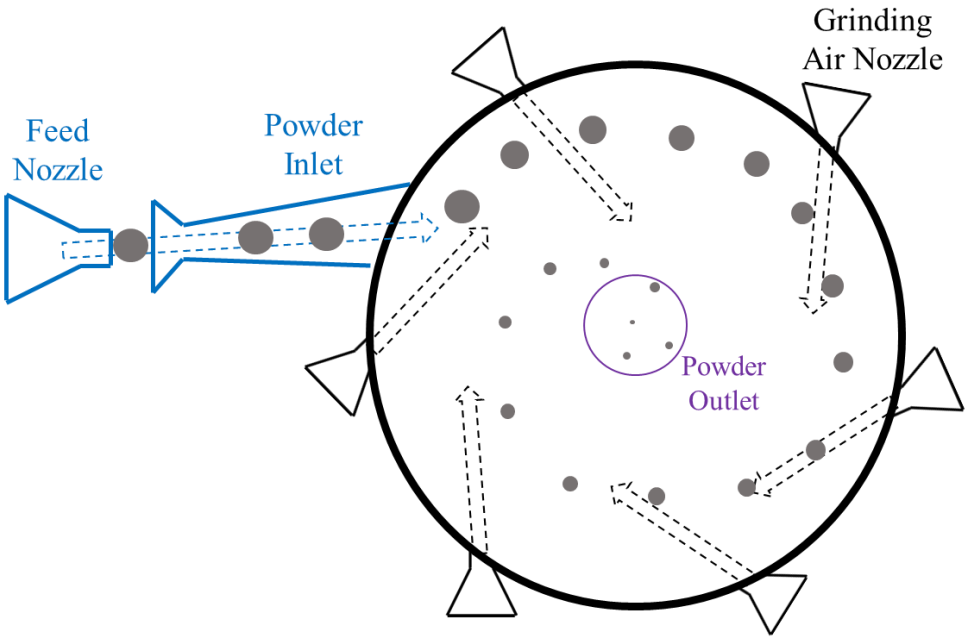

Figure 3.18: A schematic representation of the grinding chamber in a spiral jet mill. Coarse powder particles (shown in grey) are fed into the chamber via a feed nozzle. High pressure grinding air is fed into the chamber through a series of grinding nozzles. This high pressure air accelerates the particles to high velocities. The resulting high energy collisions between these fast moving particles result in size reduction. The centrifugal force means that large particles circulate at the chamber extremities while fine particles move towards the centre where they are removed from the chamber.

3.2.14 Direct Vapour Sorption

Direct Vapour Sorption (DVS) is used to measure how much moisture a material absorbs or desorbs under controlled environmental conditions. This study utilised a SPS 11-10µ Sorption Test System (ProUmid, Germany). The machine contains a high precision microbalance that continuously measures sample mass. This microbalance is housed within a measurement chamber where the temperature and humidity can be controlled. Humidity is usually altered in a stepwise or continuous manner. In this thesis, humidity was altered in a stepwise manner. In response to a change in the humidity, the powder will absorb or desorb water. The microbalance records this process by measuring the real time change in mass of the sample.

4 Selecting the Optimal Granulation Pathway by Considering Sustainability and Suitability

Abstract

Little is known about the sustainability of competing granulation technologies, despite them being key and widespread industrial processes. This study has evaluated the sustainability of four prominent granulation technology pathways with respect to material efficiency (judged according to granular yield), Specific Time (hours/kg) and Specific Energy (kWh/kg). The Fluidised Bed Granulator proved to be the most material efficient with an optimum yield of 79% while the Roller Compactor was the most time efficient with an optimum Specific Time of 0.1 hr/kg. The energy efficiency of the granulators improved in the following order: Twin Screw Granulator, Fluidised Bed Granulator, High Shear Granulator and Roller Compactor. The wet granulation techniques proved to be the less energy efficient technologies due to energy expensive sub stages such as drying. This was especially the case with the Twin Screw Granulator and High Shear Granulator where the actual granulating equipment only accounted for around 13% and 15% of the total energy consumed by the entire production pathway. Comparatively, the drying stage accounted for around 45% and 84% of the Twin Screw Granulation and High Shear Granulation production pathways. The different granulation technologies were shown to produce granules with significantly varying properties due to changing granule shape and porosities. The use of visual techniques such as parallel co-ordinate graphs and radar plots alongside analytical methods such as priority scoring are suggested as important tools to help manufacturers choose the optimum process pathway based on these varying sustainability and granule suitability factors.

Highlights

- Roller Compaction was the most energy and time efficient.
- Fluidised Bed Granulation was the most material efficient.
- Drying step consumed far more energy than the granulation step for wet granulators.
- Granule porosity and shape varied significantly between granulations technologies.
- Sustainability and suitability are key considerations when choosing the optimum granulator.

This chapter forms the basis of the following paper:

Y.H. Karunanayake, L. Brütsch, V. Meunier, A.D. Salman (2024). Sustainability vs suitability in granulation. Chemical Engineering Research and Design, Volume 202. pp 272–283

https://doi.org/10.1016/j.cherd.2023.12.032

4.1 Introduction

Process sustainability, especially with regards to energy consumption is an aspect of food production that has experienced renewed interest, with significant reductions in the energy consumption of the food manufacturing sector needed to meet upcoming sustainability targets [81]. This focus on energy consumption is driven by increased demand on manufacturers to produce cheaper products to accommodate financially pressured consumers, especially in developing markets. Meanwhile, in developed markets, manufacturers face a pressure both from the public and governmental bodies to adhere to their social responsibility of being sustainable and to reduce their carbon footprint. For instance, through recent UN Climate Change Conference's (COP29) it has been globally agreed that greenhouse gases must be reduced in order to limit temperature rises to 1.5°C and achieve net zero. The goal of net zero is even more in focus in the UK where the government has independently set the target of achieving net zero in all sectors across the economy by 2050. As a major greenhouse gas emitter, improving the sustainability and efficiency of the food sector is key to meeting these national and global commitments.

Granulation is a well-established size enlargement mechanism which is commonly used in the powder processing industry to improve material handling properties, stability and aesthetics. Granulation can occur with the use of a liquid aid (wet granulation) or without (dry granulation). Wet granulation is commonly carried out in High Shear Granulators (HSG), Fluidised Bed Granulators (FBG) and Twin-Screw Granulators (TSG). Whereas Dry Granulation is mainly carried out in Roller Compactors (RC).

While the literature investigating the mechanisms of these individual processes are quite mature, studies looking at the energy consumption of them, especially in relation to each other are very much in the infancy. With regards to the HSG, the majority of the existing work focuses on using the power requirement of the process to predict the behaviour of the granulation mix, rather than as a basis for rating energy efficiency. For instance, Pepin et al. [38] evaluated the power consumption of a HSG process as a basis for identifying the overwetting point of the mix. Meanwhile, Betz et al. [39] evaluated the ratio between temperature rise and power consumption in the HSG due to changing process and formulation parameters to evaluate whether it could be used as a tool to develop an artificial neural network for in-process control. It is a similar story with the TSG, with studies investigating the use of torque as a process control aid to monitor granule size [49], or attempting to correlate power consumption with granule shape [50]. The focus on energy efficiency is slightly more pronounced in the FBG with literature discussing how to make the technology more energy efficient through initiatives like temporally separating the spraying and drying stages [60]. The lack of literature was worst with regards to the RC with no literature evaluating the energy consumption of the process to be found. Additionally, no literature could be found which evaluates the energy consumption of the whole

granulation technology pathway by accounting for the power consumption of additional auxiliary units such as the binder pump or additional stages like drying

Furthermore, while broad multi-granulator studies do exist, they only consider a limited number of parameters such as granule attributes [82]. No study evaluating the granulation technologies against each other based on energy efficiency could be identified. In order to make informed decisions about the optimum granulation pathway, it is essential to develop knowledge of the energy economy of different granulation pathways and key process parameters effecting it. The aim of this work is to carry out a comprehensive study looking at the process energy consumption of the main granulation technologies currently used in industry, considering the entire production pathway as a whole. The process energy efficiency will be judged according to its Specific Energy (kWh per kilogram of in-specification granules produced) factor which not only accounts for the energy consumption of a process but also its granular output. Other metrics for evaluating process sustainability and affordability such as Yield and Specific Time (hours per kilogram of in-specification granules produced) have also been considered. Key granule characteristics such as flowability, friability and dissolution time were also evaluated to add a quality element to differentiate the technologies by. Graphical and analytical tools to help manufacturers make judgements based on process sustainability (judged according to the material, time and energy facets) and granule suitability (judged according to granule characteristics) together have then been proposed.

4.2 Materials and Methods

4.2.1 Materials

Glucidex IT29 (Roquette, France) has been chosen as the model granulation material due to the commonplace use of Maltodextrins in both the food and pharmaceutical industries. It has been referred to as DE29 in this chapter. The particle size characteristics of the DE29 powder can be described by a d10 of 143 µm, d50 of 255 µm and d90 of 455 µm. Powder was conditioned at 20% Relative Humidity and 20℃ for 72 hours in a Memmet IN110 Humidity Chamber (Memmet, Germany). This was done to lower the moisture content of the powder, in order to reduce the powder's Glass Transition Temperature and control the powder's tendency to cake during granulation. The chosen binder for the wet granulation processes was distilled water at 20℃.

4.2.2 Equipment and Methods

Four different granulation equipment were tested and evaluated to produce granules. The granulation equipment includes the Fluidized Bed Granulator (FBG), the High Shear Granulator (HSG), the Roller Compactor (RC) and the Twin Screw Granulator (TSG). For each evaluated granulation condition, the experiment was repeated a multiple of three times and the average taken to check for reproducibility.

When comparing the energy efficiency of competing technologies, it is important that the process conditions used to represent each technology undergo a degree of optimization. This is done to ensure that the technology is being represented in its best light to allow for fair comparison. Therefore, the process parameters were first optimized to maximize yield. This is because a higher yield results in less material wastage, which is another major consideration for food manufacturers in the drive to reduce costs and improve sustainability. For example, in the wet granulation processes this involved using the highest L/S ratio possible without caking or lumping becoming problematic to maximize total granular yield. The remaining auxiliary parameters were then honed to favor the production of in-spec granules.

After the process had been optimized for yield, the process batch size/throughput was chosen as the primary parameter of interest for this study. This is because throughput, along with the yield, determines the mass of useful granules produced and therefore will play a significant role in determining the Specific Energy (kWh/kg) of a process. For the FBG and HSG processes, this meant batch sizes between 0.3 – 1 kg and 0.2 – 0.4 kg respectively were evaluated. In the RC, throughputs between 6.66 - 16.7 kg/hr was evaluated. This was done by activating the roll gap function and altering roll speed between 3 – 9 rpm, to change the throughput of the process. In the TSG, throughputs between 0.3 and 0.7 kg/hr was evaluated. The maximum and minimum values for batch size/throughput were chosen based on the limits at which the process could be run stably.

4.2.2.1 Fluidised Bed Granulator

The FBG technology was represented by a Glatt GPCG3 Fluidised Bed (Glatt, Germany) with a side entry spray nozzle. Batch Sizes between 0.3 and 1 kg were evaluated. The inlet air speed required to maintain bed fluidization varied with batch size as follows: 2 m/s (0.3 – 0.5 kg), 2.5 m/s (0.7 kg), 3.2 m/s (1 kg). A L/S of 0.18 was used because beyond this value there was no significant increase in granular yield. A spray rate of 4.5 g/min was used because it was the fastest the liquid could be added, which minimized run time, without caking occurring. A constant L/S ratio and spray rate meant that larger batch sizes needed longer binder addition times. Therefore, the total granulation run time varied due to the changing binder spray times as follows: 12 mins (0.3 kg), 20 mins (0.5 kg), 28 mins (0.7 kg), 40 mins (1 kg). Air temperature was limited to 30°C because temperatures higher than this led to caking and collapse of the powder bed. An atomization pressure of 1 bar was used as it generated a fine droplet size and large spray zone which prevented localized bed saturation.

4.2.2.2 High Shear Granulator

The HSG technology was represented by an Eirich EL1 High Shear Granulator (Eirich GmbH, Germany). Binder was fed in using a Graseby 2100 Syringe Pump (Burtons, UK). The granulation of DE29 in HSG was highly sensitive to batch size. At batch sizes below 0.2 kg, there was insufficient powder in the bowl to capture all binder droplets, resulting in excess water contacting the granulator

surfaces. This promoted powder caking onto the equipment walls, leading to processing difficulties. Conversely, at batch sizes above 0.4 kg, the rate of heat generation within the granule bed was excessive, causing rapid and uncontrolled glass-transition-induced caking. As a result, only a narrow batch size window could be reliably evaluated, and batch sizes between 0.2 and 0.4 kg were therefore studied at three levels: 0.2 kg, 0.3 kg, and 0.4 kg. A bowl speed of 170 rpm and a relatively low impeller speed of 900 rpm was used to give a good degree of mixing while minimising heat generation due to friction. The machine was operated in a co-current mode which means the bowl and impeller were set to rotate in the same direction. The mixing pan was configured horizontally (inclination angle of 0°). A L/S of 0.07 and a spray rate of 1.5 g/min were the optimum values for each parameter that could be used while preventing caking. Wet massing time: 5 mins. Total granulation run time varied with batch size due to the changing binder spray time: 15 mins (0.2 kg), 20 mins (0.3 kg), 25 mins (0.4 kg). The range of batch sizes

4.2.2.3 Roller Compactor

The RC technology was represented by an Alexanderwerk WP120 Pharma Roller Compactor (Alexanderwerk AG, Germany). The roll speeds evaluated were between 3 - 9 rpm. This corresponds to material throughputs between 6.66 kg/hr and 16.7 kg/hr. The hydraulic pressure used was 70 bar along with a roll gap of 2 mm. A compaction pressure of 70 bar was chosen because the use of higher pressures did not result in any improvements to the granule yield faction and only increased the power consumption. A milling speed of 40 rpm and mill mesh sizes of 2.45 mm and 1.25 mm were chosen to promote the production of granules in the desired size range.

4.2.2.4 Twin Screw Granulator

The TSG technology was represented by a ThermoFisher Euro Lab 16 mm Twin Screw (ThermoFisher Scientific, UK). Incorporated into the TSG system is a loss in weight twin screw powder feeder (K-Tron Soder, Switzerland). An IC05C Water Chiller (ICS Cool Energy, UK) was used to maintain the cooling jacket on the TSG. Binder was fed in using a Graseby 2100 Syringe Pump (Burtons, UK). A screw speed of 30 rpm and L/S of 0.04 were the optimum values for granular yield before which jamming of the screws or caking over at the liquid inlet port became an issue. A barrel temperature of 10°C was used to mitigate the heat generation within the unit. A conveying element only screw configuration was chosen as the use of more aggressive kneading elements led to caking and screw jamming.

4.2.2.5 Dryer

Granules produced from the TSG and HSG were collected and drying was carried out at 50°C in a Glatt GPCG3 Fluidised Bed (Glatt, Germany) with the target being to reduce the final granule moisture content to below 2.5%.

4.2.2.6 Power Measurement

The power consumption of the equipment was measured using a Socomec Countis E27 3 Phase Power Reader (NewFound Energy, UK) or DecDeal 1 Phase Power Reader (DecDeal, UK). The power measurement technique is visualized in Figure 4.1. The power consumption of each equipment in the granulation pathway which is associated with the transition of dry powder to dry granule was measured. Figure 4.2 displays the stages and equipment involved in each granulation pathway for the evaluated technologies.

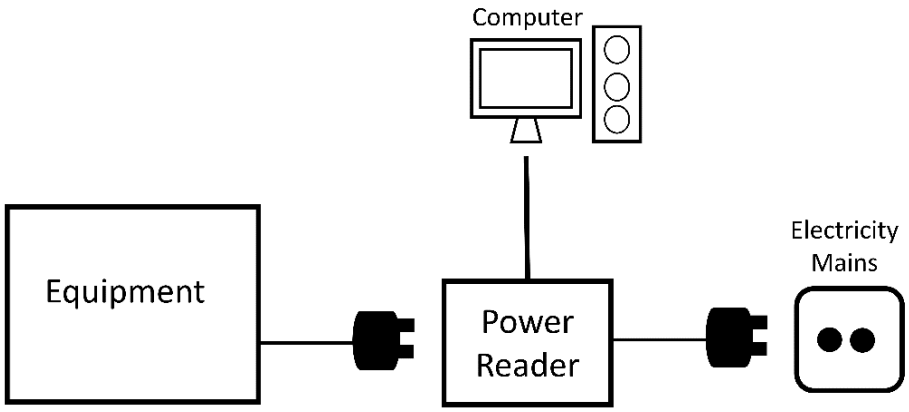

Figure 4.1: Visual representation of the power measurement technique. The equipment to be measured was plugged into the power reader and the power reader into the mains. The power drawn by the machine with time could be recorded manually or automatically by connecting the power reader to a computer.

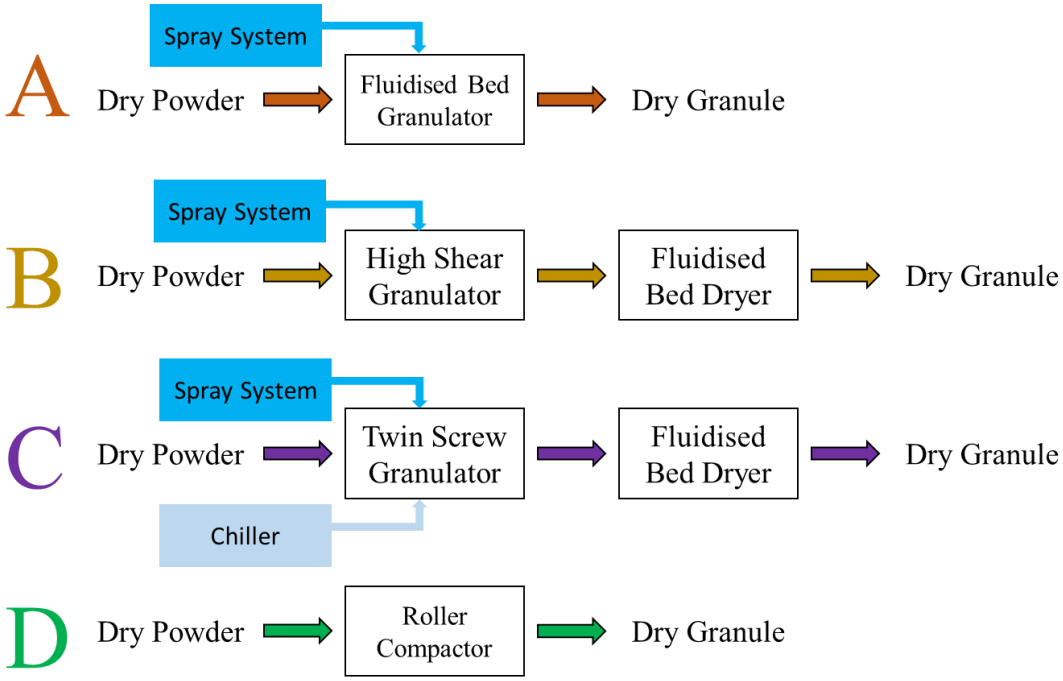

Figure 4.2: Granulation pathway showing the equipment involved in the granulation of dry powder to form dry granules. The technologies represented are as follows: Fluidised Bed Granulation (A), High Shear Granulation (B), Twin Screw Granulation (C) and Roller Compaction (D).

4.2.2.7 Granule Size Characterisation

The desired granule size was classed as being between 0.5 mm and 2 mm. Sieving using a Retsch Sieve Shaker AS200 (Retsch, UK) at an amplitude of 0.45 mm for 3 mins was used to classify the granulation products. The sieve classes used were 0.5 mm, 1 mm, 2 mm and 4 mm. Granules less than 0.5 mm were classed as fines. Those between 0.5 mm and 2 mm were classified as within specification and to be the yield faction. Granules between 2 mm and 4 mm were classified as oversized and those greater than 4 mm were classed as lumps. Additional information regarding sieving can be found in Section 3.2.5.

4.2.2.8 Granule Flowability Characterisation

A Shear Cell RST – XS.s (Dietmar-Schulze, Germany) was used to classify the flowability of granules between 1 mm and 2 mm. Three repeats were conducted for each experiment and the average taken. The normal load at pre-shear was 2000 Pa and the normal loads at shear to failure were 400 Pa, 1000 Pa, 1600 Pa and 400 Pa. Additional information regarding measuring flowability can be found in Section 3.2.6.

4.2.2.9 Granule Dissolution Characterisation

Dissolution testing was carried out using a Jenway 4520 Conductivity Meter (Jenway, UK). 4.5 g of granules between 1 mm and 2 mm was dissolved in 200 ml of distilled water at 25°C. Agitation was achieved using a magnetic stirrer at 700 rpm. The procedure was repeated a total of 5 times for each experiment and the average taken. Additional information regarding measuring dissolution time can be found in Section 3.2.7.

4.2.2.10 Granule Friability Characterisation

Friability or granule strength was assessed by evaluating the fine faction after vigorous shaking using a Retsch Sieve Shaker AS200 (Retsch, UK). 100 g of granules between 1 mm and 2 mm, was placed onto a 1 mm sieve and vibrated at an amplitude of 1.5 mm for 2 min. The friability was then calculated to be the reduced faction (mass less than 1 mm) of the product as a percentage. The experiment was repeated 3 times for each condition and an average taken. Additional information regarding measuring friability can be found in Section 3.2.5.

4.2.2.11 Granule Sphericity Characterisation

A Camsizer (Retsch, UK) was used to evaluate the sphericity of granules between 1 - 2 mm. Random sampling was used to select granule samples of 25 g and three repeats were conducted for each condition. Sphericity is defined as $4\pi A/P^2$ (ISO 9276-6) where A is the measured particle projection area and P is the measured particle projection circumference. For an ideal sphere, the sphericity is

expected to be 1. Additional information regarding sphericity characterization can be found in Section 3.2.8.

4.2.2.12 Granule Porosity Characterisation

X-Ray Tomography using a X-Ray Scanner µCT 35 (Scanco Medical, Switzerland) was used to obtain 2D imaged slices of granules between 1 mm – 2 mm. ImageJ was then used to evaluate the percentage of voids within the granular structure. For each condition, a total of 10 randomly selected granules were evaluated. Additional information regarding porosity characterization can be found in Section 3.2.9.

4.3 Sustainability in granulation

The following section will present the energy efficiency results for each individual granulator, discussing the effect that batch size/throughput had on the Specific Energy of the process. Then the Yield, Specific Energy (kWh/kg) and Specific Time (Hours/kg) of the production pathways as a whole will also be presented to allow the comparison between the technologies to determine the most sustainable option.

4.3.1 Fluidised Bed Granulator (FBG)

Figure 4.3 shows the effect of batch size on yield, energy consumption and Specific Energy for the Fluidized Bed Granulator. The yield of in-spec granules increases with batch size before reaching a plateauing point as shown by Figure 4.3. This increase in yield can be explained by considering the increased particle-droplet and particle-particle interactions occurring at larger batch sizes. This increases binder droplet capture by the powder and the increased particle-particle interactions promotes coalescence and leads to better growth [83]. Similar findings were presented by Geng et al. [84] which showed that increasing the proportion of powder in the Fluidised Bed promoted powder to powder adhesion by increasing the collision probability. However, while increasing the collision probability also promotes growth, it also results in higher attrition rates of dried granules due to impact and higher breakage rates in wet granules if its yield strength is not sufficient to resist the collision force [1]. This higher attrition and breakage rate could detract from the improved growth factors at high batch sizes resulting in the observed plateauing effect in Figure 4.3. It is also possible that there is a critical particle concentration within the FBG required for good growth to occur which is achieved at a batch size of around 0.7 kg. Increasing particle concentration beyond this point might only result in marginal improvements in granular yield causing the plateauing effect. The smallest (0.3 kg) and largest (1 kg) batch size display the greatest variation in yield. This is due to greater instability in these processes with more caking seen at a batch size of 0.3 kg and fluidization problems observed at a batch size of 1 kg.

Meanwhile, the energy consumption of the process increases with batch size. As shown in Section 4.2.2.1, both the overall batch run time and the fluidising air velocity needed to maintain bed fluidisation increased with batch size. Therefore, the higher energy requirement at larger batch sizes can be linked to this additional run time, as well as the need to generate a larger heated air flow within the unit. Despite this increase in the energy consumption, the energy efficiency of the FBG was found to improve with batch sizes before reaching a plateauing value. This is reflected in Figure 4.3 where the Specific Energy for the process decreased as batch size was increased. This decrease is due to the increased yield and material throughput of the process at higher batch sizes leading to the production of a greater mass of useful granules. This compensates for the increased energy consumption to result in a more energy economical process.

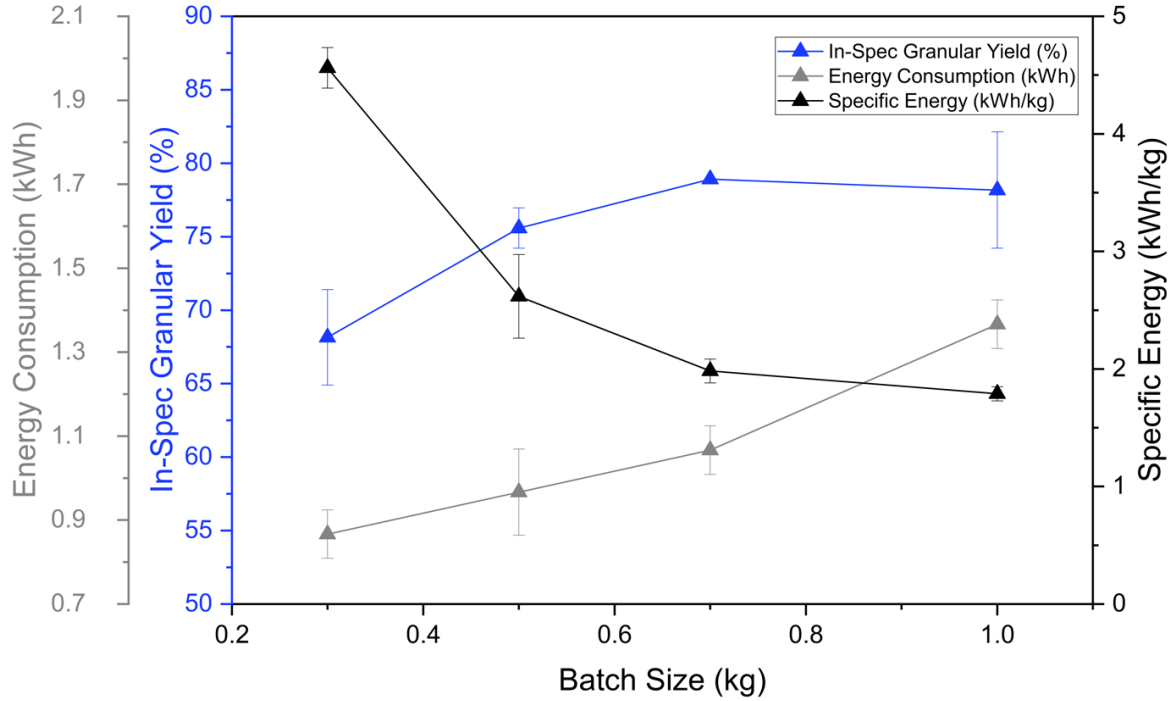

Figure 4.3 Impact of Batch Size on Energy Consumption, Yield and Specific Energy in the FBG. The energy efficiency of the process was found to improve with batch size.

4.3.2 High Shear Granulator (HSG)

The energy consumed by the HSG is a very important parameter to be aware of when granulating amorphous food powders. This is because the energy consumed in this unit is almost completely converted to heat in the wet mass, which can then become problematic when granulating heat sensitive material [85]. As shown in Figure 4.4, yield of in-spec granules first increased as batch size is increased from 0.2 kg to 0.3 kg and then decreased as batch size is further increased from 0.3 kg to 0.4 kg. This same trend is shown by the work of Terashita et al [86], which showed that this peak where the maximum granule yield occurs is linked to the fill level that corresponds to the best particle circulation

and greatest particle kinetic energy.The initial increase in yield with batch size can also be explained by considering the higher collision tendency at higher batch sizes promoting growth through coalescence. The higher collision tendency also increases the rate at which granules consolidate which forces more liquid to the granule surface which will promote better growth [30]. However, it must be noted that this increase in yield between a batch size of 0.2 kg and 0.3 kg is marginal, especially when the magnitude of the error bars is considered. Meanwhile, the reduced yield at a batch size of 0.4 kg, can be attributed to the high collision tendency at large batch sizes promoting breakage over growth in this case. This increased breakage along with the less uniform binder distribution at high fill levels result in the lower yield seen here [87]. The Eirich granulator shares many similarities with planetary centrifugal granulators where the mixing motion is primarily induced by the rotation of the bowl. Studies in planetary centrifugal granulators have linked a decreased yield at higher fill levels to greater restriction of material movement occurring at high fill levels resulting in less agglomeration [88]. This same reasoning is likely to apply to the Eirich granulator, indicating that there is an optimum fill level for mixing in the unit resulting in an optimum granulation condition for yield.

Energy consumption increased with batch size as presented in Figure 4.4. This is due to three factors, the first is the increased overall run time as a larger batch size required a longer binder addition time (since both L/S and binder addition rate were kept constant). The second is the greater load on the bowl motor, as it needs to support a greater mass as it rotates. The third is the increased load on the impeller motor which must maintain the impeller speed through a much larger bed mass. This is in agreement with the work of Betz et al. [39] which showed that the energy consumption in the HSG increased with filling level in the granulator. The lowest Specific Energy was recorded at a batch size of 0.3 kg. The 0.3 kg batch size has a lower specific energy than at 0.2 kg because its higher yield and increased throughput produces a greater mass of useful granules which offsets the increased energy consumption. Meanwhile Specific Energy was also lower at a batch size of 0.3 kg compared to 0.4 kg. This is because at 0.4 kg, the granule yield was significantly lower. This meant that the increase in the mass of in-spec granules produced as batch size is increased from 0.3 kg to 0.4 kg was insufficient to offset the associated increase in energy consumption.

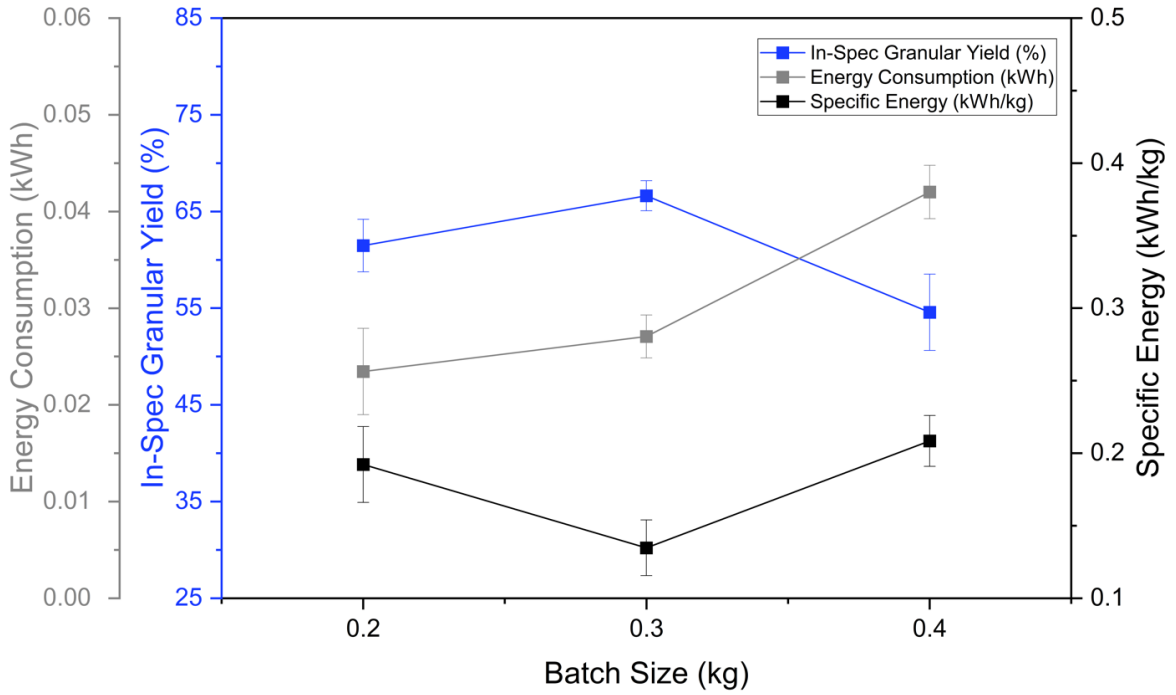

Figure 4.4: Impact of Batch Size on Energy Consumption, Yield and Specific Energy in the HSG. An optimum point for yield and energy efficiency is observed at a batch size of 0.3 kg.

4.3.3 Roller Compactor (RC)

The Roller Compactor was run with the Roller Gap control function activated. This meant the unit would automatically alter the powder feeder screw speed to keep the roll gap constant. At faster roll speeds, more material is required to maintain the roll gap which means the process throughput is higher. This increase in throughput is considerable. For instance, the following average throughputs were recorded at the evaluated roll speeds: 6.66 kg/hr (3 rpm), 11.6 kg/hr (6 rpm) and 16.7 kg/hr (9 rpm).

The effect of this change in roll speed on Yield, Energy Consumption and Specific Energy are shown in Figure 4.5. Changing roll speed caused a negligible change in yield. This trend can be explained by considering the work of Osborne [24] who granulated Maltodextrin DE21 under varying roll speeds in the same Roller Compactor as this study. Similarly, to this study, the roller gap control function was used to maintain a constant gap. Osborne [24] showed that roll speed generally did not have an impact on the ribbon strength and therefore extent of bonding when roll gap is controlled to be constant. A minimal change in bonding with increasing roller speed therefore translates to the minimal change in granular yield seen here.

Meanwhile, energy consumption increased with roller speed. This is because as roller speed is increased, the demand on the roll motors increases as well. The power requirement of the powder screw feeder motor also increases as it needs to produce a greater throughput to maintain the 2 mm ribbon gap

at higher roll speeds. This larger throughput along with the relatively stable yield means the overall mass of useful granules produced increases significantly as roll speed is increased. Therefore, despite the higher energy consumption, the specific energy decreases with increasing roll speed to result in a more energy efficient process.

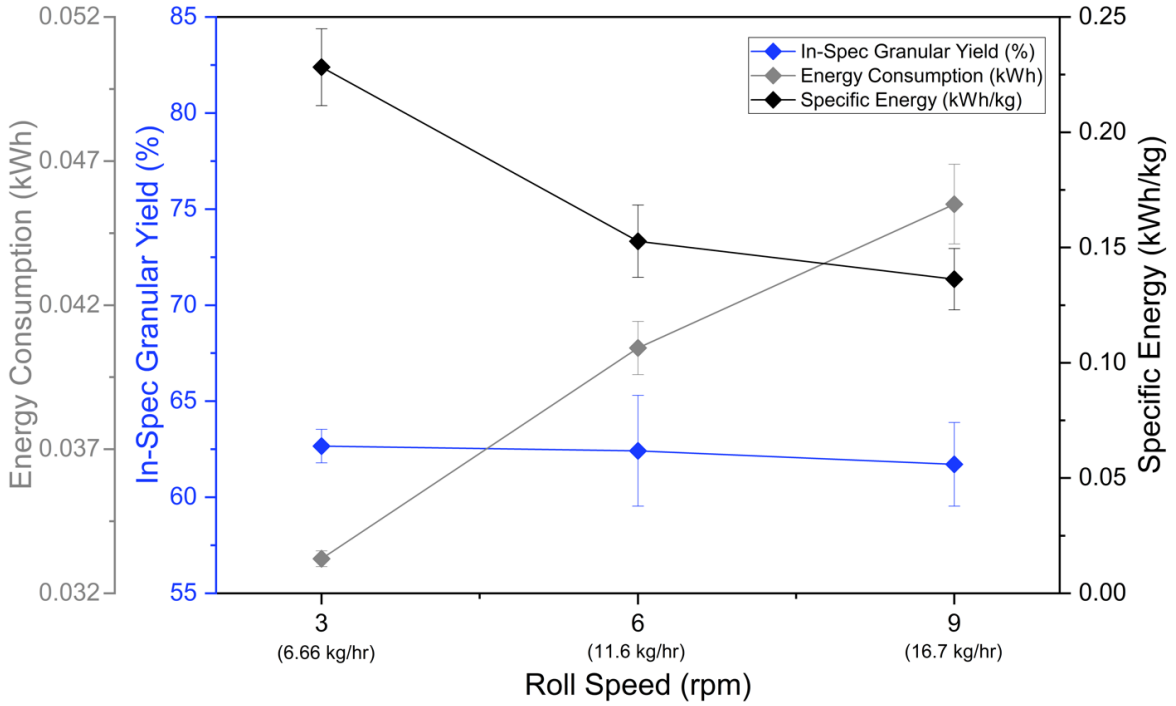

Figure 4.5: Impact of Roll Speed on Energy Consumption, Yield and Specific Energy in the Roller Compactor. Energy efficiency improves with increasing roll speed. This is because the increased throughputs at higher roll speed result in the production of more granules which offsets the increased energy consumption at this condition.

4.3.4 Twin Screw Granulator (TSG)

The in-spec granule yield for the TSG process is low compared to the other granulation techniques with the highest in-spec yield being 29% at the 0.3 kg/hr throughput as shown in Figure 4.6. This reflects the idea that agglomeration in the granulator is not effective since the screw is only composed of conveying elements which are primarily used to transport material and not for mixing [43]. This resulted in a very high ungranulated fine faction for all conditions (64%, 65% and 60% for 0.3 kg/hr, 0.5 kg/hr and 0.7 kg/hr respectively). The use of more aggressive kneading elements resulted in powder caking, which leads to screw jamming and therefore could not be utilized for the wet granulation of Maltodextrin DE29.

The highest yield is recorded at the lowest throughput of 0.3 kg/hr. This is because at this throughput, the granules that are produced are predominantly within the desired size range (0.5 mm – 2 mm). At larger throughputs, a large portion of the granules produced are larger than the 2 mm upper limit. This

means that they are classed as oversized which leads to a lower in-spec granular yield. This can be explained by considering two phenomena. The first is the increased residence time at lower powder feed rates (such as 0.3 kg/hr) as the throughput force is low [89]. This increased residence time facilitates better binder distribution and more incorporation of fine powder which leads to the preferred granule size distribution [90,91]. The second is the increased compaction forces at higher throughputs leading to more interactions between granules [89]. This leads to the production of larger granules (which are out of spec) as throughput increases [92,93].

The energy consumption of the TSG increases with throughput. At larger throughputs, the material offers more resistance to the motion of the screws meaning that more energy is required by the screw motor to overcome this resistive force. Meanwhile, the Specific Energy decreases with increasing throughput indicating an increase in energy efficiency. This is despite energy consumption increasing and yield decreasing with increasing throughput. Similarly, to the RC, this is because the actual mass of useful granules produced is larger at higher throughputs despite the decrease in yield. This offsets the higher energy consumption to produce a more energy efficient process.

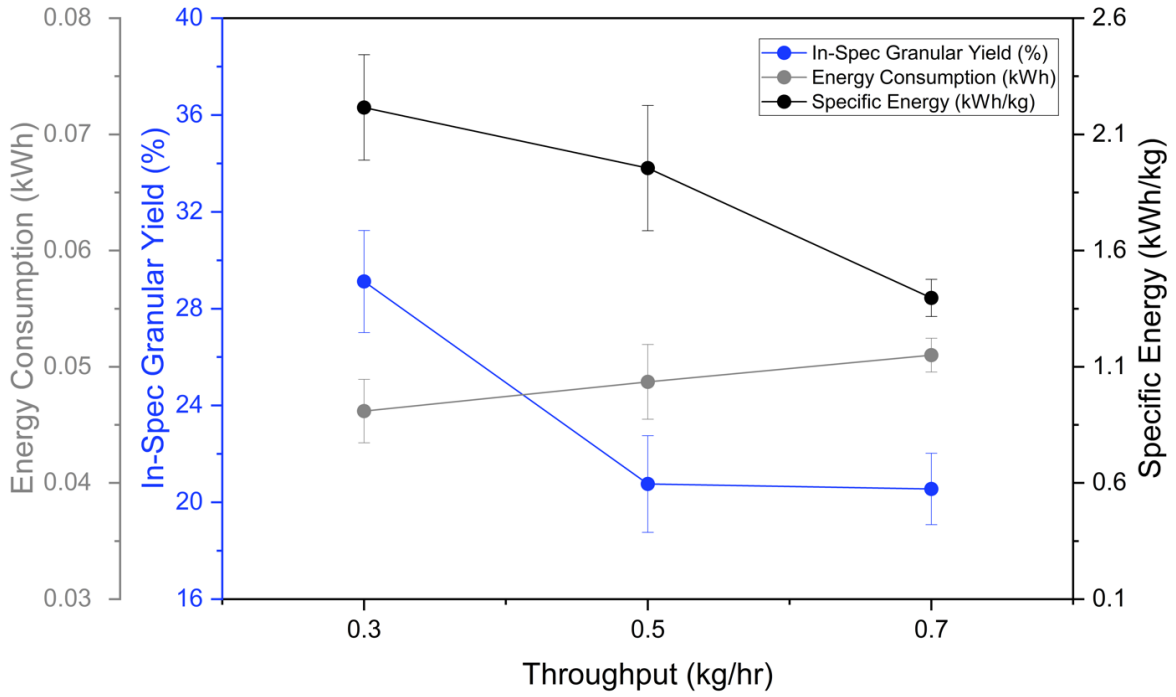

Figure 4.6: Impact of Throughput on Energy Consumption, Yield and Specific Energy in the TSG. Energy efficiency improves with increasing throughput as indicated by the decreasing Specific Energy.

4.3.5 Comparing granulation pathways

When considering the affordability and sustainability of a manufacturing process there are multiple metrics to consider. Examples of these metrics include Yield, Specific Energy and Specific Time. Yield indicates material efficiency with a lower yield indicating a less material efficient process (more

material wastage). Linking this to the cost of the raw materials, a lower yield therefore correlates to a more expensive product in the case that the fines cannot be recycled. In the case that they can be recycled, this leads to a longer processing time which reduces the sustainability and viability of the process. As mentioned in Section 4.2.2, the technologies presented in this study were optimized based on yield to reflect its importance in deciding the economic viability of the process. Figure 4.7 shows the in-spec yield achieved at the optimized conditions for the different technologies. When comparing the highest yield generated by each technology, the material efficiency was found to increase in the following order: Twin Screw Granulator, Roller Compactor, High Shear Granulator and Fluidised Bed Granulator. The yield of the TSG process is far below the rest which would result in a large amount of material wastage if it were adopted, making it the least material efficient. Next, although the RC and HSG have similar ranges of in-spec yields, the higher maximum yield achieved by the HSG indicates that it is more material-efficient than the RC. Finally, the FBG had the highest yield between the technologies at a value of 79% indicating a very material efficient process.

As displayed in Figure 4.7, the TSG was an outlier compared to the other granulation technologies, and was only capable of achieving a yield of 29% at best due to the incompatibility between the wetted DE29 and kneading elements. It is important to acknowledge that the poor performance of the TSG in the yield criteria would therefore be different if the powders used in this study had been less heat and moisture sensitive. If the TSG is removed from consideration, then it becomes evident that the Roller Compactor has a lower yield than the wet granulation technologies. This is because in dry granulation technologies, there is typically a compaction step to produce a compact which is followed by a milling step to produce granules. The milling step results in a high breakage rate which produces a lot of fines as well as granules. During milling, there is no driving force for bonding, so these produced fines cannot reform into granules. This linear pathway which ends with a breakage step limits the maximum yields possible in the Roller Compactor. Breakage also exists in wet granulation processes. However, unlike in dry granulation, the fines produced through breakage in wet granulation processes are capable of contacting binder droplets and surface wet granules to reform into granules. This cyclic pathway results in wet granulation processes typically having a higher upper limit for process yield compared to dry granulation processes.

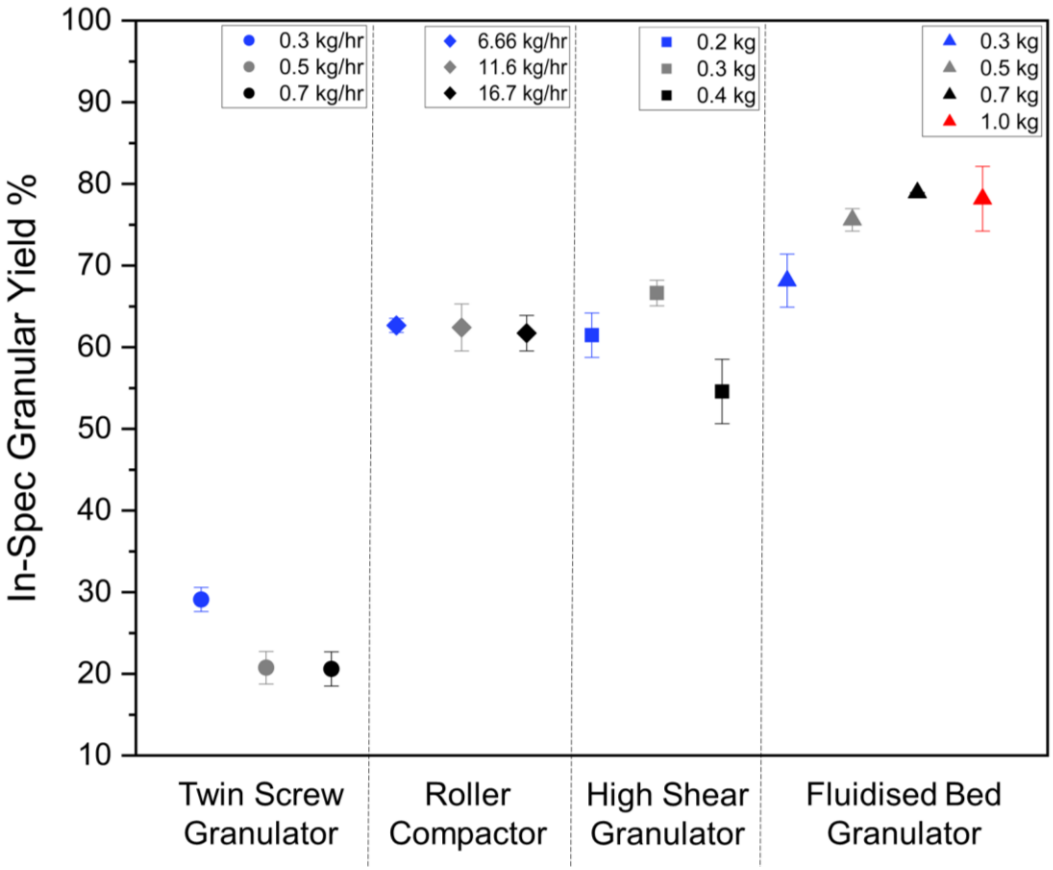

Figure 4.7: Comparing yield of the different granulation pathways. The TSG had the lowest yield and was an outlier compared to the other evaluated granulators. This is because the use of Kneading Elements proved to be incompatible with the DE29 material as it led to caking. Therefore a Conveying Element only screw configuration was used which provided a poor degree of mixing leading to the low yield. The remaining wet granulators produced better optimum yields than the RC. This is attributed to the cyclic nature of wet granulation where fines produced via breakage can undergo wetting to reform into granules. Meanwhile, dry granulation follows a linear pathway where bonding occurs first (during compaction to form a ribbon) which is followed by breakage to form granules and fines (during milling). When fines are produced during milling there is no opportunity for them to reform into granules leading to considerable material waste. This difference between the granulation pathways limits the maximum yield potential of dry granulation technologies.

Specific Energy is the second metric for evaluating process sustainability as it reflects energy efficiency. So far, Section 4.3 has only considered the energy consumption of producing granules (between 0.5 mm and 2 mm) within the granulator units themselves. However, to fairly compare different technologies, the energy consumption of the entire granulation pathway going from dry powder to dry granule must be considered. This is because not all the granulators produce the same end product, with the Roller Compactor and Fluidised Bed Granulator producing dry granules, while the High Shear Granulator and Twin Screw Granulator produce wet granules that require an additional drying stage. Figure 4.8 shows the Specific Energy of the entire granulation pathway for the different technologies compared against each other. As evidenced by the decreasing Specific Energy, the energy efficiency of the pathway improves in the following order: Twin Screw Granulator, Fluidized Bed Granulator, High Shear Granulator and Roller Compactor.

The least efficient technology by a considerable margin is the TSG. This can be attributed to two things, the first is the low yield of the unit which meant that the mass of in-spec granules produced was very low. The second is the energy expensive sub stages that are involved in the Twin Screw Granulation process. Figure 4.9 shows example energy consumption distributions for the different units involved in each granulation pathway. Each technology is represented by its most energy efficient condition. In the case of the TSG, this is at a throughput of 0.7 kg/hr. It is evident that the actual granulation process requires a minimal amount of energy (13%) compared to the drying stage (45%) and the energy drawn by the chiller (41%). The chiller is necessary to counteract the buildup of frictional heat and keep the barrel temperature low. Failing to do so means that eventually the barrel temperature increases to the point where caking occurs leading to the jamming of the screws. The need to include such an energy expensive unit in the granulation process, along with the low yield, results in a far more uneconomical process pathway compared to the other technologies. The advantage of the energy consumption distribution data shown in Figure 4.9 is that the energy expensive stages can be easily identified so manufacturers are aware of what stages require more optimization when making the overall pathway competitive from an energy efficiency perspective. For the Twin Screw Granulator, it seems that the cooling process and the drying stage need the most attention when it comes to optimizing the pathway to be as energy efficient as possible. Alternatively, a way must be found to improve the yield so that it can compensate for the energy intensive nature of the process.

The second most energy inefficient process pathway was determined to be the Fluidised Bed Granulator. This is due to the granulator itself being very energy intensive as it needs to generate and maintain a heated air flow. Despite being very energy intensive, it produced the highest yield of all the evaluated technologies as shown by Figure 4.7. This high yield compensated for its high energy usage and made it far more energy efficient than the TSG and meant its Specific Energy was more in line with the HSG and RC.

The High Shear Granulation pathway was the second most energy efficient. Similarly, to the TSG, it was found that the energy consumption by the granulator is in the minority when the production pathway is looked at as a whole. This is because the drying stage encompasses the vast majority of the energy cost of the production pathway. For instance, as shown in Figure 4.9, at the 0.3 kg batch size condition the drying step accounted for 84% of the total energy consumed. It is this drying stage that manufacturers should focus on if the aim is to produce a more energy efficient HSG pathway.

Finally, Roller Compaction was found to be the most energy efficient production pathway. As presented in Figure 4.2, only one unit – the Roller Compactor, was involved in the transition from dry powder to dry granule. This makes it a rather simple pathway requiring less stages which translates to less energy usage. For instance, since it is a form of dry granulation, it means that the energy cost associated with spraying the liquid and the subsequent high energy cost associated with drying the produced wet

granules are entirely avoided. Avoiding this drying step is a luxury that the wet granulation pathways do not have, making them far more energy expensive than the Roller Compactor.

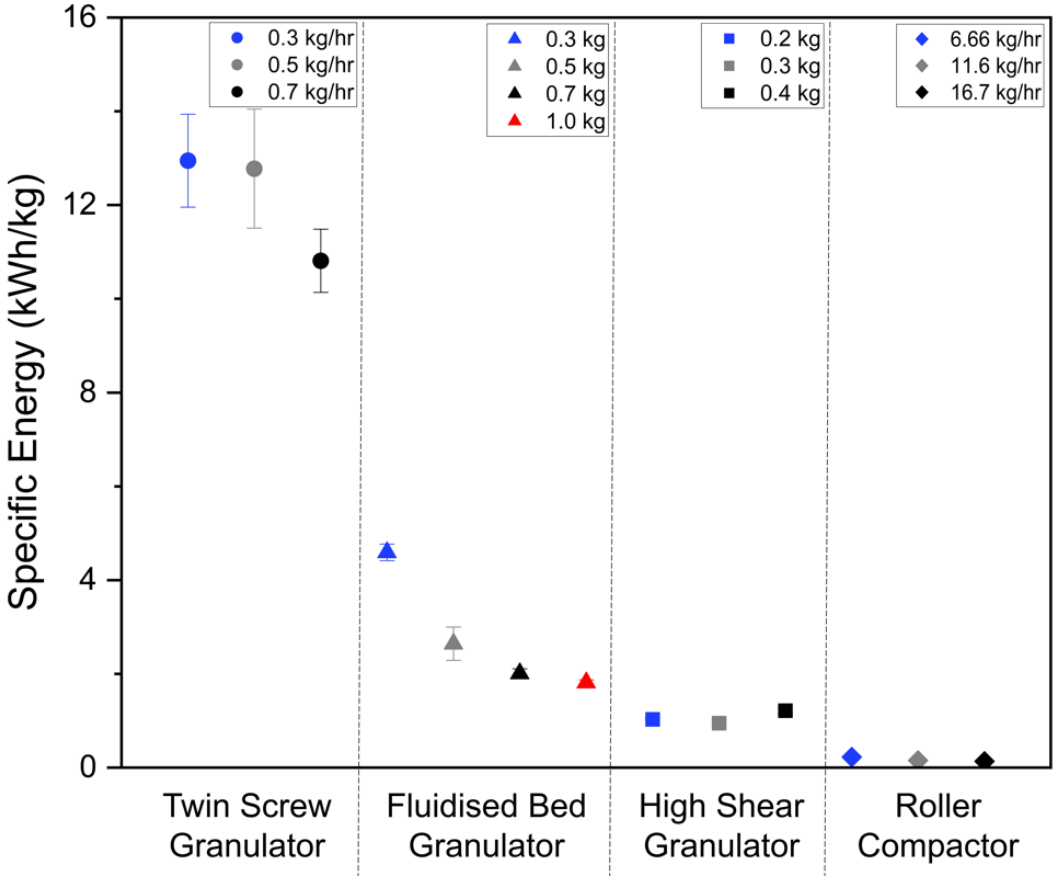

Figure 4.8: Comparing the Specific Energy of the different granulation pathways. The wet granulation pathways displayed a far higher Specific Energy than the Roller Compactor indicating that they were less efficient. This is primarily attributed to the energy intensive nature of the drying step required for the wet granulation pathways. In the case of the Twin Screw Granulator, this was further aggravated by the low yield and low throughput of the process limiting the mass (kg) of granules produced which led to a very high Specific Energy even in comparison to other wet granulation technologies. The TSG also required the use of another energy intensive unit (the chiller) to function which further increased the energy consumption of the pathway.

The energy consumed by different granulation processes directly determines their carbon footprint. For example, the UK Department for Business, Energy and Industrial Strategy reports that, on average, the generation of 1 kWh of electricity in the UK results in 0.20707 kg CO_2 equivalent emissions. Consequently, dry granulation technologies such as Roller Compaction are not only the most energy-efficient but also exhibit the smallest carbon footprint.

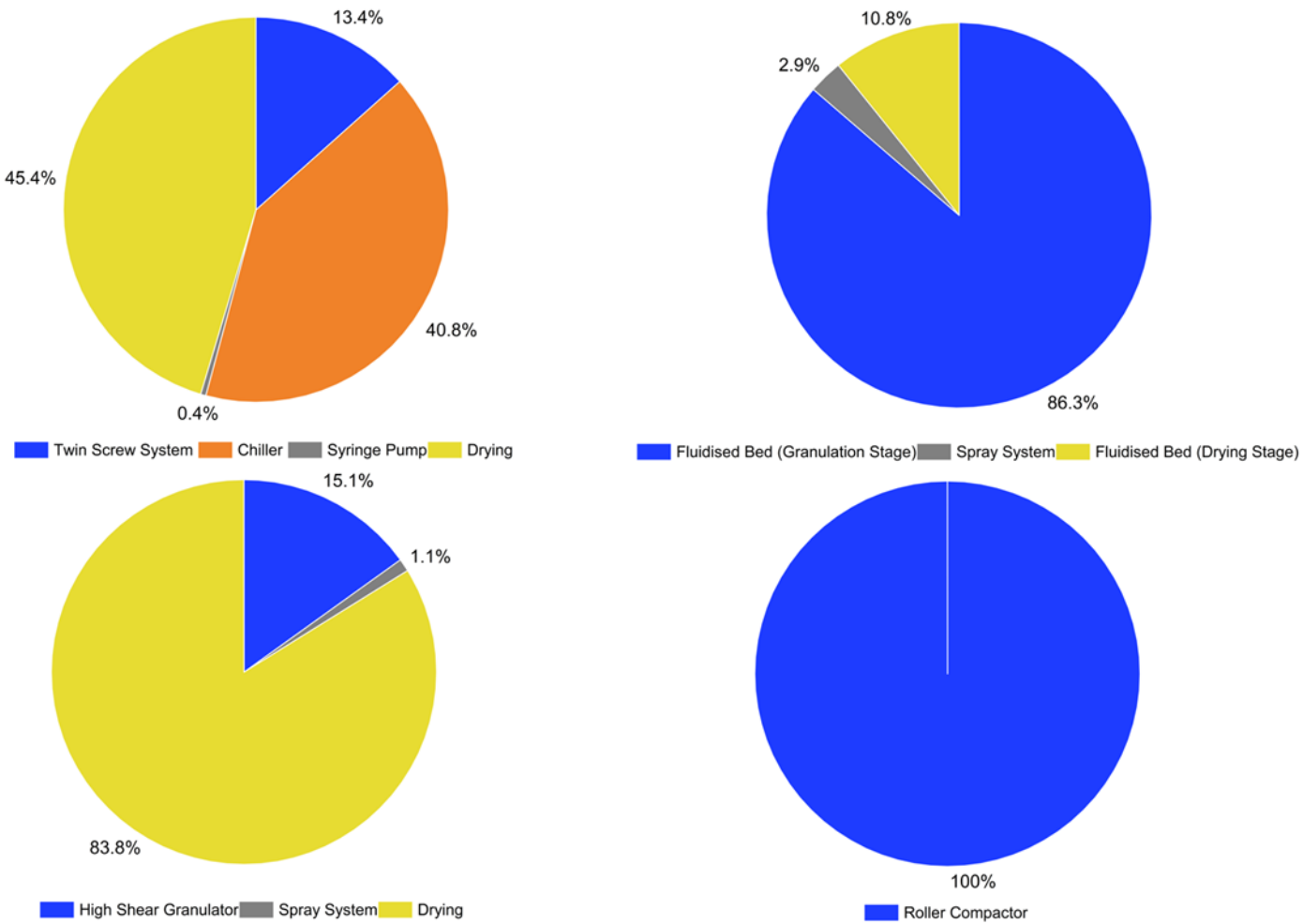

Figure 4.9: Energy consumption distribution of the different units involved in each production pathway, represented by the most energy efficient condition for each technology. Top Left: Twin Screw Granulator operating at a throughput of 0.7 kg/hr. Top Right: Fluidised Bed Granulator operating at a 1 kg batch size condition. Bottom Left: High Shear Granulator operating at a 0.3 kg batch size condition. Bottom Right: Roller Compactor operating at a roll speed of 9 rpm (16.7 kg/hr)

The final sustainability metric that competing technologies can be judged by is the rate at which in-spec granules are produced. This has been classified as the Specific Time which is the hours required to produce a kilogram of in-spec granules. A lower Specific Time means facilities need to stay active for shorter durations of time which reduces energy and labour costs leading to a more affordable and sustainable product. The total run time of the granulation pathway to produce dry granules was accounted for in the total time. Also included with the batch technologies (HSG and FBG) was the time required to clean and reset the unit so that a new run could begin. This was done to help highlight the differences between batch and continuous manufacturing technologies with regards to time. For the High Shear Granulator, the cleaning and reset time was 45 minutes. Whereas for the Fluidised Bed Granulator, this was 2 hours. Cleaning time was not included for the continuous processes such as the TSG and RC. This is because these units are capable of running indefinitely as long as the process conditions chosen prevent significant material caking in the unit. Therefore, operating at optimum conditions, their cleaning time compared to their overall run time is negligible or many multitudes smaller than the batch technologies. For this reason, the cleaning time was not included when calculating the Specific Time for the TSG and RC. Once again, the Roller Compactor proved to be the most efficient technology based on Specific Time as shown by Figure 4.10. This is due to its continuous nature, large throughput and elimination of the drying step leading to a reduction in overall operating time. Using the lowest Specific Time (indicating the best time efficiency) to represent each technology, the wet granulation technologies can be ranked with the TSG being the least efficient, followed by the HSG and finally the FBG proving to be the most efficient. Similarly to when considering Specific Energy, the poor performance of the TSG can be attributed to its low throughput (that it could be operated at without process failure occurring) and low yield. This meant that the mass of in-spec granules produced by this technology was very low compared to technologies like the Roller Compactor which operated at significantly higher throughputs. However, whereas previously when considering Yield and Specific Energy, the TSG had been a major outlier, here it proved to be more competitive with the other wet granulation technologies. This is due to the continuous nature of the process, meaning significant savings in the cleaning time, which compensates for the low throughput and low yield nature of the process.

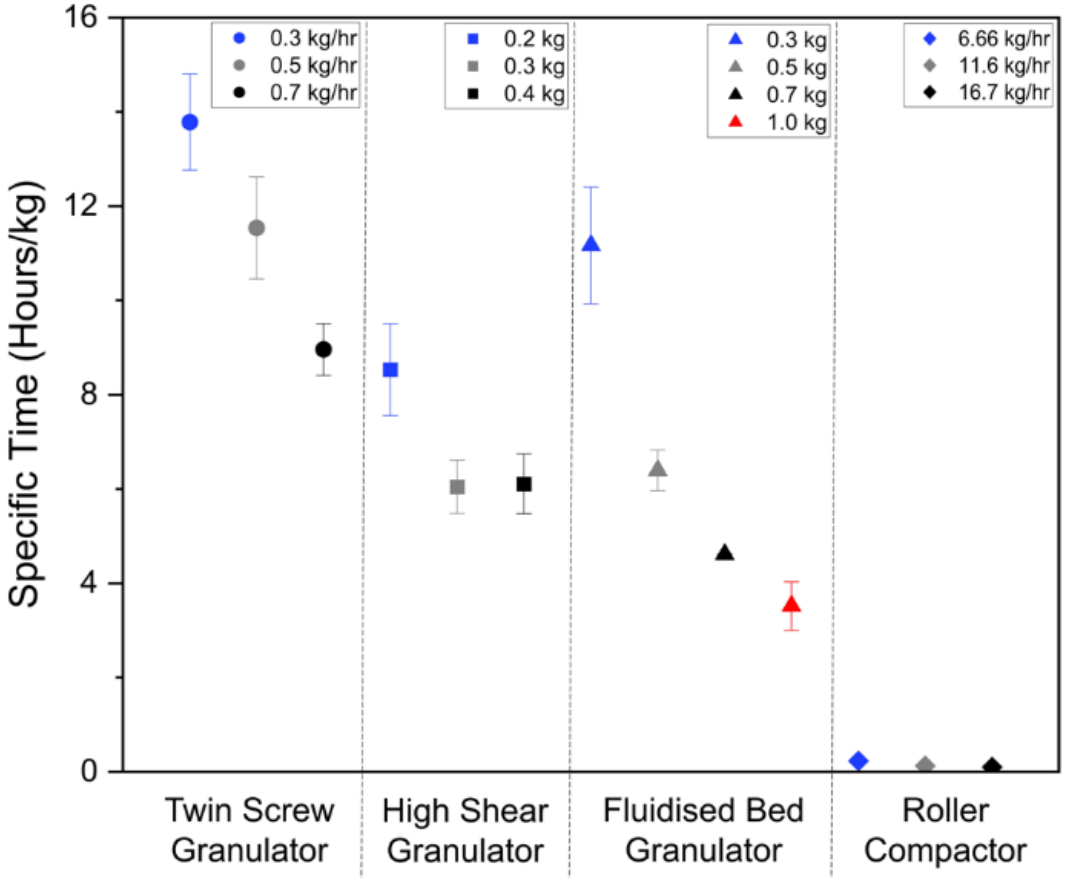

Figure 4.10: Comparing production rates of the different granulation pathways in terms of Specific Time, with a lower Specific Time indicating a more time efficient process. The Roller Compactor was found to be the most time efficient process due to its continuous nature, high throughput and elimination of the drying time (which is required by the other wet technologies) Previously, when considering Yield and Specific Energy, the TSG was a major outlier compared to the other wet granulation technologies. Here the TSG is more competitive with the HSG and FBG with its continuous nature enhancing the time efficiency of the process, despite its low yield and low throughput.

4.4 Granule suitability

When choosing the optimum granulation technology, the efficiency of the process with regards to yield, energy and time are only some of the considerations that manufacturers have to make. Other considerations include the resultant granule characteristics and whether those characteristics fit with the ultimate product specification. This is an important consideration because the different technologies produce vastly different granules. These differences are highlighted by Figure 4.11 which show X Ray scans of granules collected from the different technologies at the optimized conditions. The clearest difference is in granule porosity, with granule porosity varying significantly between the technologies. The High Shear Granulator and the Roller Compactor had the lowest porosities that were similar to each other. Porosity then increased going from the Twin Screw Granulator to the Fluidized Bed Granulator. These differences arise due to the varying extent to which granules experience consolidation in the different granulators. Maltodextrin granules undergo the greatest densification and consolidation in the High Shear Granulator under the conditions evaluated in this study. This is because the tightly

packed granules are accelerated to high velocities in the HSG where they experience a high intensity of collisions. These high energy collisions squeeze liquid to the surface and consolidate the granules producing a product that has a very low porosity. This is especially true for the parameters chosen for this HSG process, where the liquid was added slowly to prevent caking, which resulted in an extended run time that provided ample opportunity for consolidation to occur. Furthermore, the use of water binder also results in a granule with a lower porosity. This is because the water dissolves the Maltodextrin powder which then flows into the intergranular voids. During drying, the water evaporates, leaving behind solidified Maltodextrin where the voids once were, which reduces the granule porosity. The low porosity nature of HSG granules is well documented in literature [94,95]. The Roller Compactor also produce high density granules with a similar porosity to the HSG. The high density nature of Roller Compacted granules occurs because the basis for the bonding within the Roller Compactor involves minimizing the distance between particles as much as possible to increase the number of contact points and maximize the Van der Waals forces of attraction. The TSG produced the next most porous granules. In the TSG, granules undergo densification as they are compressed between the narrow channel width between the screws and barrel. However, the granule porosity produced by the TSG in this study is lower than that typically seen from the technology. This can be attributed to the lack of kneading elements used in this work which is where densification predominantly occurs in the unit. Finally, the FBG produced the most porous granules by far. This is due to the lack of consolidation and densification that occurs within the unit as there are little to no compaction forces acting within the granulator. The highly porous nature of FBG granules has been established by literature comparing HSG and FBG technologies [94,95].

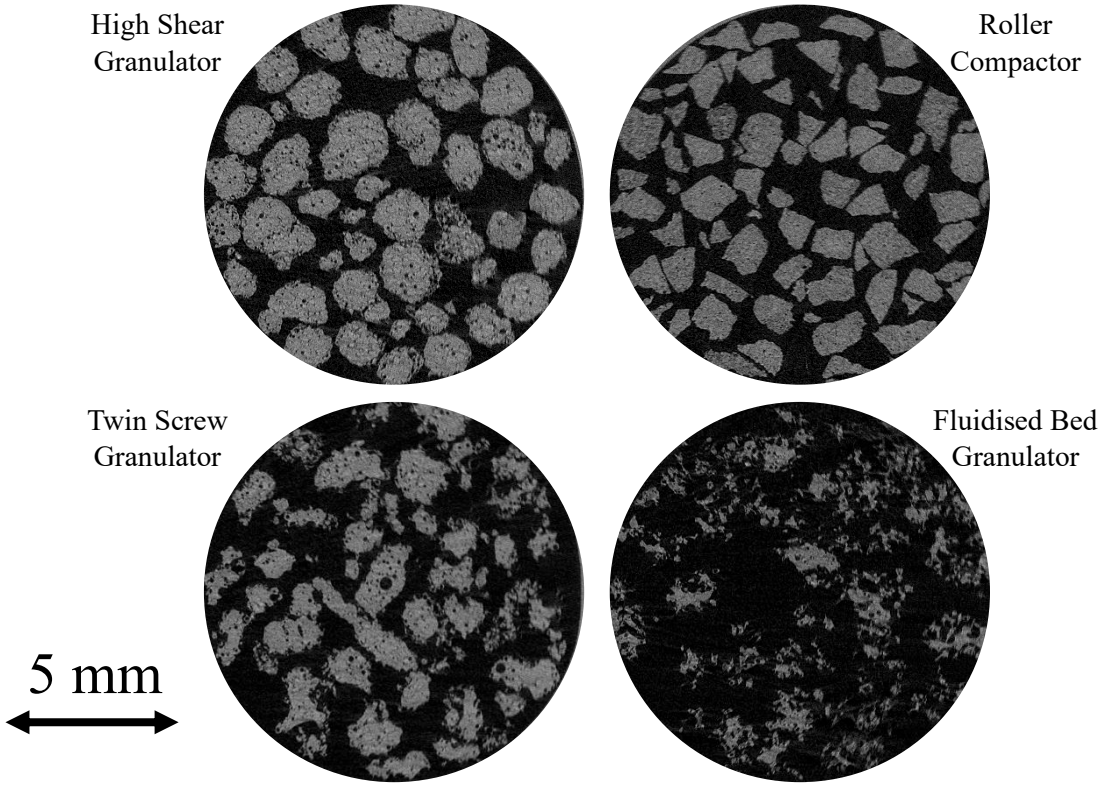

Figure 4.11: X-Ray Scans of granules from the 1 - 2 mm size class representing the different granulation technologies with white regions indicating solids while black regions indicate voids. The granules show significant variations in both shape and porosity depending on the granulation technique chosen. Granules from the most energy efficient conditions were chosen to represent each technology. Top Left (HSG 0.3 kg), Top Right (RC 9 rpm), Bottom Left (TSG 0.7 kg/hr), Bottom Right (FBG 1 kg)

These differences in granule shape and porosity will significantly affect the product granule attributes. In order to quantify the differences between the granules produced via the different manufacturing routes; Granule Flowability, Granule Friability and Dissolution Time were all evaluated. These are key attributes which will critically affect subsequent manufacturing steps and influence the perceived quality of the product by the customer. It is important to note that granule attributes can vary significantly within each technology depending on the operating conditions used to produce them. For example, the use of a higher compaction pressure has been shown to significantly reduce granule porosity during a Roller Compaction process [64,66]. Similarly, Rahmanian et al [96] and Rahmanian et al [97] highlighted how increasing impeller speeds in High Shear Granulation lead to increased compaction forces which reduce granule porosity considerably. The values presented throughout Section 4.4 are purely for the optimised operating conditions presented in Section 4.2 and are presented to highlight the variety in granule properties that arise depending on manufacturing route taken and process conditions used.

4.4.1 Granule Flowability

Figure 4.12 presents the relationship between granule flowability and granule sphericity. Figure 4.12 indicates that granule flowability decreases in line with granule sphericity. The HSG produced the most spherical and best flowing granules which are classed as free flowing as they have a ffc above 10. This is followed by the RC, then the TSG and finally the FBG. All three technologies produced granules which are classed as easy flowing which is classified as granules with an ffc between 4 and 10. The RC is at the upper limit of this range, whereas, the TSG and FBG is at the lower limit of this range. The FBG has such a low ffc that it could even be described as borderline cohesive. The superior flowability and sphericity of HSG granules compared to other technologies is well documented in literature [98–101].

The flowability of the bulk DE29 powder was measured at a ffc of 7.6. It is interesting therefore, that despite particle size increasing in all cases, only the HSG and RC led to an increase in flowability. The reason the TSG and FBG led to a worsened particle flowability can be attributed to the aspherical shape of their granules. An aspherical shape means that during motion, granules tend to interlock together to resist movement. This interlocking phenomenon is part of the reason tablets produced from TSG granules have a relatively strong tensile strength compared to other technologies [102]. The FBG granules are also much weaker than those produced by the HSG and RC. This means that when pressure is applied to them during the operation of the shear cell, they are more likely to break. This produces granule fragments which further increases the likelihood of interlocking occurring in the sample, leading to a lower flowability.

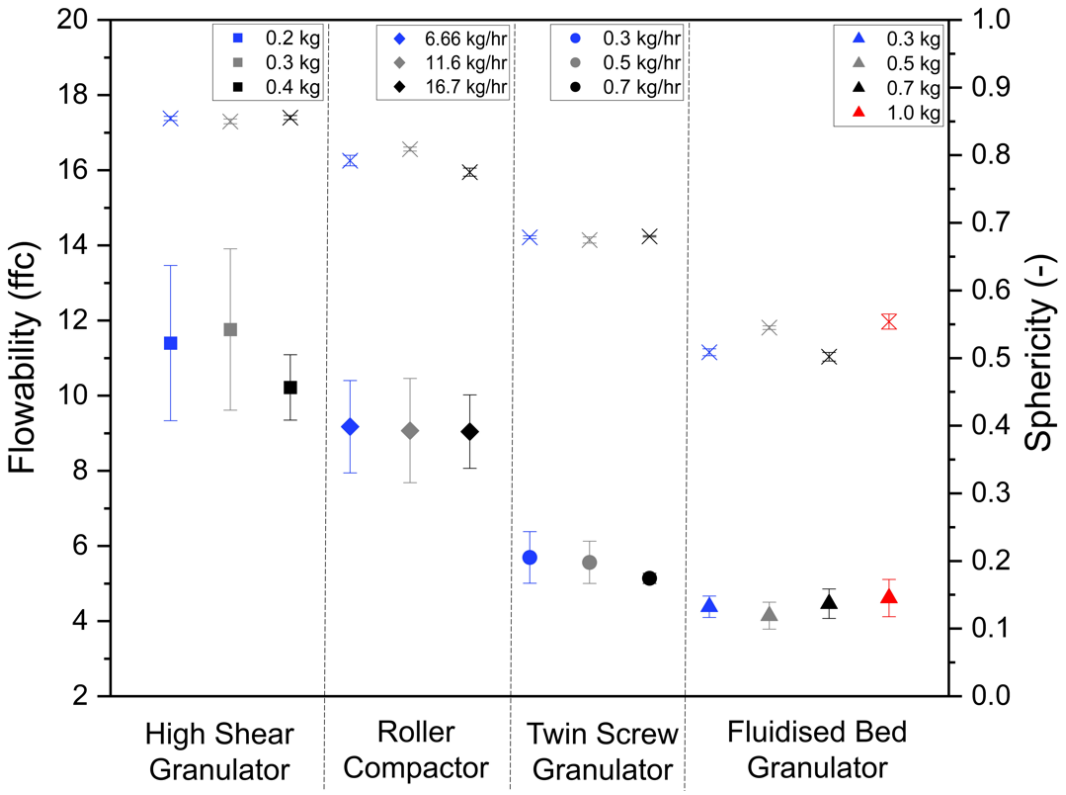

Figure 4.12: Comparing the flowability and sphericity of granules produced by the different technologies. Flowability is represented by the square (HSG), diamond (RC), circle (TSG) and triangle (FBG) symbols respectively. Granule sphericity is represented by the X symbols. Flowability increased with increasing granule sphericity.

4.4.2 Granule Friability

Figure 4.13 shows that granule friability (weakness) increases in the following order: High Shear Granulation, Roller Compaction, Twin Screw Granulation and Fluidized Bed Granulation, which is in line with that presented in literature [82]. This change in granule friability between the technologies seem to be in line with the change in granule porosity obtained via the X Ray analysis. This is because there is a direct link between granule porosity and granule strength. The lower the granule porosity, the closer the primary particles are to each other and the more contact points there are between them. This increases the attractive Van der Waals forces in the granules. Furthermore, it also leads to more mechanical strength due to more mechanical interlocking within the granule and the increased formation of solid bridges between the primary Maltodextrin particles.

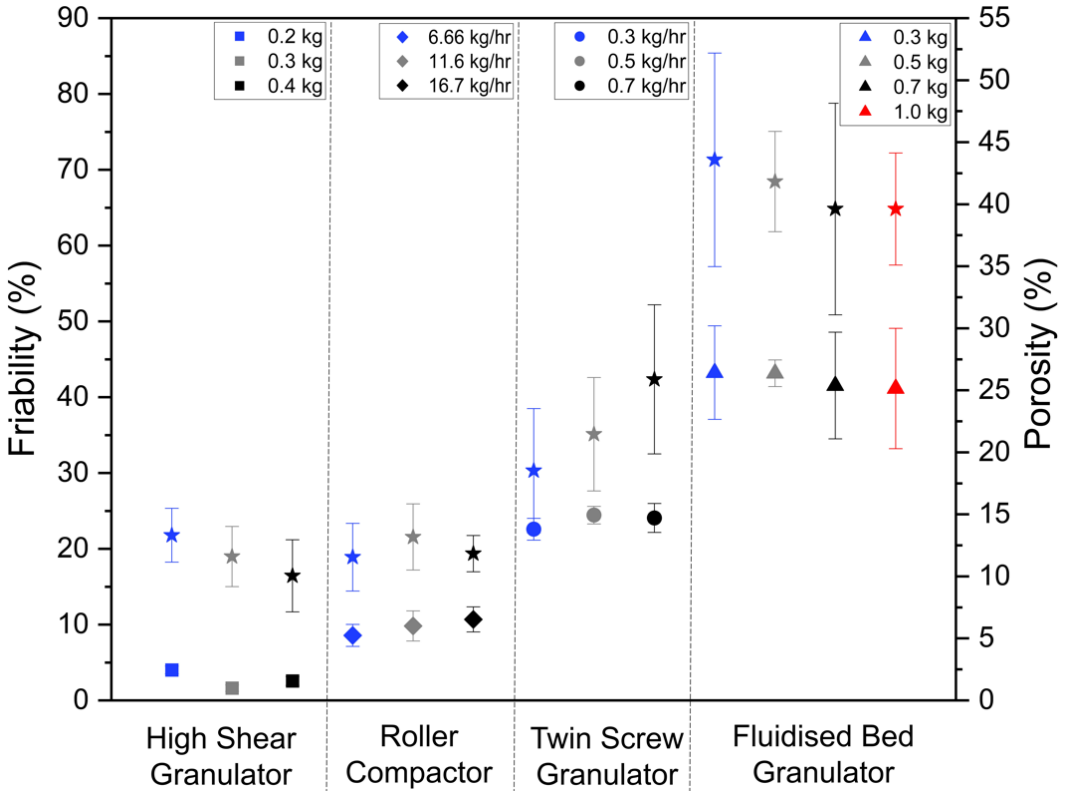

Figure 4.13: Comparing the friability of granules produced by the different technologies. Friability is represented by the square (HSG), diamond (RC), circle (TSG) and triangle (FBG) symbols respectively. Granule porosity is represented by the star symbol. Friability was found to generally increase in line with granule porosity.

4.4.3 Granule Dissolution

Dissolution time decreases in the following order: High Shear Granulation, Roller Compaction, Twin Screw Granulation and Fluidized Bed Granulation, as shown by Figure 4.14. The dissolution time of the granules produced by the different technologies is inversely related to the porosity of their respective granules [103,104]. This is because the denser the granules, the slower the penetration time of the liquid into the granules and the longer the disintegration time.

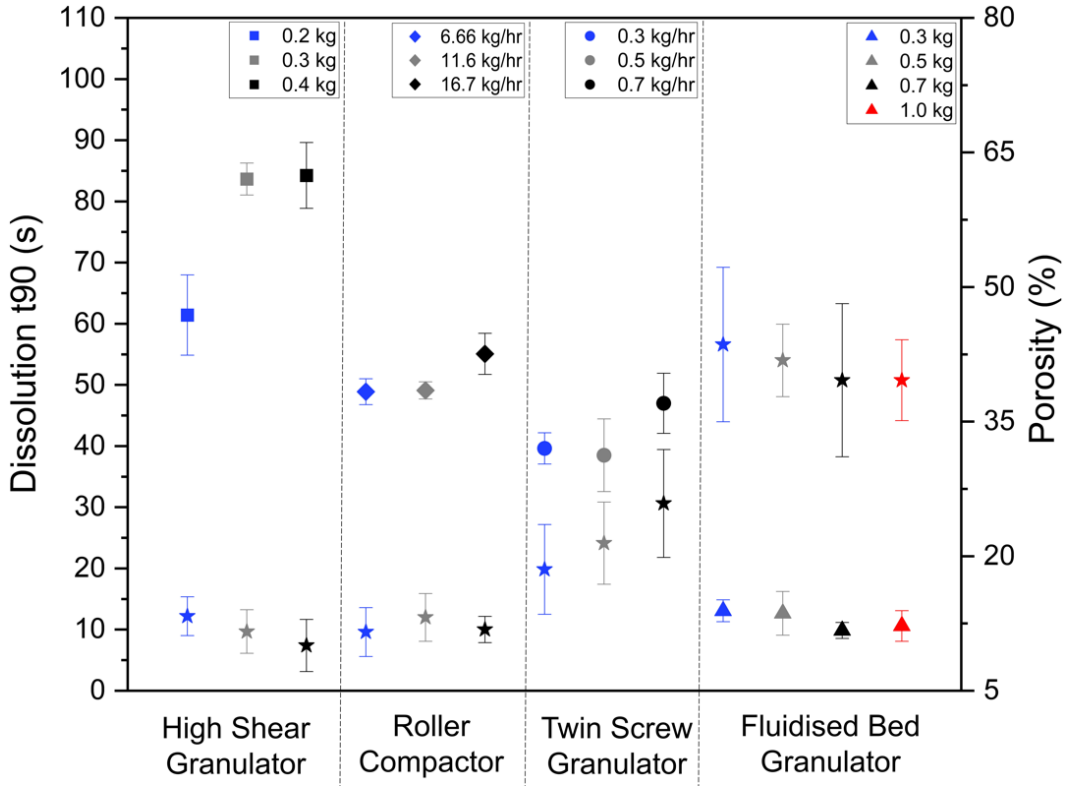

Figure 4.14: Comparing the dissolution time of granules produced by the different technologies. Dissolution time is represented by the square (HSG), diamond (RC), circle (TSG) and triangle (FBG) symbols respectively. Granule porosity is represented by the star symbol. Dissolution time was found to be inversely related to granule porosity.

4.5 Choosing the optimum granulation pathway

As discussed in this study, there are a lot of considerations that should be accounted for when deciding the optimum process route. These include those considerations looking at the efficiency and sustainability of the process with regards to material, energy and time. As important are how suitable the product granule is to its end purpose which depends on granule characteristics such as flowability, friability and dissolution time. Methods to help account for all of these parameters together in a logical and sensible way are critical to the development of a coherent decision making system. One possible approach is evaluating the technologies graphically as shown in Figure 4.15 and Figure 4.16 through the use of parallel co-ordinate graphs or radar graphs [105]. Figure 4.15 and Figure 4.16 rank the performance of the granulation technologies in each sustainability and suitability metric. The ranking is based on how desirable the performance is for an example scenario where the desired product is a strong and quickly dissolving granule. The parallel coordinate graphs and radar graphs were made using the data from the most energy efficient condition from each granulation pathway being used to represent the technology. These conditions are as follows: Fluidised Bed Granulator (1 kg), High Shear Granulator (0.3 kg), Roller Compactor (16.7 kg/hr) and Twin Screw Granulator (0.7 kg/hr). Please see Appendix Tables A1-A3 for more information on how these figures were produced.

These graphical methods allow the data to be visualized easier which facilitates better decision making. For example, the parallel co-ordinate graph shown in Figure 4.15 visually classifies the performance of each technology in the considered metrics according to the Excellent, Good and Poor regions. This graph can then be used to quickly and easily eliminate unsuitable processes from the decision making process. For this scenario (production of a strong and quickly dissolving granule), it is evident that the Twin Screw Granulator is predominantly in the poor region across the board and is therefore highly inappropriate as a general process option in this case. Furthermore, it's clear that the FBG is the only one present within the poor region for granule friability. Since the scenario requires the granules to be strong, this granulation technique can likely be discounted from further evaluation as there are better options. Meanwhile the HSG is placed in the poor category for a quickly dissolving granular product and so can also be discounted from further consideration. This means that for this example scenario, the RC can quickly be identified as the most suitable option. This illustrates how Parallel Coordinate Graphs can be used to aid the decision making process when considering different scenarios.

Meanwhile, Figure 4.16 presents a radar chart which uses normalized data to rank the performance of each technology relative to each other on a scale of 0 to 1. The closer the rank is to 1, the more desirable the performance is. If there is one key factor that the manufacturer is concerned about, then this graph can be used to visually evaluate the performance of the technology in that factor. For example, if Dissolution Time is the key parameter of importance to the manufacturer, then it is clear that the Fluidised Bed has the closest ranking to 1 and is the best option. Furthermore, if there are multiple parameters of importance, then the radar chart can be used to determine the most suitable process by determining the area encompassed by the plot produced by those parameters. For the example given in Figure 4.16, it is evident that the Roller Compactor has the largest plot area and therefore, is the most suitable process for the example scenario.

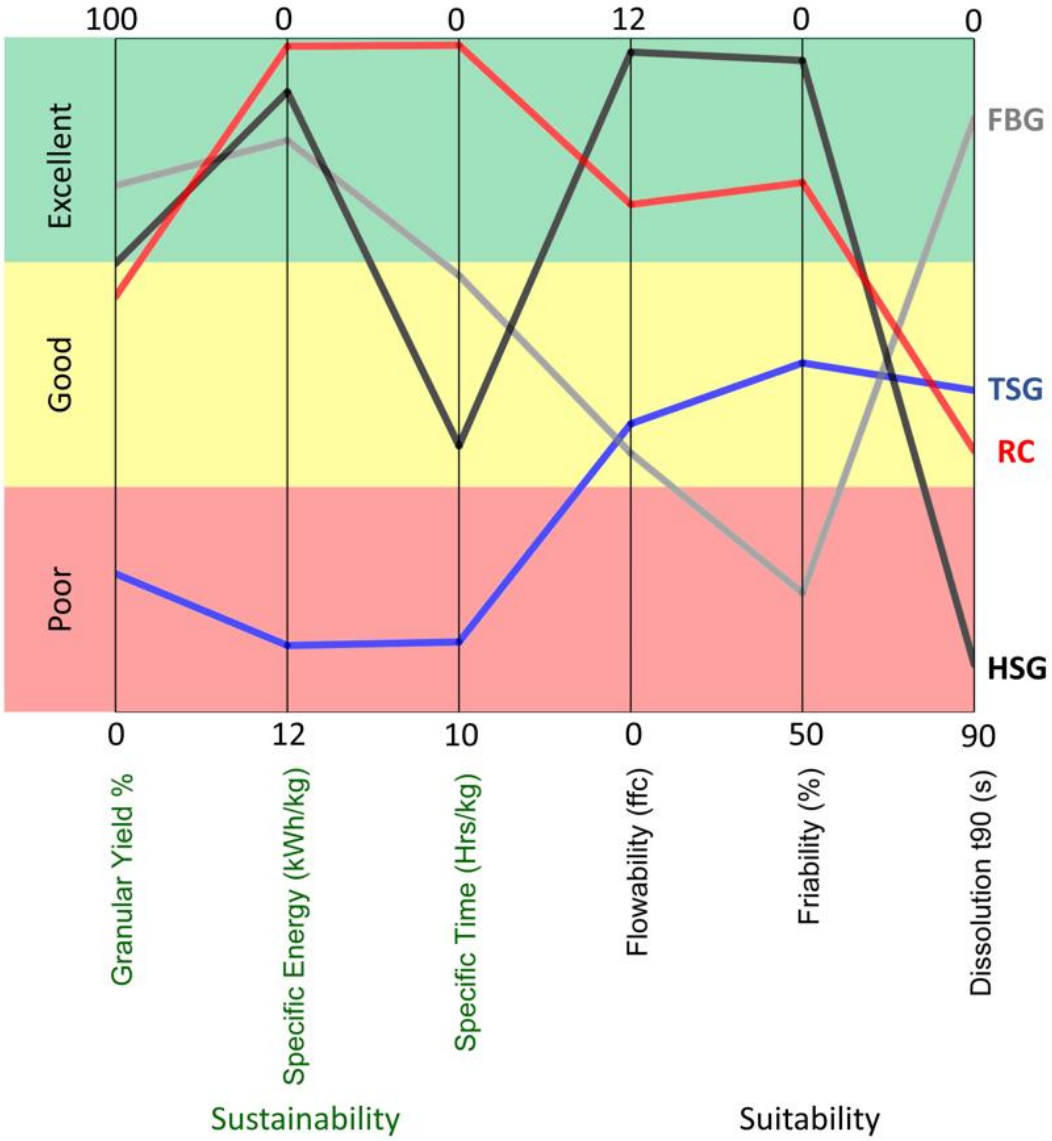

Figure 4.15: Parallel co-ordinate graph which categorises the performance of each considered aspect of the technology into poor, good or excellent. In this example, which is for the production of a strong, quickly dissolving granular product, a high friability and long dissolution time would be classed as undesirable traits leading to a poor performance. Values from the most energy efficient condition was chosen to represent each technology. The sustainability of the chosen conditions presented in Figure 4.7, Figure 4.8 and Figure 4.10 are paired with values for granule attributes shown in Figure 4.12, Figure 4.13 and Figure 4.14. The axis for each parameter is decided by whether a high value in that attribute is considered positive or negative. For instance, the higher the granule yield, the more attractive the process. Therefore, a yield of 0% indicates a poor process performance while a yield of 100% indicates an excellent process performance. On the other hand, when considering Specific Energy, a higher Specific Energy indicates a less attractive process. Therefore, a Specific Energy close to 0 kWh/kg indicates an excellent process while a high specific energy indicated by 12 kWh/kg indicates a poor process. This same principle was applied to all the attributes evaluated in this work. The values for each parameter for the different technologies was then plotted on the graph. Overall process performance can be visually determined by evaluating whether a technology is predominantly in the Excellent, Good or Poor regions.

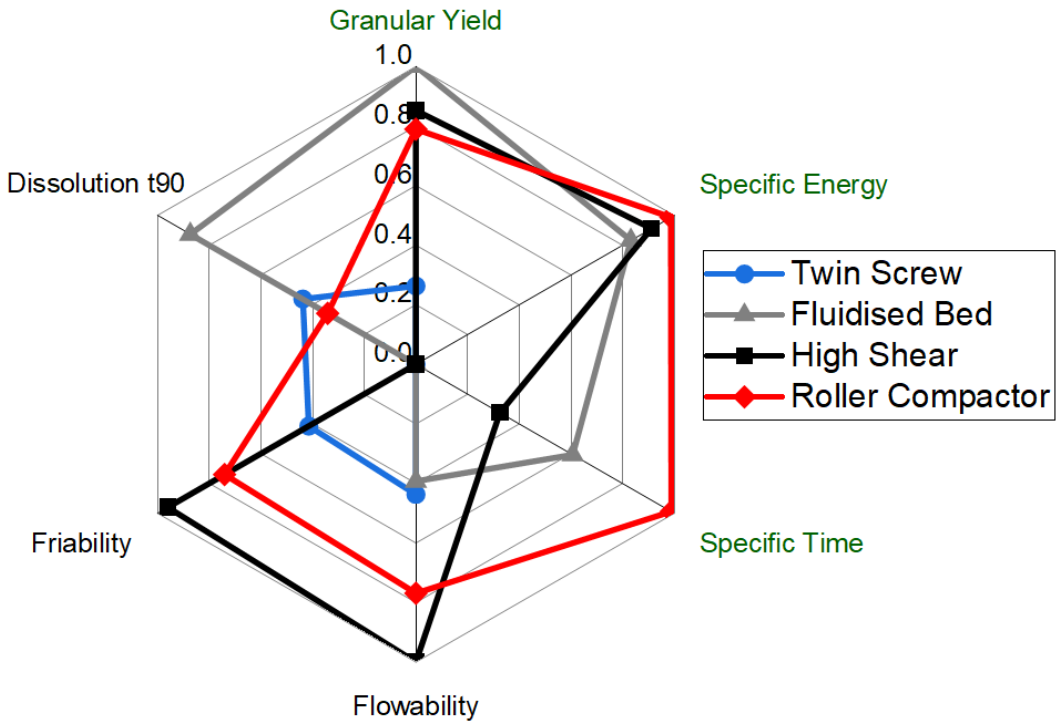

Figure 4.16: Radar chart which presents the performance of each considered aspect of the technology ranked from 0 to 1. The higher the value, the more desirable the performance of the technology in that trait. A value of 1 would indicate the most desirable and a value of 0, the least desirable. As with Figure 4.15, the radar chart was produced for an example case study where a strong, quickly dissolving granular product was required. Values from the most energy efficient condition was chosen to represent each technology. A full mathematical breakdown of how the above ranking was determined is presented in Appendix Table A1-A3. In the first step, the performance of each granulation technology in a given metric was divided by the highest value observed in that metric. For example, looking at Yield, the Yield of each chosen granulator condition is as follows: FBG (1 kg) – 78%, HSG (0.3 kg) – 67%, RC (16.7 kg/hr) – 62% and TSG (0.7 kg/hr) – 21%. Dividing each value by the highest observed yield in the set (which is 78%), gives a rating of 1 for the FBG, 0.85 for the HSG, 0.79 for the RC and 0.26 for the TSG. This procedure is repeated for every metric in a similar manner. However, in certain cases, a high value is undesirable, for instance when looking at Specific Energy and Specific Time. Also, for the chosen scenario (development of a strong and quickly dissolving granular product), a high friability and long dissolution time would also be undesirable. For these undesirable attributes, the calculated ranking for these attributes are subtracted from a value of 1. For example, the TSG had the highest Specific Time of 9 hrs/kg while the RC had the lowest at 0.1 hrs/kg. Dividing these values by the highest Specific Time (9 hrs/kg) then results in the TSG having a ranking of 1 while the RC has a ranking of 0.01 which does not reflect the idea that a ranking closer to 1 is more desirable. It is for this reason that these values are then subtracted from 1 to account for this. Subtracting by 1 gives a ranking for the TSG of 0 while giving a ranking for the RC of 0.99. In this manner the performance of each technology in a given aspect can be easily compared with each other. Overall technology performance can also be evaluated by looking at the area encompassed by the plot. The bigger the area, the better the performance. In this example, the Roller Compactor has the largest area indicating it is the most suitable.

Figure 4.16 can be used to determine the optimum granulation process for a product by calculating the area encompassed by the plot, with a bigger area indicating a more desirable process. However, this approach assumes that all the metrics are equally important. This is often not the case with certain metrics being more important due to their influence on production costs or product appeal to consumers. In those situations, an alternative approach to the graphical methods is to use a priority scoring system. A priority scoring system calculates a score for each process based on the Priority Weighting the manufacturer assigns to each parameter, which is based on their needs. An example method is presented in Table 4.1 which outlines the procedure when applied to the most energy efficient condition for the Roller Compactor (throughput of 16.7 kg/hr) for the production of a strong and quickly dissolving granular product. This quantification of desirability is a methodical and rational way of differencing

between processes based on specific requirements. An important point to note is that the Priority Weighting used in this method has a significant impact on the overall process rating. Therefore, it is important that they are chosen according to an appropriate rationale rather than arbitrarily by the user. An example rationale to base the priority weighting on could be cost. For instance, linking the importance of Yield, Specific Energy and Specific Time to the cost of the raw materials, electricity and labor. A potential rationale for evaluating granule characteristics could be their consumer-perceived importance, as determined through targeted market research studies. The user assigned Priority Weightings are multiplied by the performance of the technology in each metric (as represented by the Technology Coefficient in Table 4.1) to produce a Parameter Rating for each metric. Please see Appendix Table A4-A6 for a detailed breakdown on how these Technology Coefficients are produced. Summing the Parameter Ratings produce a Total Process Rating which judges process desirability based on manufacturer needs and process performance. The most desirable process can be identified by determining which process gives the most positive rating. The Total Process Rating for the Roller Compactor was 0.255 as shown by Table 4.1. Repeating this methodology to the remaining granulation technologies operating at their most energy efficient conditions, the following Total Process Ratings are obtained: 0.146 (Fluidised Bed Granulator), 0.249 (High Shear Granulator) and -0.311 (Twin Screw Granulator) as shown by Appendix Table A4-A10. By comparing the Total Process Rating, it becomes evident that the Roller Compactor is the most desirable process based on the manufacturer's needs with it narrowly beating the High Shear Granulator. Meanwhile, the Twin Screw Granulator is by far the worst option with it possessing the only negative rating between the evaluated conditions. In this way, process desirability can be quantified and the optimum processing route can be chosen.

Table 4.1: Presents the use of a Priority Scoring System to determine the suitability of a process based on the manufacturer needs and process performance. This system was applied to the most energy efficient conditions observed by each granulation technology. A full mathematical breakdown on how this system is applied is presented in Appendix Table A4-A10. Table 4.1 summarises the application of this technique for the Roller Compactor operating at a throughput of 16.7 kg/hr (9 rpm roll speed). In this method, the user assigns weightings for each metric based on their priority. The higher the priority, the higher the weighting given to it. For instance, in the below example, the Specific Energy was the users highest concern so it was assigned the highest Priority Weighting of 0.3. Yield followed as the second highest concern for the user and was assigned the second highest weighting of 0.25. On the other end of the scale, the Specific Time was not a significant consideration for the user and so was assigned the lowest weighting of 0.05. Please note that in this example, these Priority Weightings have been chosen just to illustrate the principle of the procedure and are not based on any underlying rationale. The Priority Weightings are then multiplied by the Technology Coefficients for each parameter. Technology Coefficients can be produced by normalising the experimental data gathered for each parameter which are presented in Figure 4.7, Figure 4.8, Figure 4.10, Figure 4.12, Figure 4.13 and Figure 4.14. Negative signs are used when higher Technology Coefficient values are undesirable. If the same scenario as Figure 4.15 and Figure 4.16 is used (production of a strong and quickly dissolving product) then a high Specific Energy, Specific Time, Friability and Dissolution Time are undesirable and therefore have been assigned negative signs. A detailed breakdown on how these coefficients are produced are shown in Appendix Table A4-A6. Multiplying the Priority Weighting with the Technology Coefficient produces a Parameter Rating for each metric which takes into account the importance and process performance in that metric. Summing the Parameter Ratings then gives a Total Process Rating which in the case of the Roller Compactor is 0.255. The most suitable process for a set of Priority Weightings can then be determined by comparing the Total Process Ratings between different processes and evaluating which has the most positive result.

Parameter	Priority Weighting	✖	Technology Coefficient	=	Parameter Rating
Yield	0.25		0.79		0.197
Specific Energy	0.3		-0.01		-0.004
Specific Time	0.05		-0.01		-0.001
Flowability	0.2		0.77		0.154
Friability	0.1		-0.26		-0.026
Dissolution Time	0.1		-0.66		-0.066
Total Process Rating					0.255

4.6 Conclusion

While multi-granulator studies do exist they are often limited in scale, only looking at a small number of granulators, and narrow in scope, often choosing to focus primarily on granule attributes. This is the first study to evaluate the four predominant granulation technologies based on such wide ranging process sustainability and granule suitability metrics. The sustainability of the process has been scrutinized with regards to material, energy and time. Also looked at was the suitability of the process to produce granules that are fit for purpose. Results showed that the granulator performance varied between the measured attributes with no granulator appearing the clear winner in all cases. The Roller Compactor was found to be the most efficient with regards to energy and time. Meanwhile, the Fluidised Bed Granulator was found to be the most efficient with regards to material usage and produced the quickest dissolving granules. The High Shear Granulator produced the best flowing and strongest granules. This highlights the difficulty faced by manufacturers when deciding the optimum production

pathway in cases where there is no clear winner. It is crucial therefore that manufacturers take a ‘big picture’ approach to the decision making process and look at all the parameters discussed by this paper as a bare minimum. Both visual and analytical methods have been proposed by this study to help in this. Utilizing them to match sustainable manufacturing technologies to products they are suited for is key in the drive to make the food industry more sustainable and affordable.

5 Development of a High Shear Wet Granulation Regime Map to Avoid Caking in Heat Sensitive Amorphous Food Powders

Abstract

Temperature and humidity induced caking of amorphous food powders is a major issue during food granulation. Caking must be avoided because it results in the permanent loss of material and process failure. The impact of key process parameters on the caking phenomenon in a High Shear Granulator was assessed across a range of Maltodextrin powders. Findings reveal that increasing impeller speed, batch size and run time promoted the rate of heat generation in the system. The resulting increase in bed temperature was found to impact the different Maltodextrin powders to varying extents depending on the powder T_g, with high DE Maltodextrins showing greater sensitivity to temperature increases. This study also highlighted that high DE Maltodextrins require less water for effective granulation. This behavior correlated with the rate at which the water binder's viscosity increases as it incorporates Maltodextrin powder during granulation. High DE Maltodextrins demonstrated a slower viscosity rise with increased solid composition than low DE counterparts, producing a binder system that remains mobile and adhesive at higher solid contents, thereby facilitating more efficient granulation. A parameter k_μ was modelled to reflect this relationship. The parameters $(T - T_g)$ and $(L/S)/k_\mu$ were then used to produce a caking regime map for the High Shear Granulation system. This regime map delineates an optimal region for granulation and a region where a high likelihood of caking occurs. The threshold of this caking region was set at a T-Tg of 40˚C and $(L/S)/k_\mu$ value of 0.0325.

Highlights

- Established regime map for caking, delineating optimum operating zone for granulation
- Critical thresholds for caking at a T-Tg value of 40˚C and $(L/S)/k_\mu$ value of 0.0325
- The higher the DE, the more sensitive to granulation temperature due to lower T_g
- High DE Maltodextrin need less water for granulation due to more efficient binding

This chapter forms the basis of the following paper:

Y.H. Karunanayake, L. Brütsch, V. Meunier, G. Niederreiter, A.D. Salman (2025). Development of a high shear wet granulation regime map for the controlled agglomeration of heat sensitive amorphous food powders. Powder Technology, Volume 466, 121470

https://doi.org/10.1016/j.powtec.2025.121470

5.1 Introduction

Granulation is a size enlargement process that is commonly employed to improve material handling properties, extend shelf life and alter reconstitution rates. Wet granulation describes a process where liquid binder is added to an agitated powder bed which results in the formation of liquid bridges between powder particles. These bridges allow particles to bind together to form larger agglomerates called granules [106]. High Shear Granulators (HSG) are popular wet granulators where agitation is achieved through a rotating impeller. This study uses a Eirich HSG, which possesses a spinning bowl alongside the rotating impeller, to further promote agitation and enhance the mixing efficiency [107].

The mechanism of wet granulation is well understood with numerous studies developing regime maps for High Shear Wet Granulation (HSWG) processes [30,36,108]. These regime maps are typically developed through experiments on heat insensitive crystalline or insoluble powders and represent the behavior of the mix in terms of the liquid content and applied stress. The most well-known regime map is that of Iveson and Litster [30] which represented the mix behavior in terms of the pore saturation (representing the liquid content) and the granule Deformation Number (representing the acting stress in the system). Similarly Tan and Hapgood [108] choose to use the L/S ratio and impeller speed to characterize granulation behavior in their regime map. While well developed, these regime maps are produced through experiments with insoluble or crystalline powders which makes them difficult to apply to amorphous powder granulation. This is because amorphous powders differ significantly from crystalline powders. One significant difference is in the existence of a Glass Transition Temperature (T_g). This describes the temperature at which an amorphous material transitions from a rigid, glassy state into a rubbery, viscous state. This transition can significantly alter the behavior of the material with respect to deformability and stickiness [109] which changes the behavior of the powder during granulation. None of the existing regime maps for HSWG currently consider the T_g parameter or T_g based phenomenon such as caking which highlights their inadequacy when applied to amorphous powders. Furthermore, amorphous powders dissolve more quickly and to a greater extent than insoluble or crystalline powders. Therefore, when exposed to water binders, they have the potential to dissolve into the binder to significantly alter binder properties such as stickiness and mobility. While existing literature has considered the effect of the initial binder viscosity on granulation [110], there were no studies found which evaluated the effect of the changing binder properties, due to binder-powder bed interactions, on the granulation process.

One of the most serious T_g based phenomena is caking. Caking describes a scenario where the powder bed temperature increases above the T_g and the powder transitions to the viscous state. This leads to an increase in the powder's stickiness and an uncontrolled, aggressive agglomeration process. Consequently, excessive powder-powder and powder-equipment adhesion occurs which results in the formation of large powder lumps and interferes with normal equipment operation [111]. It is comparable

to the overwetting phenomena when granulating crystalline powder where too much liquid is added which leads to the production of large, soft lumps or a slurry [30]. Compared to the weak, soft lumps formed during overwetting, caking is a more serious problem as it results in the formation of rigid, strong lumps, which may cause equipment damage. Furthermore, while the overwetting scenario can be 'corrected' by the addition of powder to reduce the liquid saturation of the mixture, the formation of caked material is an irreversible process which leads to the permanent wastage of material. Therefore, a thorough understanding of caking is needed so it can be avoided in the food industry. T_g based caking within granulation is an under researched topic with only a few existing studies. For example, Palzer [111] studied the caking occurring inside a Fluidised Bed Granulator while Saleh et al. [70] investigated caking in a Twin Screw Granulator and Mahmah et al. [68] studied caking onto the rollers in a Roller Compactor. However, no studies could be found which evaluated the T_g based caking process within the HSG.

The aim of this study is to comprehensively investigate the factors affecting caking in the HSG across a range of amorphous powders. The investigated factors include L/S ratio, Impeller Speed and Batch Size. The process parameter's impact on caking will be linked with the material properties of the amorphous powders to develop a regime map for the HSWG process which will identify boundary conditions for normal operation and caking. The implementation of this regime map will aid in the safe and sustainable granulation of amorphous powder by minimizing risk to equipment and material loss.

5.2 Materials and Methods

5.2.1 Materials

Maltodextrin powder was chosen for this work due to its commonplace use in the food industry. The following Glucidex Maltodextrin powders (Roquette, France) were selected for this study: IT6, IT12, IT21 and IT29. The IT grade is equivalent to the dextrose equivalent (DE) of the powders. Henceforth, the Maltodextrin grades will be referred to by their dextrose equivalent (DE) numbers. The powders were all conditioned at 20% Relative Humidity and 20°C for 72 h in a Memmet IN110 Humidity Chamber (Memmet, Germany) prior to granulation. The Onset Glass Transition Temperature of the powders prior to granulation was measured as follows: DE6 (84°C), DE12 (71°C), DE21 (58°C) and DE29 (50°C). The particle size distribution of the powders can be characterised as displayed in Table 5.1. Particle size distribution measurements were carried out in triplicate using a Camsizer (Retsch, UK) using random samples of 25 g from the bulk material. The binder used was distilled water at 20°C.

Table 5.1: Particle size distribution of the raw powders classified by the d10, d50 and d90

	Particle Size (µm)			
	DE6	DE12	DE21	DE29
d10	144 ± 9	153 ±14	141 ± 20	143 ± 17
d50	292 ± 21	271 ± 20	270 ± 15	255 ± 19
d90	651 ± 30	569 ± 37	547 ± 25	455 ± 19

5.2.2 Granulation Experiments

Granulation was carried out in an Eirich EL1 High Shear Granulator (Eirich GmbH, Germany). A Graseby 2100 Syringe Pump (Burtons, UK) was used to feed in water as binder. Batch size was evaluated between 200 g and 400 g. A bowl speed of 170 rpm was used while impeller speed was altered between 450 rpm and 1800 rpm. The granulator was operated in co-current mode where the bowl and the impeller rotate in the same direction. The mixing pan was arranged horizontally (inclination angle is 0°). The L/S ratio was varied between 0.015 and the point where caking occurred to evaluate mix behaviour under varying liquid contents. Spray rate was kept constant at 1.5 g/min. A constant spray rate meant different L/S ratio's resulted in different binder addition times as shown in Table 5.2. The wet massing time after liquid addition was 5 min. Three replicates were performed for each experiment and the average taken. The powder bed temperature for each experiment was measured using a FLIR One (FLIR, USA) thermal camera as presented in Figure 5.1. The powder bed temperature was taken as the average temperature of the observable powder bed area. The initial powder temperature and granulator temperature was 20°C in each instance.

Table 5.2: Binder addition times for example L/S ratios at different batch sizes. Binder addition rate constant at 1.5 g/min

	Binder Addition Time (min)		
L/S Ratio	200 g	300 g	400 g
0.015	2	3	4
0.045	6	9	12
0.075	10	15	20
0.105	14	21	28
0.135	18	27	36
0.165	22	33	44
0.195	26	39	52

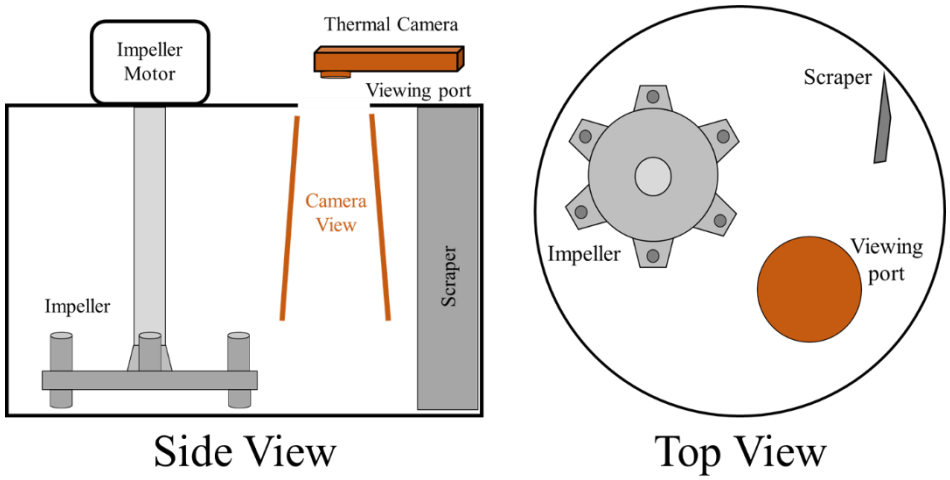

Figure 5.1: Schematic diagram of the Eirich EL1 Granulator. A thermal camera was placed to measure the powder bed temperature through a circular viewing port in the granulator lid as indicated by the highlighted orange components.

5.2.3 Granule Size Characterisation

Granule size was measured using a Retsch Sieve Shaker AS200 (Retsch, UK) and it is important that the operational settings chosen result in the generation of reliable data. The key parameters to ensure reliable sieving data are picking an appropriate shaking mass, amplitude and shaking time. First, the sieve shaking was carried out by breaking the batch into 100 g lots. This ensured that there was good particle passage during sieving by preventing sieve overloading and blocking. Secondly, it was essential to pick a high enough amplitude that it results in good particle passage through the sieves while not so high that it results in particle breakage. Breakage of granules or caked material must be avoided because it will affect the Yield and Extent of Caking. Preventing this breakage effect involved using the minimum amplitude possible which provided good particle passage and led to a amplitude of 0.45 mm being chosen. Preliminary sieving tests done with sample granules at this amplitude shows negligible breakage. To choose an appropriate shaking time, preliminary sieve shaking tests were conducted with granules samples at the chosen amplitude of 0.45 mm. The test was stopped every 30 seconds and the mass distribution of the sample within the stack measured. Mass change within the stack seized after 2.5 minutes on average during these preliminary tests. A shaking time of 3 mins was chosen as an extra precaution and to ensure the end point of the sieving had been reached.

The granule yield was defined as the product that had a size greater than the d90 of the raw powder and less than 4 mm. This means for DE6, the yield was defined as product between a sieve size of 0.7 mm and 4 mm. For DE12 and DE21 it was the product between a sieve size of 0.6 mm and 4 mm. Finally, for DE29 it was defined as the product between a sieve size of 0.5 mm and 4 mm. Material that was less than the d90 of the raw powder was classified as fines and material greater than 4 mm was classified as cake/lumps. Additional information regarding sieving can be found in Section 3.2.5.

5.2.4 Measuring Moisture Content

For certain experiments, the moisture content of the raw powder along with the moisture content of the granules and fines after granulation was measured. This wet basis moisture content was measured using an MA37 Infrared Moisture Analyzer (Sartorius, Germany). Sample mass used was 5 g and the drying temperature was set at 120°C. The equipment was run in its Fully Automatic mode where the drying end point occurs after the machine detects no further change in the sample mass during a 24 s interval. The moisture content was taken based on this end point.

5.2.5 Developing the Gordon and Taylor Model

The change in Glass Transition Temperature with moisture content of the different Maltodextrins was required to better understand the behaviour of the powder during granulation. In order to do this, powder samples were taken and conditioned at different relative humidity's for 1 month using saturated salt solutions at 20°C. The saturated salt solutions used and the corresponding relative humidity they produced are as follows: Lithium Chloride (RH 11%), Potassium Acetate (RH 23%), Magnesium Chloride (RH 33%), Potassium Carbonate (RH 43%), Sodium Bromide (RH 59%) and Sodium Chloride (RH 76%). The different relative humidity's result in varying uptakes of water vapor which produces powder samples with different moisture contents.

After conditioning, the powder samples had their water content measured using thermo-gravimetric analysis in a TGA550 (TA Instruments, Switzerland). The measurement process involved powder samples of ~25 mg being heated from 25°C to 200°C at a heating rate of 2°C/min under dry nitrogen flow (100 mL/min). The decomposition temperature of all the Maltodextrin powders is above 200°C, according to the manufacturer supplied material data sheets, ensuring no material degradation. The machine measured the weight loss of the sample with temperature. The minimum point of the weight loss derivative curve is used to determine the temperature at which water loss ends. The moisture content of the sample is then determined from the weight loss at this temperature. Additional information regarding the measurement principle for the TGA can be found in Section 3.2.11.

The Glass Transition temperature was measured using Differential Scanning Calorimetry in a DSC25 (TA Instruments, Switzerland). A double cycle scan procedure was used. The first cycle was used to erase the powder's relaxation enthalpy while the second cycle was used to measure the powder T_g. Powder samples of ~20 mg were used for the scan. The first cycle involved heating the sample at a rate of 5°C/min from 25°C to the expected T_g+30°C before the system is then cooled to -30°C. The second cycle then begins at a rate of 5°C/min, up to a temperature of the expected T_g+30°C. The glass transition temperature is taken as the onset of the steep change in heating capacity. Additional information regarding the measurement principle for T_g can be found in Section 3.2.10.

The sample moisture contents and T_g data were fitted onto the Gordon and Taylor Equation presented in Equation 5.1 [21] using a root mean squared error method in Excel. x_A and x_B are the fractions of Maltodextrin and Water in the sample respectively. $T_{g,A}$ and $T_{g,B}$ is the Glass Transition Temperature of the dry powder and of pure water. The Glass Transition Temperature of water can vary depending on the environmental pressure, with T_g increasing as pressure increases. This is because as pressure increases, the amorphous water structure changes from a low density amorphous structure to a high density amorphous structure. The creation of this denser structure increases the strength of the hydrogen bonding within it, meaning greater energy inputs (caused by higher temperatures) are needed to trigger the glass transition process. The T_g of water at ambient pressure (1 bar) is -135°C and therefore this value has been used throughout this work to reflect the conditions that the granulation experiments were carried out at. This value of -135°C has been experimentally validated [112] and is commonly used in literature to model the water component in the Gordon Taylor equation [21]. Finally, k is the fitting parameter which depends on the interactions between water and the different Maltodextrins. The fitting produced the following k values for the different Maltodextrins: 11.94 (DE6), 11.76 (DE12), 10.53 (DE21) and 9.98 (DE29).

$$T_g = \frac{x_A T_{g,A} + k x_B T_{g,B}}{x_A + k x_B}$$

Equation 5.1

5.2.6 Measuring Viscosity

Viscosity of Water-Maltodextrin mixtures at different solid contents was measured using a Malvern Kinexus Pro rheometer (Malvern, UK). The rheometer was configured using a 25 mm cup and bob geometry. The sample temperature used was 20°C to reflect the initial temperature of the raw powder and water used in granulation. The shear rates evaluated varied from 1 to 1000 s^{-1} to reflect the shear rates that are typically generated during HSWG. Measurements for each evaluated condition were performed in triplicate. Additional information measuring viscosity can be found in Section 3.2.12.

5.2.7 Powder Stickiness

The preparation step involved first dip coating a 4 mm Cellulose Acetate plastic bead in Maltodextrin to produce a Maltodextrin coated bead with a ~0.5 mm coating thickness. Then mixtures at different Maltodextrin:Water ratios were produced using a CAT R100 Mixer (CAT, UK) with an impeller speed of 300 rpm and mixing time of 20 mins. The stickiness of the mixture was then measured using a Krauss K100 Tensiometer (Krauss, Germany) at 20°C using the procedure outline in Figure 5.2. The bead was connected to the measurement probe of the tensiometer while the mixture was placed on a moving platform. Step 1 involved the platform moving upwards at 500 mm/min until the probe detected the

surface of the mixture (Step 2). Afterwards, during Step 3, the platform continued to move upwards at 500 mm/min for a further 2 mm. This resulted in the bead penetrating 2 mm into the mixture surface. The 500 mm/min movement speed represents the fastest speed that the Tensiometer could be operated at and reflects the high velocities under which adhesion needs to occur in a high shear wet granulation process. The Tensiometer will carry out the movement at the set speed unless the load rating on the sensor is reached. There was no holding time between Step 3 and Step 4, where the bead was withdrawn immediately at 500 mm/min. No holding time was used to reflect the conditions in the granulator where the collision time between granules is miniscule and adhesion needs to happen in the moment of collision to be successful. The maximum tensile force on the bead during this withdrawal process was be measured by the Tensiometer. The greater the maximum tensile force, the greater the adhesion between the bead and mixture indicating a greater stickiness.

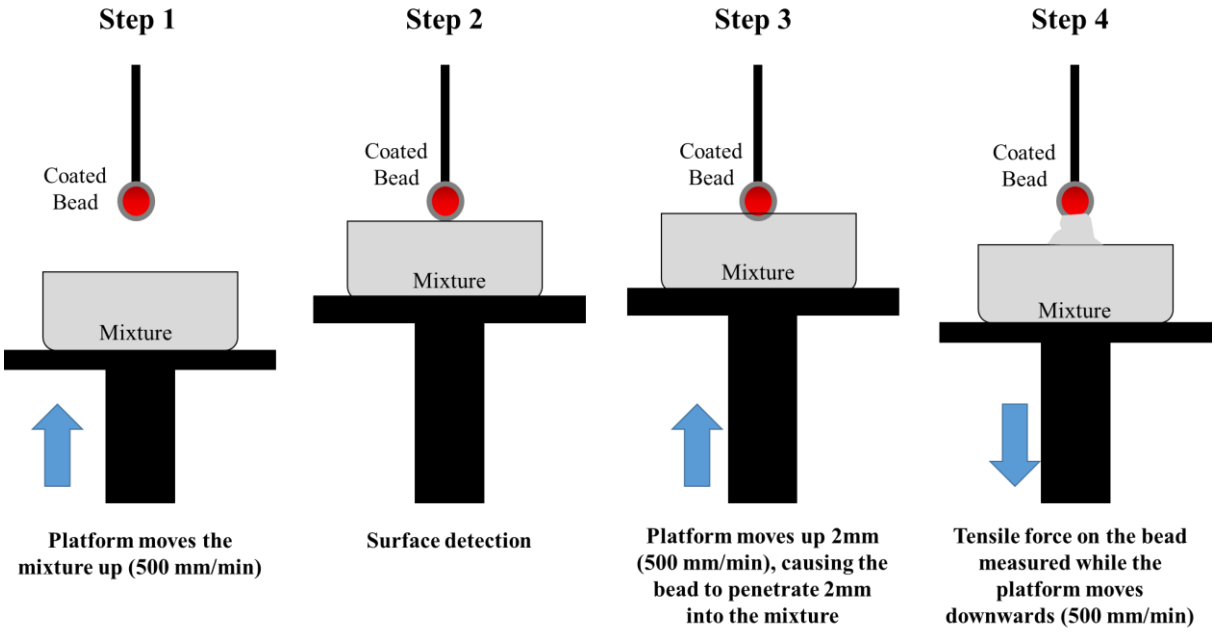

Figure 5.2: Measurement procedure to measure stickiness.

5.2.8 Particle Image Velocimetry

Particle Image Velocimetry (PIV) was carried out to determine the typical shear rate of the bed during granulation. A Photron 1024PCI High Speed Camera (Photron, USA) was used to capture high speed videos of the granulation bed at varying impeller speeds and batch sizes. The granulation bed was composed of granules between 1 – 2 mm which was the predominant granule size class produced by the system. Figure 5.3A displays an example snapshot of the granulation bed for the 200 g and 450 rpm process condition. The videos were evaluated in MATLAB's PIVLAB software [113] to determine particle velocity and the resulting shear rates throughout the bed. The area enclosed by the red border in Figure 5.3B represents the motion of the powder bed. Only this area was evaluated using the PIV

software. This was done to eliminate the motion of the rotating impeller and the rotating bowl (shown as the blue and yellow highlighted regions in Figure 5.3B) to avoid the PIV analysis from mistaking those movements for that of the powder. The recommended Image pre-processing functions and values were used. These included Enabling CLAHE with a Window size [px] of 64 and Wiener2 Denoise and Low Pass with a Window size [px] of 3. The Auto Contrast Stretch function and the Background Mean Intensity subtraction function was activated. This helped remove noise from the images and helped focus the motion of particles. For the analysis portion, the default FFT deformation algorithm was used with interrogation areas of 200, 100, 50 and 25.

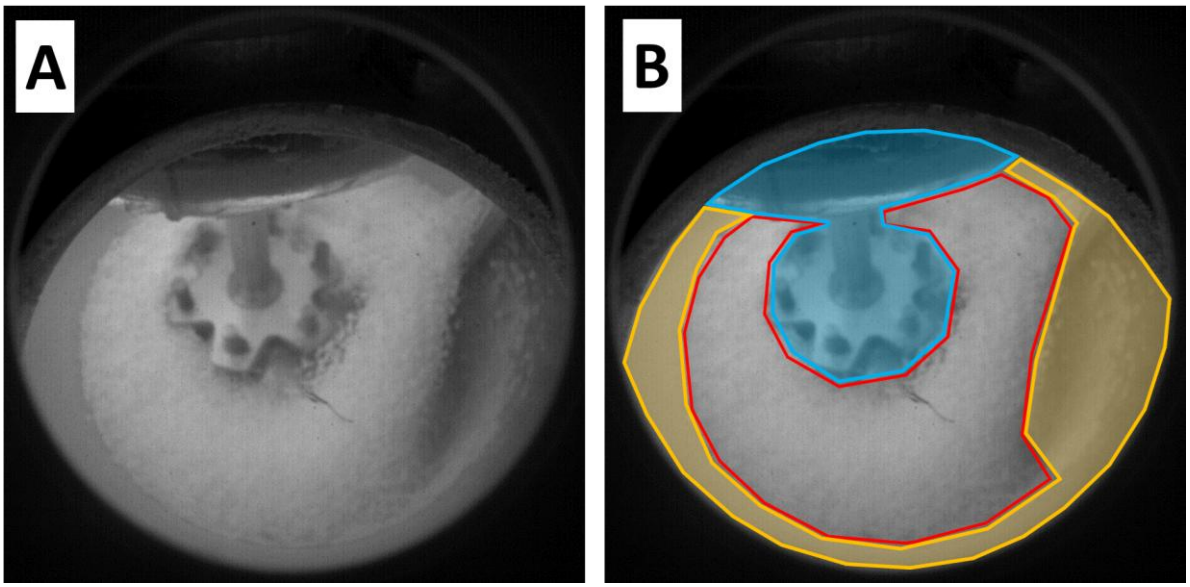

Figure 5.3: Figure 5.3A presents a snapshot of the mixing captured by the high speed camera at 200 g and 450 rpm. It displays the motion of the powder bed which is created by the rotating impeller and rotating bowl. Figure 5.3B indicates the different regions which the image can be divided into. The area within the red border represents the motion of the powder, the area within the blue border represents the motion of the impeller and the area within the yellow border represents the motion of the bowl. Only the area within the red border was evaluated during the PIV analysis.

5.3 Results: The role of Temperature within the granulation process

HSWG regime maps describe the behavior of the granulation mix based on two drivers for the process. Typically, these drivers are the liquid content on the x axis and a deformation parameter on the y axis [30,36,108]. This study considers the L/S ratio and temperature to be the two drivers of the agglomeration process for heat sensitive amorphous powders. The greater the liquid content, the more liquid bridges can form and the greater the extent of granulation [30]. Meanwhile, temperature is well established in literature as a parameter to correlate with the cohesiveness/caking of amorphous powders [71,111]. Temperature can also be used to reflect the deformation experienced by the granule during granulation. This is because at higher temperatures, the material will behave in a rubberier manner leading to more granule deformation and therefore more bonding.

This section will explore the impact of temperature on the granulation process. It will begin by discussing the glass transition behaviors of Maltodextrins and their connection to the caking phenomenon. The subsequent sub-sections will present the effect of process parameters on powder bed temperature and granular yield. These findings will emphasize the influence of temperature on the granulation behavior of amorphous powders, particularly in relation to caking. Finally, the section will conclude by explaining the rationale behind selecting the term T-T_g to model the temperature-dependent behavior of the system, along with the approach used to model this parameter within the current scenario.

5.3.1 Glass Transition behavior of Maltodextrins

Figure 5.4 shows the fitted Gordon Taylor curves for the different Maltodextrin powders. Fitting was carried out according to Section 5.2.5. For all the powders, as the moisture content increases, the T_g decreases. This is due to the plasticizing effect of water on the powder. This describes the phenomenon where water penetrates the molecular structure of the powder and forms hydrogen bonds with the polymer chains. The formation of these hydrogen bonds disrupts existing intermolecular bonds between the polymer chains giving them a greater mobility. This means less thermal energy is required to excite the material into the rubbery state resulting in a lower T_g [109]. It is also evident that at all moisture contents, the material T_g increases as the DE number decreases which is in line with accepted literature [25,26]. This is because low DE Maltodextrins have a greater portion of longer polysaccharide chains. This leads to stronger bonding and more entanglement between the polysaccharide chains. To become mobile, more thermal energy is required to overcome this greater entanglement and bonding, resulting in the higher T_g.

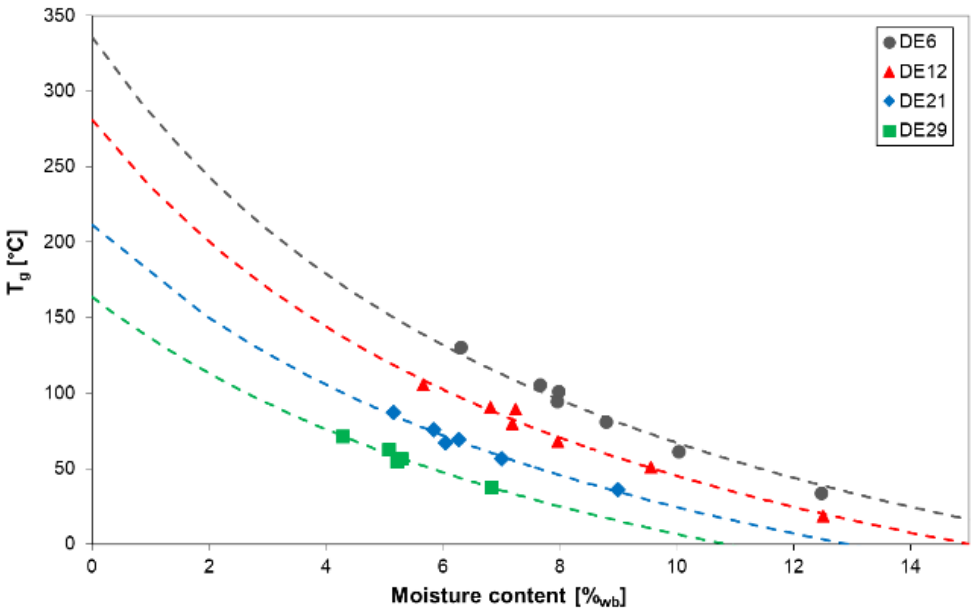

Figure 5.4: Fitted Gordon and Taylor curves for the evaluated Maltodextrins showing the decrease in T_g with increasing moisture content (wet basis). A higher DE number corresponds to lower T_g values at a given moisture content.

5.3.2 Caking behavior of Maltodextrins

When a powder undergoes glass transition, it goes from being a rigid, glassy material to being a sticky, rubbery one. This increased stickiness has the potential to promote agglomeration in the system that is both desired and undesired. Desired agglomeration is where the powder binds to other powder particles to form granules. Undesired agglomeration is where excessive agglomeration occurs within the powder bed forming large caked lumps or where the powder binds to the equipment surfaces [111]. Eventually this undesired agglomeration can become so severe that it results in process failure as visualized in Figure 5.5. Figure 5.5 shows the aftermath of severe caking that occurred during the granulation of the DE29 powder. Figure 5.5A displays an example of undesired agglomeration where the bed has become so sticky due to the glass transitioning of the powder that it has adhered together to form one solid lump. This solid lump has been extracted and pieced together in Figure 5.5A to emphasize the extent to which the bed can cake due to the glass transition phenomenon. When this caking occurs, the bed's resistance to the motion of the impeller increases and it also leads to powder adhesion onto the impeller, both of which increases the demand on the impeller motor. This demand eventually exceeds the capacity of the motor, at which point the motor shuts down, and operation cannot continue. This impeller jamming is visualized in Figure 5.5B which shows significant amounts of caked powder adhered onto the impeller which would have dramatically increased the demand on the impeller motor. Caking can therefore lead to material loss and equipment damage, especially to the impeller motor. The underlying cause of this caking is the powder undergoing glass transition which occurs depending on both the moisture content and temperature of the powder. This makes caking especially challenging to predict as both of these parameters are constantly in flux during granulation as liquid is added and heat is generated in the system.

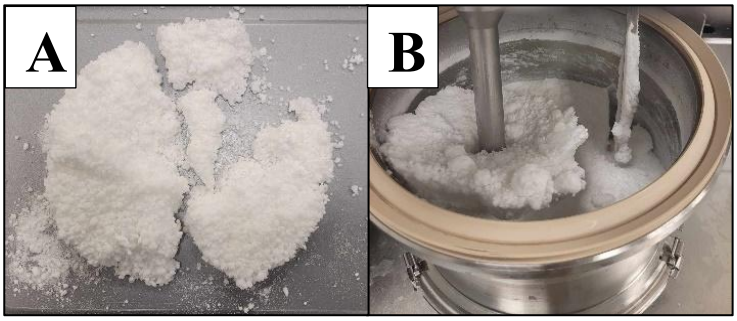

Figure 5.5: Caking of Maltodextrin DE29 in the High Shear Granulator. 4A depicts the extreme case where the whole bed has caked to form one singular lump leading to the complete loss of material (taken at the failure point of DE29 granulated at 400 g and 900 rpm). 4B depicts how this caking has the potential to jam the granulator internals (taken at the failure point of DE29 granulated at 300 g and 1350 rpm).

5.3.3 Effect of process parameters on powder bed temperature

Caking occurs when the powder temperature increases above its T_g. During granulation, the kinetic energy of the particles is converted to heat due to interparticle and particle-granulator friction. For example, Kristensen and Schaefer [85] reports that all the power consumed by the HSG is converted to heat in the wet mass. This heat generation leads to a gradual increase in bed temperature. Figure 5.6 presents the thermal images captured of the powder bed through the circular viewing port (illustrated in Figure 5.1) when granulating DE6 at 200 g and 1800 rpm. These thermal images represent the end temperature of the powder bed when granulated at different L/S ratios with the associated run times as detailed in Section 5.2.2. The bed temperature is shown to increase at higher L/S ratio's due to the increased run times. Figure 5.6 can be used to illustrate the changing characteristics of the powder bed during a granulation process. During the granulation process the bed temperature increases as kinetic energy is converted to heat in the granulator. Simultaneously water is being added to the powder bed which increases its moisture content and therefore decreases the powder bed T_g. Eventually a tipping point is reached where the bed temperature overtakes the T_g resulting in a high likelihood of caking.

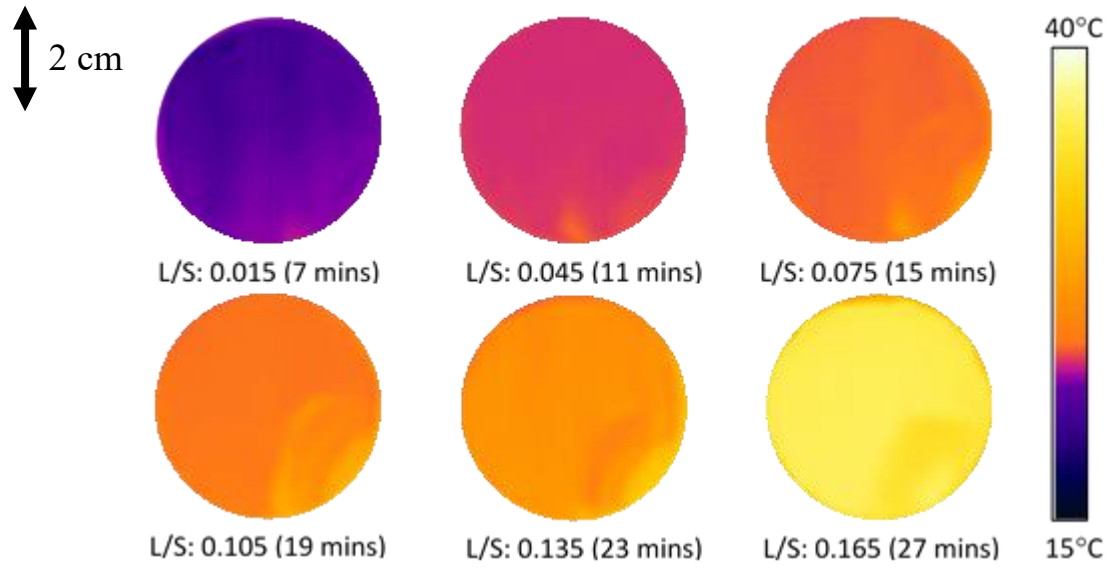

Figure 5.6: Thermal images of the DE6 powder bed when granulated at 200 g and 1800 rpm. The L/S ratio used for each experiment and the total run time is presented below each image. The figure displays the portion of the powder bed that could be observed by the thermal camera through the circular viewing window as indicated in Figure 5.1. The signature created in the powder bed by the rotating impeller is seen at the bottom right of each image.

Therefore, in order to diagnose the causes of caking, the effect of key process parameters on the powder bed temperature was evaluated. Figure 5.7 shows the changing bed temperature with impeller speed and batch size at different L/S ratio's for the varying Maltodextrins. The results show how significant the temperature rise can be with bed temperatures increasing over 25°C under certain conditions. Increasing impeller speed resulted in a greater increase in bed temperature [85,114,115]. At higher impeller speeds, the granulator motor introduces more kinetic energy into the system which is then converted into heat in the wet powder mass. Furthermore, at higher impeller speeds, the powder moves

faster. This results in more friction in the system by increasing the rate and magnitude of interparticule collisions which generates more heat. Increasing batch size also results in a significant increase in bed temperature [39]. This is because at larger batch sizes, there are more particles in the system resulting in more collisions. This leads to more friction and a greater rate of heat generation. Bed temperature was also found to increase with L/S ratio. Since the binder addition rate was kept constant, a higher L/S ratio correlates to longer binder addition times resulting in an extended overall running time as shown in Table 5.2. This increased running time allows heat to build up in the system for longer resulting in the higher bed temperature [115]. It also allows more time for the chosen impeller speed and batch size to influence the process which explains why a greater variation between bed temperatures are seen at higher L/S ratios (longer run times) than at lower L/S ratios (shorter run times).

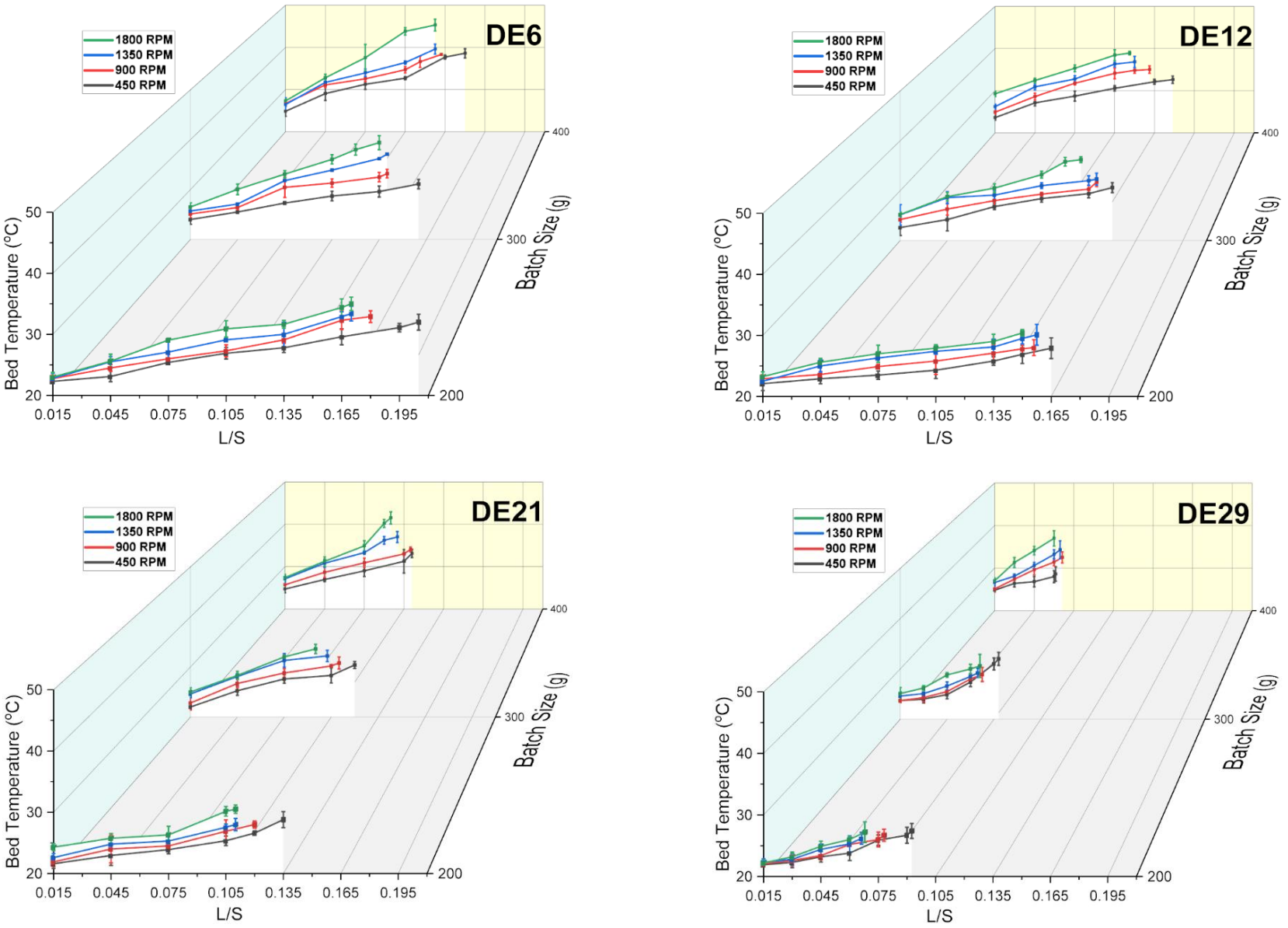

Figure 5.7: Increase in bed temperature at varying batch sizes, impeller speeds and L/S ratios. Since binder addition rate was kept constant, higher L/S ratios also correspond to longer run times. Initial raw powder temperature was 20 °C for all the different Maltodextrin powders.

5.3.4 Effect of process parameters on granular yield and caking

Figure 5.8 displays the impact of changing process parameters on the granular yield for the different Maltodextrin powders. For each combination of impeller speed and batch size, the L/S ratio was increased until process failure occurred due to caking. In this section, the failure point refers to the L/S ratio required for process failure to occur depending on the process parameters chosen. This failure point is the final data point in each series where the process was terminated due to excessive caking.

5.3.4.1 Effect of L/S Ratio

L/S is a key parameter for a HSWG process, with literature going as far as stating it is the most important process parameter [116]. Increasing L/S ratio, initially resulted in a roughly linear increase in yield as shown in Figure 5.8. However, this linear trend is not universally observed, with literature presenting varying trends depending on the material granulated. For instance, Macho et al [117] found an exponential trend between L/S ratio and yield when granulating MCC. The strong correlation between granular yield and L/S ratio exists because granule formation only occurs during a wet granulation process due to the liquid bonds that form between particles. At higher L/S ratios, more liquid is present within the system leading to the formation of more bonds between particles which facilitates the formation of more granules. However, this increase in yield with L/S ratio cannot continue indefinitely. This is shown in Figure 5.8, where at a certain point the granule yield peaks and afterwards granule yield is shown to decrease with L/S ratio. This is because after a certain point the powder starts to become saturated and excessive agglomeration occurs, resulting in the formation of lumps rather than granules [30]. With amorphous powders, increasing the L/S ratio also results in a decrease in the T_g of the mix due to the greater moisture content. Eventually this causes the T_g to decrease below the bed temperature resulting in caking. The formation of cake instead of granules results in a decreased yield and ultimately leads to process failure.

5.3.4.2 Effect of Impeller Speed

Impeller speed had a marginal impact on granule yield at low L/S ratio's where granulation occurred in the absence of caking. This is shown in Figure 5.8 where all the impeller speeds show a similar initial increase in yield with L/S ratio. However, a slight trend can be observed where higher impeller speeds result in a lower yield. This is indicated by the lower impeller speeds (450 rpm and 900 rpm) often resulting in higher yields compared to the faster impeller speeds (1350 rpm and 1800 rpm). This can be attributed to increased breakage of granules at faster impeller speeds resulting in the formation of more fines which reduces yield [4,30]. However, with DE6, an additional phenomenon is observed where at L/S ratio's greater than 0.075, an increased impeller speed results in a higher granule yield. This phenomenon becomes more pronounced with increasing batch size. This could be attributed to the increased bed temperature at higher impeller speeds and batch sizes encouraging the glass transition of

the powder. In this case, it results in desired agglomeration where the enhanced stickiness of the powder favours the formation of granules.

The predominant impact of impeller speed is observed when looking at the failure points for each condition. There is a clear trend across all Maltodextrin powders where faster impeller speeds cause failure due to caking to occur at lower L/S ratio's. This can be explained by considering the faster rate of heat generation at higher impeller speeds as shown in Figure 5.7. This increased heat generation means that the bed temperature can surpass a higher T_g, allowing caking to occur at lower L/S ratio's. However, the rate at which the failure point is reduced is not constant with increasing impeller speed. For instance, the use of a higher impeller speed of 900 rpm rather than 450 rpm results in a clear decrease in the failure point across all Maltodextrin powders. However, beyond 900 rpm, the rate of decrease diminishes with only marginal differences observed in the failure points between 1350 rpm and 1800 rpm. This can be explained by considering Figure 5.7, which displays that bed temperature only increases a few degrees as impeller speed is increased. Meanwhile, Figure 5.4 demonstrates that the T_g of the Maltodextrins rises exponentially as the moisture content decreases. Consequently, significantly higher bed temperatures are required for caking to occur at lower L/S ratios. Therefore, the minimal change in the failure point at the highest impeller speeds can be explained by the fact that the increased bed temperature at these speeds is insufficient to compensate for the large increase in T_g as moisture content decreases.

5.3.4.3 Effect of Batch Size

No clear trend is seen when comparing batch size to granule yield in the non-caking region. This is best shown in the Appendix Figure 2A which plots the data presented in Figure 5.8 in an alternative manner to better present the influence of batch size on the process. However, it must be noted that this is the case due to the broad definition of the yield (which for this study was granules between the d90 of the raw powder and 4 mm). Batch size can alter granule size and therefore a narrower definition of the desired yield size would have resulted in a different trend [88]. For instance, the work presented in Chapter 4, which focused on the granulation of DE29 to produce granules between 0.5 mm and 2 mm found yield to initially increase and then subsequently decrease with increasing batch size [118].

Similarly to impeller speed, the primary effect of batch size was found to be on the failure point of the mix. Larger batch sizes resulted in caking occurring at lower L/S ratio's. Once again this can be attributed to the increased heat generation at larger batch sizes (as shown in Figure 5.7), which compensates for a higher T_g and allows caking to occur at lower L/S ratios.

5.3.4.4 Effect of Maltodextrin Grade

It is evident in Figure 5.8, that the L/S ratio at which the failure point occurs, decreases in the following order: DE6, DE12, DE21 and DE29 when the powders are granulated under the same conditions. This

can be explained by considering the significant differences in T_g between the Maltodextrin powders. As shown by Figure 5.4, lower DE Maltodextrin have a higher T_g, especially at similar moisture contents. For example, the T_g of the raw DE6 powder used for the granulation experiments was 84°C. In comparison the T_g of the raw DE29 powder was 50°C which results in a significant 34°C difference in T_g between the two grades. Meanwhile, under the same process conditions, the Maltodextrins show similar bed temperatures as shown in Figure 5.7. For example, at 200 g and 450 rpm, the bed temperature at a L/S of 0.045 was 23.1°C for DE6, 22.9°C for DE12, 23°C for DE21 and 23.2°C for DE29. This highlights the trend shown in Figure 5.7 where similar process conditions produce similar bed temperatures regardless of powder type. Consequently, despite the powders being at the same bed temperature, their differing T_g will mean that they display distinct material behaviours. This means that higher DE Maltodextrin with a far lower T_g will cake much more readily than low DE Maltodextrin at similar bed temperatures, which results in the observed trend.

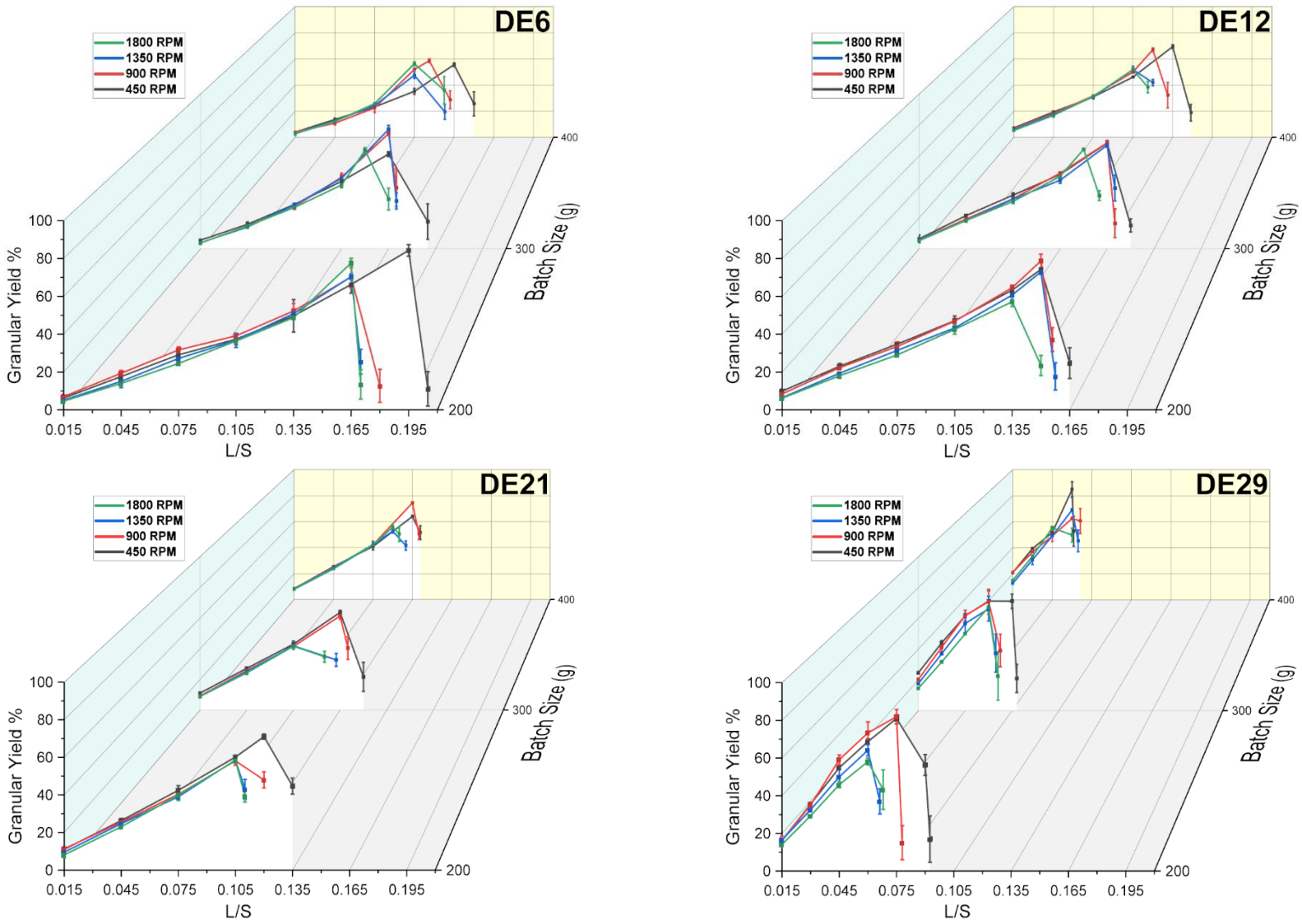

Figure 5.8: Change in granular yield with increasing L/S ratio, impeller speed and batch size. For all impeller speeds and batch sizes, as L/S ratio was increased, granular yield was found to initially increase in a roughly linear manner up to a peak value. No caking was observed in this linear region. Past this peak value, caking occurred, resulting in the formation of cake rather than granules which reduced yield. The end (failure) point for each series is the L/S ratio where caking had become so severe that it resulted in process failure. Higher DE Maltodextrin experienced caking and reached the failure point at lower L/S ratios for a given combination of impeller speed and batch size.

5.3.5 Modelling temperature interactions with Maltodextrin

The current section has emphasized the impact of bed temperature on the granulation behavior of amorphous powders, particularly in relation to caking. Experimental results demonstrate that the degree to which bed temperature affects the granulation process is closely associated with the powder T_g. The interaction between Temperature and T_g is commonly modelled using the term T-T_g [71,111] with Fries et al [67] even using it to develop a dry granulation bonding regime map for amorphous powders. Similarly, this study will also utilize the T-T_g parameter to evaluate the impact of temperature within the granulation process.

The next step involved deciding how best to determine the T_g of the granulation mix during the process. The T_g of a powder depends on its moisture content, which during granulation is the sum of the initially adsorbed water present within the powder and the water binder added during the process. Therefore, the simplest approach for determining T_g would entail calculating an average moisture content for the granulation mix based on the mass of water added and the batch size. However, this would not be a fair representation of the process, because during granulation there is an uneven distribution of water binder in the powder bed, with powder that possesses greater levels of water forming larger granules. This uneven distribution of water across different granule size fractions results in the formation of distinct size classified components with varying moisture contents. This consequently leads to differences in the T_g of these granule size class components causing them to display different behaviours to each other.

To simplify the scenario, the number of these size classified components has been reduced to two. The first is the agglomerated component which is composed of the granules and caked fraction. The second is the non-agglomerated component which is composed of the fines fraction. The moisture content between these two fractions was expected to differ significantly as there is an inherent bias in granulation that larger granules possess greater binder contents [119,120]. This is because the stresses acting on a granule during granulation increases with size. Meanwhile, granule strength increases with binder content due to the formation of stronger bonds. Therefore, granules need to possess a sufficiently high moisture content to give it the strength needed to avoid breakage as it grows. This leads to the commonly observed increase in moisture content with granule size. The fine fraction represents the smallest particulates in the system and are particles that remained below the d90 of the initial powder. This indicates that the fines received a negligible amount of water binder compared to the granule fraction, as it was not able to form bonds or survive the stresses inside the granulator to experience significant growth.

An experiment was devised to evaluate the extent to which the moisture content of the fine and granule fraction differed. For each Maltodextrin, the impeller speed and batch size were chosen that facilitated the highest possible L/S ratio without caking occurring. Granulation experiments were conducted under these process conditions and the moisture content (measured as detailed in Section 5.2.4) of the initial

powder was compared with the moisture content of the fines and granule fraction after granulation. The results are shown in Figure 5.9. Since the highest L/S possible for each Maltodextrin grade was used, Figure 5.9 displays the moisture distribution between the fine fraction and granule fraction when the amount of liquid in the system was greatest. These conditions should facilitate the greatest opportunity for the fine fraction to display an increased moisture content. Despite each granulation experiment being run at the highest possible L/S ratio, as shown in Figure 5.9, there is only a slight increase in the moisture content of the fine fraction compared to that of the initial powder. Comparatively the granule fraction shows a large increase in the moisture content. For instance, with DE29, the fine fraction only showed a 0.5% increase in moisture content while the granule fraction displayed a 9% increase. Figure 5.9 represents the liquid distribution in the system at the highest L/S possible. At lower L/S ratios this increase in the moisture content of the fines is likely to be even lower which further supports the hypothesis that the fine fraction during granulation experiences a negligible change in its moisture content.

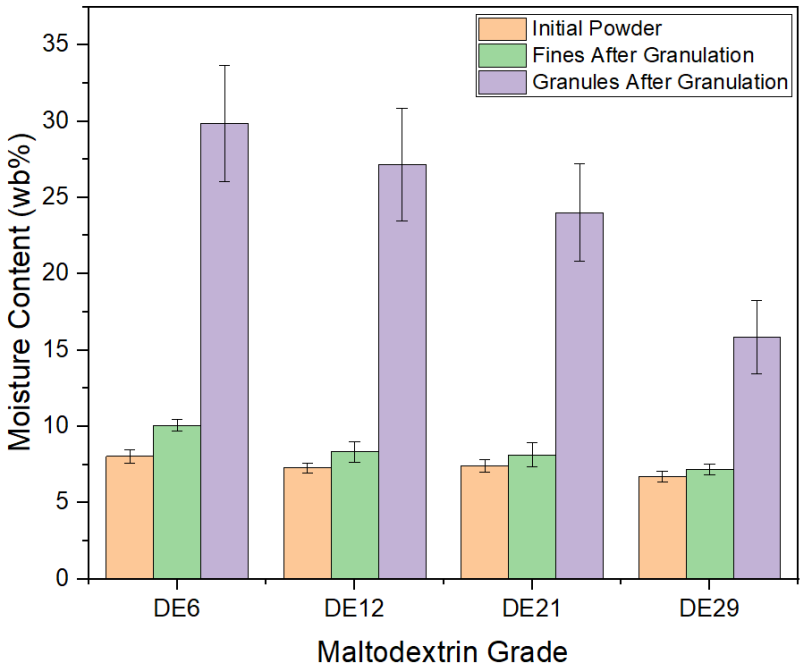

Figure 5.9: Moisture content of the initial powder compared to the moisture content of the fines and granules after granulation. Based on the results shown in Figure 5.8, process conditions were chosen which facilitated the use of the highest L/S ratio without caking occurring. Process parameters used are as follows: DE6 (200g and 450 rpm – L/S 0.195), DE12 (200 g and 450 rpm – L/S 0.15), DE21 (200 g and 450 rpm – L/S 0.12) and DE29 (200 g and 450 rpm – L/S 0.075)

A mass balance was carried out based on the results of Figure 5.9 to calculate the distribution of water that was added to the process. The results shown in Figure 5.10 indicate that almost all the added water binder was present in the granule fraction at the end of the granulation process. For example, with DE6, 38.3 g out of a total 39 g water was calculated to be present within the granule fraction. Similarly, with DE29, 14.7 g out of a total 15 g of water was calculated to be present within the granule fraction. This

confirms the uneven nature of the liquid distribution between fines and granules for this granulation system.

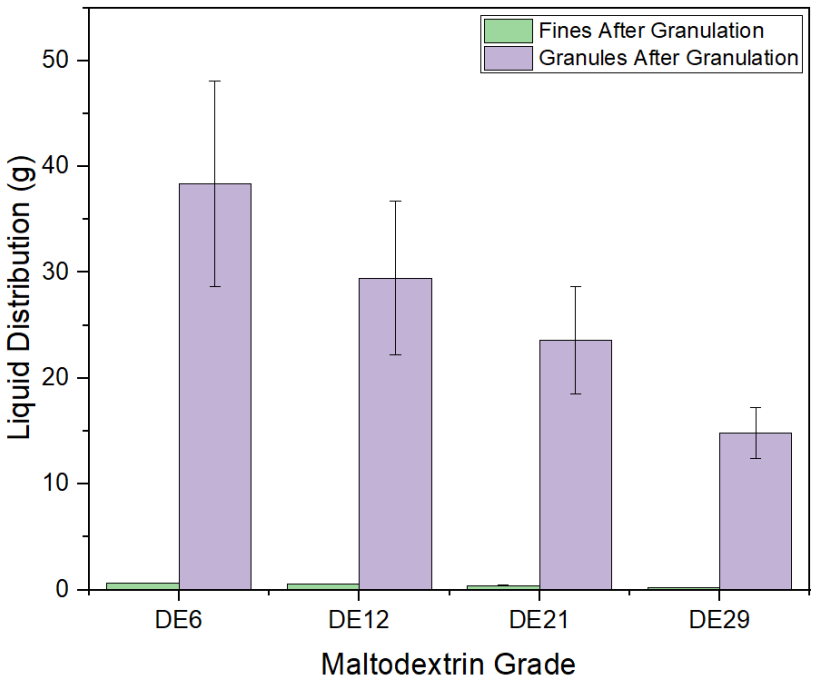

Figure 5.10: Calculated distribution of the water binder in the granule and fine fraction based on the moisture contents presented in Figure 5.9. The composition of the mix after granulation is as follows for the different powders: DE6 (84% Granule, 16% Fine), DE12 (74% Granule, 26% Fines), DE21 (71% Granule, 29% Fines) and DE29 (81% Granule, 19% Fines). The L/S ratio used and amount of liquid added for each Maltodextrin is as follows: DE6 (L/S 0.195 – 39 g), DE12 (L/S 0.15 – 30 g), DE21 (L/S 0.12 – 24 g) and DE29 (L/S 0.075 – 15 g)

The significant difference between the moisture content of the non-agglomerated (fines) and agglomerated (granule) fractions means that during granulation, these two components will possess very different T_g's. Based on this, a model has been developed to calculate the T-T_g value for each granulation mix based on the following 2 assumptions.

Assumption 1. All the water added during granulation is wholly present in the agglomerated (granule and cake) fraction and that none is present in the non-agglomerated (fine) fraction. This is based on the results illustrated in Figure 5.9 and Figure 5.10 which showed that only a marginal amount of the water binder added to the mix is found in the fine fraction. Therefore, the T_g of the non-agglomerated fraction remains as the T_g of the initial raw powder. The T_g of the agglomerated fraction is determined by first calculating its moisture content based on the initial adsorbed water content of the powder and the mass of water binder added. The corresponding T_g at that moisture content is then selected from the Gordon Taylor model presented in Figure 5.4.

Assumption 2. Both the agglomerated and non-agglomerated components have the same temperature (T) as they are in thermal equilibrium within the powder bed. This temperature is the bed temperature presented in Figure 5.7.

The T_g of the non-agglomerated and agglomerated component are determined as outlined in Assumption 1 while the temperature (T) of the non-agglomerated and agglomerated component are determined as outlined in Assumption 2. Subsequently $(T - T_{g,non-agglomerated})$ can be used to represent the caking tendency and rubbery behavior of the non-agglomerated fraction. While $(T - T_{g,agglomerated})$ can be used to represent the caking tendency and rubbery behavior of the agglomerated fraction. The mass fraction of the non-agglomerated $(x_{non-agglomerated})$ and agglomerated $(x_{agglomerated})$ components can then be used to represent the effect of $T - T_{g,non-agglomerated}$ and $T - T_{g,agglomerated}$ on the mix as a whole as shown in Equation 5.2.

$$x_{non-agglomerated}(T - T_{g,non-agglomerated}) + x_{agglomerated}(T - T_{g,agglomerated})$$

Equation 5.2

Since the mix is entirely composed of either the non-agglomerated or agglomerated components $(x_{non-agglomerated} + x_{agglomerated} = 1)$, Equation 5.2 can be simplified to the form shown in Equation 5.3. This can be further simplified through the introduction of a parameter $T_{g,Bed}$ as shown in Equation 5.4. This $T - T_{g,Bed}$ term has been used to model the temperature based granulation driver in subsequent sections in this work.

$$T - (x_{non-agglomerated}T_{g,non-agglomerated} + x_{agglomerated}T_{g,agglomerated})$$

Equation 5.3

$$T - T_{g,Bed}$$

$$where\ T_{g,Bed} = x_{non-agglomerated}T_{g,non-agglomerated} + x_{agglomerated}T_{g,agglomerated}$$

Equation 5.4

5.4 Results: The role of water binder within the granulation process

This section will explore the varying degrees to which water, acting as binder, granulates different grades of Maltodextrin. A concept will then be proposed to explain these variations, focusing on how the rate of increase in binder viscosity as the water wets the powder bed, effects the granulation process. In Section 5.3, the T_g served as a useful parameter for understanding the effects of temperature on different Maltodextrin. However, when examining interactions between water binder and amorphous powders, no established parameter like T_g exists. Thus, this section will conclude by proposing a viscosity-based parameter to explain the interactions observed between water and the various Maltodextrin grades during granulation.

5.4.1 Interaction between water and Maltodextrin grade

The primary role of the water in the process is to facilitate the formation of granules by creating liquid bridges between particles. However, the extent to which it does this is not constant between the different Maltodextrins. It is clear from Figure 5.8, that higher DE Maltodextrin granulated much faster with increasing L/S ratio than low DE Maltodextrin. Figure 5.11 shows the increase in granular yield with L/S at 200 g and 1350 rpm for the different Maltodextrins in the non-caking region. This increase has been modelled as a linear relationship which gives a good fit according to the R^2 value, with the lowest R^2 value being 0.976. The fit was set to cross the y axis at the origin (0,0). This reflects the fact that for a wet granulation process, the granular yield must be zero when the L/S ratio is 0. The gradient of this linear trend line indicates how efficiently the powder granulated when water is added. As shown in Figure 5.11, the gradients representing this granulation efficiency differs quite widely between the Maltodextrin powders with higher DE Maltodextrins possessing far larger gradients. For example, the gradient for DE29 is 2.8 times greater than that of DE6. This indicates that only a third of the water required to granulate DE6, would be needed to granulate DE29 to the same extent under those process conditions.

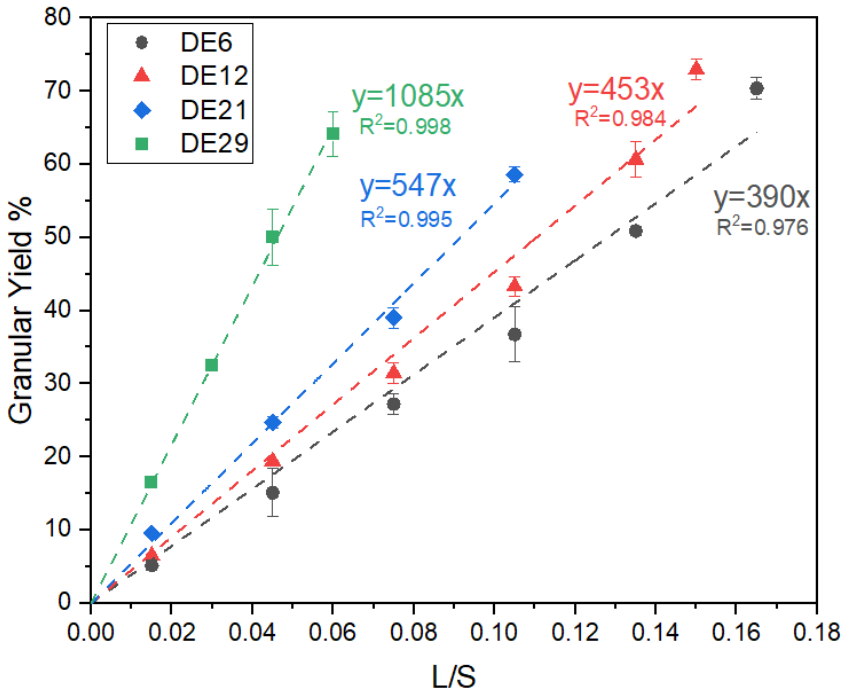

Figure 5.11: The increase in granular yield with L/S ratio for the different Maltodextrin grades, during the non-caking region at a batch size of 200 g and an impeller speed of 1350 rpm

A similar linear fitting to Figure 5.11 was carried out for all combinations of impeller speed and batch size. Once again, the suitability of the linear fit was evaluated using the R^2 value. The average R^2 value across all impeller speeds and batch sizes was 0.982 ± 0.018 with no value being lower than 0.94. This

gave a high degree of confidence in the approach and indicates that the use of a linear relationship to model the increase in yield with L/S ratio is suitable for the non-caking region. The gradient of these linear fittings which shows the increase in granular yield with L/S ratio at different processing conditions was taken and plotted according to Maltodextrin grade as shown by Figure 5.12. This increase in granular yield with L/S ratio is referred to as the Granulation Efficiency from here. Figure 5.12 confirms that regardless of the chosen process parameter, there is a trend displaying an exponential increase in the Granulation Efficiency with increasing DE number. Another observation from Figure 5.12 is that there is a far greater spread in the Granulation Efficiencies in the case of DE29 compared to the lower DE Maltodextrins. This can be attributed to the increased sensitivity of the DE29 powder compared to the lower DE Maltodextrins which amplifies the effects of process parameters such as batch size and impeller speed on the produced yield.

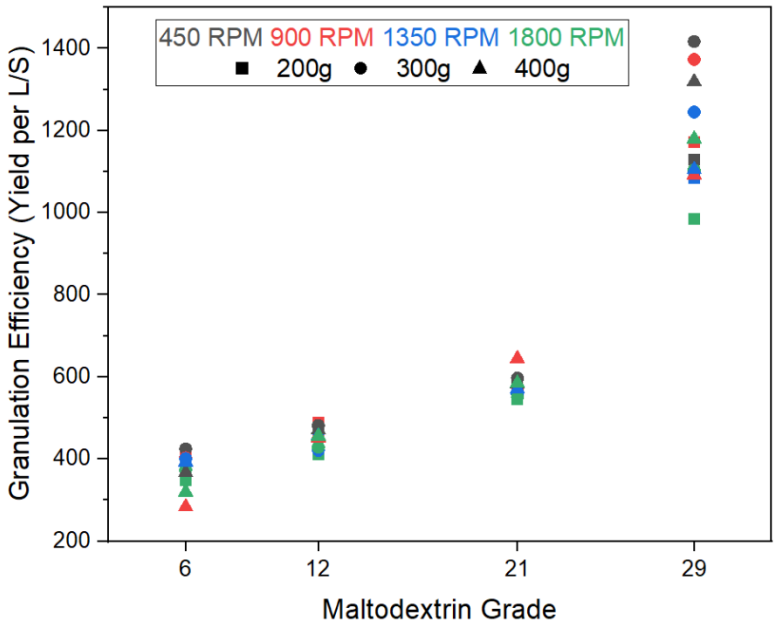

Figure 5.12: Effect of Maltodextrin Grade on the Granulation Efficiency at varying impeller speeds and batch sizes. Please note that in this context, the Granulation Efficiency is not expressed as a percentage, but rather it indicates a specific intensity based metric which reflects granulation performance. The Granulation Efficiency is the gradient of the linear fitting between Granular Yield and L/S ratio. It represents the rate of increase in granular yield with L/S for the non-caking region. Impeller Speed is denoted by the following colours: Grey (450 rpm), Red (900 rpm), Blue (1350 rpm) and Green (1800 rpm). Batch Size is denoted by the following shapes: Square (200 g), Circle (300 g) and Triangle (400 g)

5.4.2 Theory development for the interactions of water and Maltodextrin during granulation

The finding that low DE Maltodextrin require more water to granulate contradicts the general notion found in literature which indicates that granulation involving sugars with greater thickening powers require less water. However these studies, such as that by Santomaso et al, [36] involved the granulation of partially dissolving crystalline sugar with crystalline MCC. MCC absorbs water during granulation preventing water from acting as binder. When MCC is granulated with sugars of a high thickening

power, the water and sugar interact to form a highly viscous mixture which resists absorption by the MCC. This increases the water availability for the process and lowers the liquid requirement for granulation [36]. This concept is not applicable when granulating amorphous sugars with materials that do not compete for water in the same way that MCC does. This indicates that a better and new understanding of how amorphous sugar powder interacts with water is required to explain the varying granulating efficiencies of the different Maltodextrin.

At this point, the term Binder M/W (Maltodextrin/Water) will be introduced. This represents the changing Maltodextrin (solid) to water (liquid) content ($g_{Maltodextrin}/g_{Water}$) of the binder droplet after it is added to the granulation process. This is because when granulating the Maltodextrin powders, the 'true' binder in the process is the sticky Maltodextrin-water mixture that is formed during the wetting process rather than the pure water droplets that are initially added. This Binder M/W term is distinct from the term L/S ratio, which is a process parameter that represents the ratio between the mass of added water and mass of powder.

This novel approach for considering the interaction between water and Maltodextrin by considering the changing solid concentration of the binder material as it progressively wets the powder bed is visualized in Figure 5.13. During wet granulation, water droplets are added to the powder bed. Initially the binder droplet is pure water before it contacts the powder bed meaning it has a Binder M/W of 0. After being added to the granulator, it contacts and begins to wet the powder. At this stage the binder is primarily water and has a very low viscosity meaning it spreads easily and dissolves the Maltodextrin quickly. During this spreading process, the solid content within the binder (represented by the Binder M/W term) increases due to the dissolution and incorporation of Maltodextrin powder by the water. This increase in the Binder M/W causes the viscosity of the wetted binder material to increase. As the viscosity increases, the mobility of the binder drops, eventually reaching the point where it is no longer capable of spreading. Furthermore, as viscosity increases, the point is eventually reached where the binder becomes so viscous and solid like that it is no longer sticky. As the wetted material loses its mobility and stickiness, its performance as a binder is reduced. Once it has lost all mobility and stickiness then it can no longer function as binder and granulation stops. Powder-water systems that display a slower increase in viscosity with increasing Binder M/W are able to remain mobile and sticky for longer, resulting in a more water efficient granulation process.

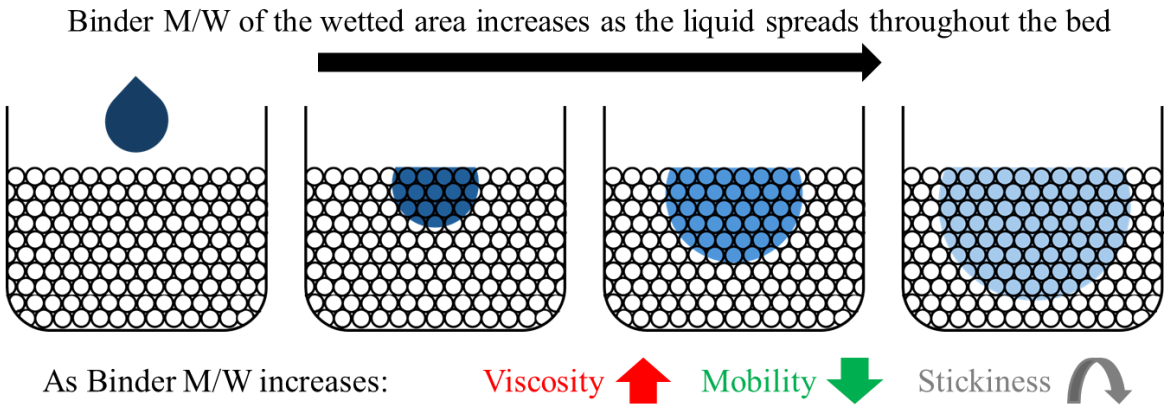

Figure 5.13: Visualisation of the spreading of a binder droplet after it contacts and wets the powder bed. As this spreading occurs the solid content (Binder M/W) within the binder increases. This increase in the Binder M/W causes binder properties such as viscosity, mobility and stickiness to change significantly.

To apply this concept to this work, the stickiness of Maltodextrin mixtures at different Maltodextrin/Water (M/W) ratios were measured as outlined in Section 5.2.7. This was done to get an impression of the changing adhesion behaviour of the binder in the granulation process as it incorporates more and more solid. The Maltodextrin coated bead can be seen to represent a solid particle in the granulation process while the Maltodextrin-water mixture can be seen as the binder driving agglomeration. The greater the stickiness between the bead and mixture, the higher the likelihood of adhesion occurring during granulation involving binder at that solid content.

Figure 5.14 shows the bridge developed at different M/W ratios for DE29 while Figure 5.15 shows the maximum tensile force recorded at each M/W ratio for the different Maltodextrins. Looking at Figure 5.14, it is evident that the nature of Maltodextrin-water mixture changes significantly as M/W is increased. At a M/W of 1 the DE29-Water solution is completely transparent with a very low viscosity. This low viscosity means the liquid is very mobile and any bridge produced during withdrawal of the bead is easily broken. This is shown in Figure 5.14 where there is no bridge to be observed at that separation distance. This low viscosity also results in a very low tensile force (stickiness) as indicated in Figure 5.15. As M/W is increased to 2, the viscosity of the mixture increases resulting in a stronger bridge developing between the bead and the mixture during withdrawal. At a M/W of 4, the saturation point of the water is starting to be reached as indicated by the mixture visually changing from a transparent, clear finish to a glossy/white finish. Beyond this point, as M/W increases from 4 to 7, the size and viscosity of the bridge increase significantly. This results in a dramatic increase in the tensile force detected by the machine indicating a sharp increase in stickiness in this region. At a M/W of 8 the mixture has become a semi solid. When the probe is dipped in, the mixture deforms to accommodate it, but there is no bridge formation indicating the mixture is losing its mobility. Despite this, there is still adhesion occurring as indicated by the significant tensile force presented in Figure 5.15. Meanwhile, increasing M/W to 10 sees the material becoming fully solid. At this condition the DE29-Water mixture

does not even allow the bead to penetrate its surface and no adhesion between the bead and mixture can be detected. At this point the mixture can no longer function as a binder in the granulation process as it has lost its stickiness and mobility. The bell shaped trend shown in Figure 5.15, where the stickiness of sugar mixtures first increases and then decreases with increasing solid content is well documented in literature [121–123]. These literature studies all utilized a probe tack test to evaluate stickiness where a steel probe was inserted into a sugar solution and held for period of time before being removed. The tensile force during removal was measured. There are several differences between this work and literature which include the use of a Maltodextrin coated bead to create a Maltodextrin-Maltodextrin contact surface, elimination of the hold time and much faster movement speeds (500 mm/min as opposed to 6 mm/min [122], 30 mm/min [123] and 60 mm/min [121]). This was done to better represent the conditions under which adhesion occurs during the High Shear Granulation process as justified in Section 5.2.7.

These mixtures at different M/W ratios represent the binder material at different stages during the wetting process as it incorporates more and more solid. Over time it loses its ability to spread and stick powder together and becomes less effective. Different Maltodextrin go through the described stages at different rates. As shown in Figure 5.15, lower DE Maltodextrins display quicker increases in their stickiness and reach their peak stickiness at lower M/W ratios. They then subsequently show a rapid decrease in stickiness with increasing M/W ratios and reach the point where they no longer adhere at lower M/W ratios compared with high DE Maltodextrins. This result is supported by the work of Wang and Hartel, [121] as well as that of Nowakowski and Hartel [122], which found that an increase in DE number in corn syrups resulted in the peak stickiness and adhesive failure point occurring at higher solid contents. This means that as water wets a powder bed of low DE Maltodextrins, the water loses its mobility and stickiness after incorporating less powder. This inefficiency means more water is needed to granulate low DE Maltodextrins than high DE Maltodextrins supporting the trend seen in Figure 5.12.

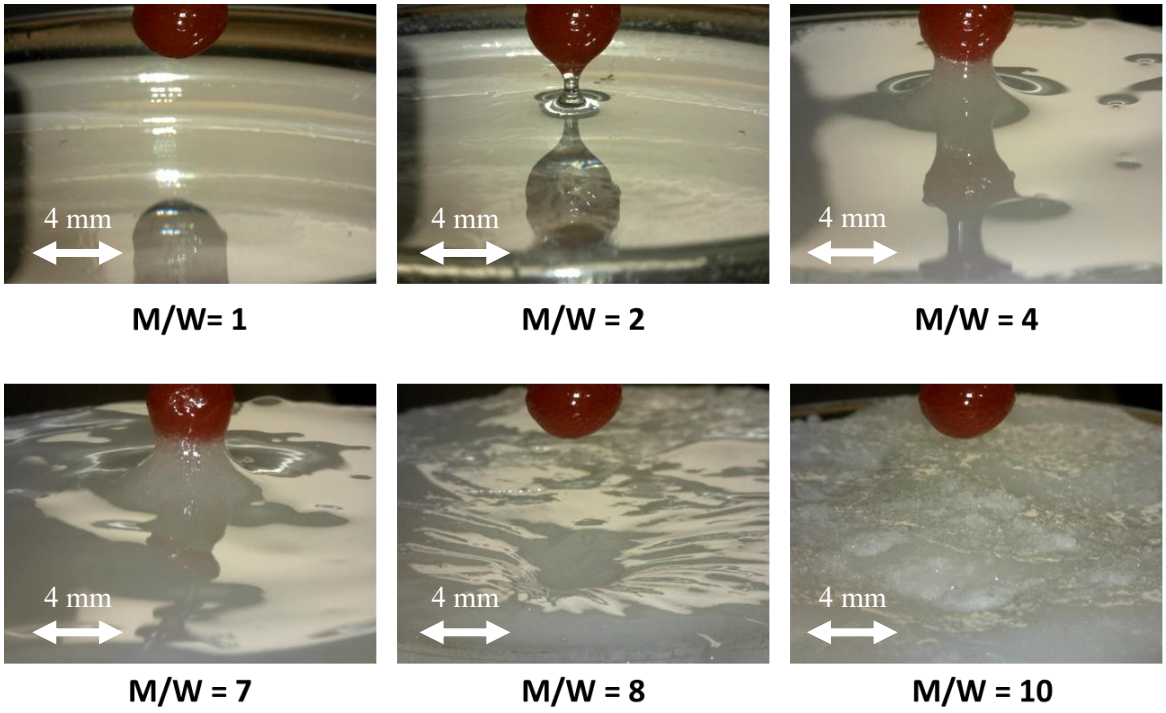

Figure 5.14: Freeze frames of the DE29 coated bead during the withdrawal process from DE29-water mixtures at different M/W ratios. Mixture viscosity increased with M/W ratio, initially leading to a more pronounced sticking effect as evidenced by better bridge development during withdrawal. As M/W ratio was increased beyond 8 and viscosity continued to increase, the mixture became more solid like and lost its adhesive properties. This led to no bridge development and eventually no sticking.

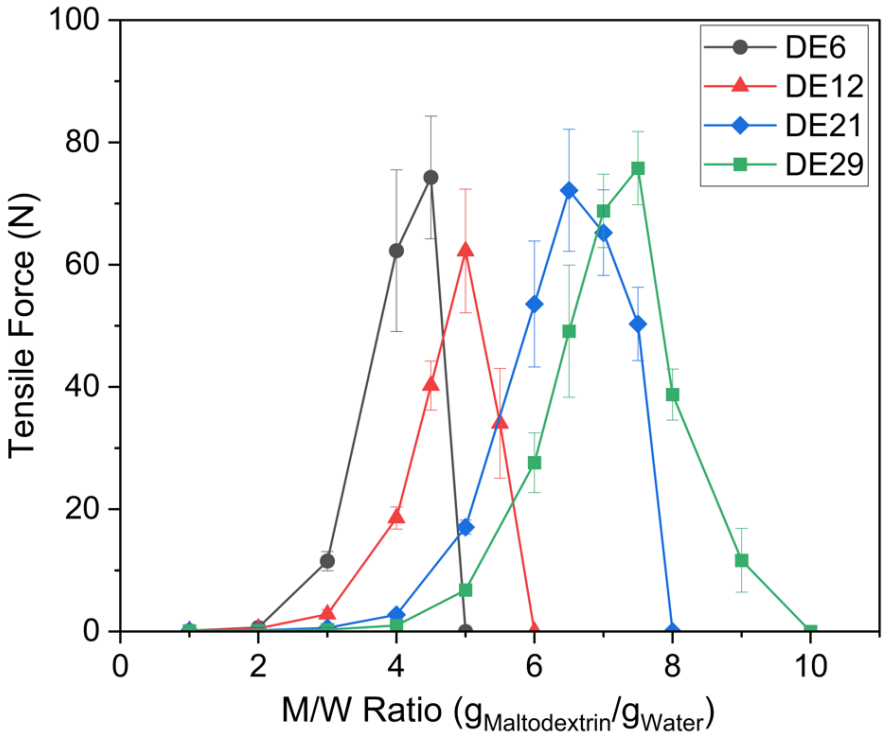

Figure 5.15: Maximum Tensile Force acting on the bead during the withdrawal process for Maltodextrin-water mixtures at different M/W ratios. A high tensile force indicates a greater stickiness of the mixture.

5.4.3 Viscosity measurement

This change in binder mobility and stickiness with M/W ratio is due to the increase in viscosity of the water binder as powder incorporation occurs. Viscosity of Maltodextrin-water mixtures at different solid contents (M/W ratio) was measured to evaluate how the viscosity of the binder would change as it mixed with the powder bed. Figure 5.16 displays the effect of shear rate on the viscosity of Maltodextrin-water mixtures for the different Maltodextrin at varying M/W ratios. The maximum measurable M/W ratio was smaller for lower DE Maltodextrins. For example, the maximum measurable M/W ratio for DE6 and DE12 was 1.5, while for DE21 it was 2, and for DE29 it was 3. This is because low DE Maltodextrins produced highly viscous mixtures that would exceed the rheometer's operating range at lower M/W ratios compared with high DE Maltodextrins.

For all Maltodextrins, increasing the M/W ratio results in an increase in viscosity which is best displayed by Figure 5.16b [25]. This is because Maltodextrin molecular chains possess hydroxyl groups which form hydrogen bonds with water. As more Maltodextrin is added to the mixture, they form more hydrogen bonds with water molecules and more intermolecular bonds with existing sugar chains in the solution. This network of bonding limits mobility and resists motion to a greater extent, resulting in a greater viscosity. It is also evident from Figure 5.16a, that this increase in viscosity is not directly proportional to M/W ratio with a greater increase in viscosity seen at higher M/W ratios than at lower M/W ratios. For example, for DE6, the increase in viscosity is greater when comparing a M/W of 1 to 1.5, than when comparing a M/W of 0.5 to 1. This can be attributed to saturation effects. This describes what occurs when the mixture nears the saturation point of the solvent and the water cannot hold more sugar. This leads to excess sugar in the system which interacts more strongly with each other resulting in the formation of more complex networks and more entanglement. This increases the structuring of the solution to a greater extent and results in a disproportionate increase in resistance to flow.

The increased entanglement at high M/W ratios can also be linked to the shear thinning behavior displayed by Maltodextrins at high M/W ratios. Shear thinning describes the phenomenon where viscosity decreases as shear rate increases. This behavior is most evident when looking at the effect of shear rate on the viscosity of DE6 at a M/W of 1.5 in Figure 5.16a. Shear thinning behavior occurs because as shear rate increases, it can lead to disentanglement of the polymer chains which reduces the viscosity of the mixture. At high M/W ratios when the degree of entanglement is high, the disentanglement caused by the high shear rates results in a more pronounced effect on viscosity than at low M/W when there is little entanglement to begin with [124].

The different Maltodextrins produce mixtures of different viscosities at the same M/W ratio which is best displayed by Figure 5.16b. For a given M/W ratio, viscosity was found to decrease in the following order: DE6, DE12, DE21, DE29. The decrease in viscosity with increasing DE number is well documented in literature [25] and meant higher maximum M/W ratios could be evaluated for higher DE

Maltodextrins. This is because lower DE Maltodextrins have longer polymer chains with more hydroxyl groups. This means when low DE Maltodextrins are added to water they form more hydrogen bonds and entangle with each other more easily than high DE Maltodextrins do. This leads to the creation of more complex networks in the solution which resist flow more strongly.

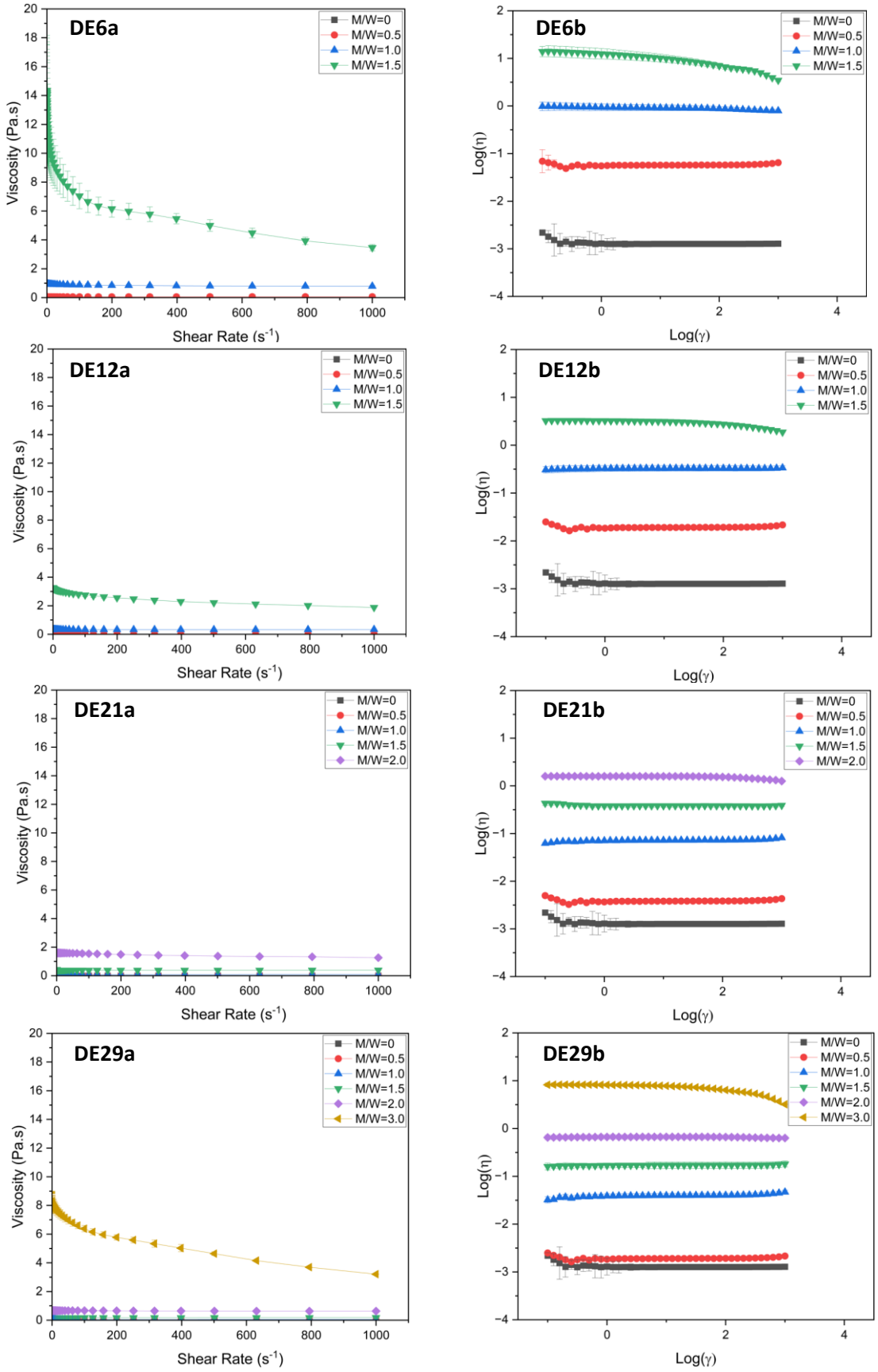

Figure 5.16: Effect of shear rate on the viscosity of the Maltodextrin-water mixture for the different Maltodextrin grades at varying M/W ratios. 15a plots viscosity against shear rate while 15b plots the natural log of viscosity against the natural log of shear rate. M/W indicates the ratio of Maltodextrin powder to liquid water in the measured sample. M/W of 0 indicates the viscosity of pure water.

5.4.4 Selection of a suitable shear rate

The next step involved linking this increase in viscosity with M/W to the Granulation Efficiency of the Maltodextrin powders. However, when considering viscosity, the shear thinning nature of Maltodextrin solutions must be considered. Therefore, to evaluate the increase in viscosity during granulation, a suitable value for shear rate must be chosen at which to select viscosity values. To achieve this, PIV analysis was carried out to determine a maximum realistic shear rate for the High Shear Granulation system studied in this work. Figure 5.17 displays the conditions that created the lowest and highest shear rate in the bed and the associated powder bed velocities from the PIV analysis. The lowest powder bed velocities and shear rates was seen at a batch size of 200 g and impeller speed of 450 rpm while the highest powder bed velocity and shear rate was seen at 400 g and 1800 rpm.

The bed surface velocity and shear rate was found to increase as batch size was increased. This is attributed to the increased filling height of the powder bed resulting in better contact between the powder bed and impeller. This is displayed by Figure 5.17, where at 200 g, only the lower part of the impeller is contacting the powder. While at 400 g, both the upper and lower part of the impeller are in contact with the powder bed which would have allowed better transfer of energy from the impeller to the powder, increasing bed velocity. The increased fill height also resulted in better contact between the powder bed and the scraper which resulted in the powder flow profile becoming more turbulent. This increased turbulent flow resulted in more intense velocity gradients in the powder bed, increasing the shear rate.

Increasing impeller speed was found to increase bed surface velocity [125,126]. This can be attributed to the higher impeller speed imparting more kinetic energy onto the powder flow and resulting in higher particle velocities. The increased impeller speed creates a more prominent layer of powder near the impeller that moves at faster speeds when compared with the bulk of the powder bed (which primarily rotates depending on the bowl velocity). The velocity gradient between powder influenced by the rotation of the impeller and powder influenced by the rotation of the bowl increases with impeller speed resulting in the localized high shear rates observed near the impeller in Figure 5.17.

The largest shear rate observed in the system was around 100 s^{-1} which was in the localized area around the impeller at a batch size of 400 g and impeller speed of 1800 rpm as indicated by the highlighted red square in Figure 5.17. This region around the impeller is where the greatest input of energy into the system will be and therefore it is the critical area for granulation to occur. Therefore, this maximum observed shear rate value of 100 s^{-1} in this region was chosen as the shear rate at which to evaluate viscosity. The velocities and shear rates generated at the other evaluated process conditions are shown in the Appendix Figure 3A and 4A for the readers interest.

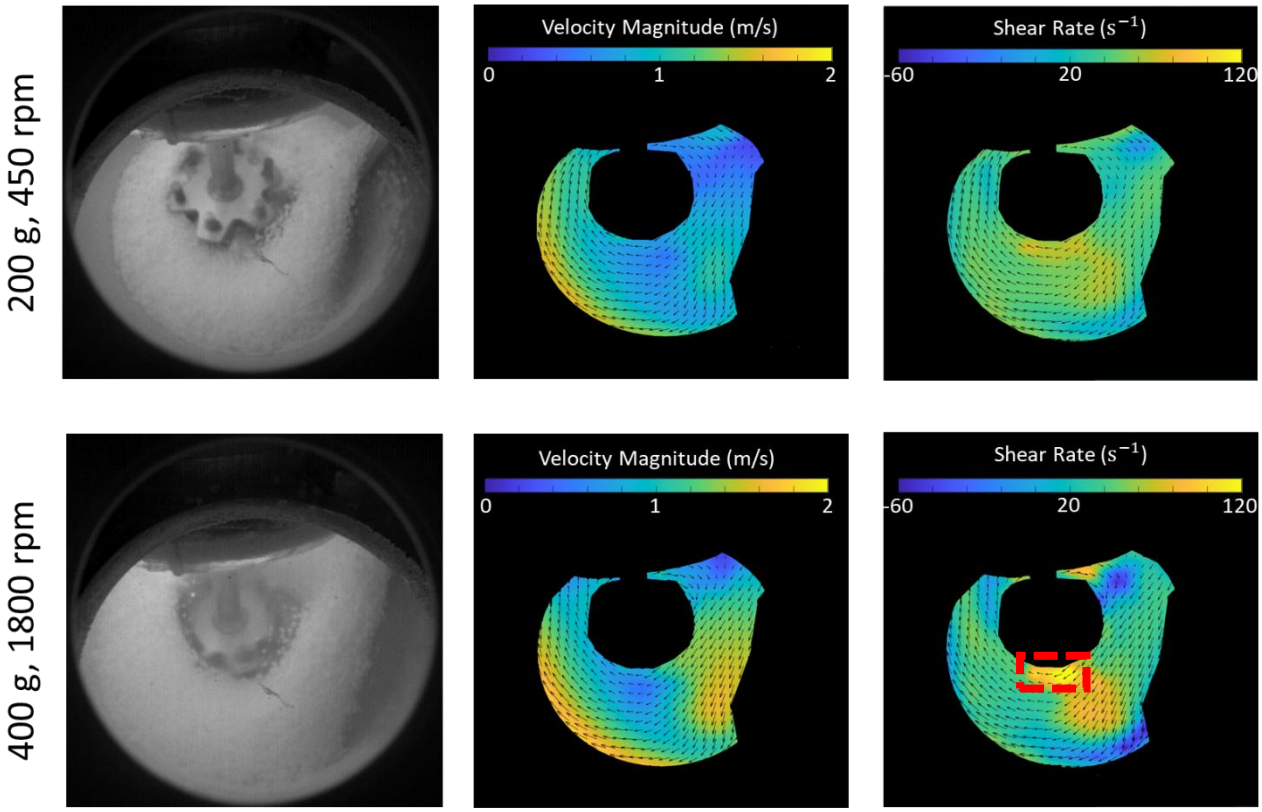

Figure 5.17: Presents the minimum (200 g and 450 rpm) and maximum (400 g and 1800 rpm) surface powder bed velocity and shear rates developed in the Eirich Granulator using PIV. The area representing the impeller and rotating bowl were masked during the analysis to focus on the motion of the powder as detailed in Section 5.2.8. The dotted red square (on the bottom right image) indicates the region near the impeller that developed the highest modelled shear rate of 100 s^{-1} .

5.4.5 Linking Viscosity to Granular Yield

Figure 5.18 shows the increase in viscosity with M/W ratio between the different Maltodextrin at a shear rate of 100 s^{-1} (viscosity data extracted from Figure 5.16). For all Maltodextrin, viscosity increased in an exponential manner with M/W ratio. This exponential relationship exists because at higher M/W ratios, the hydrogen bonds that are formed between the polymer chains result in the creation of increasingly more complex networks that resist motion to a greater extent. Furthermore, as M/W increases, the degree to which the polymer chains entangle with each other increases at a disproportionate rate. The general equation for an exponential growth expression is given by Equation 5.5. Here A is the y intercept and k_μ is the growth rate constant which determines how quickly viscosity (y variable) increases with M/W ratio (x variable). This equation was used to model the exponential growth trend line for the Maltodextrin powders in Figure 5.18.

$$y = Ae^{k_\mu x}$$

Equation 5.5

When the M/W is 0 then there is no Maltodextrin in the mixture and it is entirely composed of water. This means that the viscosity at a M/W of 0 is the viscosity of pure water, which was measured to be 0.0011 Pa.s. This value has been set as the A variable for all the Maltodextrin as shown in Figure 5.18.

The growth rate constant (k_μ) meanwhile varies with lower DE Maltodextrin possessing a larger k_μ. The larger the k_μ, the quicker the binder viscosity will increase as it incorporates powder during granulation. Consequently, the binding material loses its stickiness and mobility at a faster pace. This results in a less efficient binding system and increases the water content needed for granulation. Therefore, the reciprocal of k_μ ($1/k_\mu$) can be used to mathematically reflect the idea that larger k_μ values result in a lower Granulation Efficiency. Figure 5.19 plots the change in $1/ k_\mu$ across the Maltodextrin grades alongside the Granulation Efficiency. Both parameters exhibit nearly parallel trend lines, as evidenced by their closely aligned exponential rate constants (0.047 for Granulation Efficiency and 0.039 for $1/ k_\mu$). This suggests a strong correlation between the Granulation Efficiency and $1/ k_\mu$.

Typically, when considering viscosity in the context of granulation, literature focuses on the effect of binder viscosity and its effect on the strength of the bonds formed between granules [127,128]. Meanwhile, this study looks at the change in viscosity of the powder-binder mixture that is formed during wetting to establish a correlation with the L/S ratio required to granulate the powder. This novel approach can prove to be highly valuable for future studies looking at predicting L/S requirements to maximize yields while minimizing the risk of adding excess liquid such as caking and needless drying.

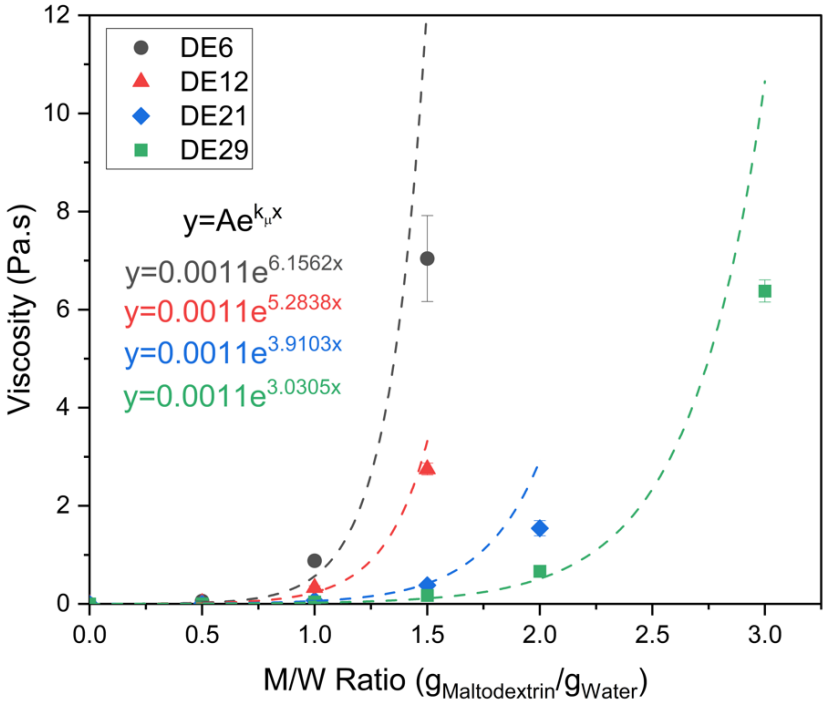

Figure 5.18: Increase in viscosity with M/W ratio for the different Maltodextrins at a shear rate of 100 s^{-1}. The increase has been modelled by an exponential growth trend line where A is the y intercept and k_μ is the growth rate constant.

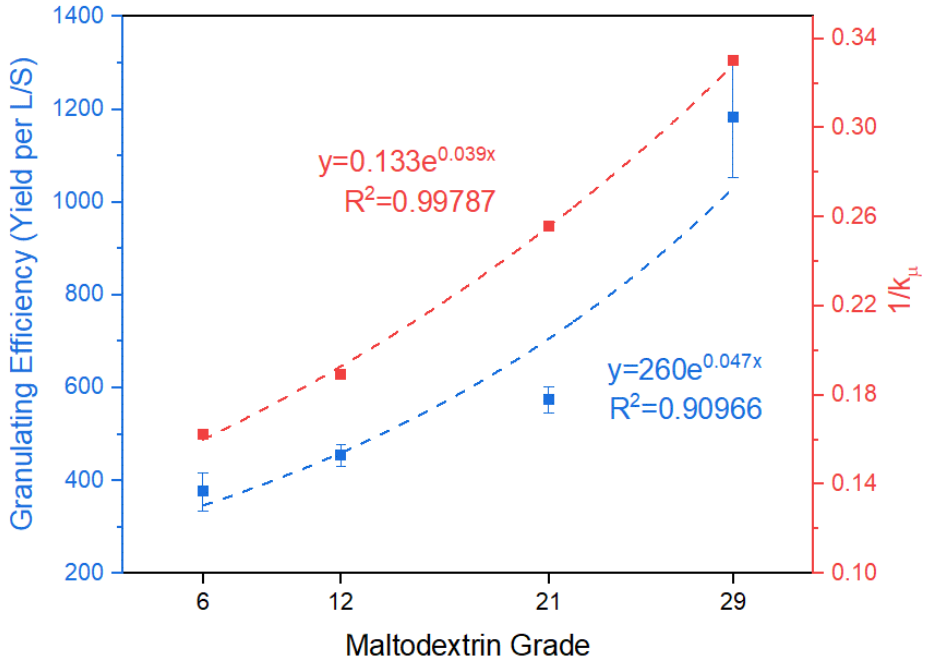

Figure 5.19: Effect of Maltodextrin grade on the average Granulation Efficiency (increase in granular yield with L/S ratio) and the reciprocal of the viscosity growth rate constant (1/ k_μ). The trendlines of these two relationships show a similar growth constant which indicates a good correlation with each other.

5.5 Regime Map

This work has highlighted the predominant effect of L/S ratio and temperature in determining the granulation behavior of amorphous powders. The L/S ratio represents the amount of water added to the process. When added the water binder will quickly dissolve and incorporate the amorphous powder, changing the properties of the binder as it does so. This is a big departure from the granulation of insoluble powders where the properties of the binder remain relatively unchanged during the granulation process. The addition of water will also affect the T_g of the amorphous powder. The difference between the powder temperature and powder Glass Transition Temperature (T-T_g) will decide whether the material is in the glassy or rubbery state. The more positive this T-T_g value, the rubberier the material will be and the more likely it will display caking behavior. This interaction with temperature is something that is unique to amorphous powders and is completely absent when considering crystalline powders.

To reflect the importance of the L/S ratio and T-T_g parameter, the granulation data previously presented in Figure 5.8 has been displayed in terms of L/S and T-T_g in Figure 5.20. Here the effect of impeller speed and batch size is represented through the Temperature (T) parameter with higher impeller speeds and larger batch sizes resulting in higher bed temperatures. Figure 5.20 has been divided into two regions, the first is the granulation zone where normal operation can be carried out. The second is the caking zone where a heightened risk of caking exists which will cause process failure and material loss.

L/S and T-T_g are the drivers for the agglomeration process. Figure 5.20 shows that as L/S and T-T_g increase, the yield increases as there is a stronger motive for granulation. Beyond a certain value of T-T_g the driving force for agglomeration becomes too strong and excessive agglomeration results in caking. This caking leads to severe loss of material and a significant decrease in the yield. This is indicated in Figure 5.20 as color transitions from a yellow/orange/red complexion to a green/blue colour, which represents the decrease in yield due to caking. The T-T_g value where caking occurs appears to occur between +30 to +45˚C. Existing literature states that the sticking point of amorphous sugar mixtures is around 10 to 20°C higher than the Onset T_g [129]. It is also known that the caking temperature is higher than the sticky point temperature. This work has established it to be 30 – 45°C greater than the Onset T_g for the Eirich HSG system. Another point of note is that the degree of separation between the normal operation zone and caking point decreases as the DE number increases. For example, in the case of DE6 and DE12, there is a very clear separation between the green/blue points indicating caking and the points below indicating a high yield and normal operation. Whereas, with DE21 and DE29, the points indicating caking start to become more intermixed with those indicating normal operation. This reflects the extra sensitivity of Maltodextrin with increasing DE number and highlights how more care must be taken monitoring bed temperature with high DE Maltodextrins in order to avoid caking.

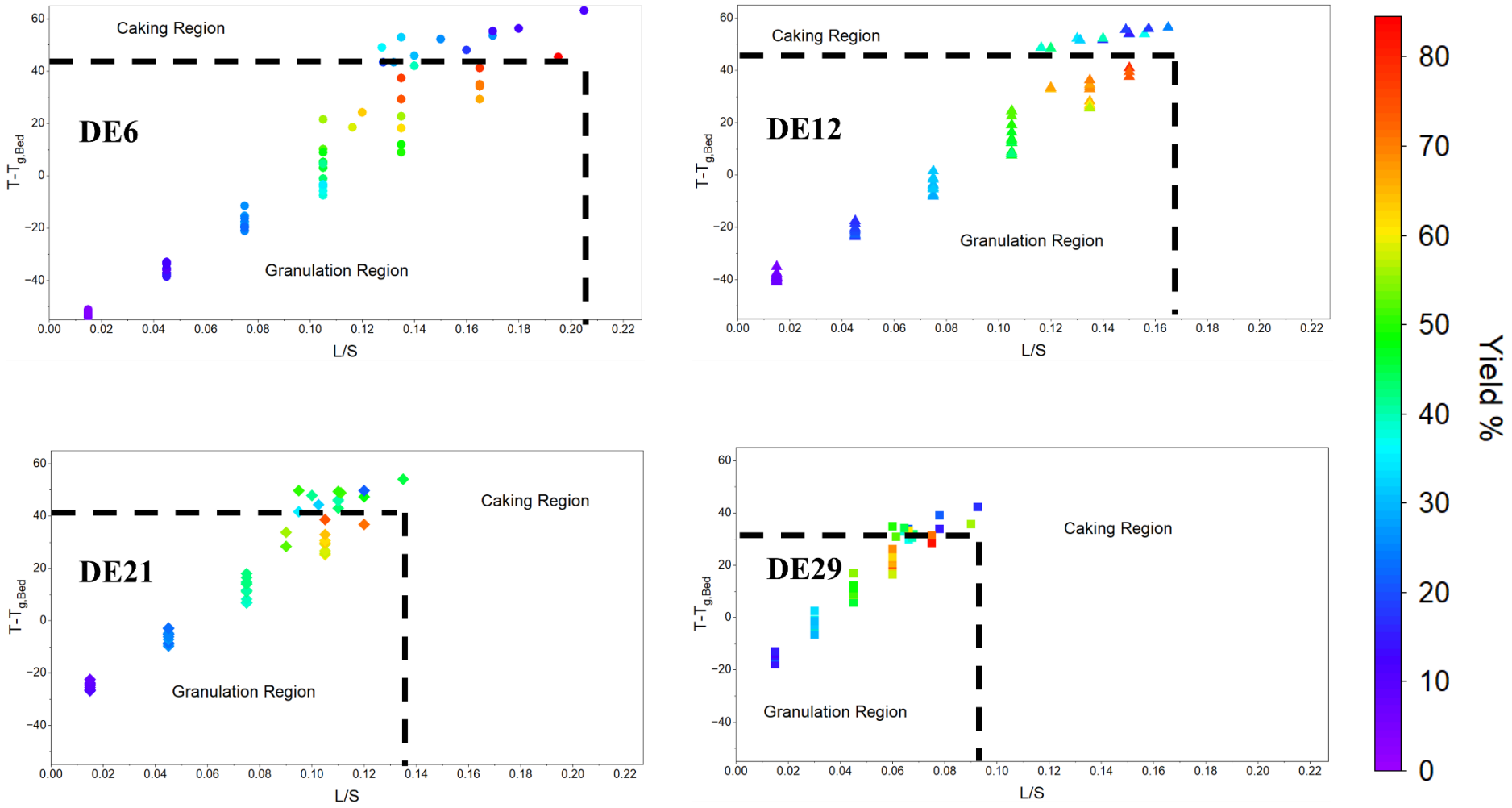

Figure 5.20: Shows the effect of changing L/S ratio and T-$T_{g,Bed}$ on granular yield. A dividing line seperating the yield points representing normal operation and representing caking has been added. The T- $T_{g,Bed}$ value where caking happens appears to occur between +30 to +45˚C. The L/S ratio at which caking occurs decreases with increasing DE number for the different Maltodextrins.

Currently Figure 5.20 plots the granulation behaviors of the Maltodextrin powders independently of each other. The reason they cannot be plotted together yet is because there is no parameter on the L/S axis that accounts for the fact that water interacts with the Maltodextrins differently. This is because during wetting, the water mixes with the Maltodextrin powder which leads to the formation of binders with different effectiveness's. In the field of wet granulation, binder viscosity is typically used to evaluate the effectiveness of different binding systems. For example, existing regime maps for wet granulation in the Twin Screw Granulator multiply the L/S term with the binder viscosity to account for the effectiveness of different binders in the system [110,130]. This is a suitable approach for a scenario where the binder properties remain relatively unchanged during granulation. However as shown by this study, when liquid water is used to granulate amorphous powders, the properties of the binding material can change significantly during the granulation process as it incorporates more solid into itself. Consequently, for the granulation of amorphous powders with water, it is the rate at which binder viscosity increases during wetting that determines the effectiveness of the binding system. The faster the increase in binder viscosity, the quicker the binder loses its mobility and stickiness which leads to the loss of its ability to function as a binder. To reflect this, Figure 5.20 was further developed by introducing the material parameter k_μ into the x axis as shown in Figure 5.21. This parameter is the growth rate constant of viscosity with M/W ratio as presented in Figure 5.18 and correlates well with the varying Granulation Efficiency of the different Maltodextrin as shown by Figure 5.19. Its introduction changed the term on the x axis to L/S divided by k_μ. This is to reflect the concept that the greater the k_μ value, the less effective the water added will be as a driver towards agglomeration. The introduction of the k_μ value means that all the Maltodextrins can be plotted on the same graph to produce the complete regime map. This map combines process parameters such as L/S, Impeller Speed and Batch Size (represented through the Temperature term) with material properties such as T_g and Viscosity (represented through the k_μ value) to predict granulation behavior. Currently the map presents two regions. The first is the granulation region where normal operation occurs without caking. The second is the caking region which occurs at T-T_g values of more than 40˚C and (L/S)/ k_μ of 0.0325. In this region there exists a heightened risk of caking. Special care should be taken to ensure that the granulation process should not exceed these boundary conditions. The use of PAT tool such as temperature sensors can be employed to ensure this. Furthermore, a caking study by Palzer [111] found that the difference between the Bed Collapse (caking) Temperature and Glass Transition Temperature in the Fluidised Bed Granulator was around 40°C for a DE21 powder. This is similar to the result observed here for the HSG system and indicates that this work could potentially be applied to other wet granulation systems.

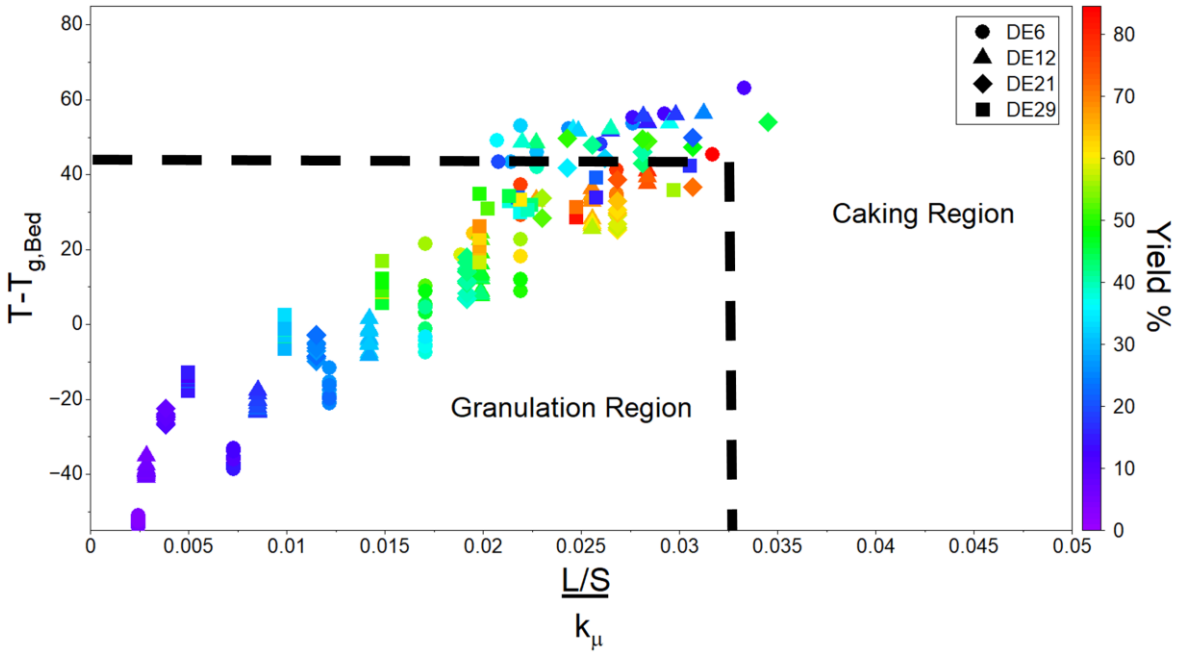

Figure 5.21: Completed regime map indicating the normal operation and caking region for all the evaluated powders. The viscosity growth rate constant k_μ has been introduced here as a parameter accounting for the interaction of water with the different Maltodextrin powders. Threshold for caking has been established to be at T – T_g value of 40°C and (L/S)/k_μ value of 0.0325

5.6 Conclusion

This work comprehensively studied the caking phenomenon of amorphous powders in the High Shear Granulator. Through this work, the influence of key process parameters such as impeller speed and batch size on caking has been evaluated. Furthermore, the interaction between the water binder and amorphous powder has been critically analyzed. This analysis revealed a link between the exponential growth rate constant of binder viscosity with increasing solid content (presented in this work as k_μ) and the Granulating Efficiency (indicating the increase in granular yield with L/S ratio) of the different Maltodextrins. This parameter can be used in future studies to develop a model predicting the L/S ratio required to achieve optimum yields without the need for costly experimental trials. This k_μ parameter was incorporated to account for the differing impact of water binder on various Maltodextrin types through the $(L/S)/k_\mu$ parameter. The $(L/S)/k_\mu$ parameter alongside the (T-T_g) parameter was used to produce a HSWG regime map for amorphous powders that presents two key regions: the granulation region and the caking region. The boundary conditions presented in the map should be used as a tool to help avoid operation in this caking region. This will minimize potential damage to the equipment as well as reducing material wastage due to caking.

6 Layered Granulation to Enhance the Shelf Life of Granular Food Systems

Abstract

Humidity-induced caking of granular products during storage is a significant issue that reduces shelf life and leads to material waste. Traditional approaches to preventing caking rely on metal and plastic packaging to create effective moisture barriers; however, these methods are material-intensive and unsustainable. This study explores an alternative strategy which involves modifying the granular structure to develop a layered granular system with enhanced resistance to humidity. In this granular system, moisture-insensitive components are preferentially positioned on the granule surface, while moisture-sensitive components are confined to the core. A novel multi-operation process incorporating Roller Compaction, Dry Coating, and High Shear Granulation was employed to produce Layered Granules composed of Maltodextrin DE6 and Coffee. The storage properties of the Layered Granules were compared with Standard Granules (in which DE6 and Coffee were randomly distributed). Over a 16-day storage period, the Layered Granules demonstrated significantly lower amounts of caking compared to Standard Granules across all evaluated formulations. Additionally, greyscale analysis revealed that the Layered Granules experienced less colour change, preserving product aesthetics more effectively. The Layered Granules also maintained their size better by displaying reduced shrinkage, particularly at low DE6 compositions. Overall, adopting a layered granular structure significantly mitigates humidity-induced degradation, offering a promising approach to developing food products with extended shelf life while reducing reliance on traditional moisture barrier packaging. This work concluded by proposing a 3-layer granular system designed to further mitigate caking while simultaneously preventing moisture migration toward the granule core, protecting the moisture-sensitive materials placed there.

Highlights

- Developed a novel, layered wet granulation process for moisture sensitive material
- Layered Granules were less prone to caking than Standard Granules
- Layered Granule structure displayed less colour change and granule shrinkage
- Novel 3 Layer Granule structure proposed to hinder moisture migration into granule core

This chapter forms the basis of the following paper:

Y.H. Karunanayake, L. Brütsch, V. Meunier, A.D. Salman (2025). Layered granulation to enhance the shelf life of granular food systems. Chemical Engineering Research and Design, Volume 223. pp 425-438

https://doi.org/10.1016/j.cherd.2025.10.016

6.1 Introduction

Granulation is a common size enlargement process that is carried out in the food industry to produce a more stable particulate. Despite the enhanced stability, the caking of these granules during storage is a persistent problem. This describes a process where bridges form between granules leading to adhesion [77,131]. The adhesion between particles leads to a growth in granule size, change in product texture and can affect key quality attributes such as the dissolution time. Over time, caking mutates the product to such an extent that it becomes unusable and it must be discarded, leading to material waste. Therefore granules that are more susceptible to caking suffer from a short shelf life resulting in a less sustainable and economical product.

Granules in the food industry are multicomponent structures that contain elements of various hygroscopicity and tendencies to undergo caking. For example, these elements can include hydrophobic substances such as oils and fats, moisture insensitive crystalline powders, and amorphous powders of varying moisture sensitivity. The bridge formation between these components that leads to caking, can be caused by many factors including the melting of fatty components [132], capillary condensation [133] and mechanical stresses [133]. When considering the caking of amorphous powders, the humidity driven decrease in the Glass Transition Temperature (T_g) is of special concern [131]. The T_g of an amorphous powder represents the point at which it transitions from a rigid, glassy material to a viscous, sticky substance. During storage, amorphous powders absorb moisture from the atmosphere which acts as a plasticiser to decrease the powder T_g. As the T_g decreases, eventually the point is reached where it decreases below the storage temperature. At this point, the powder gains the ability to flow and forms material bridges with neighbouring particles resulting in caking.

Currently, research into the prevention of caking during storage has focused on investigating the role of different packaging in preventing moisture uptake. For example Zang et al [73] evaluated the effect of packaging such as plastic polypropylene and aluminium on the caking of whole egg powder while Kumar and Mishra [74] conducted a similar study focusing on the caking of mango powder. However, there is a desire in the food industry to reduce the amount of packaging (especially plastics and metal) in the drive for increased sustainability. Therefore, it would be beneficial if particulate systems themselves could be engineered to be more stable to reduce the industry's reliance on packaging. Another approach involves adding anticaking agents which operate by hindering moisture uptake or act as physical barriers to stop bridge formation from occurring [75,77,131]. For instance, Fu et al [75] evaluated the effect of anticaking agents such as calcium stearate and silicon dioxide on the caking properties of peptide powders. However, the addition of extra components to a food formulation can be complicated because it can lead to taste, compliance and compatibility issues. This has resulted in a movement known as clean labelling in the food industry where recipes are tailored to be simple and contain fewer ingredients.

Instead of additional packaging or extra ingredients, this work proposes modifying the granulation production process to better engineer a more caking resistant product. Typically, for both wet and dry granulation, there is a dry mix stage prior to the granulation step to create a randomly distributed mix [134]. A randomly distributed mix describes the scenario where components in the mix are distributed in an unsystematic and arbitrary manner. In wet granulation, liquid is then added, and these blended elements are agglomerated to form granules. Meanwhile in dry granulation, high stresses are applied to the blend to produce a compact which then undergoes milling to form granules. These granulation pathways produce granules with a random distribution of components within the granule. In this work, this is referred to as the Standard granulation pathway and the granular product as the Standard Granule. This study proposes that this current approach where components are randomly distributed within a granule to be antiquated and unsustainable. Rather, the granulation philosophy should involve the production of a multi-tiered granule where components are layered together to form a shell shaped granule structure. The inner most layers should be formed of the materials with the greatest sensitivity to moisture while the outermost layers are formed of the materials with the greatest resistance to moisture. Since the granule surface will be predominantly composed of moisture insensitive material, it should reduce the stickiness at the granule surface and hinder humidity induced bridge formation during storage. The importance of surface composition was highlighted by Ozkan et al [135]. They observed that whole milk powder had a high caking tendency because its surface was predominantly covered in fat (despite the average overall fat composition only being 27%) which melted and formed bridges. Similarly, Fitzpatrick et al [136] noticed that the high non-amorphous surface content of skimmed milk hindered bridge development by amorphous lactose (which is the majority component).

The primary aim of this work is to evaluate the benefits of a Layered Granule structure in preventing humidity induced caking during storage. To produce these Layered Granules, a novel, multi-operation process has been developed which facilitates the layered granulation of water sensitive powders without inducing structural collapse. This layered granulation process was used to produce multicomponent, Layered Granules which preferentially placed moisture insensitive elements at the granule surface. A comparison study was then carried out comparing the caking of these Layered Granules against Standard Granules (where the different elements are randomly distributed) to highlight its benefits with regards to extending shelf life.

6.2 Materials and Methods

6.2.1 Materials

Five types of Maltodextrin powders (IT6, IT12, IT21, IT29 and IT47) were acquired from Roquette (France). The IT grade is equivalent to the dextrose equivalent (DE) of the Maltodextrin and henceforth the Maltodextrin powders will be referred to by their DE number. Instant soluble Coffee powder was

supplied by Nestle Research (Switzerland). The particle size of the Maltodextrin and Coffee powders are shown in Table 6.1 below.

Table 6.1: Particle size distribution of the raw powders used in this study

	Particle Size (µm)					
	DE6	DE12	DE21	DE29	DE47	Coffee
d10	144 ± 9	153 ±14	141 ± 20	143 ± 17	55 ± 2	33 ± 2
d50	292 ± 21	271 ± 20	270 ± 15	255 ± 19	153 ± 1	126 ± 7
d90	651 ± 30	569 ± 37	547 ± 25	455 ± 19	248 ± 9	287 ± 46

To produce the Standard and Layered Granule structures, DE6 was chosen as the moisture insensitive component and Coffee was chosen as the moisture sensitive component. The colour difference between the two materials (DE6 being white while Coffee being brown) means that visual techniques such as optical microscopy can be used to easily evaluate the effectiveness of the layering process. Furthermore, Coffee is a widely consumed powder and forms a key component of many food and beverage products. Identifying ways to better protect it from caking highlights the real-world benefits of this work.

6.2.2 Sieving and Micronisation of Maltodextrin DE6 for Layered Granulation

Two distinct particle size classifications of Maltodextrin DE6 was used in the procedure to form the Layered Granule. In this work, they are referred to as Micronized DE6 and Fine DE6. The particle size distribution of the Micronized and Fine DE6 alongside the raw DE6 powder is shown in Table 6.2.

A J-20 Fluid Jet Mill (Tecnologia Meccanica, Italy) was used to micronize the raw DE6 powder. The feeding pressure was 5.5 bar and the grinding pressure was 5 bar. This powder would then be used in a dry coating process of the Coffee granules prior to undergoing wet layered granulation. The dry coating process is better described in Section 6.2.7.

The Fine DE6 powder was used in the layered wet granulation process to form the Layered Granule. It was produced by sieving the raw DE6 powder using a sieve mesh size of 200 µm to isolate the fraction of the raw DE6 Maltodextrin powder with a particle size less than 200 µm. This operation was carried out in a Retsch Sieve Shaker AS200 (Retsch, UK) at an amplitude of 1.5 mm for 10 mins.

Table 6.2: Particle size distribution of the Raw, Fine and Micronized DE6 powder

	Particle Size (µm)		
	Raw DE6	**Fine DE6**	**Micronised DE6**
d10	144 ± 9	22 ±1	4.9 ± 0.2
d50	292 ± 21	69 ± 2	10 ± 1.6
d90	651 ± 30	144 ± 2	21.3 ± 1.4

6.2.3 Production of Pure Maltodextrin granules

Pure Maltodextrin granules of DE6, DE12, DE21 and DE29 were produced using an Eirich EL1 High Shear Granulator (Eirich GmbH, Germany). The batch size used was 400 g and the impeller speed was 450 rpm. The bowl speed was set at 170 rpm, and the granulator was used in the horizontal configuration (inclination angle is 0˚). The granulator was operated in the co-current mode where the impeller and bowl both rotated in a clockwise motion. The liquid addition rate was 1.5 g/min and the following L/S ratios were used depending on DE grade: 0.135 (DE6), 0.135 (DE12), 0.105 (DE21), 0.06 (DE29). The L/S ratio was chosen to maximise the amount of granules produced without over wetting occurring. These granules were used to test the effect of key material properties such as T_g on granule caking.

6.2.4 Production of pure Coffee granules

Roller Compaction was used to produce pure Coffee granules. A dry granulation technology like Roller Compaction was chosen as opposed to wet High Shear Granulation because Coffee is very soluble in water and therefore even a small amount of water has the potential to interact with and collapse the structure of the Coffee powder. This structural collapse negatively impacts Coffee quality attributes such as dissolution time. The use of a dry granulation technique where no water is used, eliminates this concern. Furthermore, Roller Compaction is far more energy efficient compared to wet granulation technologies as it does not need a very energy intensive drying stage making the overall production of granules more sustainable [137].

Roller Compaction was carried out using an Alexanderwerk WP120 Pharma Roller Compactor (Alexanderwerk AG, Germany). The compaction pressure used was 40 bar. This was the highest pressure that could be used before the Coffee powder began to display a tendency to glass transition. The roll gap used was 3 mm and the roll speed was 3 rpm. The milling speed was 40 rpm, and system was configured with mill mesh sizes of 3.5 mm and 2.45 mm to maximise the production of granules between 1 - 2 mm. Similarly, to the pure Maltodextrin granules, the pure Coffee granules were used to evaluate the effect of material properties on granule caking.

6.2.5 Theory for Layered Granulation

The primary aim of this work is to highlight the benefits of a Layered Granule microstructure compared to a Standard Granule microstructure in preventing caking and extending product shelf life. Figure 6.1 displays an illustration of a Standard Granule (A) cross section composing of a moisture sensitive and moisture insensitive material formed from the standard granulation process. The moisture sensitive material in this work is represented by Coffee and the moisture insensitive material is represented by DE6. As visualised, the two materials are randomly distributed in the Standard Granule, with the granule surface composition including both moisture sensitive and insensitive materials. During storage, these

powders will absorb moisture and their T_g will decrease. If the T_g decreases below the storage temperature, then these materials will become mobile and experience viscous flow. In a high humidity environment, the moisture sensitive material (Coffee) will quickly absorb moisture due to its hygroscopic nature. This will cause its already low T_g to decrease further to below the storage temperature which results in Glass Transition induced material flow. The moisture insensitive material (DE6) will similarly absorb moisture but not enough to sufficiently depress its T_g below the storage temperature. Therefore, it will not undergo Glass Transition and will not experience material flow. However, the random distribution of elements in the granule means that localised areas on the granule surface which hosts high concentrations of Coffee will display a high degree of material mobility. This high mobility will lead to bridge development from these areas on the granule surface which results in adhesion and caking as visualised in Figure 6.1. This study will develop a granulation process that is capable of structuring these elements in a layered manner where the moisture sensitive material (Coffee) is confined to the core and the moisture insensitive material (DE6) forms the outer layer. This granule structure is presented as the Layered Granule (B) in Figure 6.1. In this scenario, while the Coffee may still undergo glass transition, its viscous flow will be better contained and restricted by the outer DE6 layer. This means that the granule surface will be less sticky and experience less bridging leading to less caking. The granulation pathways used to produce the Standard and Layered Granule structures are presented in Section 6.2.6 and 6.2.7 respectively. Studying the effect of structural arrangement differentiates this work from previous literature investigating the caking of binary mixtures which has focused primarily on composition [138–140].

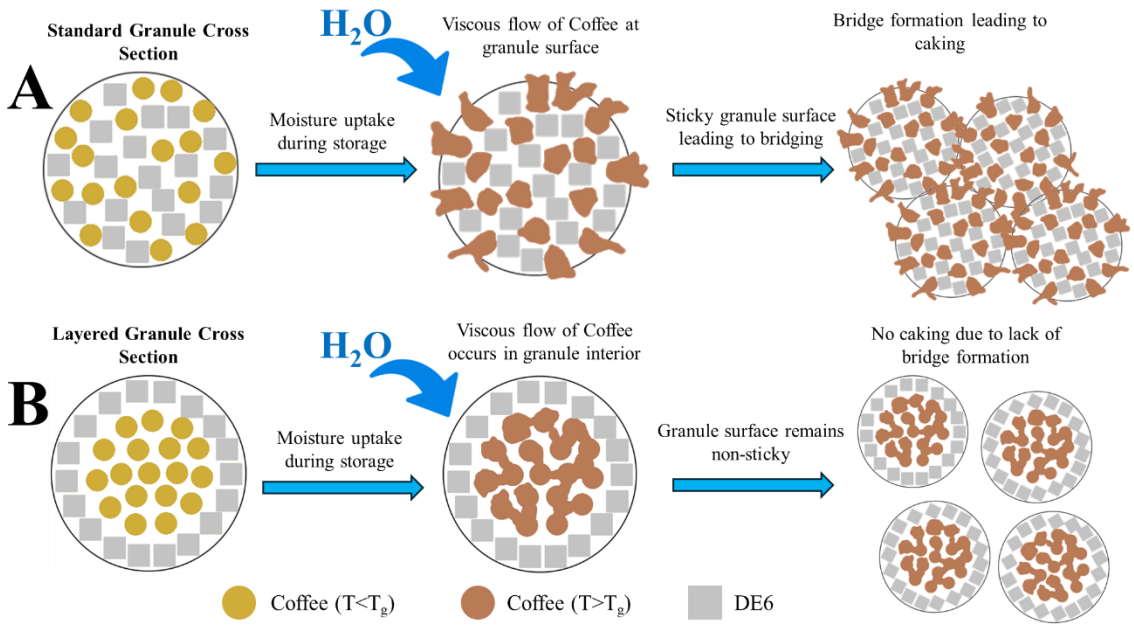

Figure 6.1: Illustration of a granule cross section formed from the Standard granulation pathway (A) and the Layered granulation pathway (B). In the Standard granulation pathway, the random distribution of material means that there are significant amounts of moisture sensitive material (in this case Coffee) on the granule surface. Uptake in moisture during storage causes this material to undergo glass transition leading to bridge formation and caking. In the Layered granulation pathway, the moisture insensitive material is preferentially placed on the granule surface. This helps protect against caking during storage as this material undergoes little to no change when exposed to high humidity. It is then capable of acting as a physical barrier to contain the viscous flow of the Coffee undergoing glass transition in the granule core.

6.2.6 Production of the Standard Coffee-Maltodextrin Granule Structure

This section will outline the procedure used to produce Coffee-DE6 granules with the Standard Granule structure as illustrated in Figure 6.1A. The procedure follows the previously described Standard granulation pathway where the different components are first dry mixed together to form a randomly distributed mixture before being granulated. The dry mixing was carried out in a Eirich EL1 High Shear Mixer (Eirich, GmbH, Germany) at an impeller speed of 450 rpm and bowl speed of 85 rpm for 5 min. The bowl and the impeller were both set to rotate in a clockwise motion. This was used to produce three different formulation blends of Coffee-DE6 where the DE6 percentage was 25%, 40% and 50%. These blends were then Roller Compacted under the same conditions presented in Section 6.2.4. The granulation of these randomly dispersed blends produces granules with a random distribution of components.

6.2.7 Production of the Layered Coffee-Maltodextrin Granule Structure

The following section will outline the procedure used to produce Coffee-DE6 granules with the Layered Granule structure as illustrated in Figure 6.1B. This was a multi-step process which first involved Roller Compaction to produce the core Coffee granule. These Roller Compacted Coffee granules were then dry coated with Micronized DE6 and then steam treated to lock this coating in place. Finally, these

coated granules underwent wet layered granulation in the Eirich EL1 High Shear Granulator to produce the Layered Granule structure. High Shear Granulators are far better suited for the production of Layered Granules compared to Roller Compactors. In Roller Compaction, the different components are mixed within the feeding system of the unit, creating a random mix, which results in a randomly organised ribbon being produced. Whereas, in High Shear Granulation, components can be introduced into the granulator sequentially which encourages the formation of layers. The production pathway to produce the Layered Granule structure is presented in Figure 6.2 and will be explained in greater detail throughout this section.

Step 1 involves producing pure Coffee granules through Roller Compaction as outlined in Section 6.2.4. Coffee granules between 1 – 2 mm that were produced in this manner were selected to act as the core of the Layered Granules, onto which DE6 would be layered upon in subsequent steps.

Step 2 involved dry coating the core Coffee granules with micronized DE6, which was a necessary intermediate step prior to wet granulation to limit the Coffee granules exposure to water. This necessity arises because water has the potential to very quickly compromise and collapse the Coffee structure which would degrade the Coffee's quality attributes. It was important to ensure that the production method for producing the Layered Granule would not result in significant changes to the Coffee structure. Changes in the Coffee structure would mean that any benefits gained by the reduction in the caking tendency of the Layered Granule, would be detracted by the loss of granule functionality due to Coffee degradation during the wet granulation process. To prevent this degradation, a very thin layer of micronized DE6 would be developed on the Coffee granule surface using dry coating prior to granulation. This is because, aside from being moisture insensitive, DE6 is also a sugar with a high thickening power which means that it mixes with water to form a highly viscous substance. During granulation, the water binder would contact this thin DE6 outer layer first, which would then interact with the water to form a viscous mixture. The high viscosity of the mixture resists the movement of water through its matrix. This essentially locks the water in this layer, which prevents water from passing through to the core coffee granule and collapsing it. The ability of high viscous sugars to lock in water has been demonstrated in other contexts. For example, Santomaso et al [141] evaluated the amount of water needed to granulate various MCC/sugar formulations. MCC typically absorbs water during the granulation process which prevents the water from acting as a binder. Santomaso et al [141] highlighted how sugars with high thickening powers form highly viscous sugar/water mixtures that prevents water absorption by MCC during the granulation process. This increased the water availability in the system meaning less water was needed for the granulation of MCC and high thickening power sugars. Whereas in the study of Santomaso et al [141], high thickening power sugars limited absorbance of water by MCC, in this study it will be used to limit the dissolution and collapse of the Coffee by water.

The formation of this DE6 layer was done by dry coating the Coffee granules with micronized DE6 using the Eirich High Shear mixer. The small particle size of the micronized DE6 gave them very high Van der Waal forces, allowing them to dry coat the Coffee granules with great efficacy. The granulator configuration was altered by replacing the impeller with a 3D printed cone as shown in Figure 6.3. The replacement was carried out because the impeller would exert excessive stress on the Coffee granules, even at the lowest speeds, resulting in a high attrition rate. Therefore, it was important to eliminate this source of stress to keep the Coffee granules intact. However, the removal of the impeller led to the development of an agitation dead spot in the bowl. To eliminate this dead spot, a 3D printed cone was glued to the centre of the bowl, which then rotated with the bowl during operation. The gentle slope of the cone resulted in little attrition and allowed a gentle dry coating process to occur.

The dry coating was carried out at a bowl speed of 85 rpm with a batch size of 100 g Coffee granules and 200 g micronized DE6. A high composition of micronized DE6 in the mix was used to promote contact between the Coffee granules and micronized DE6 to create as complete a coating coverage as possible. After dry coating, gentle sieving at an amplitude of 0.2 mm for 3 min was used to recover the coated granules and remove the unbound micronized DE6 powder. The subsequent dry coated layer of DE6 on the Coffee granules was found to be very fragile. This meant that if the coated granules were taken and directly used in the wet granulation process, the high speeds generated in the High Shear Granulator would quickly strip the coating away.

Step 3 involved steam treating the dry coated Coffee-DE6 granules. This was carried out by taking the dry coated Coffee-DE6 granules and placing them on a raised cellulose paper bed. Steam from a HY-128 Handheld Steamer (Rolipo, UK) was then passed over the granules for approximately 5 seconds. The porous nature of the cellulose paper meant that the steam could easily pass through the bed while still interacting with the granules. This prevented the build-up of moisture and sticking at the paper surface. This steam treatment causes the coated granule surface to become viscous and adhered the DE6 outer layer onto the Coffee. This increases the strength of the coating and allows it to survive inside the Eirich Granulator during the wet granulation step. Importantly, since steam contains little water, it does not cause the collapse of the core Coffee granule interior. This thin DE6 coating will act as a protective shield for the Coffee granules during the wet granulation process by hindering the movement of water into the Coffee. From comparing the mass of the granules prior to the dry coating (before Step 2) and after the steam treatment (after Step 3), it was estimated that the coated granules were composed of 4% DE6 at this point.

Step 4 involves granulating the steam treated Coffee-DE6 granules alongside Fine DE6 Maltodextrin powder using the Eirich Granulator in the modified configuration as shown in Figure 6.3. It is commonly expressed in literature that smaller particles perform better during layering processes. For example, Rahmanian et al. [142] stated that the diameter of the seed granule had to be at least two times

greater than that of the layering particle for seed granulation to occur. The smallest seed Coffee granule is 1 mm while the largest Fine DE6 particle is 144 μm. This gives a minimum ratio of 6.94 for the seed granulation process undertaken here which indicates it aligns well with the criteria set by Rahmanian et al. [142]. Therefore, the use of the Fine DE6 as opposed to the raw DE6 facilitated a more efficient layering mechanism. Micronized DE6 could not be used in this step because it was too cohesive and tended to promote the formation of large agglomerates rather than Layered Granules. The granulation batch consisted of 100 g Coffee with sufficient Fine DE6 to produce formulations with Maltodextrin percentages of 25%, 40% and 50%. Water binder was sprayed in at 1 g/min for 1 minute at a time after which there was a 1-minute mixing step to prevent the mix from becoming oversaturated. The number of liquid addition steps needed to granulate the different formulations are as follows: 5 (25% DE6), 9 (40% DE6), 12 (50% DE6). Step 4 produced Layered Granules with approximately the same composition as the Standard Coffee-Maltodextrin granules produced in Section 6.2.6 for comparison purposes.

In this manner, a process was developed which facilitates the wet granulation of Coffee without any degradation or loss of functionality. This process utilises a dry coating step to develop a thin coating of a high thickening power sugar onto the Coffee, which is followed by steam treatment to lock this coating in place. During the wet granulation process, this coating limits the interaction between the water binder and Coffee. The use of this process is not limited to Coffee and could be applied to a variety of moisture sensitive materials that previously could not be wet granulated due to structural degradation.

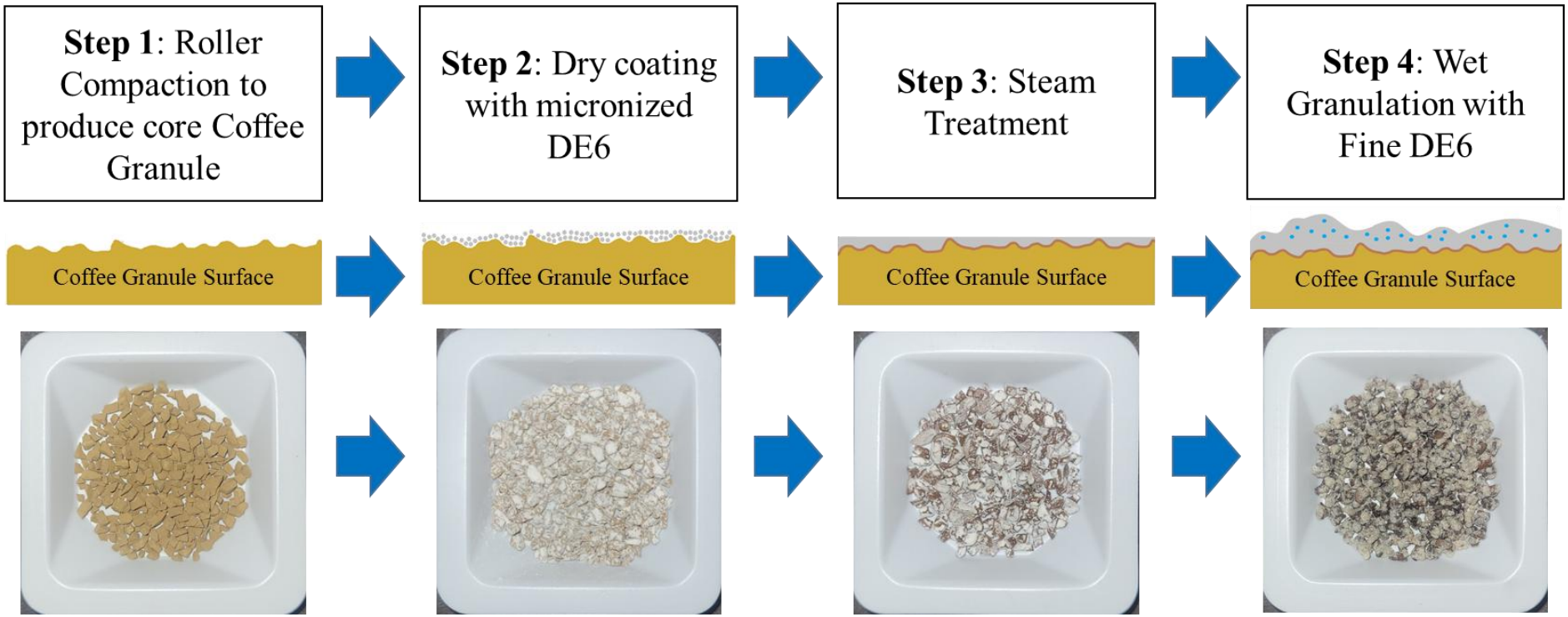

Figure 6.2: Process pathway to produce the Layered Coffee – DE6 Granule. Step 1 involves forming the core Coffee granule using Roller Compaction. In Step 2, the core Coffee granules (1 – 2 mm) are then taken and dry coated with micronized DE6 to form a very thin, fragile coating on the granule surface. In Step 3, this coating is then locked in place using a steam treatment. Finally, in Step 4, the steam treated granules are then layered with DE6 through wet granulation in a High Shear Granulator. This forms the Layered Coffee – DE6 Granule structure.

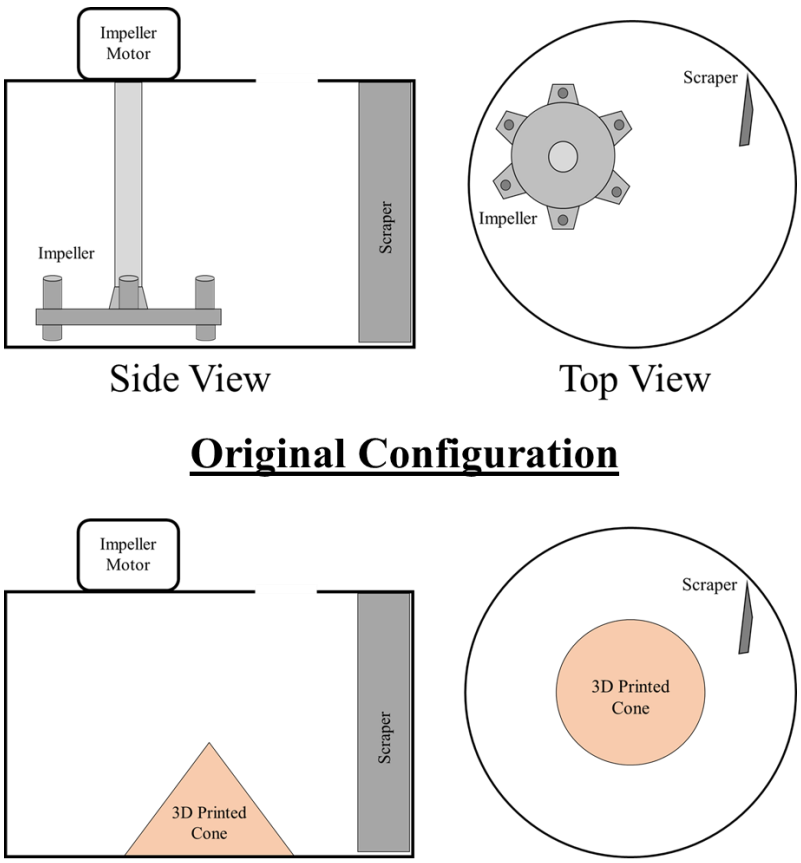

Figure 6.3: Schematic showing the Eirich granulator in its original and new configuration. The impeller was removed as it resulted in too much attrition of the core Coffee granules. It was replaced by a 3D printed cone which prevented an agitation dead spot from forming at the centre of the bowl. The cone was glued to the centre of the bowl and therefore rotates at the same speed as the bowl.

6.2.8 Determining layer thickness

To evaluate the DE6 layer thickness, granules were first taken and sliced open down the middle. The granule cross sections were then captured using a VHX-S550E Microscope (Keyence, UK). An example cross section is presented in Figure 6.4. ImageJ was then used to split the image along 18 lines, with each line being 20˚ apart as visualised by the black lines in Figure 6.4. The locations at which these black lines cross the interface between the core Coffee granule and the outer DE6 layer were taken as the points where layer thickness would be measured. For each granule, layer thickness would be measured at 18 points as shown by the 1-18 numbers in Figure 6.4. Layer thickness was then measured at each of these points as the perpendicular distance between the Coffee granule surface and the outer edge of the DE6 layer. The red dotted line visualises this in Figure 6.4 for Point 1 as an example. The layer thickness for each granule was then taken as the average of the 18 measured thicknesses associated with that granule. Ten randomly selected granules were evaluated for each formulation and the average of these ten used to represent that condition.

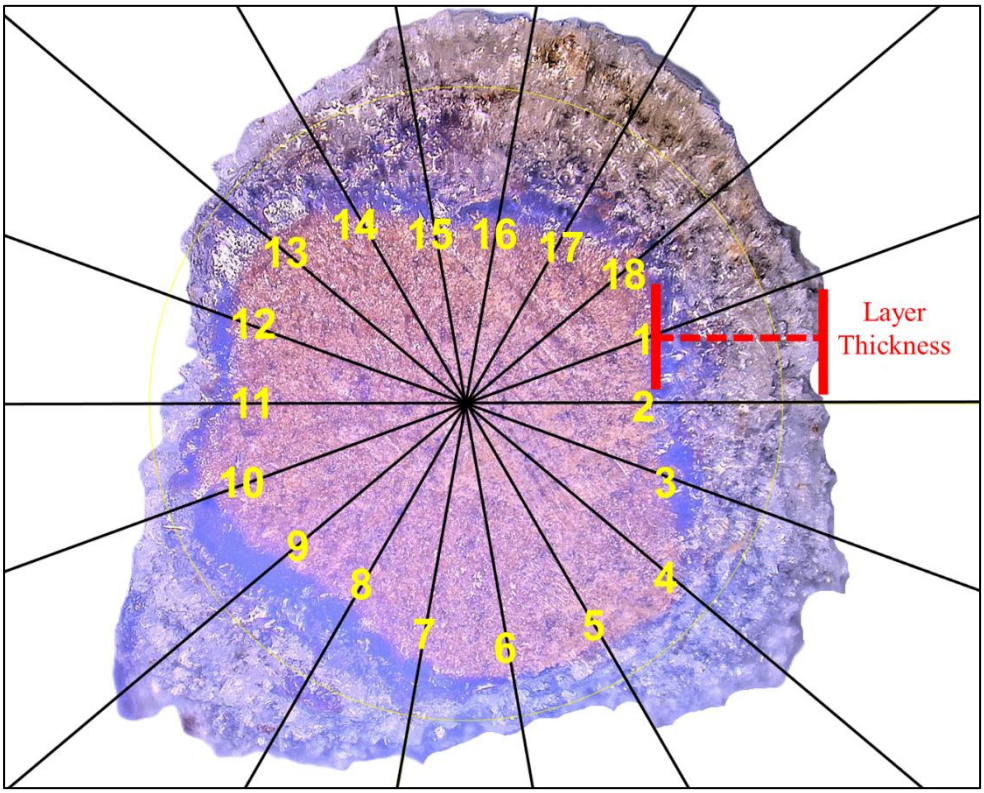

Figure 6.4. Example methodology for measuring granule thickness. Granule thickness was measured at each point where the black segment lines crossed the interface between the Coffee granule and DE6 layer. Granule thickness was measured perpendicular to the Coffee granule surface as shown by the example at Point 1. The overall granule thickness was taken as the average of the 18 thicknesses associated with the granule.

6.2.9 Evaluating Caking Index

The extent of caking was evaluated using a sieving approach to determine the Caking Index [72]. Granules between 1 – 2 mm were used in all cases to ensure that material type and granule structure were the predominant factor affecting caking rather than particle size. These granules were first conditioned at 20˚C and 10% RH using Silica Gel for 1 week to equilibrate them. They were then taken and placed into cylindrical glass dishes with a height of 1 cm. These samples were then placed at 20˚C and 60 - 80% RH using a Memmet IN110 Humidity Chamber (Memmet, Germany) to represent possible storage conditions. The total storage time was 16 days. Samples were taken out at set time intervals and sieved at an amplitude of 0.45 mm for 1 min. The sieve size used was 2 mm. Since all the granules were originally below 2 mm, any material found on the sieve can be attributed to agglomeration due to caking. The caking index was then used to classify the extent of caking as shown in Equation 6.1.

$$\textbf{Caking Index}\ (\%) = \frac{\text{Mass retained on sieve}}{\text{Total Mass}} \times 100$$

Equation 6.1

For certain materials, the caking of the raw powder was also evaluated. First the raw powder presented in Table 6.1 was sieved to isolate the powder faction between 300 µm and 400 µm. This ensures a narrow size distribution across samples which prevents variations in particle size dominating results. Then the caking of these powder samples were evaluated using the sieving method with a mesh size of 500 µm in a similar manner to the granules.

6.2.10 Evaluating changing granule morphology during storage

Changing granule surface morphology during storage was evaluated using a VHX-S550E Microscope (Keyence, UK). The polarised light setting was used alongside a magnification of 100x. Five randomly chosen granules were used to represent each condition. The images obtained via microscopy were also used to investigate the size change of these 5 granules during storage. The images were evaluated using ImageJ where the wand tool was used to automatically select the granules based on the difference in contrast between the granule and background colour. The selected area was then measured. The average change in the area occupied by the 5 granules over time was taken to represent granule deformation.

The change in colour of bulk samples during storage was also evaluated. Samples were loaded into a circular dish before being placed into storage. The dish was then removed at given time intervals and the aesthetic of the bulk sample surface recorded using a Sony $RX10_{IV}$ camera. The images were then evaluated in ImageJ where colour change was judged according to their greyscale value.

6.2.11 Dynamic vapor sorption

Dynamic vapor sorption (DVS) was used to measure the humidity based uptake in moisture content of different powders using a SPS 11-10µ Sorption Test System (ProUmid, Germany) at 20°C. Samples of ~1.5 g first underwent an equilibration stage in the machine. During the equilibration stage, the environmental humidity was set to plateau at 0% RH until the change in mass of each sample was less than 0.01% per 40 mins. This was done to condition each sample to the same initial environment. After this criterion was reached, the humidity was set to increase to the set value and mass change measured with time. The increase in mass of each sample was used to measure the moisture uptake over time at the given environmental condition. Measurements were conducted in triplicate.

6.2.12 Production of Gordon Taylor Model and GAB Model

To establish the Gordon Taylor model and Guggenheim-Anderson-de Boer (GAB) model for the different materials, it was necessary to measure the Glass Transition Temperature and water activity of the materials at different moisture contents. This paragraph outlines the preparation step used to produce powder samples with different moisture contents for the Maltodextrin and Coffee powders. The powders were conditioned using different saturated salt solutions at 20˚C. The different salt solutions produced

environments with different relative humidity's resulting in varying rates of moisture uptake in the powder. The saturated salt solutions used and the corresponding relative humidity they produced are as follows: Lithium Chloride (RH 11%), Potassium Acetate (RH 23%), Magnesium Chloride (RH 33%), Potassium Carbonate (RH 43%), Sodium Bromide (RH 59%) and Sodium Chloride (RH 76%).

Thermo-gravimetric analysis (TGA) in a TGA550 (TA Instruments, Switzerland) was used to evaluate the moisture content of the powders. TGA involves measuring the weight loss in a sample as it's dried across a range of temperatures. Samples of ~25 mg were heated from 25°C to 200°C at a rate of 2°C/min. The temperature at the minimum point of the weight loss derivative curve was used to determine when water loss ends. The weight loss at this temperature was then used to calculate the moisture content of the sample. Water activity of the samples were measured using a AquaLab 4TE Decagon (Decagon Devices Inc, US) and samples were left to equilibrate inside the device for 1 hr.

The Glass Transition Temperature (T_g) was measured using Differential Scanning Calorimetry in a DSC25 (TA Instruments, Switzerland). A two cycle procedure was used. The first cycle was used to erase the powder's relaxation enthalpy while the second cycle was used to measure the powder T_g. Powder samples of ~20 mg were used for the scan. The first cycle involved heating the sample at a rate of 5°C/min from 25°C to the expected T_g+30°C before the system is then cooled to -30°C. The second cycle then begins at a rate of 5°C/min up to a temperature of the expected T_g+30°C. The Glass Transition Temperature is taken as the onset of the steep change in heating capacity.

The moisture content and T_g data for each material was then fitted to the Gordon and Taylor Equation which is displayed by Equation 6.2. x_A and x_B are the mass fractions of the (Maltodextrin or Coffee) powder and water in the sample respectively. $T_{g,A}$ and $T_{g,B}$ is the Glass Transition Temperature of the dry (Maltodextrin or Coffee) powder and pure water (taken to be -135°C as justified in Section 5.2.5). The Gordon Taylor constant (k) was determined to be as follows for the evaluated materials: 11.94 (DE6), 11.76 (DE12), 10.53 (DE21), 9.98 (DE29) and 6.58 (Coffee).

$$T_g = \frac{x_A T_{g,A} + k x_B T_{g,B}}{x_A + k x_B}$$

Equation 6.2

The moisture content and water activity (a_w) data was fitted onto the GAB equation as shown in Equation 6.3. Wm and C represent Monolayer Moisture Value and the Energy of absorption while B represents non-ideal behaviour. These parameters are obtained from the fitting. The obtained Wm parameters are as follows 8.2 (DE6), 6.5 (DE12), 4.8 (DE21), 4.7 (DE29) and 4.9 (Coffee). The obtained C parameters are as follows 41 (DE6), 46 (DE12), 144 (DE21), 14 (DE29) and 3.4 (Coffee). The obtained B parameters are as follows 0.56 (DE6), 0.77 (DE12), 0.97 (DE21), 1 (DE29) and 1 (Coffee)

$$Moisture\ content_{Dry\ Basis} = \frac{W_m C a_w}{(1 - Ba_w)(1 + (C - 1)Ba_w)}$$

Equation 6.3

6.2.13 Granule shape and size

Granule shape and size were evaluated using a Camsizer (Retsch, UK) using randomly collected samples of ~25 g. Three repeats were conducted for each condition. Sphericity is defined as $4\pi A/P^2$ where A is the measured particle projection area and P is the measured particle projection circumference. A sphericity of 1 indicates a perfect sphere.

6.2.14 Internal granule structure evaluation

A µCT 35 Scanner (Scanco Medical, Switzerland) was utilised to obtain X-Ray scans of the Layered Granules. The scan intensity was 70 kV and 114 µA.

6.2.15 Tabletting

Layered tablets were produced to better investigate how a layered structure can be used to inhibit moisture diffusion into the Coffee in the granule core. These layered tablets were composed of three components: Coffee, DE47 and DE6. The preparation step involved sequentially filling the tabletting die with different materials. Coffee was filled first so that it would form the bottom layer. Subsequently DE47 was filled to form the middle layer and finally DE6 was added to form the top layer. The filled dies were then tabletted using an Instron 3367 Universal Tester (UK). The tabletting pressure used was 3 KN and the punch speed 1 mm/min. The tabletting parameters were chosen arbitrarily as the purpose of this work was to evaluate the effect of formulation rather than the effect of the tabletting process on the model system. The compositions of the layered tablets were tested as follows: Tablet A (0.6 g Coffee, 0 g DE47 and 0.6 g DE6), Tablet B (0.6 g Coffee, 0.24 g DE47 and 0.36 g DE6) and Tablet C (0.6 g Coffee, 0.48 g DE47 and 0.12 g DE6). The order of the layers was as follows: DE6 (top), DE47 and Coffee (bottom).

6.3 Simple size enlargement to prevent caking

This section will investigate the caking tendency of single component granules compared to their raw powder forms to establish the effectiveness of simple size enlargement using granulation to prevent caking. Effectiveness will be judged by considering the rate at which the different materials cake and the humidity threshold at which caking occurs. Results will be linked back to key material properties such as the Glass Transition Temperature and moisture absorption behaviours. Amongst the materials tested will be Coffee and DE6 which will form the Standard and Layered Granules in subsequent

sections. This section will establish the caking of these materials to better understand the behaviours displayed when they are combined together.

6.3.1 Comparing the caking tendency between granules and raw powder

The caking of single component granule and powder samples was evaluated according to the Caking Index over a 16-day period as outlined in Section 6.2.9. Figure 6.5 shows the increase in the Caking Index of these materials during storage at 20˚C and a relative humidity of 60% - 80%. It is evident from the results that particle size has a strong impact on the rate at which caking occurs, with the powder samples (small particle size) showing more rapid increases in the Caking Index to their granule counterparts (large particle size). For instance, at 20˚C and 70% RH, DE12 required only 7 days to fully cake in the powder form while it required 16 days to cake when in the granular form. The faster rate of caking can be linked to the greater number of contact points that exist for the powder form which more easily facilitates bridge formation leading to caking. It can also be linked to the increased rate at which powder, due to their larger specific surface area, absorb moisture from the atmosphere. A quicker absorbance of moisture means that the material T_g depresses faster which leads to quicker glass transition induced caking. This is shown in Figure 6.6 which presents the rate at which powder and granule samples of the different materials absorb water at 20˚C and 80% RH. Figure 6.6 highlights the faster moisture uptake for powder samples compared to granule samples as the higher specific area of the raw powder facilitates more active sites for moisture absorption to occur, resulting in a faster moisture uptake [143]. The only exception is with Coffee where both the powder and granule sample showed similar rates of moisture uptake. This indicates that the Coffee granule structure collapses so quickly when exposed to high humidity that it does little to hinder moisture absorption compared to the raw powder. The quick collapse can be attributed to the highly moisture sensitive nature of Coffee which means that very low amounts of moisture absorption can lead to structural collapse, this essentially reduces the powder and granule forms to the same collapsed state, resulting in both the powder and granule possessing a similar moisture absorption profile. This illustrates that size enlargement in itself is not sufficient to ensure shelf life stability when dealing with highly moisture sensitive materials.

Another interesting observation from Figure 6.6 is that the point at which moisture uptake appears to plateau is slightly higher for the powder form compared to the granule form when considering the less moisture sensitive materials like DE6 and DE12. Therefore, possibly indicating that the granule structures for these materials are able to successfully reduce moisture diffusion into the granule structure and therefore slow down moisture uptake considerably to the point where it appears to plateau within the evaluated time scale. However, over a longer evaluated time scale it is expected that the equilibria moisture content for both the powder and granule samples would be the same as that is decided by material property rather than a physical characteristic such as size. Rather particle size will primarily affect moisture sorption kinetics. Therefore, Figure 6.6 highlights how in the case of certain materials,

granulation can be utilised to significantly slow down moisture sorption kinetics leading to the production of more shelf life stable particles.

A key observation from Figure 6.5 is that there was no instance where the raw powder (small particle size) experienced caking without the granules (large particle size) also experiencing caking. Both powder and granules experiencing caking together (albeit at different rates) indicates that the relative humidity at which caking occurs for these materials is primarily determined by material properties rather than a characteristic such as size. The lowest evaluated relative humidity was 60% and at this level both types of Coffee and DE29 experienced caking while DE6-DE21 experienced no caking. At a relative humidity of 70%, both forms of Coffee, DE29 and DE21 experienced caking, while DE6 – DE12 experienced no caking. Finally, at a relative humidity of 80%, all the materials experienced some degree of caking. To link this caking behaviour to material property, the GAB and Gordon Taylor models for the Maltodextrin and Coffee materials were produced as shown in Figure 6.7A and Figure 6.7B. Figure 6.7A presents the hygrocapacity of the different materials. For a closed system at equilibrium the Water Activity correlates with the relative humidity (For instance, a_w = 0.6 would correspond to 60% RH). As Water Activity increases, the material moisture content increases due to the higher amount of water vapour in the air, which increases the driving force for absorption of water into the powder structure. Materials such as Coffee and high DE Maltodextrin which are composed of smaller chained molecules have more potential binding sites for moisture to absorb onto, and therefore display a greater hygrocapacity [144,145]. Being composed of smaller chained molecules also means that less energy is needed to excite them into the rubbery state [26,146] . This leads to Coffee and High DE Maltodextrins having lower Glass Transition Temperatures as shown by Figure 6.7B. Material hygrostability can be evaluated using Figure 6.7C. Figure 6.7C was produced by combining the BET model with the Gordon Taylor model using the moisture content parameter as a common variable, which allows Glass Transition Temperature to be plotted against Water Activity. For caking to occur, Water Activity must be sufficient to depress the T_g to be equal to or less than the storage temperature, which was 20˚C for the scenario considered in Figure 6.5. From Figure 6.7C, it can be estimated that the water activity needed to reach a T_g of 20˚C is as follows: 0.94 (DE6), 0.71 (DE12), 0.62 (DE21), 0.53 (DE29) and 0.48 (Coffee). Knowing that under equilibrium the water activity correlates to Relative Humidity, this means the minimum estimated RH needed for caking to occur is: 94% (DE6), 71% (DE12), 62% (DE21), 53% (DE29) and 48% (Coffee). There is some correlation between these estimations and the behaviours seen in Figure 6.5 where caking did not occur till these humidity thresholds had been reached for Coffee and DE12-DE29. The only exception is DE6 which displayed a tendency to cake at 80% RH despite the estimated threshold being 94%. This could be caused by the irregular composition of Maltodextrins, which means that all DE grades have some faction of short and long polymer chains within them. It is possible therefore that at 80% RH, DE6 material with a localised high composition of moisture sensitive short chained polymers underwent Glass Transition leading to the limited caking

seen in Figure 6.5C. Another explanation could be the tendency for water to condense on the particle surface at such high relative humidity's. Small fluctuations in the temperature within the humidity chamber, which can easily occur during normal operation, can be sufficient to induce this surface condensation at 80% RH. The presence of this condensed water on the granule surface would have then triggered the caking seen in Figure 6.5C. To summarise, the results indicate that the probability of a material caking is dependent on the hygrostability of the material rather than particle size. However, if caking were to occur, size enlargement via granulation has been shown to be a useful tool which can be used to slow down the rate at which caking occurs considerably.

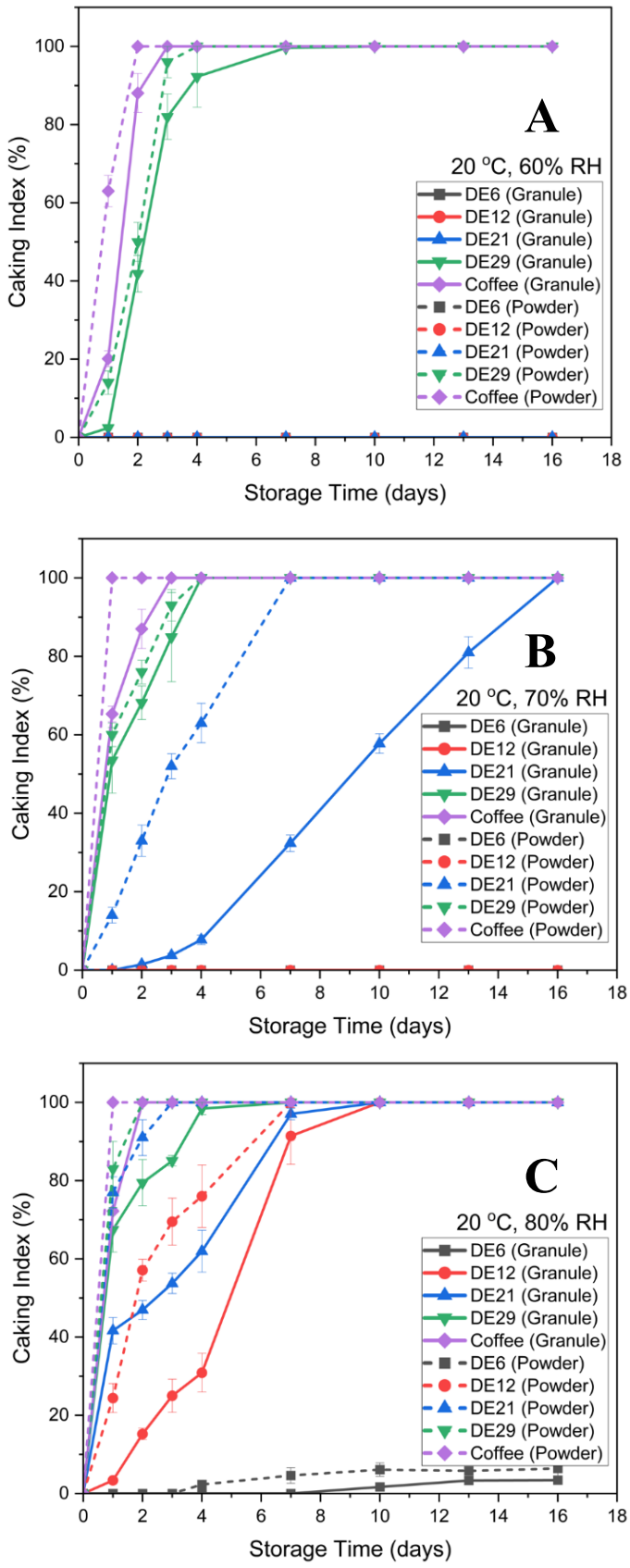

Figure 6.5: Caking behaviour of granules compared with powder for different Maltodextrin grades and Coffee. Samples were stored at 20˚C and 60% (A), 70% (B) and 80% (C) Relative Humidity. Particle size was found to impact the rate of caking with the powder form caking far faster than the granule form. Humidity under which caking occurred was found to be dependent on material type rather than particle size. Coffee was found to have the greatest caking tendency followed by high DE Maltodextrins.

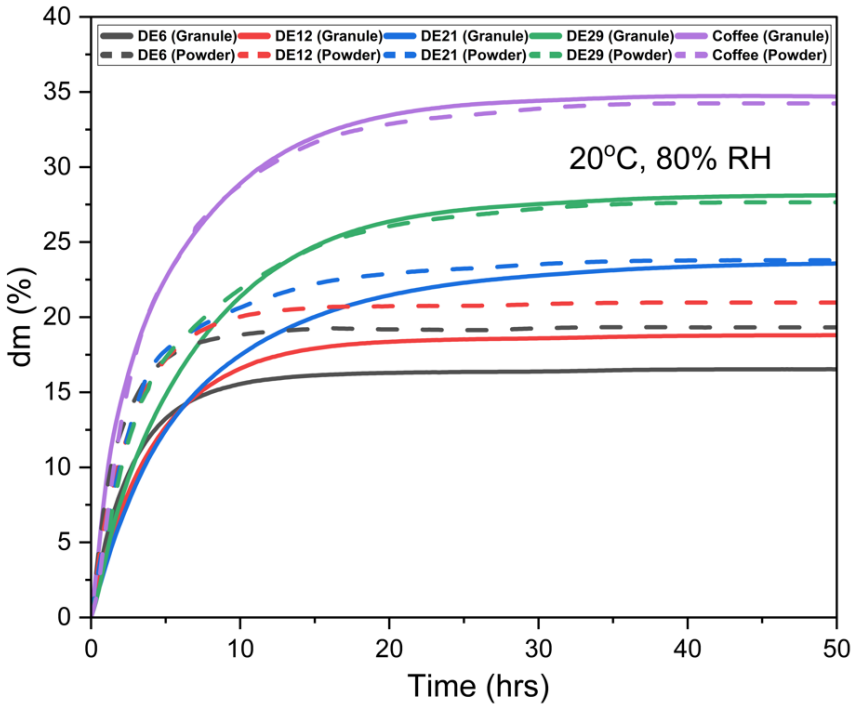

Figure 6.6: Displays the increase in mass (indicating moisture uptake) between the different materials over time at 20˚C and 80% Relative Humidity. Generally, the powder samples display faster moisture uptake which can be attributed to their increased specific surface area. The exception is Coffee where both the powder and granule form show similar rates of moisture absorption which could reflect the speed at which the Coffee structure collapses at 80% RH to form a caked mass. This quick collapse means that the effect of the initial particle size becomes less significant when considering moisture uptake in the Coffee.

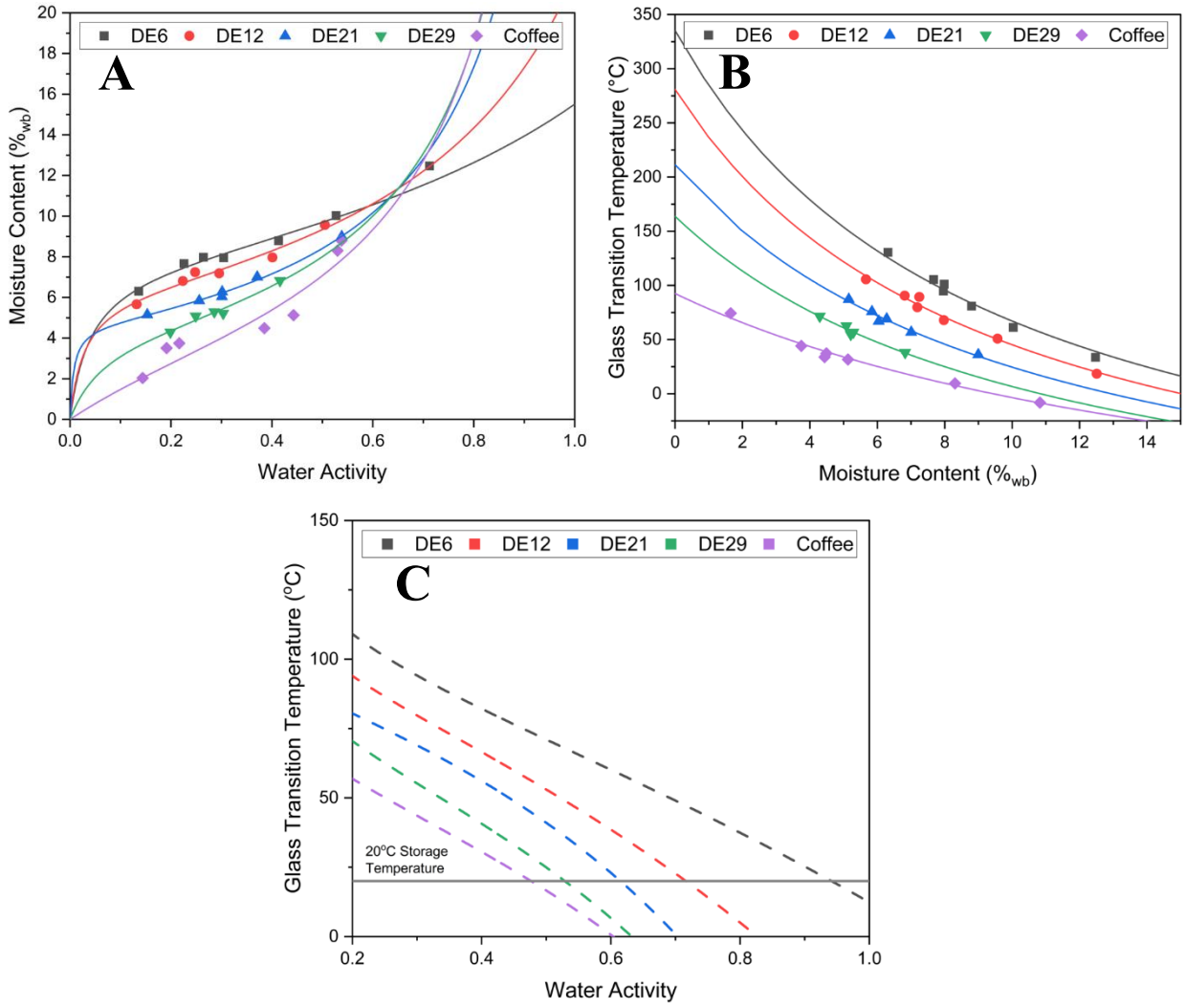

Figure 6.7: Fitted GAB Model (A) and Gordon Taylor Model (B) for the different evaluated materials. Material hygrostability (C) has been evaluated by plotting Glass Transition Temperature against Water Activity. From (C) it is evident that the water activity required for caking to occur at 20°C has been estimated to be 0.94 (DE6), 0.71 (DE12), 0.62 (DE21), 0.53 (DE29) and 0.48 (Coffee). These values can also be obtained from (A) and (B) by evaluating the moisture content required to produce a T_g of 20°C using the Gordon Taylor Model (B) and determing the corresponding water activity at that moisture content from the GAB Model (A).

Figure 6.8a displays the changing characteristics of a bulk sample of Coffee granules stored at 20˚C and 60% RH, while Figure 6.8b shows the change in the granule morphology of five randomly chosen Coffee granules under this condition. Figure 6.8a highlights how even within 6 hours of storage, there is a visible change with the colour of the Coffee starting to darken. This discolouration rapidly progresses with the Coffee granules becoming darker and then finally turning black over the course of the 16 days the granules were evaluated for. In the case of the granules shown in Figure 6.8b, the changes were observed to occur more rapidly. For instance, within 6 hrs, the Coffee granule had completely browned, and its surface had softened. After 1 day of exposure, the surface has lost all texture and after 6 days the granules have completely collapsed – losing their shape and shrinking in size significantly. The final granule at the end of this process is completely unfit for purpose and would be considered waste. The slower visual change in the bulk sample compared to the five-granule sample is attributed

to increased competition for moisture between Coffee granules in the bulk sample resulting in less moisture uptake by individual granules, leading to less colour degradation. This changing colour and texture due to structural collapse during the caking process is commonly reported across a wide range of food powders such as soymilk powder [147] and highlights what a significant problem caking can be. It is also evident that in the case of the microscopy images shown in Figure 6.8b that the Coffee granules obtain a blue hue during the caking process. This is because as the granule surface becomes more viscous and liquefies, it reflects light more. The reflection of the microscope light from the liquefying surface, which occurred even at the lowest light intensity possible in the microscope, created the blue highlights around the Coffee granules. This phenomenon will be discussed further when comparing the caking of the Standard and Layered Granules.

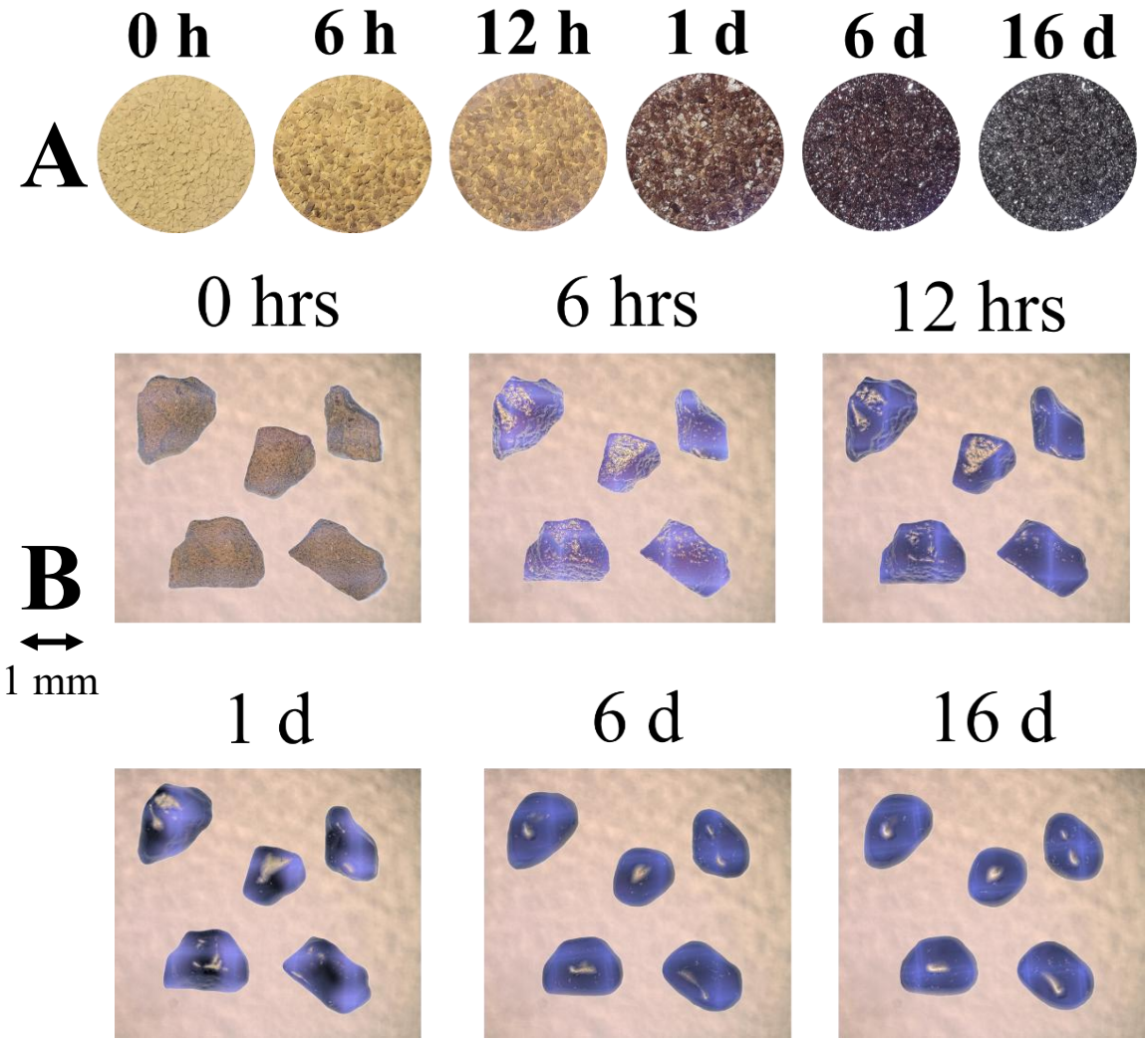

Figure 6.8: Changing characteristics of Coffee granules stored at 20˚C and 60% relative humidity over a 16 day period. Figure 6.8A presents the bulk Roller Compacted Coffee sample contained in a circular dish. Figure 6.8B presents five randomly selected Roller Compacted Coffee granules observed under a microscope. Both samples display humidity induced changes to their morphology over time. The collapse of the five granules (B) occurs at a much faster rate compared to the bulk sample (A). The blue hue of the collapsed granules seen in Figure 6.8B is caused by the reflection of microscope light from the liquefying Coffee surface.

6.4 Evaluation of the Layered Granule

The primary aim of this work was to evaluate whether a Layered Granule structure would mitigate caking. Section 6.2.7 outlines the procedure used to produce the layered Coffee-DE6 granules which is composed of a Coffee core and DE6 outer layer. Section 6.4 will outline the changing characteristics of the granules during the different production steps to better understand the pathway shown in Figure 6.2. Characteristics evaluated include granule size, granule shape and DE6 layer thickness. This section will then conclude by comparing the storage properties of the Layered Granule with the Standard Granule to determine which form presents the best protection against humidity induced degradation. Caking Tendency, Granule Colour Change and Granule Shrinkage are all metrics under which humidity degradation was judged.

6.4.1 Granule Size

Figure 6.9 shows the change in granule size across the different production steps presented in Section 6.2.7. Step 1 involved Roller Compacting Coffee to produce the core Coffee granule. The Purple line shown in Figure 6.9 shows the granule size distribution of these core Coffee granules. The Green line represents the granules after Step 3. At this point the Roller Compacted core Coffee granules have been dry coated with micronized DE6 before being steam treated to 'lock' the coating in place. There appears to be no significant change in the granule size distribution between Step 1 and Step 3. The lack of growth in the distribution can be explained by considering that the developed dry coating is very thin and not consistently applied. This results in no significant increase in granule size. Meanwhile, there is also no noticeable reduction in the granule size distribution which indicates there was little breakage during the dry coating step. This is because of the mild mixing conditions chosen and the large amount of micronized DE6 used in the mixing which would have 'cushioned' and protected the Coffee granules from breakage.

The grey, red and blue lines represent the granule size distribution after wet granulation to produce layered Coffee-DE6 granules with a formulation of 25%, 40% and 50% DE6 respectively. A higher DE6 percentage in the formulation represents more water added to the mix and longer mix times as outlined in Section 6.2.7. Therefore, the amount of water added and the mix time was lowest for the 25% formulation (grey line) and greatest for the 50% formulation (blue line). Comparing the 25% formulation (grey line) with the Steam Treated Granules (green line), it is evident that the steam treated granules undergo significant breakage during granulation despite the removal of the impeller from the Eirich granulator. This is shown by the peak of the grey line moving significantly to the left and the fraction of material less than 1 mm increasing considerably. However, there is some growth evident as the fraction of material greater than 2 mm also displays an increase which indicates that layering is occurring. The red (40% DE6) and blue (50% DE6) lines show the density distribution peak move

rightwards from the grey line (25% DE6) indicating progressive granule growth. This can be attributed to the higher amounts of water binder and longer mix times used for the 40% and 50% DE6 formulation facilitating a greater extent of layering leading to more granule growth.

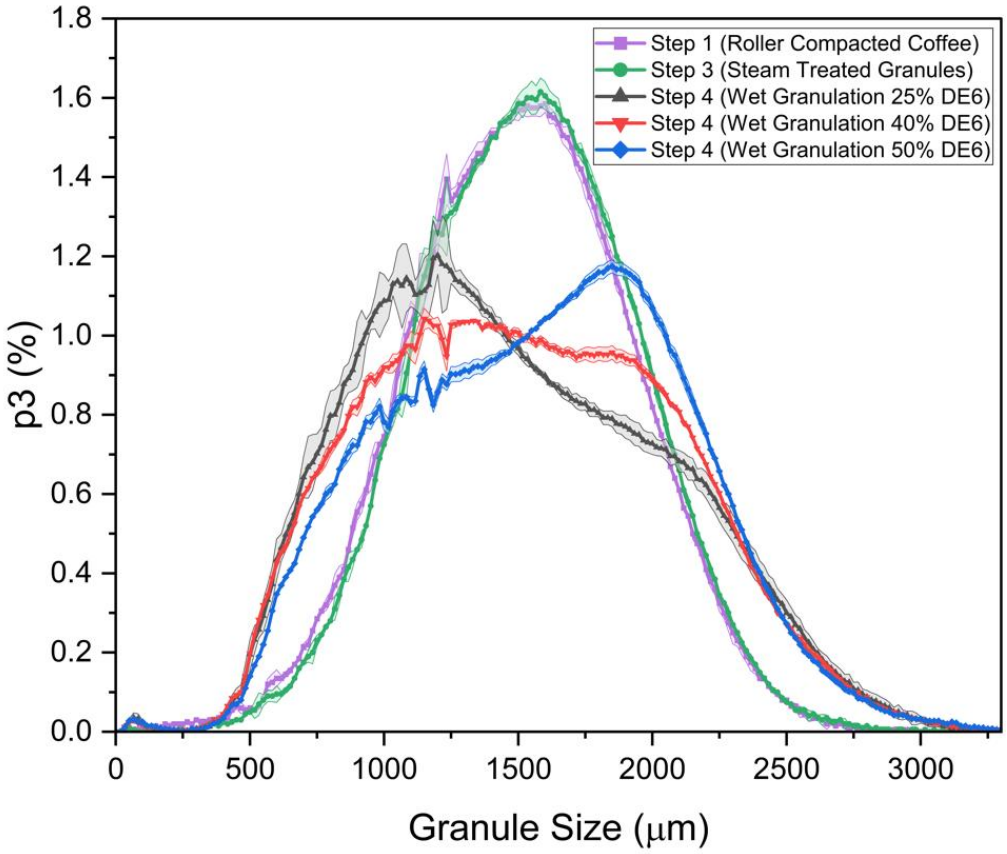

Figure 6.9: Changing granule size distribution through the layered granule production process outlined in Section 6.2.7 (as measured by the Camsizer).

6.4.2 Granule Shape

Figure 6.10 shows that granule shape was also found to change through the production process. This is important because granule shape partly determines granule flowability which is a key granule property for many applications. Sphericity is also relevant when considering caking because larger and more spherical particles display less bridge formation and therefore experience less caking [132]. Figure 6.10 shows that there was little change in shape between Step 1 and Step 3. This supports the theory mentioned in Section 6.4.1 that the dry coating step resulted in little breakage as any breakage would have resulted in the production of fragments which would have effected granule shape. The lack of breakage can be attributed to the short mix times and low bowl speed (85 rpm) used. The large amount of micronized DE6 used in the mixing process was also suspected of cushioning the Coffee granules and protecting them from breakage. A decrease in granule sphericity is observed between the Steam Treated Granules (Step 3) and the 25% DE6 formulation (Step 4). This can be associated with the breakage occurring during the wet granulation in Step 4 which involved a bowl speed of 170 rpm and

a much longer mix time. The amount of DE6 used here was also far less than during the dry coating meaning they would have less effectively cushioned the granules from collisions and impact. This breakage would have produced irregular granule fragments and lowered the sphericity as seen in Figure 6.10. However, sphericity subsequently improved for the 40% DE6 and 50% DE6 conditions. This can be explained by considering the rolling motion of the High Shear Granulator promoting the formation of a spherical DE6 outer layer. More water binder and longer mixing times were employed for the 40% and 50% DE6 formulation. This facilitates the development of a more complete, thicker and spherical outer layer of DE6 which improves the sphericity of the granules.

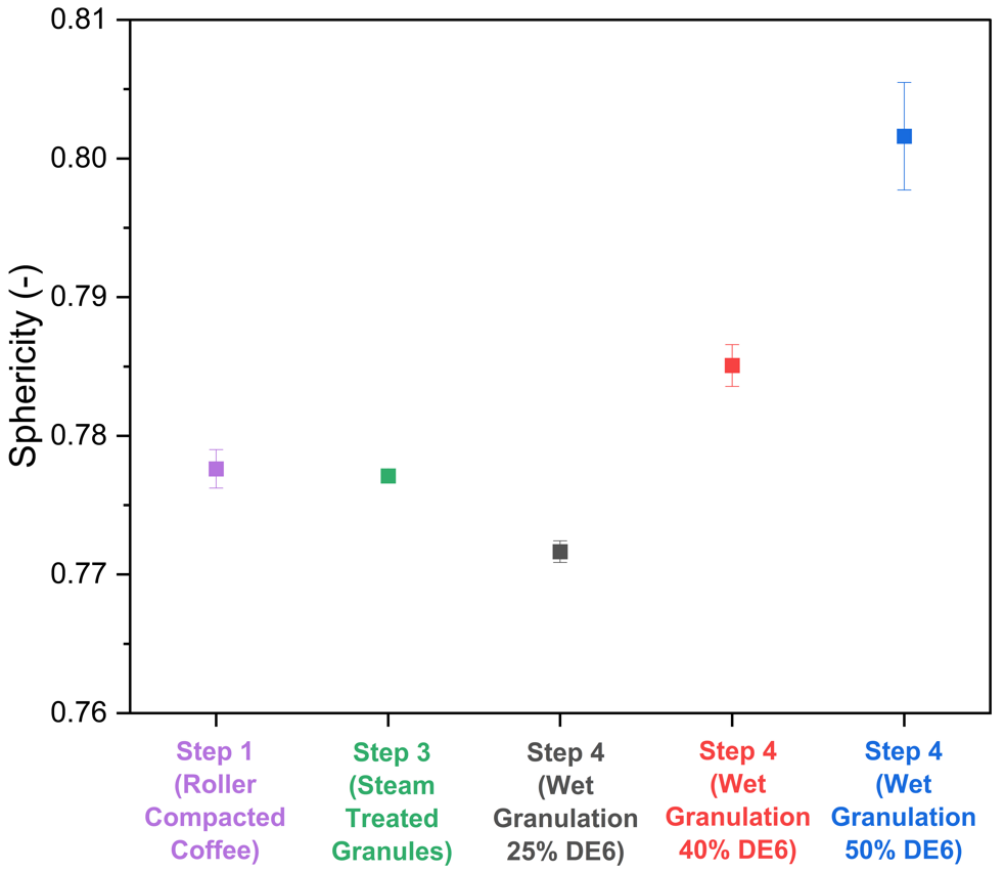

Figure 6.10: Changing granule sphericity through the Layered Granule production process. Sphericity initially shows no change during Step 1 to 3 due to a lack of breakage. Then there is a decrease in granule sphericity between the Steam Treated Granules (Step 3) and the 25% DE6 formulation (Step 4) which indicates that significant breakage initially occurs during granulation which produces aspherical fragments. However, sphericity improves sharply for the 40% and 50% DE6 formulation. This is attributed to the formation of a more spherical, thicker DE6 outer layer due to the rolling motion of the High Shear Granulator at higher DE6 compositions

6.4.3 Granule layer Thickness

DE6 layer thickness for granules produced during Step 3 and Step 4 was evaluated as outlined in Section 6.2.8. The layer thickness is a pivotal parameter to explain how effective each formulation will be at preventing caking during storage. A thicker layer will perform better as a physical barrier which contains

the viscous flow of the Coffee core as Coffee undergoes glass transition and prevents material bridges forming between granules. Figure 6.11 displays the layer thickness developed by the granules across the different production steps. The steam treated granules produced during Step 3 possessed the lowest average layer thickness of 50 µm. This was expected because at this stage the percentage of DE6 on the granules was estimated to be only 4% after the dry coating step. For the granules produced via wet granulation during Step 4, as the percentage of DE6 in the formulation increases, the layer thickness also increases with the 50% DE6 formulation having the thickest layer of 228 µm. This is because formulations with a higher percentage of DE6 are produced with more DE6 powder and liquid addition steps which facilitates the building of a much thicker and more complete layer. Figure 6.12 shows a visual representation of example granule cross sections taken from each formulation. The coated micronized DE6 layer in Figure 6.12a appears far whiter compared with the layers in Figure 6.12b-d which appear greyer and more glasslike. This is because the DE6 layer in Figure 6.12a is rough, porous and irregular which scatters the light to give a bright, white appearance. Meanwhile, the DE6 layers in Figure 6.12b-d are a lot denser and smoother due to the Maltodextrin experiencing high stresses and water saturation during granulation. This denser, smoother surface scatters light to a lesser extent and increases transparency resulting in the duller, glass like appearance.

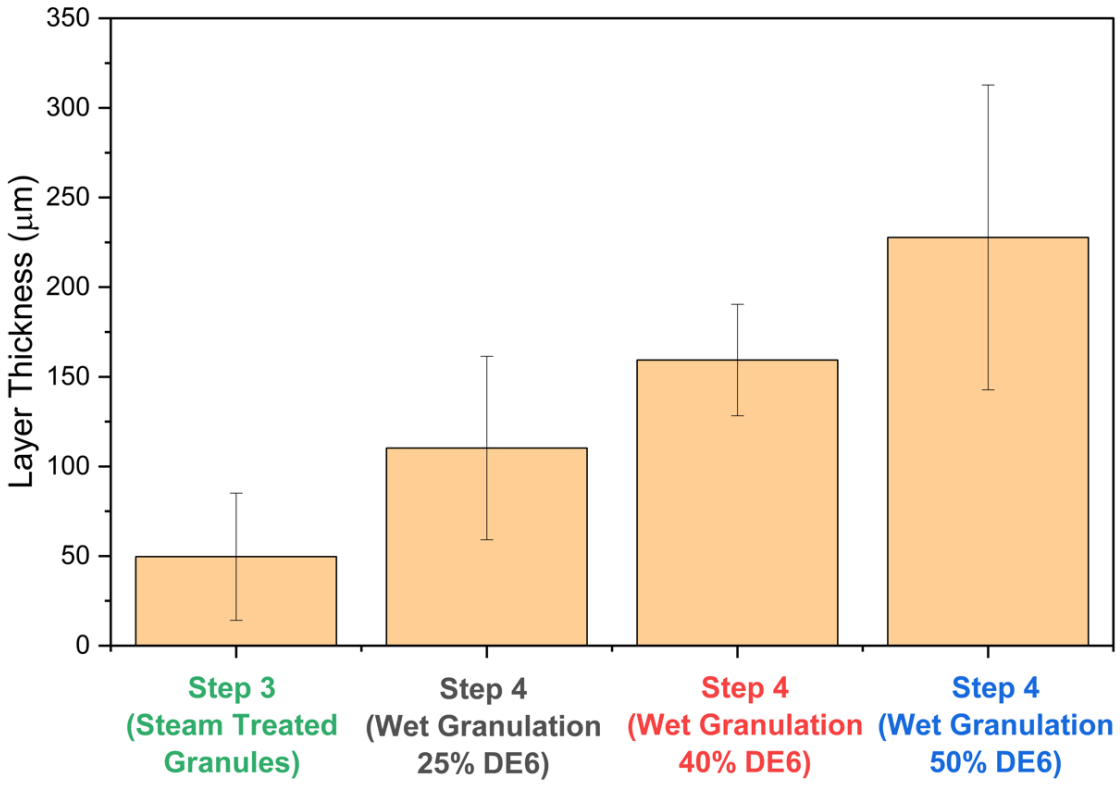

Figure 6.11: Changing DE6 layer thickness through the layered granule production process.

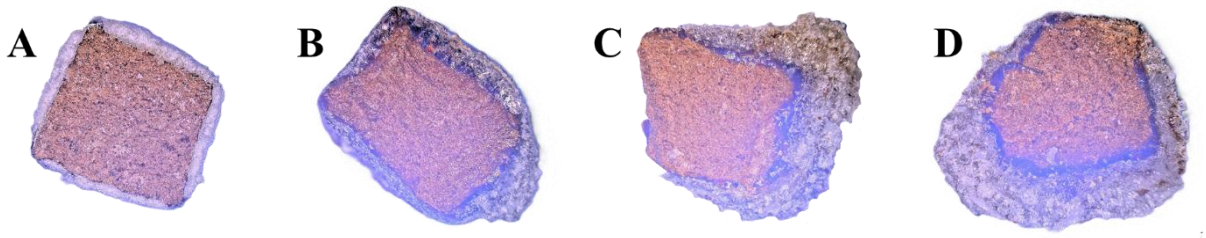

Figure 6.12: Visual representation of the changing layer characteristics between the Step 3 Steam Treated Granules (A), Wet Granulated 25% DE6 Granules (B), Wet Granulated 40% DE6 Granules (C) and Wet Granulated 50% DE6 Granules (D).

6.4.4 Caking tendency of the Standard Versus Layered Granule structures

This section will compare the caking behaviour of the Standard Coffee-DE6 Granule with the Layered Coffee-DE6 Granule. The Standard Granule is manufactured via Roller Compaction as described in Section 6.2.6 and describes the scenario where the two components are randomly distributed in the granule. The Layered Granule involves the production of core Coffee granules via Roller Compaction and then High Shear Wet Granulation to produce an outer DE6 layer as outlined in Section 6.2.7. The components are not randomly distributed in the Layered Granule, instead, DE6 is preferentially placed on the granule surface. The caking of these granules was evaluated during storage at 20˚C and 60% RH as this represents realistic storage conditions for particulate food products. As shown by Figure 6.5, Coffee showed a high caking tendency at 20˚C and 60% RH where its Caking Index rapidly increased and reached 100% within 3 days. Meanwhile at 20˚C and 60% RH, DE6 displayed no caking tendency whatsoever with its caking index remaining at 0% for the evaluated 16-day period. Therefore, any bridge formation and caking evident in the Standard and Layered Granules can be attributed to the Glass Transition of the Coffee component.

Figure 6.13 shows the change in the Caking Index for granules of pure Coffee alongside the three evaluated Coffee-DE6 formulations produced through the Standard and Layered pathways. Figure 6.13 shows that the inclusion of Maltodextrin in both the Standard and Layered Granules caused caking to occur at a slower rate compared to the Pure Coffee sample. This is shown by these systems showing far slower increases in their caking index compared to the Pure Coffee (purple line). Additionally, for both the Standard and Layered Granules, as the amount of DE6 in the formulation is increased, the extent of caking decreases. In the case of the Standard Roller Compacted Granules, the more DE6 in the formulation, the greater the likelihood that there is a higher DE6 surface composition. A higher DE6 composition results in a less sticky surface and therefore less caking. In the case of the Layered Granule, a higher DE6 composition results in a thicker outer DE6 layer as shown by Figure 6.11, which is better able to contain the viscous flow of the Coffee core and prevent bridge formation.

Overall, it is evident that the Layered Granule structure offers much better caking protection compared to the Standard Granule structure. This is shown in Figure 6.13 where the increase in the Caking Index of the Layered Granule is significantly lower than that of the Standard Granule for each respective formulation. The Layered Granule structure also showed a delayed start to the caking process, with caking starting around day 6-8 depending on formulation. Comparatively, caking began on day 2 for all the Standard Granule formulations. The enhanced caking protection provided by the layered structure is best emphasised by the Layered 25% DE6 Granule, which outperformed the Standard 40% DE6 Granule despite containing far less DE6. Additionally, the Layered 25% DE6 Granule demonstrated significant advantages over the Standard 50% DE6 Granule, including a delayed onset of caking and only a slightly higher caking index at the end of the 16-day evaluation period. The Caking Index at the end of the 16-day period is presented in Figure 6.14. Figure 6.14 highlights how after the 16-day storage period, each of the Standard Granule formulations had caked to roughly double the same extent as their Layered Granule counterpart, highlighting the benefits of the Layered Granule approach. The improved protection stems from the fact that the DE6 outer layer is able to better hinder the viscous flow of the rubbery Coffee which prevents bridge formation and caking from occurring.

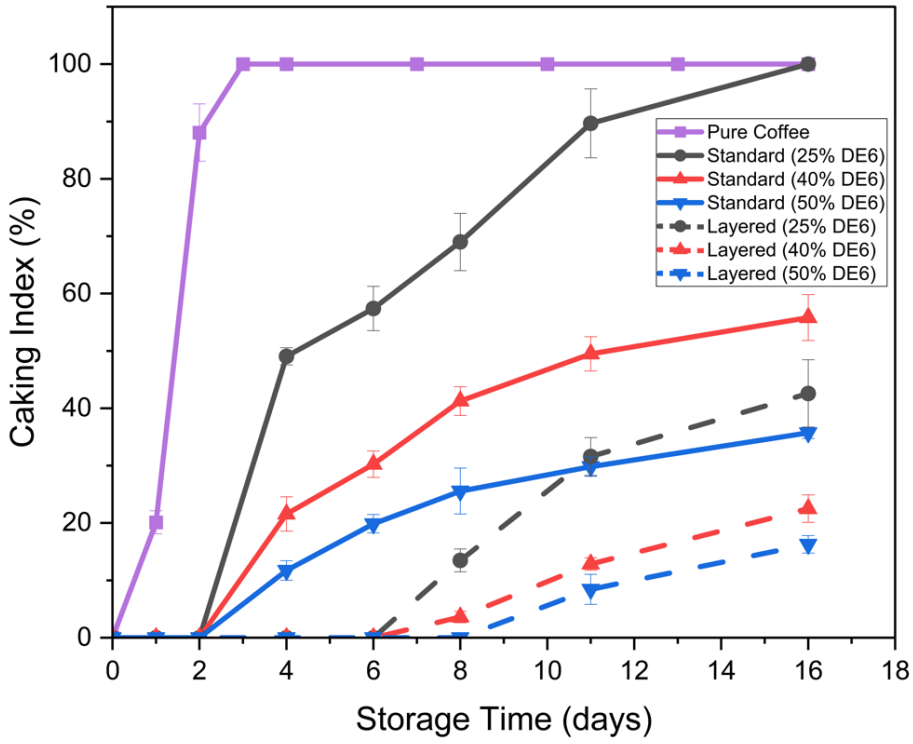

Figure 6.13: Change in the Caking Index over time for three formulations produced via the Standard and Layered production processes. The Layered Granule approach showed significant benefits in its caking protection over its Standard Granule counterpart. Storage conditions: 20˚C and 60% RH

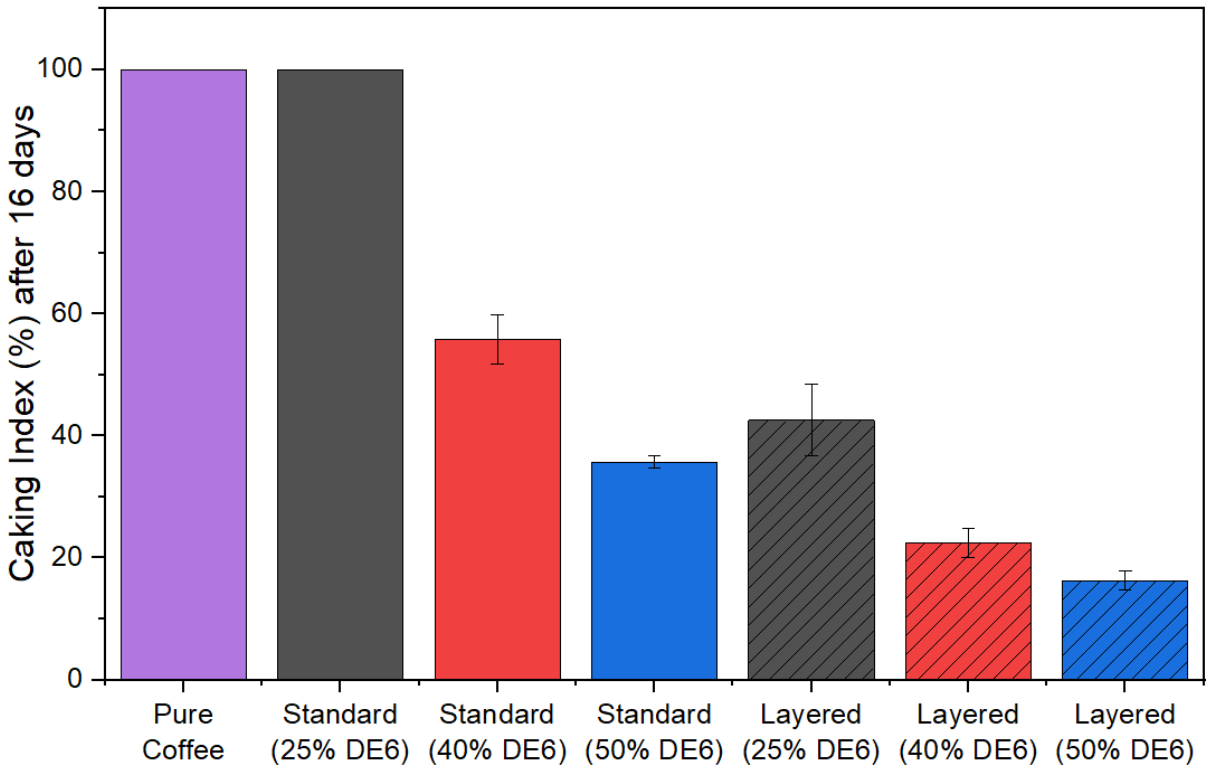

Figure 6.14: Caking Index after 16 days of storage (at 20˚C and 60% RH) comparing the Standard and Layered Granule structures. The Layered Granules displayed roughly half the Caking Index of the Standard Granules for each formulation, highlighting the effectiveness of a layered structure at preventing caking.

6.4.5 Change in colour of the Standard Versus Layered Granule structures

Figure 6.15 presents images of the different formulations during storage. The first observation is that granules formed from the different production pathways look very different to each other. The Standard Granule where the Coffee and DE6 are randomly distributed, retained the colour of Coffee and appeared golden brown at the start of the storage period. Meanwhile the Layered Granule appeared primarily white/grey to reflect the higher surface composition of DE6. This highlights how granules could be tailored to achieve different aesthetics for consumer acceptance by using a Layered Granule methodology.

During storage both granule forms experienced a colour change. Humidity induced colour changes can have serious consequences for food products due to negative consumer perception if it looks different to what they expect. Therefore, it would be beneficial if the granule structure proved to be more resistant to colour change as well as caking. Colour change of the images shown in Figure 6.15 were evaluated according to their greyscale value in Figure 6.16. A greyscale value of 0 indicates pure black while a greyscale value of 255 indicates pure white. Figure 6.16 shows that both the Standard and Layered granules start at similar greyscale values. However, the initial greyscale values for the Layered Granules are slightly higher to reflect the higher concentration of white Maltodextrin on the granule surface. During storage, the Coffee darkens and blackens as it collapses. This causes the greyscale value to decrease over time. The greatest decrease in the greyscale value was shown by the Pure Coffee granules with it displaying a dramatic decrease from 167 to 72 during the 16-day period. The inclusion of Maltodextrin in the granule reduced this darkening effect considerably with both the Standard and Layered Coffee-DE6 Granules showing far less drastic changes in their greyscale values compared to the pure Coffee granules.

Comparing between the two different granule structures, the Standard Granules experienced greater changes to their colour than the Layered Granules. This is shown visually in Figure 6.15. It is also shown through the greater decrease in their greyscale value in Figure 6.16. All formulations of Standard Granules experienced a greater decrease in their greyscale value compared to any of the Layered Granule formulations. This highlights the superiority of the Layered Granule structure in preserving granule aesthetics. Meanwhile, the Layered Granules only experienced a slight decrease in their greyscale values. This decrease can be attributed to the darkening of the exposed Coffee on the granule surface. This exposed Coffee existed because the highly viscous nature of DE6 meant it was not very mobile and did not spread well. Therefore, it was challenging to achieve complete coverage of the core Coffee granule surface, even at a 50% DE6 composition. These exposed areas started off as a reddish brown which slowly greyed and then blackened. These exposed Coffee surfaces are the reasons why the Layered granules showed caking tendencies in Figure 6.13. However, it is expected that the ability of this exposed Coffee to successfully form bridges would have been hindered. This is because they

were usually found in depressions in the granule surface and therefore would have to form much larger bridges to contact and bind with neighbouring granules. Furthermore, Fitzpatrick et al [139] found that mixtures with a higher composition of ‘sticky’ components caked more because the bridge formed between two ‘sticky’ components is stronger than the bridge formed between a sticky and non-sticky component. In this study, while there might still be Coffee partially exposed at the granule surface, any Coffee bridges that do form are likely to contact with DE6 on the surface of neighbouring granules. This leads to a weaker Coffee-DE6 bridge (compared to strong Coffee-Coffee bridges that are more likely to form in the Standard Granule scenario) resulting in less caking.

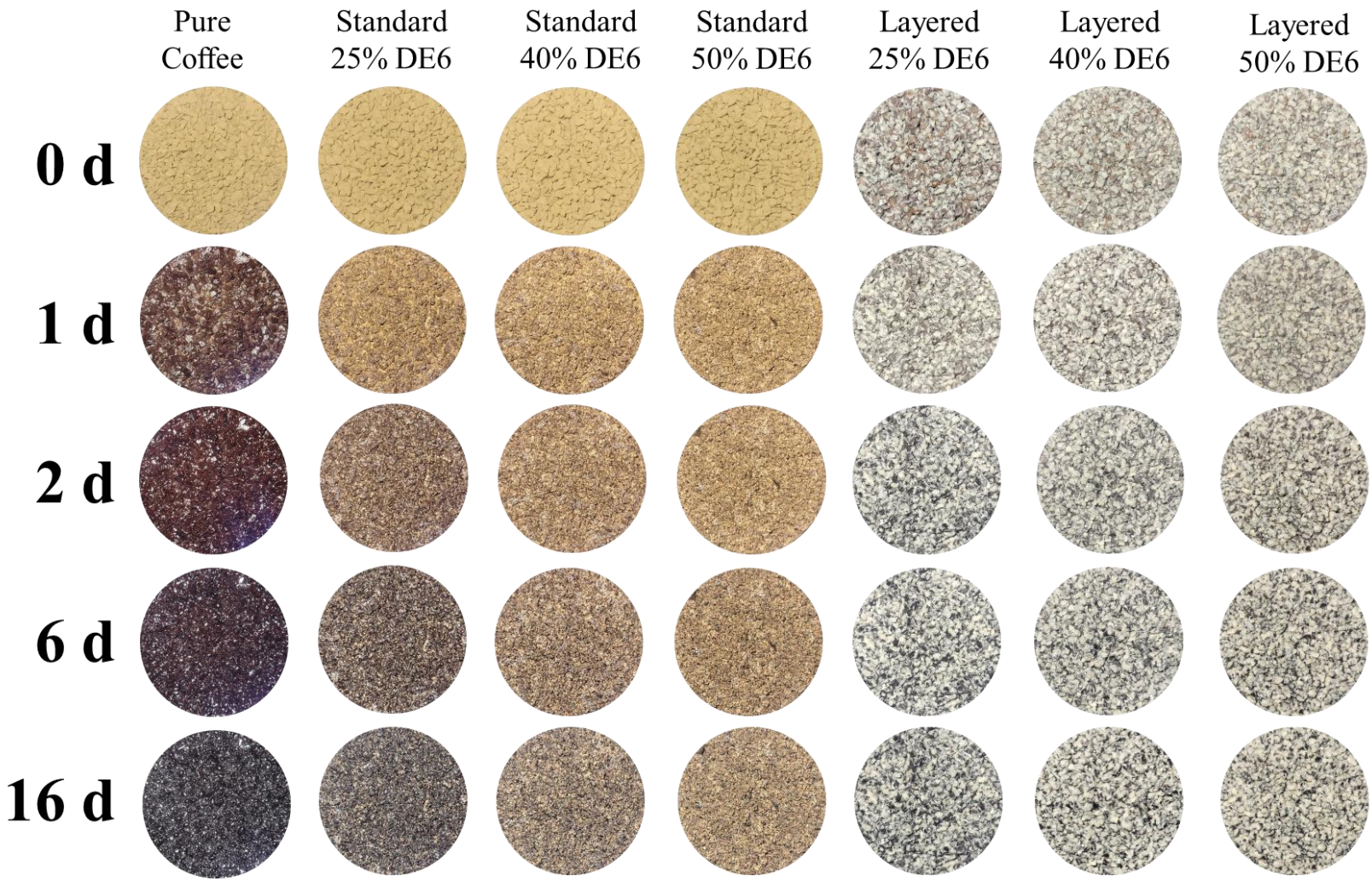

Figure 6.15: Changing characteristics of bulk samples of the different evaluated formulations over time. Storage conditions: 20˚C and 60% RH. This figure highlights the contrasting visual appearance of the granules produced by the two production pathways. The Standard Granules appear golden brown and slowly darken during storage with granules containing a greater coffee composition experiencing more darkening. Meanwhile, the Layered Granules appear predominantly white/grey with dark brown regions indicating the exposed core coffee granule. During storage, the areas housing this exposed coffee experience significant darkening.

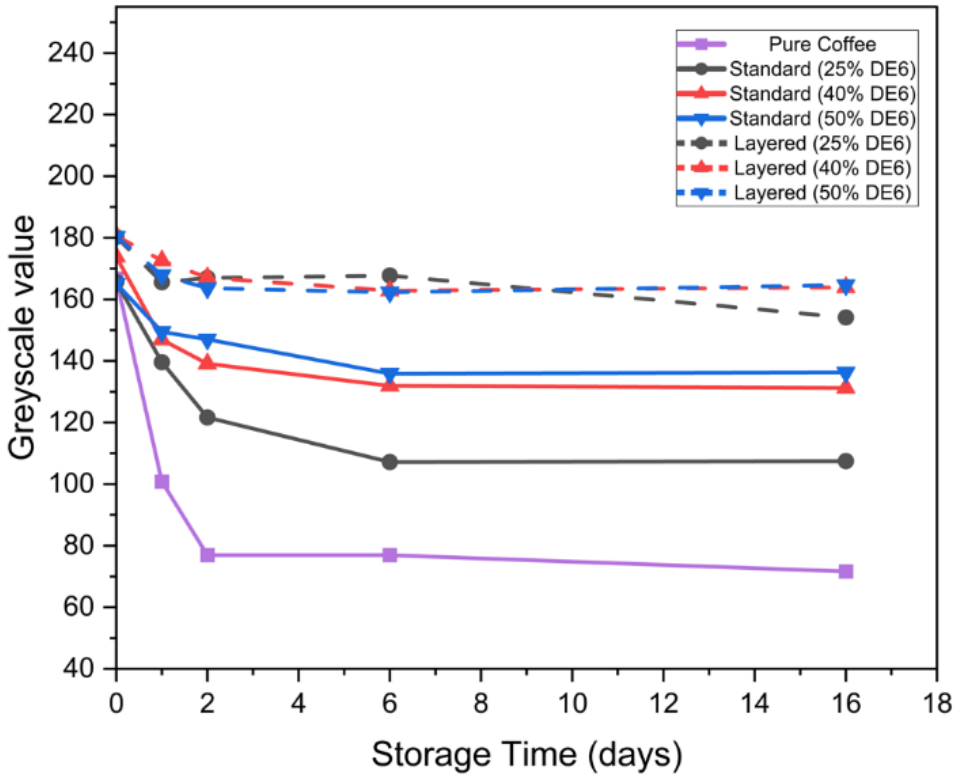

Figure 6.16: Changing greyscale value of the bulk sample surfaces shown in Figure 6.15. A greyscale value of 0 indicates pure black while a greyscale value of 255 indicates pure white. The Standard Granule structure showed far greater changes in the greyscale value compared to the Layered Granule structure.

6.4.6 Granule deformation of the Standard Versus Layered Granule structures

Figure 6.17 and Figure 6.18 show the changing morphology of 5 random granules belonging to each formulation during storage as observed by a microscope. Figure 6.17 shows that within 6 hours, the Standard Granules experience liquefying of the granule surface. This is especially evident in the case of the Standard 25% DE6 formulation where a thick, smooth, dark Coffee layer has formed on the granule surface. If these granules had been in contact with each other, this layer would have led to bridging and caking. Meanwhile, as shown in Figure 6.18, the Layered Granules displays no significant changes in granule surface morphology after 6 hours of storage, apart from a slight darkening of the exposed Coffee regions. Furthermore, as mentioned in Section 6.3.1, the blue hue seen over the granules in Figure 6.17 and Figure 6.18 is caused by the reflection of the microscope light on the liquefying granule surface. Therefore, it can be used to qualitatively compare the extent to which the surfaces of the Standard and Layered granules liquefy. In the case of the Standard Granules, all of the formulations present a blue hue after 6 hours. On the other hand, the Layered Granules only present a blue hue at a significantly later stage during storage. For example, the Layered 25% DE6 formulation only starts to show a slight blue hue after 6 days. This further emphasises the slower rate at which the Layered Granule structure liquefies and develops a viscous outer surface which is capable of caking.

The granules presented in Figure 6.8, Figure 6.17 and Figure 6.18 show that granule shape and size can change considerably during the course of storage. The granules can increase in size as the Coffee absorbs moisture and swells. They can also decrease in size as the Coffee structure collapses due to glass transition and the material becomes less porous. This granule shrinkage is best demonstrated by the pure Coffee granules in Figure 6.8. The deformation experienced by the granules in Figure 6.8, Figure 6.17 and Figure 6.18 has been quantified according to Section 6.2.10. The results are presented in Figure 6.19. As was the case when evaluating the change in colour, the Pure Coffee granules display the greatest change during storage. This is highlighted by Figure 6.19 which displays these granules shrinking ~20% over the course of 16 days. The inclusion of Maltodextrin significantly reduced this shrinking as the Maltodextrin acts as a 'skeleton' which strengthens the granule structure for both the Standard and Layered Granules. Overall, the Layered Granule structure limited the extent to which the granules experienced deformation compared to the Standard Granules. For instance, at the end of the 16-day storage period, the 25% DE6 Layered Granule had only deformed 7.6% compared to 14% in the case of the 25% DE6 Standard Granule. Similarly, the 40% DE6 Layered Granule had only deformed 3.2% compared to the 8.5% deformation experienced by the 40% Standard Granule. This can be attributed to the shell structure formed by the Maltodextrin outer layer in the Layered Granules helping to better maintain granule form. The results do indicate that at high DE6 compositions, the benefits of the Layered Granule Structure Compared to the Standard Granule Structure become more limited with both the Layered and Standard 50% DE6 granule experiencing similar levels of deformation.

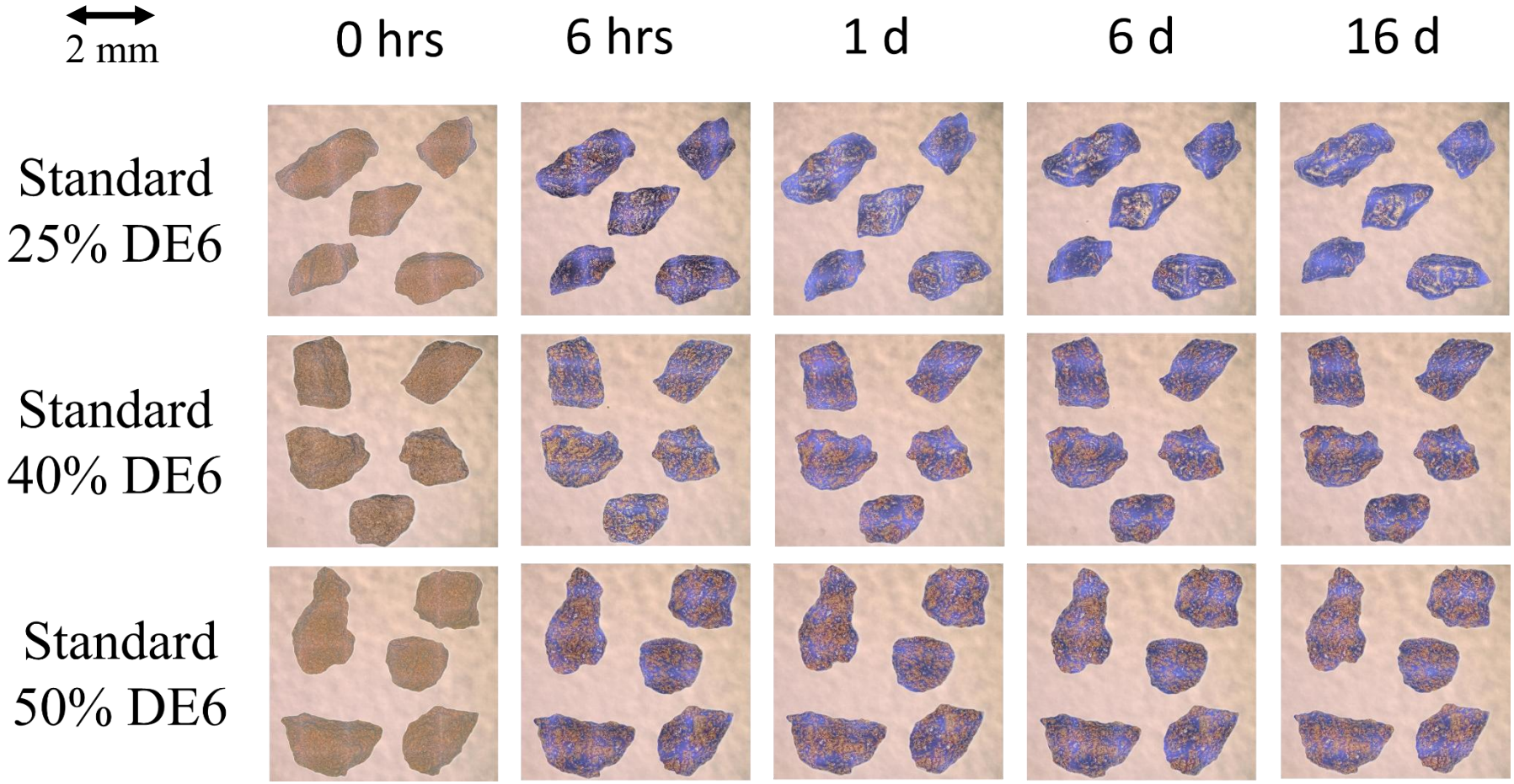

Figure 6.17: Changing characteristics of 5 random Standard Granules from the three evaluated formulations over time (Storage conditions: 20˚C and 60% RH). It is evident that the surface Coffee in the Standard Granules quickly liquifies and begins to flow on the granule surface within 6 hours of storage. This phenomenon is best displayed by the 25% DE6 formulation which contained the highest proportion of Coffee. The liquifying of the granule surface results in the reflection of the microscope light and the granules obtaining the blue hue in a similar manner to Figure 6.8. The granules also undergo significant changes to their size and shape as the Coffee structure in the granule collapses as clearly shown by the shrinkage experienced by the 25% DE6 granules.

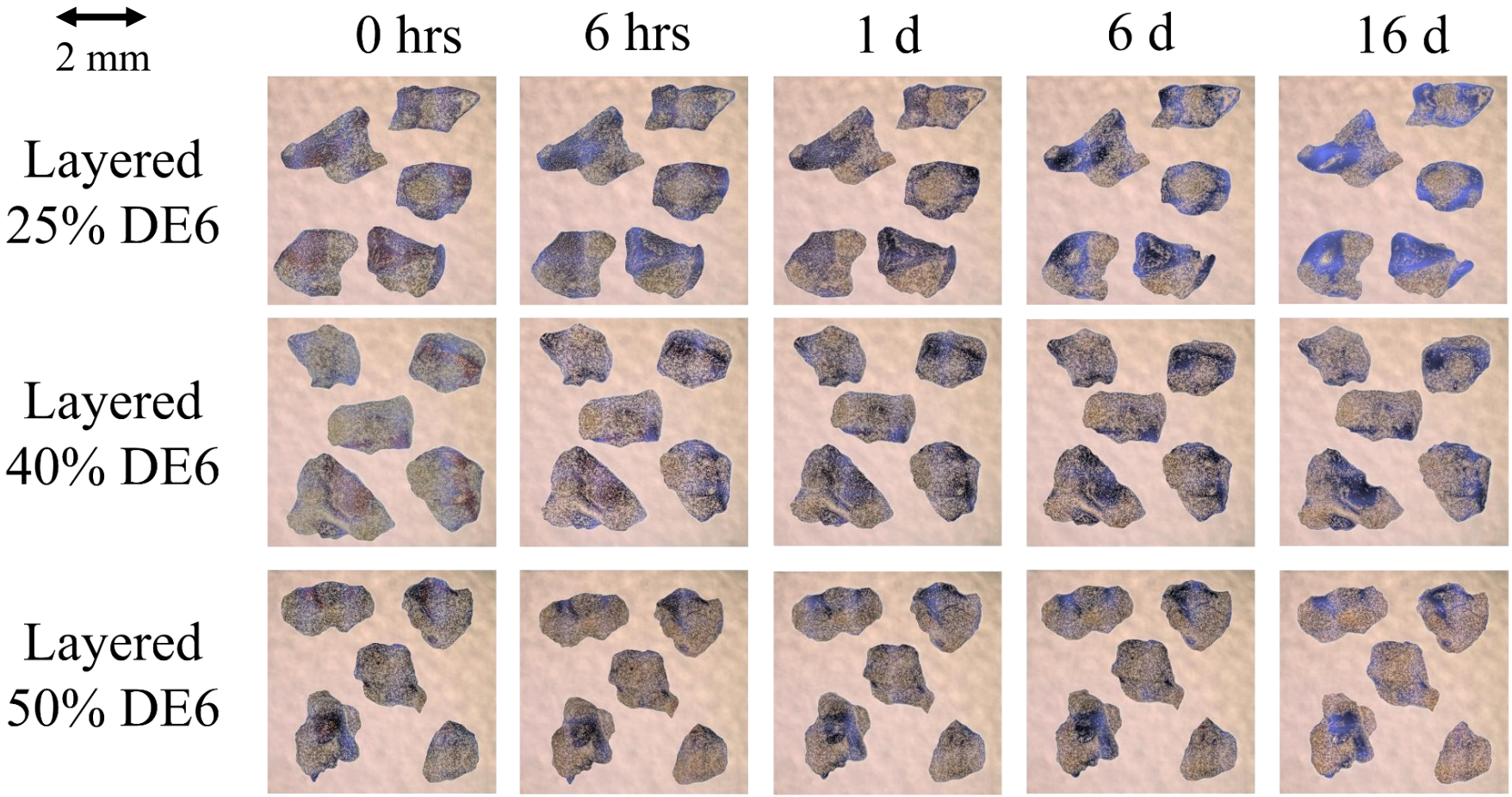

Figure 6.18: Changing characteristics of 5 random Layered Granules from the three evaluated formulations over time (Storage conditions: 20˚C and 60% RH). Similar to Figure 6.17, the exposed Coffee on the surface of the Layered Granules also liquifies leading to a change in granule size and shape as best displayed by the 25% DE6 granules. However, these changes occur at a delayed rate compared to those seen in Figure 6.17 which can be attributed to the shell like structure of the Maltodextrin helping to better maintain granule form.

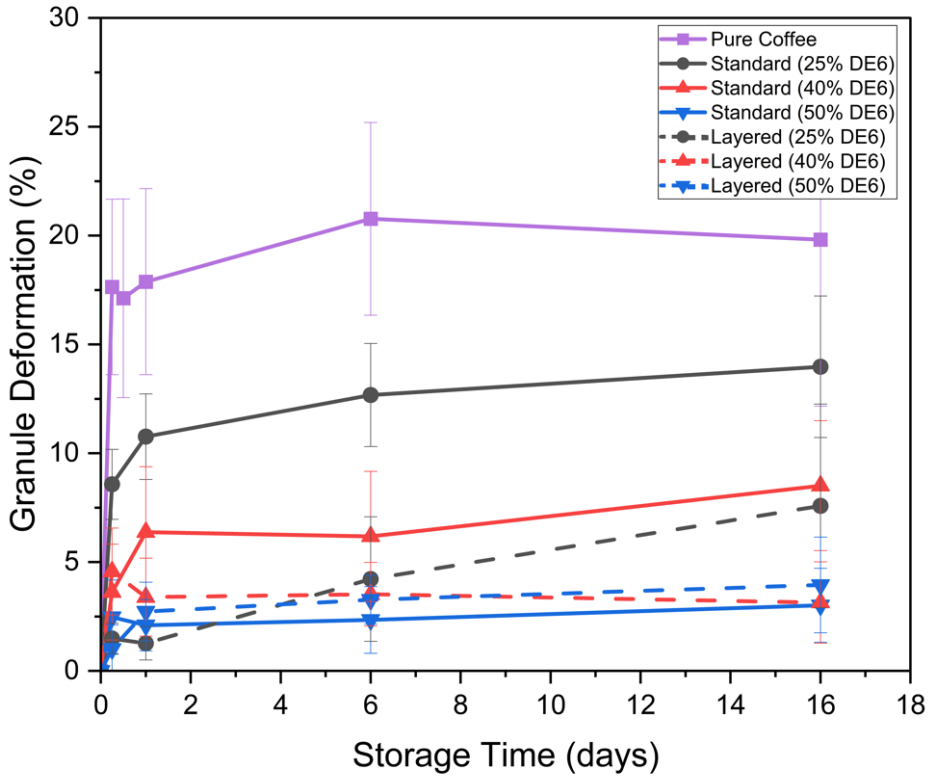

Figure 6.19: Granule deformation during storage as evaluated according Section 6.2.10. The Standard Granules were found to display greater changes in granule deformation compared to the Layered Granules, especially at low DE compositions. This is attributed to the outer DE6 layer in the Layered Granules acting as a 'skeleton' to help maintain granule form.

6.5 Layered structure to prevent moisture migration into granule core

Section 6.4.4 - 6.4.6 demonstrated how a Layered Granule approach can be used to lower the risk of caking, maintain granule size and mitigate colour change. However, these Layered Granules still displayed collapse of the Coffee at the granule core. This collapse even occurred in granules that had a complete outer DE6 layer, indicating that moisture is able to penetrate the DE6 outer layer and migrate towards the Coffee at the core. Moisture penetration is enabled by the intergranular pores in the granular structure. A representation of these pores is shown in Figure 6.20. It shows a Layered Granule composing of 50% DE6. The core of the granule is formed from the dense Roller Compacted Coffee. The outer layer meanwhile is formed from DE6 through wet granulation and displays large pores. During storage, these pores will aid the diffusion of moisture through it. The structural collapse of the moisture sensitive material (in this case Coffee) at the granule core is important because it can affect the functionality of the material. In the case of Coffee, it would lead to an extended dissolution time.

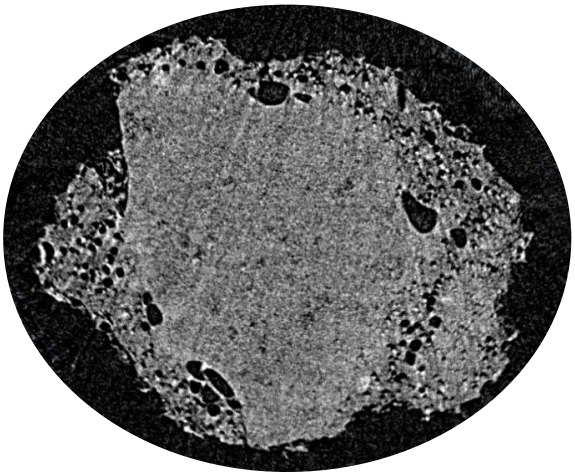

Figure 6.20: X-RAY scan of a Layered Granule composing of 50% DE6. The outer DE6 Layer is characterised by a high porosity which facilitates the diffusion of moisture towards the granule core during storage.

Therefore, it would be beneficial to develop a granule structure that could prevent the structural collapse of key ingredients while also mitigating caking. One such approach is presented in Figure 6.21. As before, the moisture insensitive ingredient (DE6) is layered on the granule surface to ensure the surface remains non-sticky. Similarly, the moisture sensitive component (Coffee) whose structure must be protected to maintain functionality is at the centre. However, an intermediate layer (DE47) between the inner and outer layer has now been added. The material forming this layer must be more moisture sensitive than the core material. This means this intermediate material will gain mobility and enter the viscous state first. As it does so, it should flow into any existing pores to close them and form a less porous layer around the core material. This less porous layer then acts as a physical barrier to better prevent the diffusion of moisture into the core.

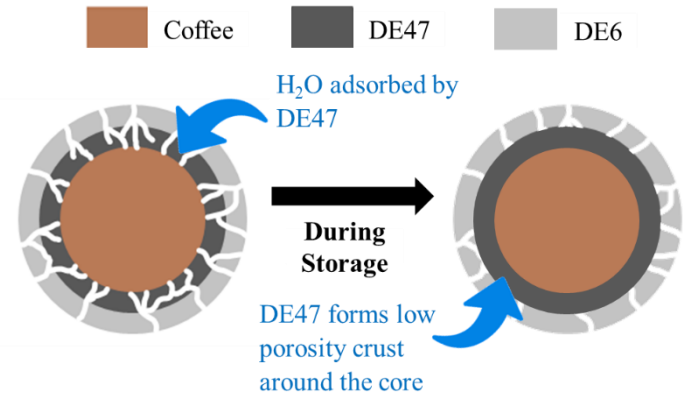

Figure 6.21: Shows a hypothetical three component granule composed of a moisture sensitive material whose structure is important (coffee for example), a hyper moisture sensitive material (DE47 for example) and a moisture insensitive material (DE6 for example). During storage, the hyper sensitive material undergoes glass transition first. The resulting flow of this material reduces the intergranular pores and forms a dense crust around the Coffee which hinders the diffusion of moisture into the core.

This hypothesis was tested through the creation of layered tablets as outlined in Section 6.2.15. The tablets were made to mimic the 3-layer granular structure that is presented in Figure 6.21. The layered tablets were organised as follows: Coffee (bottom of the tablet), DE47 (middle of the tablet) and DE6 (top of the tablet). These tablets were kept inside the plastic dies used to compact them, meaning they were only exposed to the environment from the top. Therefore, moisture would have to travel through the pores in the DE6 and then DE47 layer before reaching the Coffee at the bottom. This mimics the mechanism under which moisture would penetrate the proposed granule in Figure 6.21. The effectiveness of the DE47 layer in preventing the migration of moisture through it can be evaluated by observing the change in state of the bottom Coffee layer in these tablets.

The results are shown in Figure 6.22. It shows that the Coffee layer in Tablet A (which is purely consisting of Coffee and DE6) darkens at a much faster rate than the other two tablets containing an intermediate DE47 layer. This can be attributed to the DE47 undergoing glass transition to form a less porous protective layer around the Coffee which hinders the migration of moisture through it. Tablet C which contained the thickest DE47 layer shows minimal change in the colour of the Coffee layer at the end of the 42-day period, highlighting the effectiveness of this DE47 layer at prevent moisture migration through it. It is hoped that future studies can build upon this theory to produce granules with this multi-layered structure that can not only protect against caking but can also prevent the structural collapse of key components.

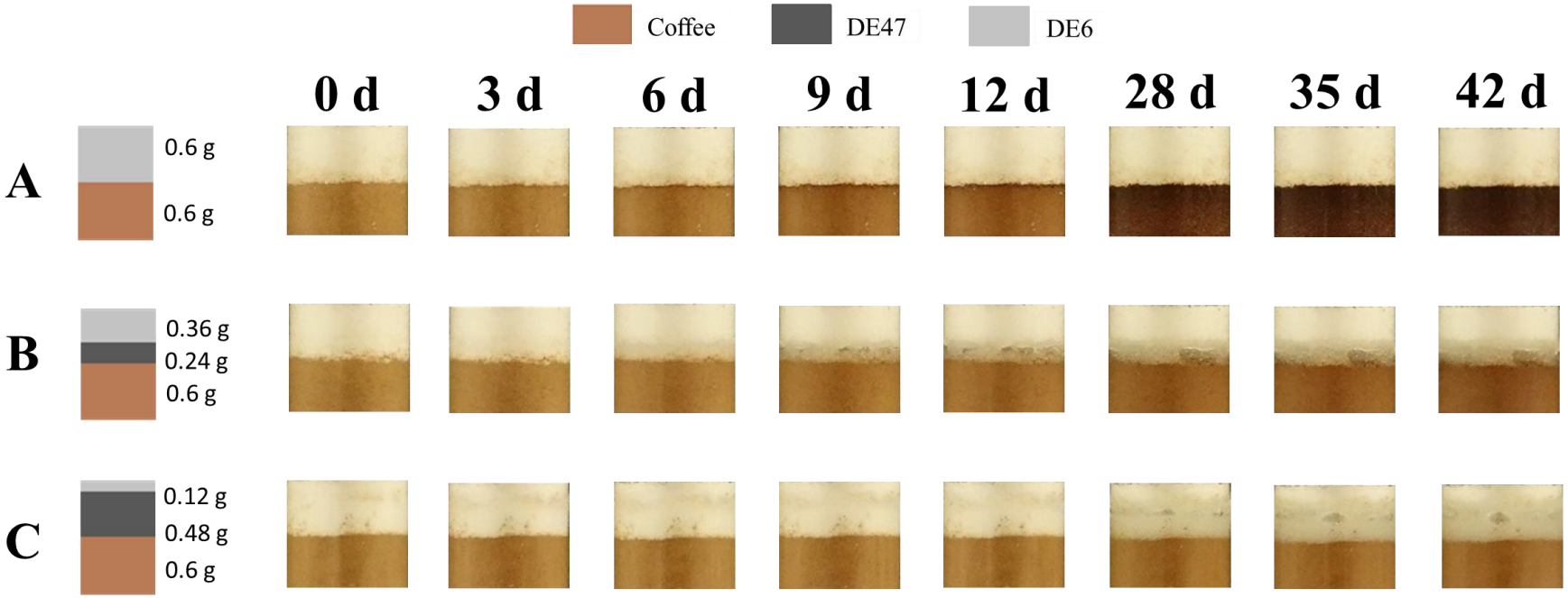

Figure 6.22: Change in colour profile in the 3 tablet formulations over time. The tablets were kept inside the transparent dies used to produce them. Therefore, they are only open to the environment from the top and moisture must migrate through the DE6 and DE47 layers to interact with the Coffee. The presence of the DE47 layer has been found to lessen the collapse experienced by the Coffee during storage as shown by the Coffee maintaining its colour better for Tablets B and C compared to Tablet A. This is attributed to the DE47 layer caking to form a dense crust which resists the penetration of moisture.

6.6 Conclusion

In conclusion, this work has demonstrated that size enlargement through granulation is an effective strategy to mitigate caking tendencies in food powders. The comparative analysis between single component granules and their raw powder forms revealed that particle size significantly influences the rate of caking, with smaller particles exhibiting a higher propensity for caking due to their increased surface area and number of contact points which facilitates moisture absorption and bridge formation.

Nevertheless, when dealing with highly moisture sensitive food powders such as Coffee, size enlargement by itself was not sufficient to significantly delay or prevent caking. Co-granulation of Coffee with less moisture sensitive ingredients such as DE6 helps increase the stability of granules, with stability increase being proportional to the amount of DE6 present. Two competing granule microstructures were tested to evaluate what impact the distribution of moisture sensitive and moisture insensitive components in the granule structure had on granule stability. One structure was the Standard Granule where the Coffee and DE6 were randomly distributed within the granule matrix. The second structure was a Layered Granule (composed of a Coffee core and DE6 outer layer) which was produced through a novel production pathway involving dry coating, steam treatment and wet granulation. The Layered Granule structure demonstrated superior caking resistance compared to the Standard Granule, as evidenced by a delayed onset of caking and reduced caking indices during storage. The Layered Granules were also shown to preserve key characteristics including colour and size better than their Standard Granule counterparts. This work emphasizes the importance of formulation strategies, such as the use of protective outer layers, in enhancing the stability of food powders under varying humidity conditions. The insights gained from this study provide a foundation for further research into optimizing granule formulations to improve product performance and consumer acceptance in the food industry.

7 Dry Twin Screw Granulation: The future of amorphous food granulation?

Chapter Abstract

Dry Twin Screw Granulation is a recently proposed form of granulation that has numerous potential benefits for the agglomeration of amorphous food powders. This process involves the kneading segment applying sufficient stress on the powder to induce glass transition. The glass transition process converts a portion of the powder into a sticky, viscous material that then acts as binder to drive agglomeration. This work presents the application of a dry Twin Screw Granulation process to a model food powder (Maltodextrin DE29) while evaluating changing process parameters and screw design. The work showed the importance of Throughput, Screw Speed and Kneading Segment Length in determining granule attributes and process behaviour. Several possible process behaviours were exhibited by the system depending on the process parameters chosen. These behaviours included a region where granulation did not occur as the stress applied on the powder was insufficient, a region where the barrel fill level was too high leading to barrel blocking and a region where the energy introduced into the powder was too great leading to extrusion. These behaviours were captured to produce the first operational regime map for a Dry Twin Screw Granulation process. Comparing the material, energy and time efficiencies indicates that this process is far more sustainable than wet Twin Screw Granulation. Furthermore, there are strong indications that it can compete with the other established forms of granulation once the cooling capability of the Twin Screw is improved to facilitate the stable use of higher screw speeds and throughputs.

Chapter Highlights

- Production of the first regime map for Dry Twin Screw Granulation
- Map delineates key regions describing behaviours such as Barrel Blocking and Extrusion
- Established the need for a strong cooling capability to expand the Operable region
- Evaluated the sustainability of the process compared to established granulation techniques

7.1 Introduction

Granulation is a size enlargement mechanism which is carried out to prevent segregation, improve particle flowability, reduce dust and modify particle structure [148–150]. There are many different processing routes that can be utilised for a granulation process. Most of these processing routes can be grouped under the two following categories: Wet Granulation and Dry Granulation.

Wet granulation can be considered the most common form of industrial granulation, with it being used to produce 70% of granular products worldwide [151]. The typical wet granulation process can be described as the addition of a liquid binder to an agitated powder bed to produce wet agglomerates. This is followed by a drying step to remove the moisture from the wet mass and finally a sizing step to collect granules within the desired size range [6]. It is this drying step which is the major drawback due to its very energy intensive nature which decreases energy efficiency as highlighted by Chapter 4. The need for a drying step also leads to an increase in process complexity, total processing time, facility space requirement and operating costs [9,118,152,153]. However, there are also benefits to wet granulation pathways. For example, the use of strong material bridges to bond the particles together and the cyclic nature of the granulation mechanism enable wet granulation processes to achieve very high yields as presented in Chapter 4.

Meanwhile, Dry granulation typically involves the use of high stresses to compact the powder particles. This increases their Van der Waals forces of attraction and leads to mechanical interlocking resulting in agglomeration. Roller Compaction is the most common form of Dry Granulation where powder is compressed to form a ribbon which then undergoes a milling process to produce granules [6,154]. As shown in Chapter 4, since water is not used in the process, there is no need for a drying step making dry granulation technologies like Roller Compaction very energy efficient. However, as also discussed in Chapter 4, the main issue with Roller Compaction is the high amount of fine generation during milling which leads to a lower yield and increased material waste [154–156].

These issues with each granulation method highlights the need for further innovation and improvement in the field. The ultimate aim should be the development of an ‘ideal’ granulation process for the future which can be described according to the following statement: (1) High Yield, (2) Energy Efficient, (3) Low Complexity and (4) Continuous Operation. This chapter aims to determine whether a recently proposed Dry Twin Screw Granulation process can meet these mission statements and act as a granulation technology of the future for amorphous food powders. The Twin Screw Granulator is a continuous granulator which is primarily used for wet granulation. In the Twin Screw Granulator, a pair of co-rotating screws are used to apply a large amount of stress and agitate a wetted powder flow to create granules. In this wet granulation process, a liquid binder such as water is added to specifically act as a bonding agent. However, the ability of the Twin Screw Granulator to develop large stresses

offers an alternative pathway for the granulation of amorphous powders. This pathway utilises an intrinsic property of amorphous powders – the Glass Transition Temperature (T_g). When the powder temperature exceeds T_g, these materials undergo a phase transition from a glassy state to a rubbery state. Within a Twin Screw Granulator, this transition can be mechanically induced using the high stresses imparted by the rotating screw elements which results in a temperature rise in the powder. The extent of this stress—and consequently, the temperature rise—is governed by the screw design and process parameters. Upon reaching the rubbery state, the amorphous material becomes sticky and viscous enough to function as a binder, facilitating the agglomeration of surrounding particles. This mechanism underpins a dry granulation approach wherein the formulation self-induces granulation through localized glass transition, eliminating the need for liquid binders.

This innovative concept of using a wet granulation unit to carry out dry granulation creates a technology where the benefits of each processing route are maintained without the drawbacks. For example, since the process utilises no water, there is no need for a drying step which will allow Dry Twin Screw Granulation to achieve a high energy efficiency which is a characteristic benefit of dry granulation techniques like Roller Compaction. Unlike Roller Compaction, no destructive milling stage is required to produce granules in the Dry Twin Screw Granulator. The absence of this milling stage, as well as the strong material bonds formed by the molten amorphous material, will enable Dry Twin Screw Granulation to achieve high yields which are characteristics of wet granulation processes.

There are a limited number of studies exploring Dry Twin Screw Granulation originating from the pharmaceutical granulation field. These studies involve the granulation of a pharmaceutical formulation (composed of an API and filler) with different polymer binders. Frictional stress generated by the kneading segment in the TSG was used to induce the glass transition or melting of these polymer binders to initiate agglomeration [55,56,157]. Existing literature mainly focused on proving that dry granulation is possible while evaluating a narrow range of quality attributes such as API degradation [55,56,157]. The literature showed that this Dry TSG process was capable of granulating pharmaceutical formulations with little API degradation due to exposure to moisture (as it did not need water unlike wet TSG) and exposure to high temperatures (as opposed to melt TSG).

This work seeks to evaluate the feasibility of Dry Twin Screw Granulation as an ‘ideal’ food granulation technology for the future by focusing on three main aims. The first aim will be the identification of which process parameters are critical in affecting process stability and granule attributes. This will improve the ease at which the process can be understood, transferred and optimised outside of this work. Secondly, the development of a regime map to better understand the operating window within which controlled agglomeration without process issues can be achieved. Currently there is only one dry granulation regime map which exists and it applies to Roller Compaction [67]. The establishment of a second dry granulation regime map for a completely different unit highlights the novelty of this work.

Thirdly, the sustainability of the Dry Twin Screw Granulation process at this early stage will be compared to the established granulation technologies. Sustainability will be judged by comparing the material, energy and time efficiencies of the technologies in a similar manner to Chapter 4.

7.2 Materials and Methods

7.2.1 Materials

Glucidex IT29 (Roquette, France) has been chosen as the model granulation material as it allows the direct comparison of results between this work and Chapter 4 (which also utilised IT29) when evaluating process sustainability. Henceforth, as is the convention in this thesis, the powder will be referred to as DE29. The powder size characteristics can be described by a d10 of 143 µm, d50 of 255 µm and d90 of 455 µm. Powder was conditioned at 50% Relative Humidity and 20˚C for 72 hours in a Memmet IN110 Humidity Chamber (Memmet, Germany). This was the highest relative humidity the powder could be conditioned at before it underwent glass transition. The powder was conditioned at a high relative humidity to maximise the moisture absorbed by the powder and therefore decrease the T_g as much as possible. A lower T_g reduces the amount of stress that needs to be exerted for the material to transition to the viscous, sticky state where it can act as binder and form agglomerates. The T_g of the powder after conditioning was measured at 31˚C. The conditioning process was shown to be key during preliminary work with agglomeration not being possible or far more aggressive mixing conditions needed for agglomeration when the powder was conditioned at lower relative humidity's.

7.2.2 Dry Twin Screw Granulator Set-up

The Twin Screw Granulator used in this study was the ThermoFisher Euro Lab 16 mm Twin Screw (ThermoFisher Scientific, UK). Incorporated into the TSG system is a loss in weight twin screw powder feeder (K-Tron Soder, Switzerland). An IC05C Water Chiller (ICS Cool Energy, UK) was used to provide cooling. The granulator barrel is split into 6 compartments, each of which can be individually temperature controlled as presented in Figure 3.6. This control is achieved by using cooling water which flows into the upper half of the barrel or heating elements which are present in the lower half of the barrel. The ability to have both barrel cooling and heating offers significant benefits in terms of unit flexibility. However, a key drawback of this assembly is that the direct effect of the cooling or heating function is only active over half the barrel. It then relies on conduction to transfer that cooling or heating to the other half of the barrel. This can severely limit the cooling capability of the machine when dealing with rapid heat generation due to friction within the barrel.

The barrel configuration for this work is shown in Figure 7.1 below. Powder is fed in at Compartment 1 (C1). The first 5 compartments (C1-C5) were set to a raised temperature of 45˚C. The screw configuration during this 5-compartment section is entirely conveying elements. The intent is for no

granulation to occur during this section with the conveying elements purely transporting the powder along the barrel. As the powder is transported along the barrel it will gain thermal energy from the heated barrel, which increases powder temperature (T). This reduces the energy barrier required for glass transition to occur in the subsequent C6 granulation compartment (as less energy now needs to be applied to the powder to cause $T>T_g$ and trigger glass transition) which makes a successful agglomeration process more likely. Therefore, it is important to ensure that the barrel temperature is sufficiently high to facilitate granulation with literature stating that agglomeration is not possible or very difficult to induce if the chosen barrel temperature is too low [157]. Also, a high barrel temperature means that the other operating conditions need to be less severe in order to induce glass transition in the granulation compartment (C6). This facilitates the use of lower screw speeds and throughputs, which is important because the use of higher screw speeds/throughputs resulted in a much faster rate of heat generation during granulation which leads to process instability. Therefore, to promote process stability, milder screw speeds and throughputs are preferred. For instance, operating at a heated barrel (C1-C5) temperature of 20˚C significantly increased the severity of the screw speeds/throughputs needed for granulation which dramatically increased the likelihood of process instability and failure. Conversely, the heated barrel temperature (C1-C5) cannot be too high, otherwise the material will glass transition or melt in compartments C1-C5 resulting in material sticking to the barrel walls and screw jamming. Following this logic, a (C1-C5) barrel temperature of 45˚C was chosen because it was the highest that could be used without the DE29 powder undergoing glass transition in the conveying section and sticking to the barrel wall.

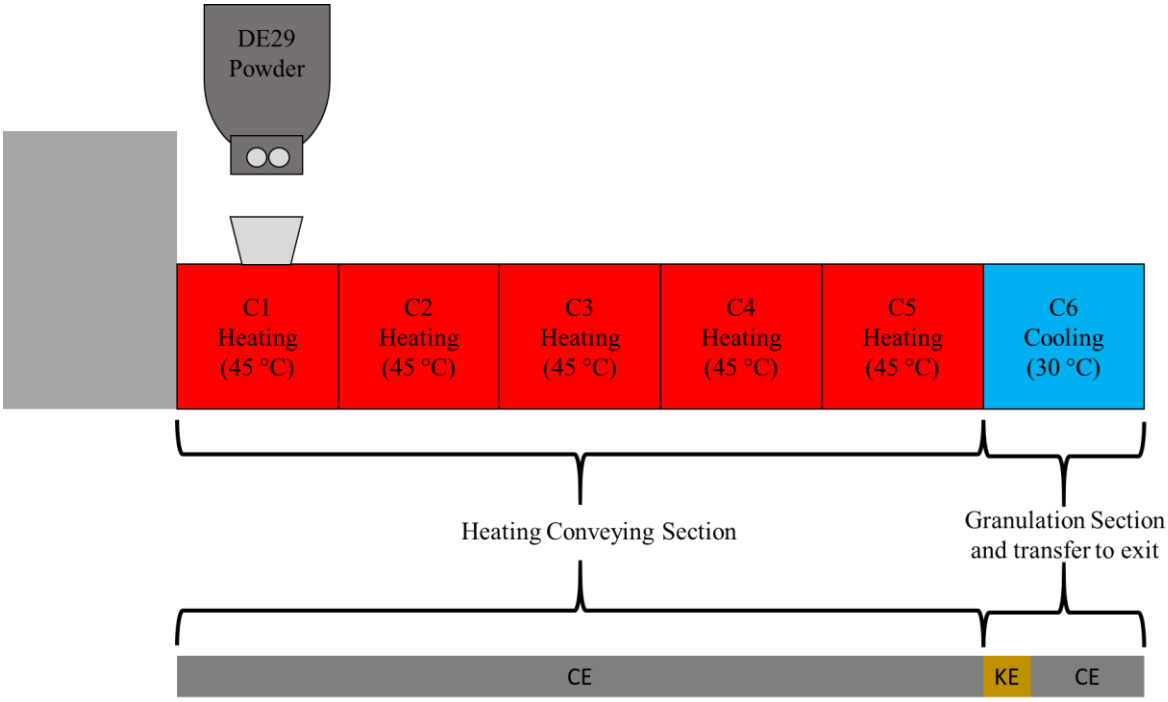

Figure 7.1: Schematic diagram of the Twin Screw Granulation set-up. The first 5 compartments (C1 - C5) of the barrel were heated to a temperature of 45°C. The screw elements in these 5 compartments were solely Conveying Elements (CE). The last compartment (C6) was set to cool with the target temperature being 30°C. This compartment housed the Kneading Elements (KE) which drives the granulation process. The cooling effect was needed to mitigate the heat generation due to the high frictional forces involved during the granulation in Compartment 6.

The last compartment (C6) where granulation occurs was cooled in order to maintain a compartment temperature of 30˚C. Cooling is needed here because the granulation process produces a significant amount of frictional heat. If not mitigated, this frictional heat builds up causing excessive glass transition of the Maltodextrin which leads to the formation of a paste and/or screw jamming. The screw configuration in C6 is composed of kneading elements and conveying elements. The kneading elements are key because they exert a very strong compaction and shear stress on the material. This leads to a portion of the Maltodextrin powder transitioning to form a viscous paste that agglomerates the un-transitioned powder to form granules. Meanwhile, the subsequent conveying elements transport the produced granules to the exit.

The temperature profile for the granulator used here in this work differs significantly from that used in literature. The temperature profile used by literature configured the compartment where granulation occurred to have the highest temperature to aid in the granulation process [55,56,78,157]. Meanwhile, this setup uses cooling to ensure the compartment where granulation occurs (C6) has the lowest temperature. The differing configurations can be explained by considering the nature of the granulation mix evaluated by literature. Literature applied the dry TSG process to a pharmaceutical formulation where only part of the mix would undergo glass transition. In these studies, it was intended that the binder would undergo glass transition/melting to become sticky while the API/filler remained as non-sticky components. Conversely, in this work the entire powder flow is capable of undergoing glass

transition. Therefore, not as much energy needs to be input into the system described here in order to achieve agglomeration, compared with the system described in literature where only a part of the powder flow is capable of entering the viscous state. Compared with powder flow where only a partial component undergoes glass transition, powder flows that are entirely capable of entering the viscous state also show greater tendencies to over-agglomerate or form an extrudate when excessive energy is introduced into the system. Therefore, to also reduce the risk of this over-agglomeration occurring, this work chose to keep the temperature in Compartment 6 at a relatively low 30°C.

The two screw configurations evaluated in this study are shown in Figure 7.2. The main difference between the screw configurations is the number of kneading elements in the granulation zone with one configuration possessing 2 elements while the other possessed 4 elements. These are referred to as the 2 Kneading Element and 4 Kneading Element Configuration throughout this work. Apart from these configurations, additional extra screw configurations also underwent preliminary investigation, however, they were found to be unsuitable for the Dry Twin Screw Granulation of DE29. For example, regardless of the process parameters chosen, no DE29 granules could be produced when the kneading segment in the granulation compartment (C6) was composed of only 1 kneading element. This is attributed to the short powder residence time in the granulation zone when the number of kneading elements was 1, which resulted in insufficient stress being applied on the powder to result in glass transition. Furthermore, DE29 powder could not be well granulated when there were 5 or more kneading elements in the granulation compartment (C6). This is because the poor transportability of material in the kneading segment alongside the excessive stress on the material under these conditions promoted excessive glass transition and caused barrel jamming to occur. Therefore, the two screw configurations presented in Figure 7.2, were the most suitable for evaluation with DE29.

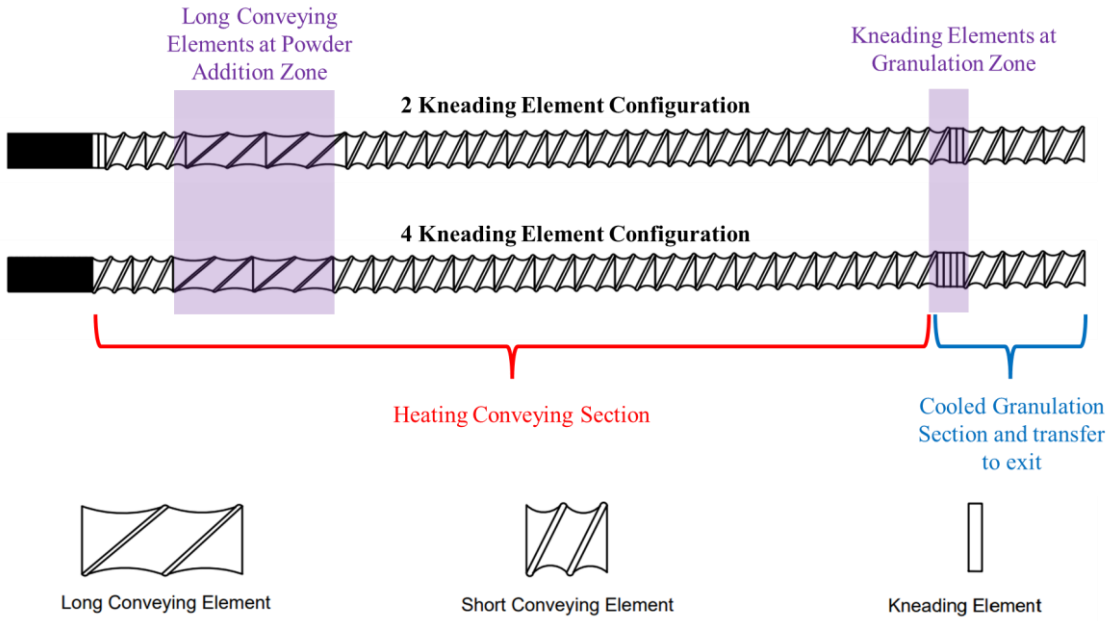

Figure 7.2: The two main screw configurations evaluated in this work, each with a differently sized kneading segment in the granulation zone - Top (2 Kneading Elements) and Bottom (4 Kneading Elements). The offset angle between the Kneading Elements was 60°.

There is a significant difference in the screw configurations that were shown to be feasible in literature and the two configurations (as presented in Figure 7.2) used in this work. Literature evaluated screw configurations where the kneading block contained as many as 10 kneading elements and there were multiple kneading blocks present [55,56,78,157]. Meanwhile, for the DE29 powder used in this study, the use of more than 4 kneading elements was found to lead to screw jamming. This is linked to the previously discussed ease at which over-agglomeration and extrusion occurs in powder flows which can entirely glass transition (as is the case in this study) compared with powder flows where only a partial component can glass transition (as is the case in literature). Over-agglomeration occurs at shorter kneading segment lengths for powder flows that can entirely glass transition compared to powder flow which only partially glass transition. This meant that far fewer kneading elements could be included in the screw configuration when granulating DE29 compared to the pharmaceutical formulations evaluated in literature. Furthermore, in this work only 1 kneading block is present in the screw configuration. This is because the DE29 granules produced by this process were found to be dense, strong and tended to resist deformation. This made it very hard for these granules to navigate secondary kneading blocks without barrel jamming occurring and even resulted in conveying issues during transport by the conveying elements. Therefore, only 1 kneading block was utilised in this work and it was placed near the barrel exit so that the produced granules can be quickly removed from the unit, minimising the risk that they get caught in the screw and cause screw jamming. This is in contrast to literature where the kneading blocks are placed relatively earlier along the screw to promote further agglomeration by the conveying elements after glass transition of the binder has been achieved

[55,56,78,157]. These differences emphasise how formulation material properties heavily influences the development of viable screw configurations for the Dry Twin Screw Granulation process.

Unlike existing literature, this work did not include the use of Magnesium Stearate (MgSt) as a lubricant [55,56,78,157]. Literature found MgSt necessary because the formulations used in those studies include a large powder component that does not undergo glass transition. This component remains glassy and generates a lot of friction and grinding at the kneading block. To mitigate this, MgSt was added to protect the equipment by reducing the metal-powder friction [55,56,78,157]. In this study, the process proved to function well without the use of MgSt. This is because in this work, the entire powder flow is capable of undergoing glass transition which produces a majority viscous DE29 component at the kneading element. This viscous DE29 that is produced then goes on to lubricate the TSG elements and cause less grinding at the kneading block. The elimination of the need for MgSt is significant for the food industry as it reduces non-essential components from the recipe and for the pharmaceutical industry where excessive amounts of MgSt have been shown to negatively impact tablet properties.

7.2.3 Granulation Compartment (C6) Temperature Measurement

The temperature of the granulation compartment (C6) would increase if the cooling system was unable to mitigate the frictional heat generated at the kneading elements. This compartment temperature increase was measured by using the inbuilt temperature sensor function inside the Twin Screw Granulator unit.

7.2.4 Yield

Sieving using a Retsch Sieve Shaker AS200 (Retsch, UK) at an amplitude of 0.45 mm for 3 mins was used to classify the Granulation Yield. The sieve classes used were 0.5 mm, 1 mm, 2 mm and 4 mm. Granules less than 0.5 mm were classed as fines. Granules between 0.5 mm and 4 mm were classified as the Total Yield faction. Granules greater than 4 mm were classed as lumps. Similarly to Chapter 4, granules between 0.5 mm and 2 mm were classified as the In-Spec Yield faction. This In-Spec Yield was used to compare sustainability metrics between the Dry TSG process and the established granulation technologies presented in Chapter 4.

7.2.5 Granule Size and Sphericity Characterisation

A Camsizer (Retsch, UK) was used to evaluate the size and sphericity of granules. Three repeats were conducted for each condition. Sphericity is defined as $4\pi A/P^2$ (ISO 9276-6) where A is the measured particle projection area and P is the measured particle projection circumference. For an ideal sphere, the sphericity is expected to be 1.

7.2.6 ANOVA analysis

When evaluating experimental data, it is essential to determine whether observed trends are statistically meaningful or simply the result of random variability within the dataset. Analysis of Variance (ANOVA) is a commonly used technique for this purpose. ANOVA works by comparing the variation within groups to the variation between groups. When the variation between groups is large relative to the variation within groups, the observed trends are more likely to be statistically significant and reliable. ANOVA analysis was carried out using JMP Statistical Discovery to evaluate which of the process parameters displayed the greatest significance towards the process stability and granule attributes. The data was analyzed using a Standard Least Squares approach with the parameters analyzed according to a full factorial design. Parameter significance was determined by considering the Logworth value for each process condition. The higher the Logworth value, the greater the significance of the condition. The Logworth value is the negative log of the p value (-Log[p]). Typically, a p value of 0.01 is required for the parameter to be classed as significant which corresponds to a Logworth value of 2.

7.2.7 Barrel Fill Level

The approach used to calculate the Barrel Fill Level is presented in Equation 7.1. The Barrel Fill Level is defined as the ratio between the powder volume in the barrel and the barrel free volume. The barrel free volume is the space inside the barrel that is not occupied by the screw. Barrel and screw volume was determined by modelling the geometries in Fusion 360 and analyzing the fill volume of the model. Figure 7.3 presents the modelled geometries for the barrel and the two screw configurations. The values for screw volume were verified using water displacement. This involved dipping the screw configuration into a tube filled with water and measuring the increase in the water level to determine the volume of water displaced. The screw volume would equal the volume of water displaced. The barrel free volume was then determined by subtracting the screw volume from the barrel volume.

The powder volume inside the barrel at different processing conditions was determined by first running the unit for 2 minute (for steady state to be achieved) then using the emergency stop function to pause the entire unit. The mass of powder inside the barrel was then collected. The powder bulk density of the raw powder (450 kg/m^3) as supplied by the manufacturer was used to estimate the powder volume by using the relationship: Volume = Mass/Density.

$$Barrel\ Fill\ Level\ \% = 100 * \frac{Powder\ Volume}{Barrel\ Free\ Volume} = 100 * \frac{Powder\ Volume}{Barrel\ Volume - Screw\ Volume}$$

Equation 7.1

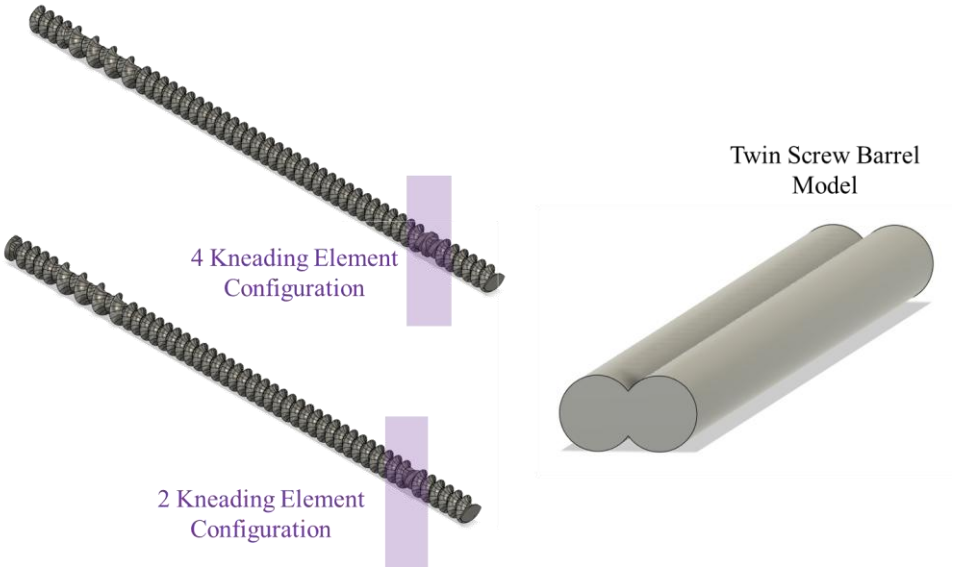

Figure 7.3: Fusion360 was used to model the barrel and screw geometries. The barrel volume was determined to be 0.00015 m^3 while the screw configuration volume was determined to be 0.000078 m^3 (4 Kneading Element) and 0.000076 m^3 (2 Kneading Element) respectively. Barrel Free Volume was determined as the Barrel Volume subtracted by the Screw Volume.

7.2.8 Peak Shear Rate

The peak shear rate for the Twin Screw Granulator was determined according to Equation 7.2 as is common in literature. Where D is the screw diameter (16 mm), N is the screw speed (rpm) and h is the overflight gap (0.2 mm) [158]. This equation calculates the maximum shear rate which exists between the tip of the rotating screw and the stationary barrel surface.

$$Peak\ Shear\ Rate = \frac{\pi \times D \times N}{60 \times h}$$

Equation 7.2

7.3 Results and Discussion

7.3.1 Process Stability

This section will present the work carried out looking at process feasibility and the practical considerations necessary for a successful, stable Dry Twin Screw Granulation process. Process stability was evaluated by looking at the temperature rise in the granulation compartment (C6) during the run and how long the TSG could operate for without process failure occurring. There were two criteria needed for the process to be considered stable. The first criteria was that the process should display no temperature rise in the granulation compartment (C6) over time. This would indicate that the cooling system was capable of managing the frictional heat generation in the system and a constant temperature profile would result in the production of a more consistent product. The second criteria was that the

process should run for 30 minutes (which was the maximum evaluated run time) without process failure occurring. Figure 7.4 presents the observed Temperature Rise and Maximum Operating Time possible for various combinations of screw speed and throughput in the case of the 2 and 4 Kneading Element screw configurations. Figure 7.4 also highlights the operating spaces where granules could and could not be produced. The production of granules was possible in Region A and not possible in Regions B, C and D.

Region A indicates the screw speed and throughputs under which granules could be produced. The observed Temperature Rise and maximum Operating Time within this region has been plotted to better understand the effects of process parameters on process stability in this region. For both screw configurations, increasing screw speed resulted in a higher Temperature Rise in the granulation compartment (C6) as shown by Figure 7.4. For example, in the case of the 2 Kneading Element Configuration, at a throughput of 0.1 kg/hr, the Temperature Rise increases from 0 °C/min at 15 rpm to 2.7 °C/min at 95 rpm. Furthermore, increasing throughput also resulted in higher Temperature Rises for both screw configurations. For instance, the 2 Kneading Element Configuration at a screw speed of 45 rpm, displays a Temperature Rise increase from 0.9 °C/min at 0.1 kg/hr to 2.8 °C/min at 0.5 kg/hr. These trends exists because heat generation in this compartment depends on the amount of friction that the chosen process parameters generate. A higher throughput will result in more particles being present within the kneading segment leading to more particle-particle interactions, resulting in more friction. Meanwhile, higher screw speeds will increase the friction between the screw and the barrel resulting in more heat generation. It will also increase the rate of collisions between particles and the energy involved in those collisions, both of which will result in the generation of more frictional heat.

Comparing between the 2 Kneading Element and 4 Kneading Element configuration, increasing the number of kneading elements also results in an increase in the compartment temperature, especially at high throughputs and screw speeds. For example, for the 2 Kneading Element Configuration at 0.3 kg/hr, the following Temperature Rises were observed: 1 °C/min (35 rpm), 1.8 °C/min (45 rpm) and 1.8 °C/min (55 rpm). Meanwhile for the 4 Kneading Element Configuration at 0.3 kg/hr, the Temperature Rise was 2 °C/min (35 rpm), 2.8 °C/min (45 rpm) and 3.3 °C/min (55 rpm). This is due to the increasing applied stress and powder residence time in the kneading zone as the kneading segment is lengthened leading to more friction. To summarise, increasing the screw speed, throughput and number of kneading elements will all result in more friction leading to more energy dissipation via heat resulting in a greater Temperature Rise.

The Temperature Rise observed in the granulation compartment (C6) shows a clear correlation with the Maximum Operating Time. A higher Temperature Rise results in lower Operating Times as displayed by Figure 7.4. For instance, the 2 Kneading Element configuration displayed a Temperature Rise increase from 0 °C/min at 15 rpm to 2.7 °C/min at 95 rpm when operating at a throughput of 0.1 kg/hr.

This correlates with a decrease in the operating time from 30 mins at 15 rpm to 4.5 mins at 95 rpm at a throughput of 0.1 kg/hr. This is because the higher the Temperature Rise, the greater the risk of process instabilities occurring. For example, if heat continues to build up in the granulation compartment (C6), eventually the barrel temperature at this location would increase to the point where the Maltodextrin powder sticks and melts onto it, resulting in jamming or the formation of an extrudate. A higher Temperature Rise increases the risk of this occurring. The only 'stable' region for the DE29 material under the evaluated conditions is presented within the area highlighted by the blue border for the 2 Kneading Element Configuration in Figure 7.4. In this region, there was no temperature rise in the granulation compartment (C6), indicating that the cooling system was capable of controlling the heat generation under those conditions. The granulator was also capable of running for the full 30 minute run time without any processing issues within this highlighted region. There was no similar 'stable' region for the 4 Kneading Element Configuration, with all combinations of throughput and screw speed either resulting in a Temperature Rise or process failure before the 30 min run time criteria was reached.

Granulation was not feasible in Region B, C and D. Region B represents the operating space where the low screw speeds and low throughputs mean that the stress applied on the material is insufficient to cause glass transition. The lack of glass transition means that no sticky, viscous DE29 is formed to initiate agglomeration, resulting in the production of no granules. Region C represents the operating space where low screw speeds and high throughputs result in a high barrel fill level. The high barrel fill level generates large frictional and adhesive forces inside the unit which act to resist the conveying of the powder. Under these conditions the motor cannot supply the torque required for the screw to overcome these forces and continue rotating, which leads to barrel jamming. Region D represents the operating space at relatively high screw speeds. The high screw speed means there is a large energy input into the system resulting in the DE29 undergoing glass transition to an excessive degree. This makes the DE29 too viscous and leads to an extrusion process. The product of this extrusion process is a Maltodextrin paste rather than granules. Process conditions that resulted in process failure due to barrel jamming or the forming of a paste less than 3 minutes after start up were placed in Regions C and D respectively. These scenarios' will be further discussed in this work when presenting the regime map.

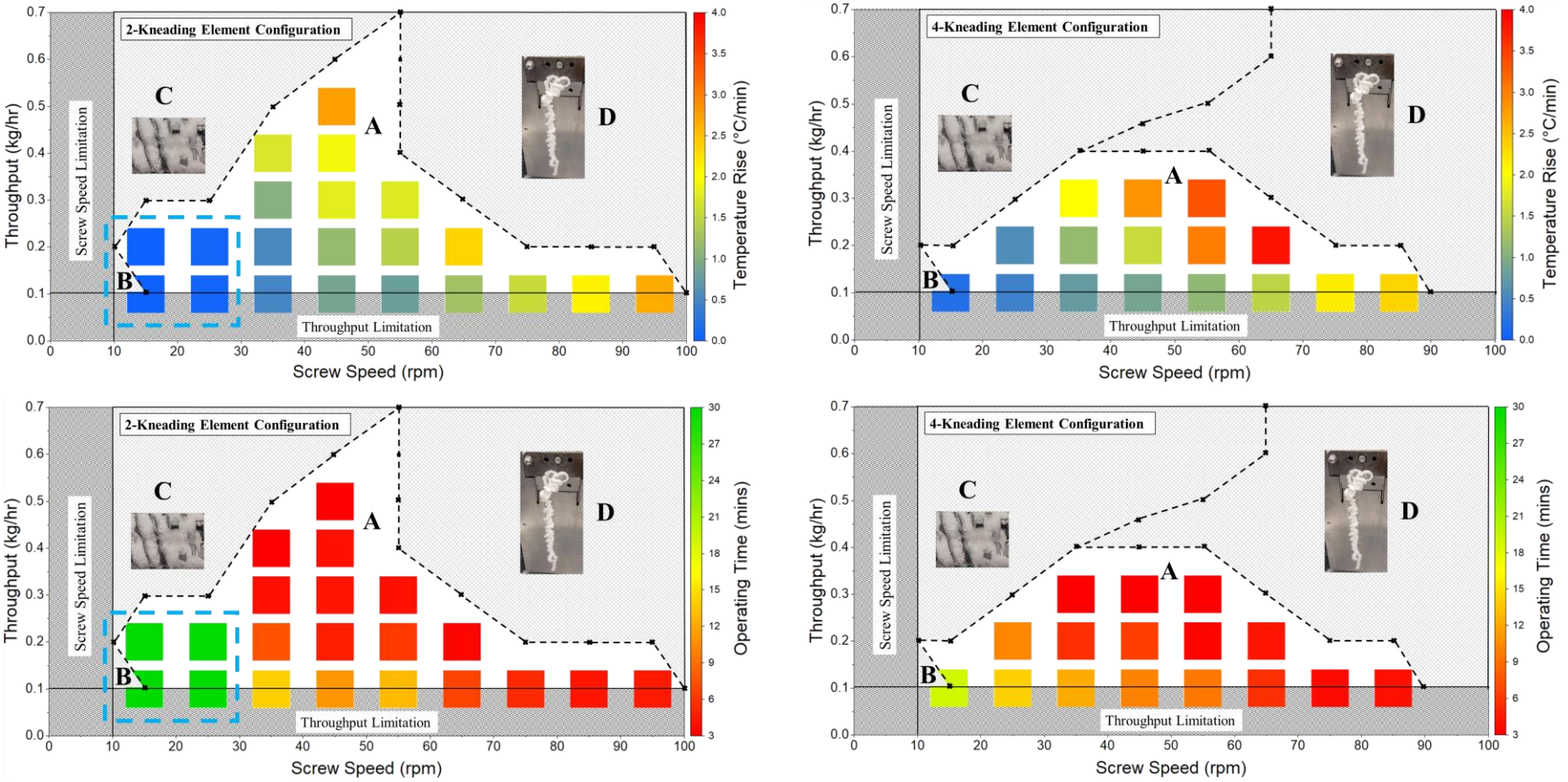

Figure 7.4: Temperature Rise and the Maximum Operating Time were used to evaluate process stability at varying screw speed and throughput for the 2 Kneading Element Configuration (Left) and 4 Kneading Element Configuration (Right). Several different process behaviours were observed which were defined into the following regimes: Operable region (A), No granulation due to insufficient stress (B), Barrel jamming (C) and Extrusion (D). The zone highlighted by the blue border for the 2 Kneading Element Configuration indicates the only region where the process is classed as being stable. This meant no temperature rise was recorded at those conditions and the process ran for the full 30 min without issue. When the 4 Kneading Element Configuration was used, the process displayed a temperature increase in the granulation compartment (C6) or failed before a running time of 30 mins was reached, at all the evaluated process conditions. This means no region could be classed as stable for that screw configuration.

ANOVA analysis was used to evaluate the relative significance of throughput and screw speed on Temperature Rise as shown by Figure 7.5. The analysis shows that for both screw configurations, throughput and screw speed had a Logworth value far higher than 2, which indicates that both parameters have a very significant impact on the temperature generation. For the 2 Kneading Element configuration, throughput had a greater effect than screw speed. However, in the case of the 4 Kneading Element configuration, screw speed has a slightly more dominant effect. This indicates that increasing the kneading segment length amplifies the frictional stress resulting from higher screw speeds over higher throughputs.

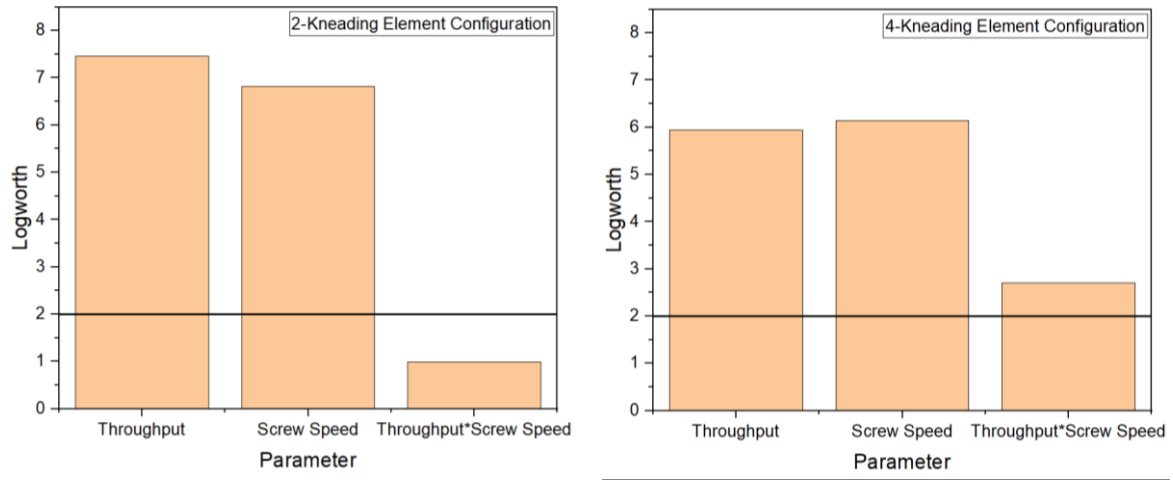

Figure 7.5: ANOVA analysis evaluating significance of process parameters on Temperature Rise. 2 Kneading Element Configuration (Left) and 4 Kneading Element Configuration (Right). A Logworth value of 2 (correlates to a p value of 0.01) is required for a parameter to be classed as significant. Both Throughput and Screw Speed classed as significant parameters in determining Temperature Rise.

The Temperature Rise produced by the chosen process parameters is important because it indicates process stability. Any condition where the Temperature Rise cannot be mitigated will eventually result in the barrel heating up to the point where process failure occurs. Under the evaluated conditions, the process is only stable for the 2-Kneading Element Configuration at low screw speed and throughputs. These stable conditions are shown on Figure 7.4 as the blue highlighted region. While this may indicate that the operating space for this technology is limited, it is worth bearing in mind the limitations of this machine with regards to its cooling capability as mentioned in Section 7.2.2. More modern TSG have cooling jackets which operate over the entire barrel and not just the upper half. They also utilise much more powerful coolants than that used in this study which offer more rapid responses to heat generation within the system. In such a TSG, a far greater Temperature Rise, can be controlled leading to a more expansive operating space than that indicated here.

7.3.2 Granule Size

Figure 7.6 displays the change in granule size with changing screw speed and throughput. The results highlight, that for both screw configurations, granule size tends to increase significantly with increasing throughput. For instance, in the case of the 2 Kneading Element Configuration at a screw speed of 45 rpm, granule size increased from 1.43 mm at 0.1 kg/hr to 2.84 at 0.5 kg/hr. This trend occurs because the higher barrel fill levels at larger throughputs generate greater compaction forces which promotes agglomeration leading to the formation of bigger granules. This notion is strongly established in literature evaluating the wet granulation process in the TSG [89,92,93] and the same reasoning can be applied here for the Dry Twin Screw Granulation..

Meanwhile, no clear trend was observed for the 2 Kneading Element Configuration when looking at the relationship between screw speed and granule size. At the same throughput, the 2 Kneading Element Configuration displayed similar granule sizes regardless of the screw speed as shown by Figure 7.6. Similarly, for the 4 Kneading Element Configuration, there was no significant change in granule size with screw speed at a throughput of 0.1 kg/hr. However, for the 4 Kneading Element Configuration, there appeared to be a trend between screw speed and granule size at throughputs of 0.2 and 0.3 kg/hr. At these high throughputs, increasing screw speed resulted in a decrease in granule size. For example, at a throughput of 0.2 kg/hr, granule size decreases from 2.6 mm at 25 rpm to 1.65 mm at 65 rpm. This reduction in granule size can be attributed to the higher breakage forces at faster screw speeds. The influential effect of screw speed at high throughputs for the 4 Kneading Element Configuration compared with its negligible effect at low throughputs and for the 2 Kneading Element Configuration could be explained by considering the granule sizes formed at these conditions. The granules produced at low throughputs and by the 2 Kneading Element Configuration, are much smaller and therefore less prone to breakage than the large granules produced by the 4 Kneading Element Configuration at high throughputs. This leads to a less pronounced breakage effect on these smaller granules at higher screw speeds which results in a negligible effect on granule size.

The 4 Kneading Element Configuration produced much larger granules than the 2 Kneading Element configuration at the same process conditions. This is because the kneading segment has a poor conveying power. Therefore, increasing the kneading segment length will increase the residence time of material in the kneading segment, promoting agglomeration and resulting in the formation of larger granules [159]. Increasing the kneading segment length also increases the stress on the material, promoting more Maltodextrin to undergo glass transition which leads to the formation of more binding material. Increased binder composition then facilitates the formation of larger granules in a similar manner to the Wet Twin Screw Granulation process [160].

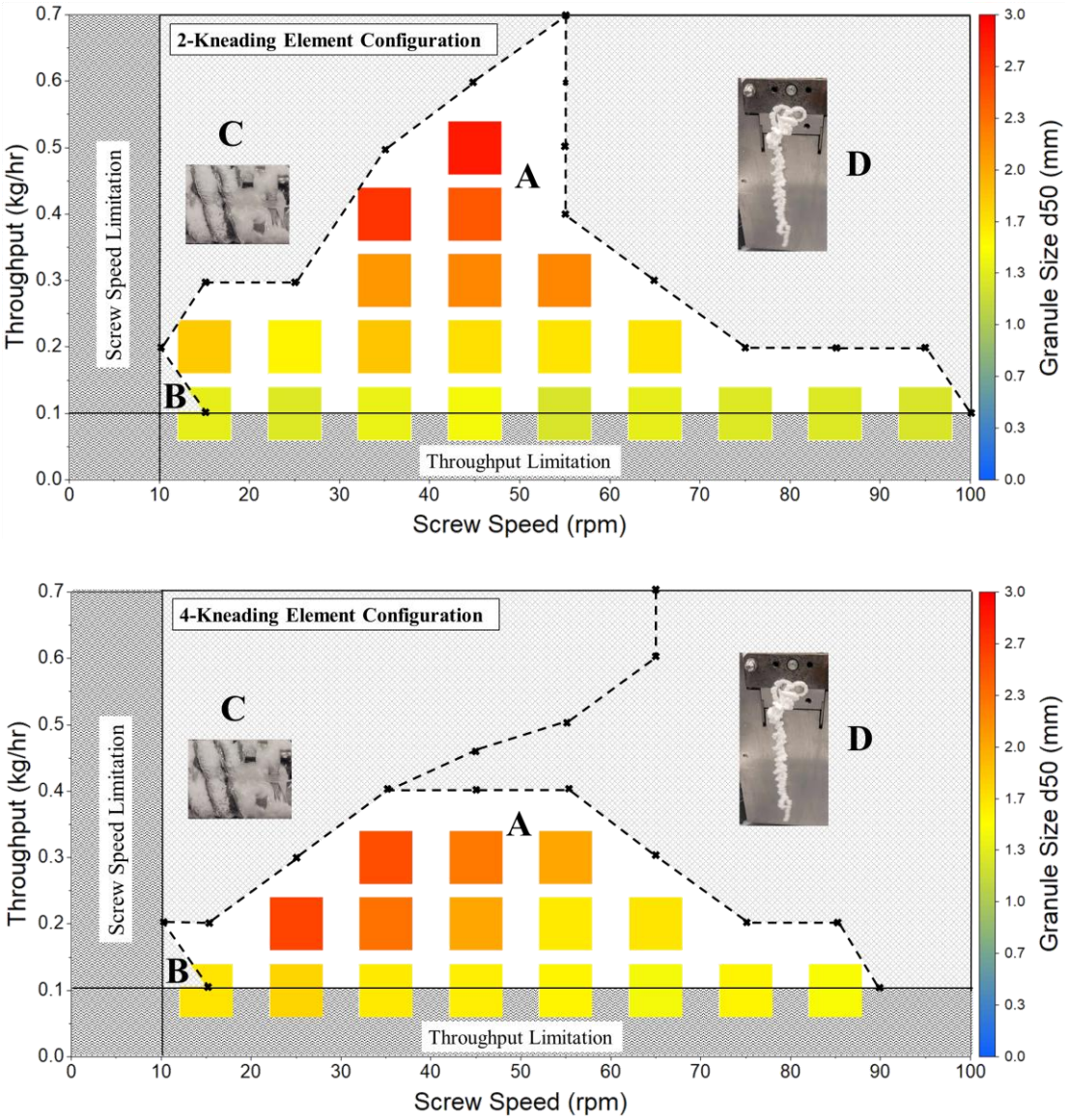

Figure 7.6: Change in Granule Size at varying screw speeds and throughputs. 2 Kneading Element Configuration (Top) and 4 Kneading Element Configuration (Bottom). For both screw configurations, granule size increases with increasing throughput. No significant change in granule size with screw speed is shown for the 2 Kneading Element Configuration. Similarly, for the 4 Kneading Element Configuration, no change in granule size with screw speed is seen at 0.1 kg/hr. However, at 0.2 and 0.3 kg/hr, a trend is observed where granule size decreases with increasing screw speed.

Figure 7.7 presents the ANOVA analysis evaluating the effect of screw speed and throughput on granule size. The results confirmed that when evaluating the 2 Kneading Element Configuration, throughput was the only significant parameter with a Logworth value of 8.92. By comparison the Logworth for Screw Speed and the interaction Throughput*Screw Speed was less than 2 indicating that they were not significant in determining granule size. However, for the 4 Kneading Element Configuration, there is a significant change in the behaviour with all three factors now having a Logworth greater than 2 indicating that they are all significant. Furthermore, in this scenario, screw speed has become an even more influential parameter than throughput as indicated by its higher Logworth value (5.05 compared with 4.29). This growing influence of screw speed as kneading segment length increases is similar to

that seen when evaluating Temperature Rise. This indicates that as the kneading segment lengthens, screw speed becomes significantly more important across a range of process outputs.

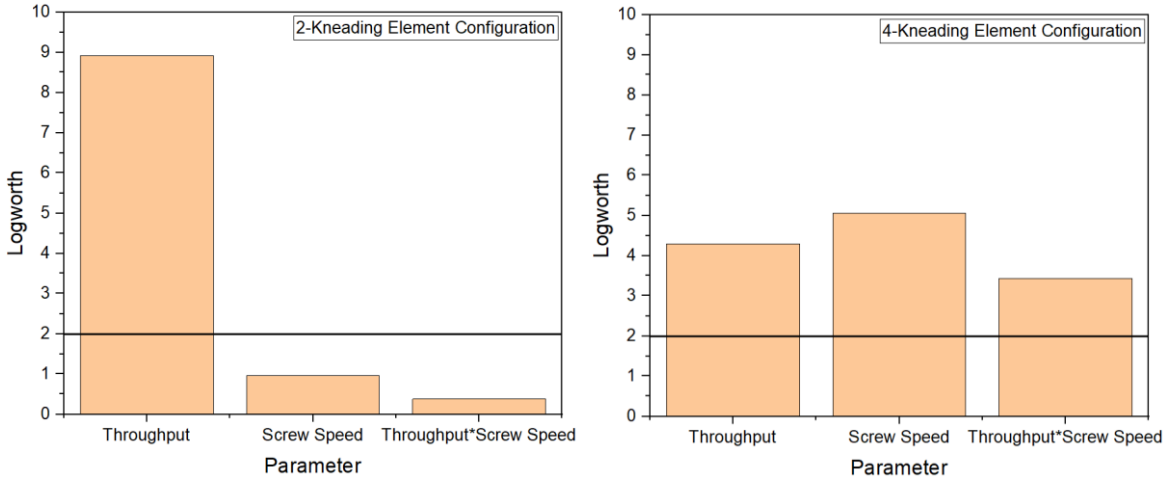

Figure 7.7: ANOVA analysis evaluating significance of the considered parameters on Granule Size. 2 Kneading Element Configuration (Left) and 4 Kneading Element Configuration (Right). A Logworth value of 2 (correlates to a p value of 0.01) is required for a parameter to be classed as significant. Temperature is the only significant parameter for the 2 Kneading Element Configuration. Meanwhile, both temperature and screw speed along with their interaction is classed as significant for the 4 Kneading Element Configuration.

7.3.3 Total Process Yield

The granule faction between 0.5 mm and 4 mm was classed as the Total Yield of the process. Since a high yield indicates a greater proportion of granulated material in the product, total granular yield can also be considered to represent the extent of granulation. Figure 7.8 shows that the Dry Twin Screw Granulation process has a very high Total Yield output across the operating space with the lowest Total Yield being 80% and the highest Total Yield being 95%. This indicates that the Dry Twin Screw Granulation process is capable of achieving a very high extent of granulation. This is important because yield is an indicator of process sustainability. A higher yield results in less material wastage which improves process sustainability.

There is no clear trend between the process Total Yield and either screw speed nor throughput for either screw configuration presented in Figure 7.8. In theory, adjusting these parameters should alter the stress applied to the material. In turn, this should change the extent to which the Maltodextrin undergoes glass transition which changes the proportion of 'binder' in the mix which will then affect the granule yield. Therefore, the negligible impact of these process parameters on granule yield indicates that the DE29 material is very susceptible to undergoing glass transitioning and that very little energy input is required to trigger the transition. This is also implied by how small Region B is in Figure 7.8, which highlights that the operating space where there is a lack of glass transition is extremely narrow. As a result, increasing screw speed or throughput does not significantly promote a greater extent of granulation, as

the material transitions readily even under low stress conditions to produce a high Total Yield granulation process.

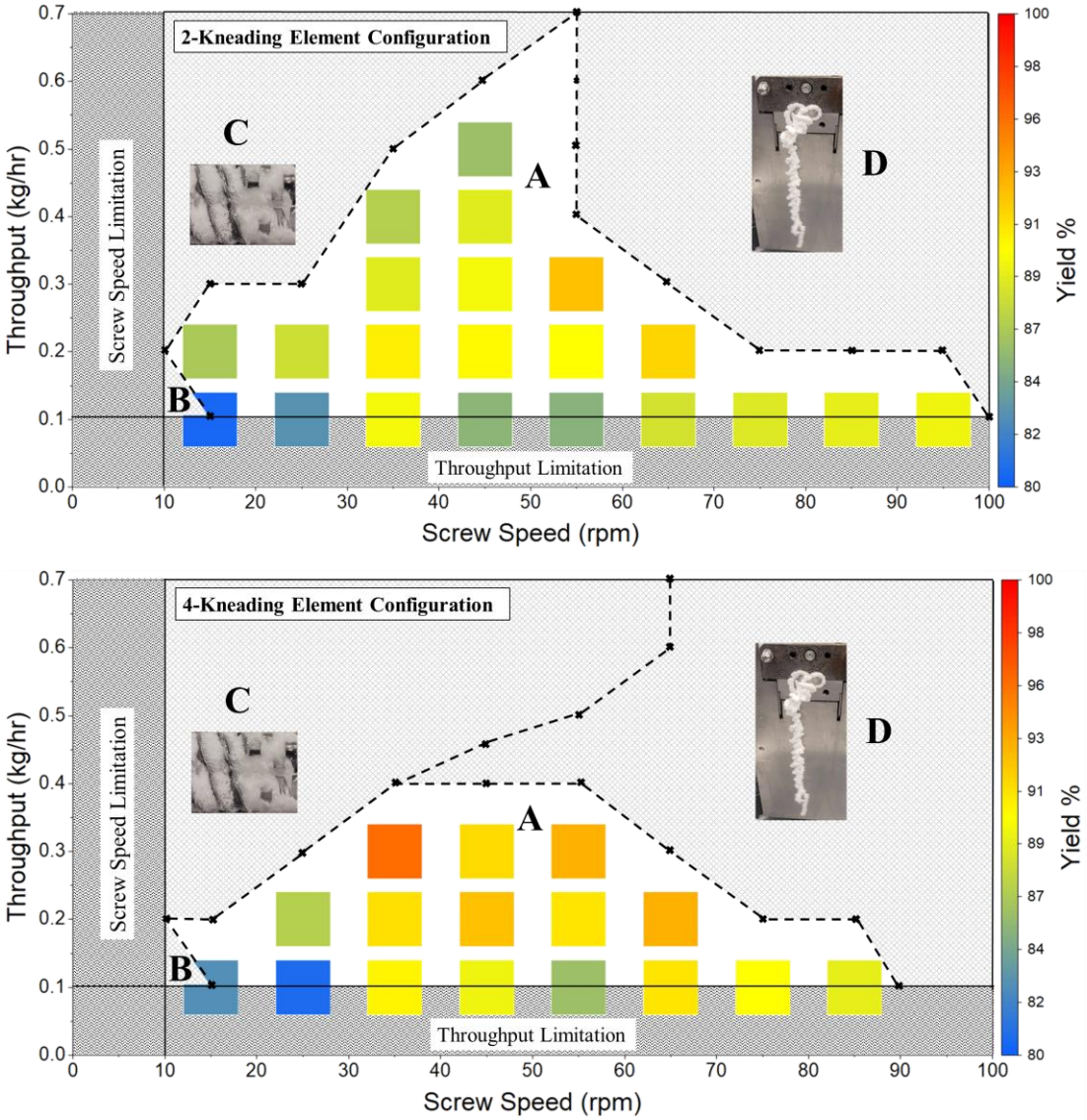

Figure 7.8: Granule Yield (0.5 mm – 4 mm) at varying screw speeds and throughputs. 2 Kneading Element Configuration (Top) and 4 Kneading Element Configuration (Bottom). No significant change in Total Yield is observed with changing Throughput or Screw Speed. This is attributed to the ease at which the DE29 undergoes Glass Transition at low screw speeds and throughputs. Since the material readily undergoes Glass Transition, there is no significant Yield benefit in increasing the energy input into the system by increasing screw speed or throughput.

The ANOVA analysis presented in Figure 7.9 emphasises just how inconsequential throughput and screw speed were when determining process yield for the 2 and 4 Kneading Element Configurations, with neither screw speed and throughput or their interaction, having a Logworth more than 2. The influence of these parameters was far lower for the 4 Kneading Element Configuration compared with the 2 Kneading Element Configuration as indicated by their lower Logworth values. This suggests that increasing the number of kneading elements appears to further reduce the influence of these parameters. However, it must be noted that these conclusions depend on the definition of the yield size class which

is 0.5 – 4 mm here. Both throughput and screw speed are influential in deciding granule size as explained by Section 7.3.2 and therefore, will affect the yield to different extents depending on the yield size classification.

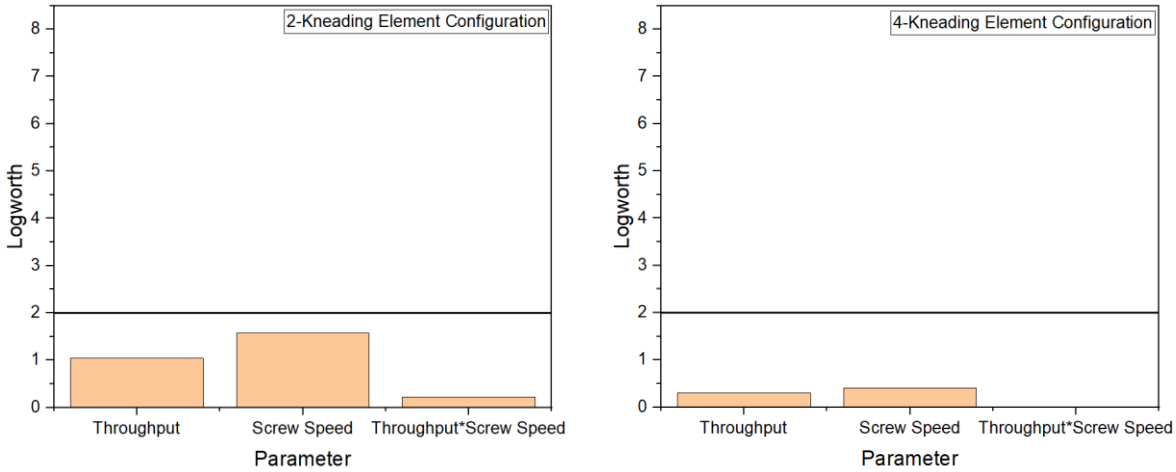

Figure 7.9: ANOVA analysis evaluating significance of the considered parameters on Yield. 2 Kneading Element Configuration (Left) and 4 Kneading Element Configuration (Right). A Logworth value of 2 (correlates to a p value of 0.01) is required for a parameter to be classed as significant. No parameters were found to be significant when considering Total Yield.

7.3.4 Granule Shape

Granule shape is an often overlooked yet crucial granule property because it influences granule flowability. Figure 7.10 presents the change in granule sphericity as a result of changing screw speed and throughput. For the 2 Kneading Element Configuration, increasing throughput causes granule sphericity to increase slightly as shown by Figure 7.10. For example, at 45 rpm, granule sphericity increases from 0.612 at 0.1 kg/hr to 0.68 at 0.5 kg/hr. This is attributed to the greater stresses generated at larger throughputs which result in more of the powder undergoing glass transition. This increases the amount of available binder for granule formation. A greater binder composition makes the mix softer and more pliable meaning it can be molded more easily which could result in a more spherical shape. This has been found to be the case in Wet Twin Screw Granulation. For instance, Dhenge et al [161] found sphericity increased with binder composition. Dhenge et al [161] also found that sphericity increased with throughput which was attributed to the increased shearing force of the barrel on the powder mass at higher throughputs.

Meanwhile, Figure 7.10 also indicates that increasing screw speed results in less spherical granules for the 2 Kneading Element Configuration. For example at 0.1 kg/hr, sphericity decreases from 0.67 at 15 rpm to 0.6 at 95 rpm. This can be explained by considering that at faster screw speeds, material travels through the kneading segment at a faster speed. This can lead to a stretching effect on the granules that are produced, making them more elongated. While there is no reference literature for Dry Twin Screw

Granulation considering granule shape, in the Wet Twin Screw Granulation process, increasing screw speeds has been found to result in more elongated granules due to the greater granule attrition rate at high screw speeds resulting in the formation of shard-like fragments [161].

The trends observed for the 2 Kneading Element Configuration are only observed with the 4 Kneading Element Configuration at low screw speeds (15 - 35 rpm). In this range, increasing throughput causes sphericity to increase, while, increasing screw speed causes sphericity to decrease. Outside of this range (screw speeds greater than 45 rpm), no clear trend is observed with either throughput or screw speed. For example, at a screw speed of 45 rpm, no significant increase in sphericity with throughput was observed. Similarly, at a throughput of 0.2 kg/hr, no decrease in sphericity between screw speeds of 45 and 65 rpm was observed. This lack of correlation between the process parameters and sphericity in this range can be attributed to greater process instability (as discussed in Section 7.3.1) at high screw speeds affecting the results. It could also be that the effect of the kneading segment has become so dominant in this zone that screw speed and throughput have a negligible effect on granule shape.

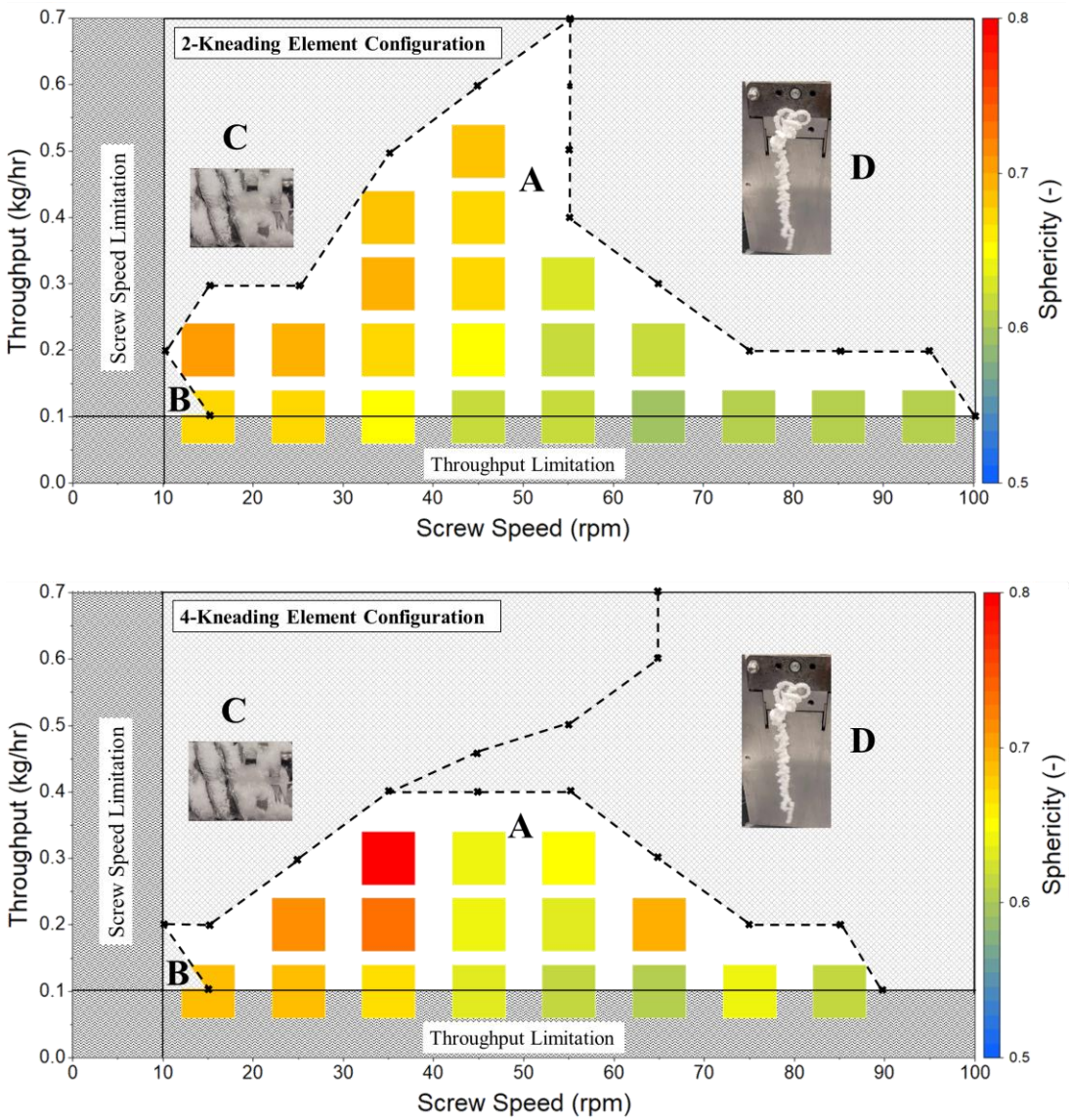

Figure 7.10: Granule Sphericity at varying screw speeds and throughputs. 2 Kneading Element Configuration (Top) and 4 Kneading Element Configuration (Bottom). For the 2 Kneading Element Configuration, granule shape became more spherical at higher throughputs and lower screw speeds. For the 4 Kneading Element Configuration, the same trend is observed at screw speeds between 15 – 35 rpm. Within this range, granule shape becomes more spherical as throughput increases and screw speed decreases. However, for the 4 Kneading Element Configuration, at screw speeds greater than 35 rpm, no trend is seen between process parameters and granule sphericity which is attributed to greater process instability in this region.

The ANOVA analysis, shown in Figure 7.11, highlights that screw speed was the significant parameter in determining granule sphericity, with it being the parameter with the highest Logworth value for both configurations. For the 2 Kneading Element Configuration, the screw speed was found to be the most dominant parameter by far with neither throughput and the interaction being classed as significant. In the case of the 4 Kneading Element Configuration, the increased number of kneading elements decreased the significance of all the parameters considerably. This indicates that the length of the kneading segment itself could be the most dominant parameter.

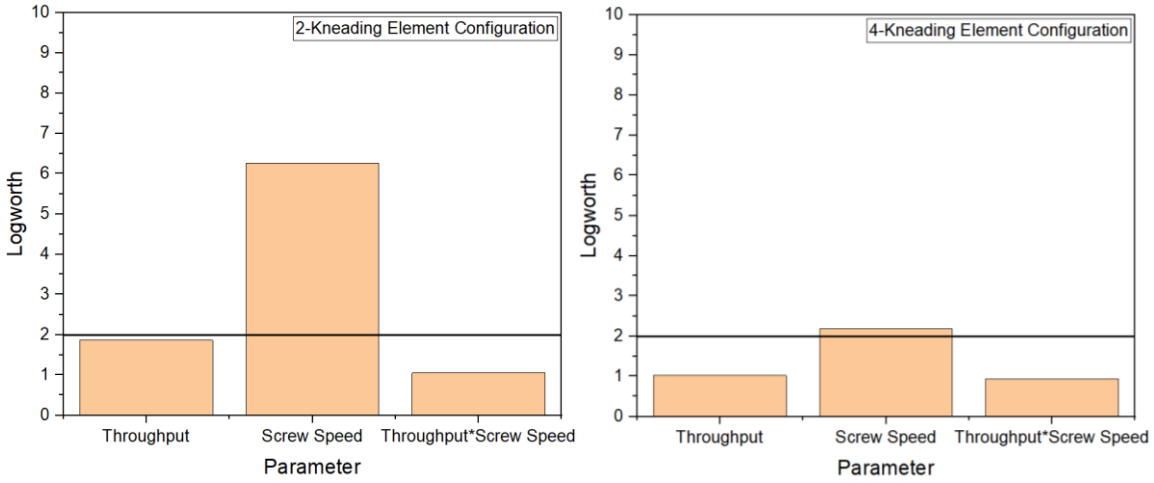

Figure 7.11: ANOVA analysis evaluating significance of the considered parameters on Sphericity. 2 Kneading Element Configuration (Left) and 4 Kneading Element Configuration (Right). A Logworth value of 2 (correlates to a p value of 0.01) is required for a parameter to be classed as significant. Screw Speed was found to be the only significant parameter when determining granule sphericity.

7.3.5 Granule Porosity

Figure 7.12 presents the porosity of the granules produced in the operable region for the two different screw configurations. Meanwhile, Figure 7.13 displays X-RAY scans of granules representing the least and most porous granules that were produced by each screw configuration. As shown by Figure 7.12, for both screw configurations, it is clear that increasing the throughput leads to a decrease in porosity. This can be linked to the increased barrel fill level at higher throughputs resulting in more compaction of the granules. This increased compaction squashes pores and leads to a reduced porosity. Furthermore, at higher throughputs, greater stresses and more frictional heat is generated which facilitates a greater extent of glass transition. This leads to the DE29 softening more and produces more deformable granules. The increased deformation means that they undergo consolidation more easily which produces less porous agglomerates.

For the 2 Kneading Element Configuration, two behaviours are evidenced depending on the throughput. The first behaviour is observed at a throughput of 0.1 kg/hr. At a throughput of 0.1 kg/hr, as screw speed is initially increased from 15 to 45 rpm, granule porosity slightly increases from 10.5% to 12.9%. This can be attributed to the decreased barrel fill level at higher screw speeds resulting in less granule compaction and therefore the production of more porous granules. Faster screw speeds may also result in a greater stretching effect on the granules passing through the kneading segment, which enlarges pores within the granule structure. However, at this throughput of 0.1 kg/hr, there is a limited effect of screw speed on granule porosity at screw speeds greater than 45 rpm, with porosity remaining constant around ~12.5%. Meanwhile, the 2 Kneading Element Configuration displays a different behaviour at throughputs of 0.2 – 0.5 kg/hr. At these throughputs, granule porosity appears to decrease with

increasing screw speed as best displayed by the 0.2 kg/hr condition which shows porosity decreasing from 9.4% to 7.2% as screw speed is increased from 15 rpm to 65 rpm. This differing behaviour could be explained by considering that at high throughputs, the effect of decreasing barrel fill level with screw speed is not as significant. Instead in this case, granule porosity could decrease due to the increase in energy input and applied stress with increasing screw speed acting to compact the granules to a greater extent.

The 4 Kneading Element Configuration showed a similar relationship between screw speed and granule porosity to the 2 Kneading Element Configuration, at a throughput of 0.1 kg/hr. At this throughput, granule porosity once again increased (from 6.1% to 9.6%) as screw speed was increased from 15 rpm to 45 rpm. Beyond this 45 rpm threshold, no significant change in granule porosity was seen with increasing screw speed, with granule porosity remaining stable around ~9.5%. Whereas for the 2 Kneading Element Configuration, higher throughputs (≥ 0.2 kg/hr) led to granule porosity decreasing with increasing screw speed, the 4 Kneading Element configuration showed no significant change in granule porosity at throughputs of 0.2 – 0.3 kg/hr. This can be attributed to the highly dense nature of the granules at these conditions making further reductions in porosity extremely unlikely.

Comparing the 2 Kneading and 4 Kneading Element configurations, it is evident that the increased number of kneading elements resulted in the production of denser granules for the 4 Kneading Element configuration. This can be attributed to the increased compaction force exerted by the kneading segment as more kneading elements are added. Overall, the Dry Twin Screw Granulation process for DE29 seems to produce very dense granules with porosities between 5 – 13%, which is far denser than those produced by the established technologies in Chapter 4. This is linked to the ease at which DE29 undergoes glass transition in this process as discussed previously. This ease means that the majority of the mix would have entered the viscous state where it deformed easily. This high deformability combined with the high stresses applied by the kneading segment resulted in the formation of a highly dense granular product.

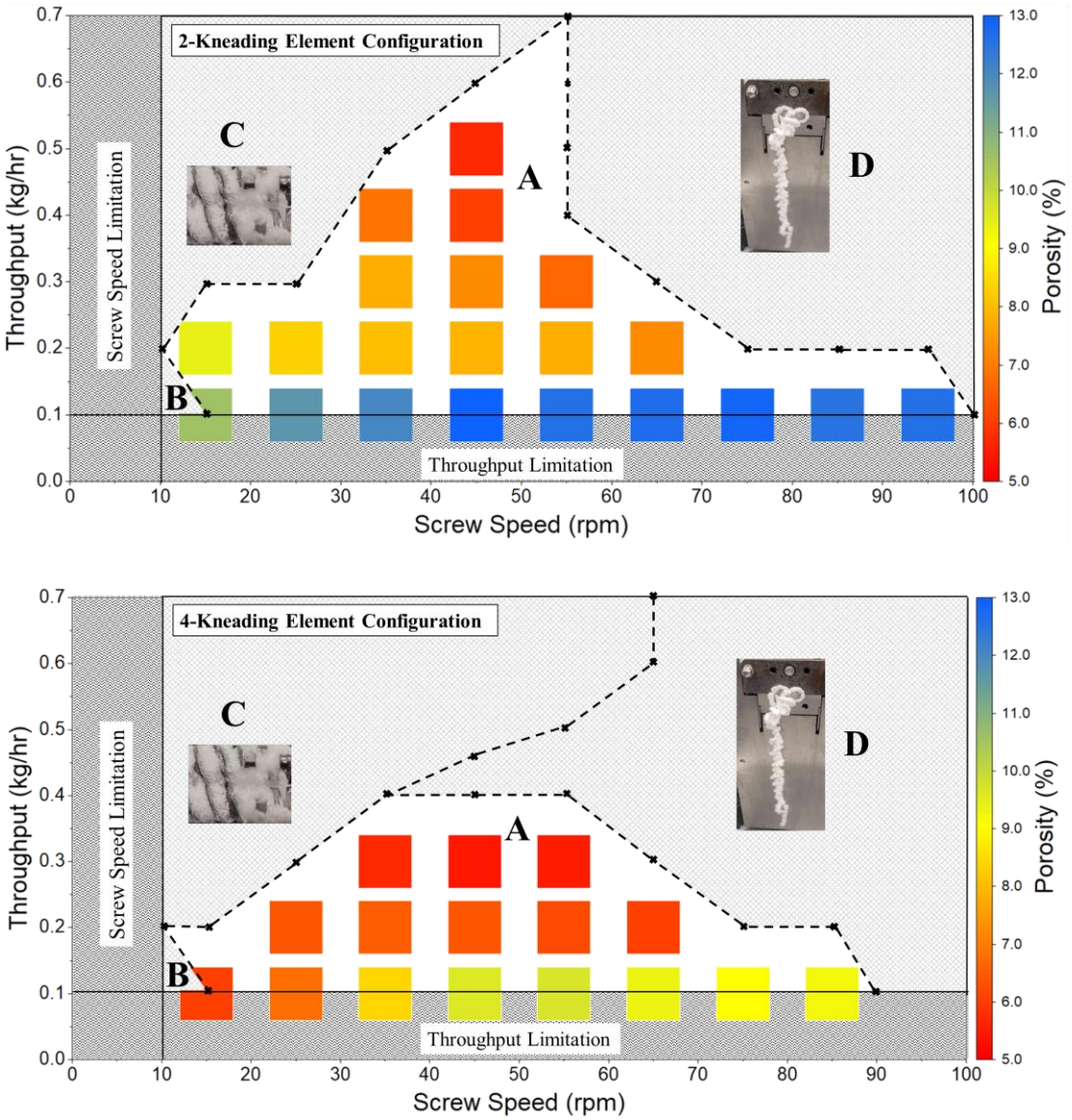

Figure 7.12: Granule Porosity at varying screw speeds and throughputs. 2 Kneading Element Configuration (Top) and 4 Kneading Element Configuration (Bottom). Increasing Throughput resulted in a decrease in porosity for both screw configurations. For the 2 Kneading Element Configuration, at a Throughput of 0.1 kg/hr, granule porosity increases with increasing screw speed between 15 – 45 rpm. However, at 0.1 kg/hr, little change in porosity is seen at screw speeds higher than 45 rpm. For the 2 Kneading Element Configuration, at Throughputs of 0.2 kg/hr and higher, increasing screw speed appears to decrease granule porosity. The 4 Kneading Element configuration displayed the same behaviour as the 2 Kneading Element Configuration at a Throughput of 0.1 kg/hr, where granule porosity initially increased with increasing screw speed before plateauing at screw speeds greater than 45 rpm. At Throughputs of 0.2 and 0.3 kg/hr, the 4 Kneading Element Configuration showed no change in porosity with changing screw speed.

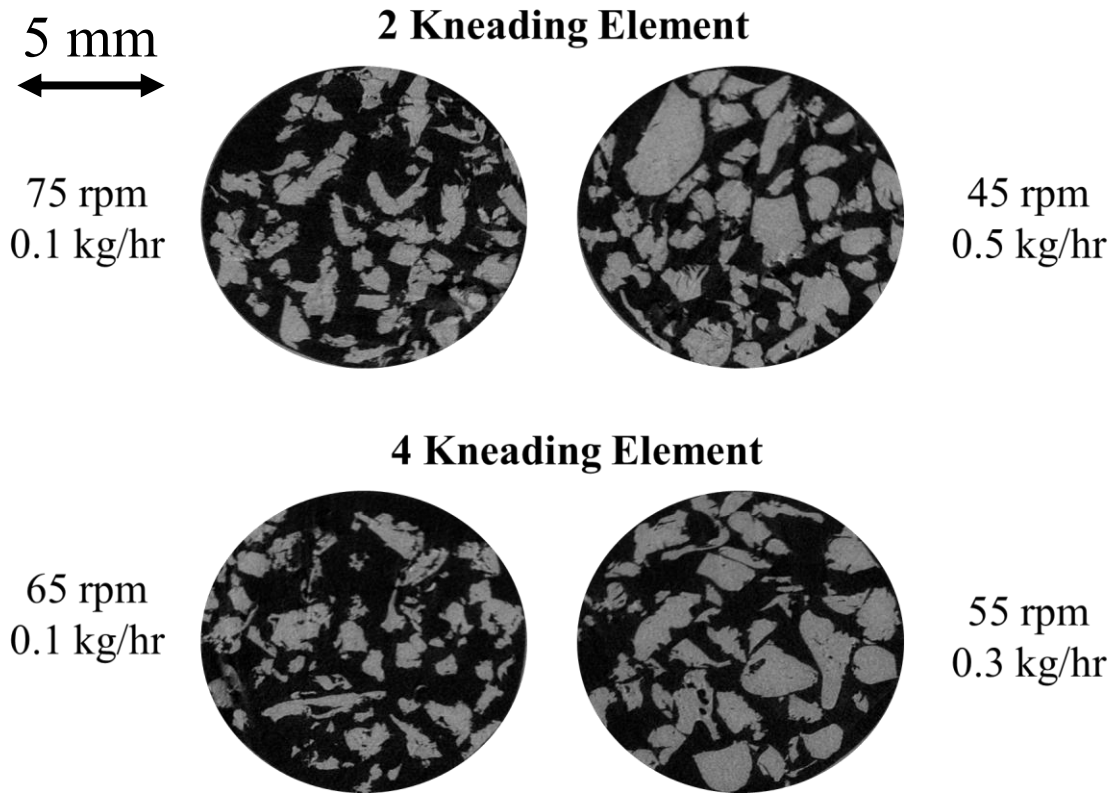

Figure 7.13: X-Ray images of granules from the process conditions that resulted in the most porous (left) and least porous granules (right) for each screw configuration

The ANOVA analysis shown in Figure 7.14 indicates that Throughput is the only statistically significant parameter when determining Porosity. This is shown by the Logworth parameter representing Throughput being 6.69 and 4.47 for the 2 and 4 Kneading Element configurations respectively. This is far more than the minimum required value of 2. Meanwhile, Screw Speed and the interaction Throughput*Screw Speed was not considered significant by the ANOVA analysis.

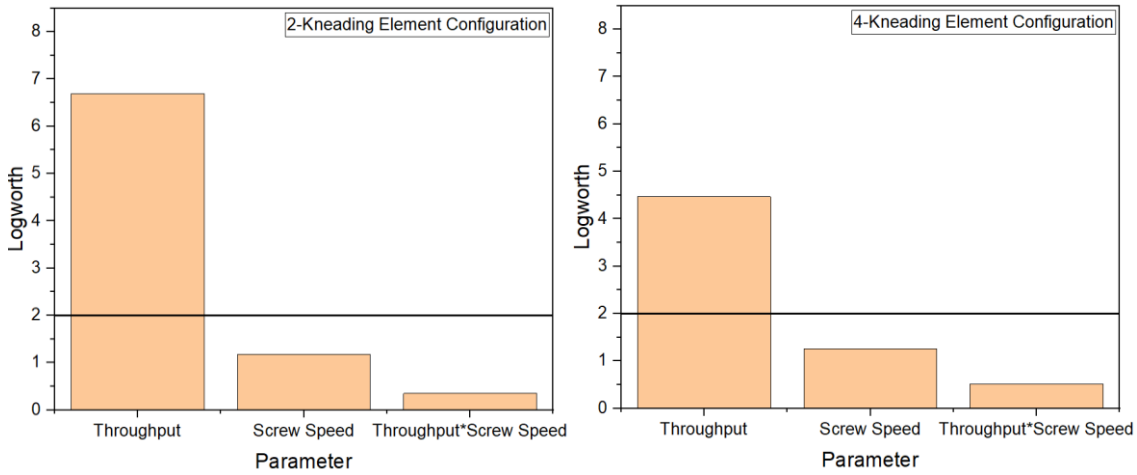

Figure 7.14: ANOVA analysis evaluating significance of the considered parameters on Porosity. 2 Kneading Element Configuration (Left) and 4 Kneading Element Configuration (Right). A Logworth value of 2 (correlates to a p value of 0.01) is required for a parameter to be classed as significant. Throughput was classed as the only significant parameter effecting granule porosity.

7.3.6 Regime Map Development

There is currently no existing regime map for the dry granulation process in the Twin Screw Granulator. The development of a regime map would be a novel contribution to the field which will facilitate better process understanding and transferability of process knowledge. Currently, this work has identified four possible behavioural regions for the granulation process: Operable Region (A), Insufficient Stress Region (B), Barrel Blocking Region (C) and Extrusion Region (D). These are similar to the Production, Blocked and Extrudate regions identified by Tu et al [47] when developing a TSG Wet Granulation Regime Map. The regions have been characterised by screw speed and throughput so far in this study. However, that limits their future usefulness to the same ThermoFisher Euro Lab 16 mm Twin Screw used here. To broaden the applicability of the work, the Regime Map will characterise the possible granulation behaviours according to Barrel Fill Level and Peak Shear Rate. These were chosen because the dry granulation process is driven by the stresses generated by the kneading elements. Of these stresses, the dominant ones are the compaction stress and the shear stress. The compaction stress is dependent on the Barrel Fill Level which is a function of the powder throughput and screw speed as outlined in Section 7.2.7. Meanwhile, the Peak Shear Rate has been used to represent the shear stress. This Peak Shear Rate depends on the screw speed used and is calculated according to Equation 7.2. The produced regime maps for each screw configuration are presented in Figure 7.15. Peak Shear Rates less than 40 s^{-1} were not possible as this corresponded to the Peak Shear Rate developed at the minimum screw speed of 10 rpm. The shaded area at the base of each map represents the range of Barrel Fill Levels that could not be evaluated due to the throughput limitation (with throughputs less than 0.1 kg/hr not possible) for the machine. The Operable Region (A) has been characterised by the Temperature Rise factor as this is the most relevant to explain process behaviour for the Dry Twin Screw Granulator.

7.3.6.1 Operable Region (A)

The operable region presented in Figure 7.15 indicates the regions where glass transition of the DE29 powder could be achieved in a controlled manner for long enough that granules could be produced. It exists in the middle of the regime map and is bordered by all the other regimes. It occurs at Barrel Fill Levels and Peak Shear Rates that are high enough to initiate glass transition but not too high to result in barrel jamming or extrusion. This region generally has a sloping shape at the bottom (lower limit). This is because both the compaction stress (represented by Barrel Fill Level) and shear stress (represented by the Peak Shear Rate) contribute towards initiating the glass transition process. Therefore, as Peak Shear Rate increases, the minimum possible Barrel Fill Level required to generate sufficient total stress to facilitate granulation also decreases. This leads to the sloping curve at the bottom of Region A. Meanwhile, the sloping curve at the top of Region A exists because the maximum possible Barrel Fill Level tolerated in the operable region also decreases as the Peak Shear Rate increases. This is because more glass transitioning at higher Peak Shear Rates result in the production

of more sticky, viscous DE29 which makes Barrel Blocking more likely. To prevent Barrel Blocking and keep the mix in the Operable Region, the Barrel Fill Level has to decrease to lower the stress on the material as Peak Shear Rate increases.

The area of the operable region was greatest when looking at the 2 Kneading Element Configuration. This is because the 2 Kneading Element Configuration results in less stress being applied at a given Barrel Fill Level and Peak Shear Rate compared to the 4 Kneading Element Configuration. The 2 Kneading Element Configuration also facilitates better flowability of material through the kneading segment compared to the 4 Kneading Element Configuration. This meant far greater Barrel Fill Levels and Peak Shear Rates could be tolerated in the process without the behaviour being pushed into the Extrusion (where excess stress is applied on the material) and Barrel Blocking (where the material cannot flow through the kneading segment) regions.

Also within this region, there were instabilities arising from the Temperature Rise in the granulation compartment (C6) during the course of the run. The Temperature Rise occurred because the TSG design meant that the cooling water used to maintain the cooling jacket could only be fed into the top half of the barrel as outlined in Section 7.2.2. This led to an inefficient cooling process within the compartment. Since the frictional heat generated by the granulation process was significant, the inefficient cooling process meant that the compartment temperature would increase over time. Eventually the compartment temperature would reach the point where excessive glass transition would occur resulting in process failure. Therefore, the size of the operable region depends on the rate of heat generation in the system and the cooling capability of the TSG. Systems that generate less friction and cool better are expected to have larger operable regions.

7.3.6.2 Insufficient Stress Region (B)

During the process, the powder experiences both compaction stresses and shear stresses as they pass through the kneading segment. In the Insufficient Stress region presented in Figure 7.15, the Barrel Fill Level and/or the Peak Shear Rate is too low which results in a weak compaction and shear stress. This means the total stress applied on the powder is insufficient to induce the glass transition process. Without this key phenomenon occurring, no viscous DE29 is formed to act as binder, and the product is ungranulated fine powder.

For both screw configurations, the insufficient stress region is relatively small which is reflective of how easily the DE29 powder glass transitions under the evaluated conditions. It is expected that the granulation of a powder with a higher T_g would result in this region becoming significantly bigger as more aggressive mixing conditions would be needed to provide the necessary energy input to induce the material to undergo glass transition.

7.3.6.3 Barrel Blocking (C)

The kneading elements display a poor flowability through them, especially compared to the conveying elements [43]. This leads to significant material buildup in this segment which must be overcome by the screw motor. If the selected screw speed is too low and the material throughput too high, then this will lead to a high Barrel Fill Level which results in a low conveying power in the kneading segment. At a certain Barrel Fill Level, the torque required to convey the material becomes greater than the motor's safety threshold. At this point, the motor will shut down to protect the drive system and the barrel is classed as blocked. Region C represents the conditions where this scenario is realised, and barrel blocking occurs.

The Barrel Blocking region is in the top left of the map for both screw configurations as shown by Figure 7.15. It occurs at high Barrel Fill Levels and low Peak Shear Rates. As the Peak Shear Rate increases, the Barrel Fill Level required for Barrel Blocking to occur decreases. This can be attributed to the increased shear stress at higher Peak Shear Rates causing more of the material to undergo glass transition. This produces a stickier, more viscous flow of DE6, which resists the motion of the screws and increases the likelihood of the screw motor's torque safety threshold being breached. The Barrel Fill Level at which Barrel Blocking occurs is much lower for the 4 Kneading Element configuration compared to the 2 Kneading Element Configuration. This can be attributed to the decreased transportability of the kneading segment as more elements are added which result in higher torques being generated at lower Barrel Fill Levels resulting in Barrel Blocking.

7.3.6.4 Extrusion (D)

During a standard Twin Screw extrusion process, the application of compaction stress and high thermal energy converts the dry powder into a molten flow. This molten flow is then forced through a die plate to shape it into a continuous strand of material [162]. Similarly to the extrusion process, in Region D, the stresses applied on the material are very high resulting in a lot of energy being applied on the powder. This results in the formation of a continuous flow of Maltodextrin 'vines' rather than a discrete granular product. The region is located at the top right of the regime map where the Peak Shear Rate is high. At such high Peak Shear Rates, the powder is in a very soft state having undergone excessive glass transition. This makes it less viscous and allows it to flow better preventing barrel blocking from occurring. This region is comparable to the TSG Wet Granulation extrudate region presented by Tu et al [47] which occurred because excess water had been added to the mixture. This saturated the mixture and caused it to soften to the extent that it formed a paste. Comparatively, for the dry granulation process, it is the excess application of thermal energy that is driving this softening.

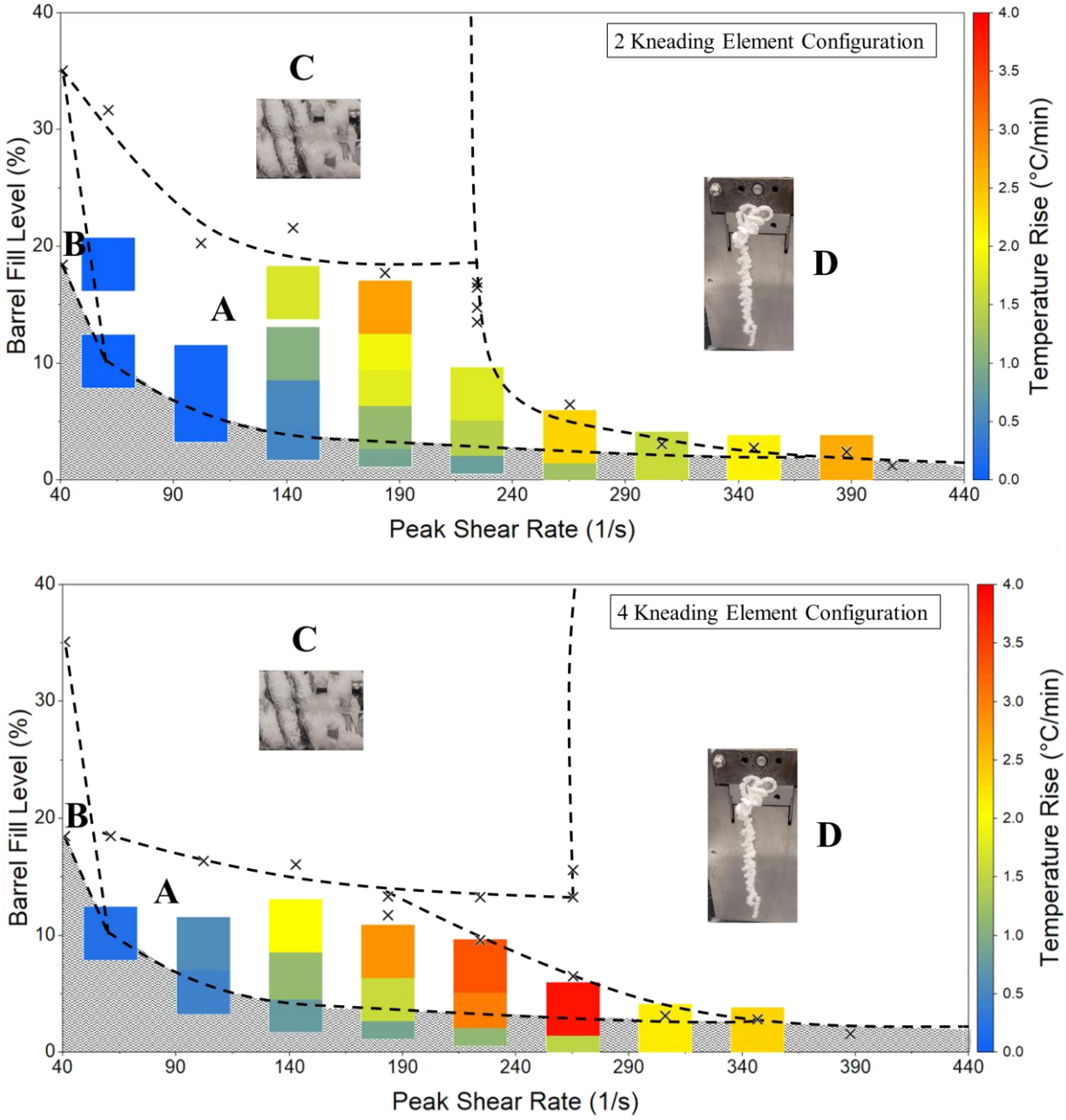

Figure 7.15: Process Regime Map for the 2 Kneading Element Configuration (Top) and the 4 Kneading Element Configuration (Bottom). The map classified the four possible regions depending on Barrel Fill Level and Peak Shear Rate. The possible regions include: Operable Region (A), Insufficient Stress Region (B), Barrel Blocking (C) and Extrusion (D). Peak Shear rates less than 40 s^{-1} could not be evaluated because this corresponds to the Peak Shear Rate generated at the lowest possible screw speed (10 rpm). The shaded region indicates the range of Barrel Fill Levels that could not be evaluated due to the minimum possible throughput being 0.1 kg/hr.

7.4 Comparison with existing technologies

The study so far has evaluated the feasibility of a dry granulation process in the Twin Screw Granulator and established key process understanding for it through the development of the first dry granulation regime map for the TSG. This section will discuss the sustainability of the process when compared to the mainstream granulation technologies. This will be done by comparing the process efficiencies with

regards to material, energy and time, with that of the established granulation technologies evaluated in Chapter 4. The stable region highlighted by the blue border in Figure 7.4 was chosen to represent the dry granulation technology for this comparison study.

7.4.1 Material Efficiency

Yield is the key indicator of material efficiency with a higher yield representing a more sustainable process with less waste. As with Chapter 4, the yield of granules between 0.5 mm and 2 mm was used to compare the material efficiency of the Dry Twin Screw Granulation process to its counterparts. Results are presented in Figure 7.16, which highlights the superior In-Spec Yield of the Dry Twin Screw Granulation process when compared to Wet Twin Screw Granulation. Dry Twin Screw Granulation also proved to be very competitive with both the Roller Compaction process and the High Shear Granulation process when comparing peak yield for each technology. However, it was not as material efficient as the Fluidised Bed Granulation process, with the Fluidised Bed Granulation process having a peak yield of 79% while for the dry Twin Screw Granulation process it was 63%.

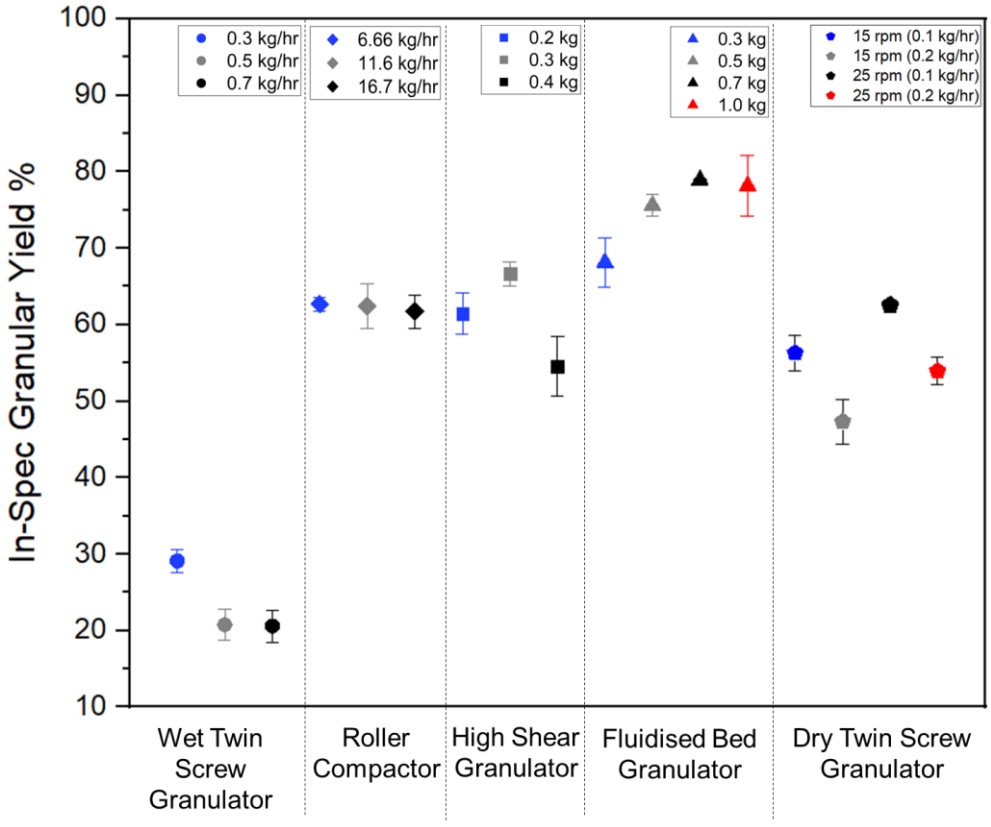

Figure 7.16: Comparing the material efficiency of the Dry Twin Screw Granulation Process with the established granulation technologies. The criteria for evaluating material efficiency is the granule yield between 0.5 mm and 2 mm (as in Chapter 4). The Dry TSG process proved to be far more material efficient than the wet TSG process. The Dry TSG process also had a comparable optimum yield (63%) to the Roller Compactor (63%) and High Shear Granulator (67%).

7.4.2 Energy Efficiency

Specific Energy (kWh/kg) is the indicator by which this thesis evaluated energy efficiency with lower Specific Energy's indicating a more energy efficient process. It is important that processes are made as energy efficient as possible to reduce carbon emissions and reduce costs. As shown in Chapter 4, the drying step is the major energy consumer in a wet granulation process. Since the Dry Twin Screw Granulation process eliminated the need for this step, it was expected to be highly energy efficient. However, the comparison between the Specific Energy of the Dry Twin Screw Granulation process with the other technologies, as shown in Figure 7.17, indicates that this process has one of the worst energy efficiencies as highlighted by its high Specific Energy. In fact, it is only better (when comparing the lowest Specific Energy achieved by each technology) than the Wet Twin Screw Granulation process which had the worst efficiency from the technologies evaluated in Chapter 4. This is mainly due to the low throughput of the Dry Twin Screw Granulation process. For example, the largest stable throughput possible in the dry TSG process was 0.2 kg/hr. Comparatively, in the Wet Twin Screw Granulation process it was 0.7 kg/hr. The contrast was even more extreme when considering the Roller Compactor, which was able to handle throughputs up to 16.7 kg/hr. This meant that even though the Dry Twin Screw Granulation process produced a high yield and consumed little energy, the overall mass of granules produced was much lower compared to the established technologies resulting in the high Specific Energy. However, the results shown in Figure 7.17, indicate that increasing throughput results in big improvements in energy efficiency. For instance, at 15 rpm, the specific energy decreased from 15.1 kWh/kg to 9.1 kWh/kg as throughput was increased from 0.1 kg/hr to 0.2 kg/hr. This corresponds to a 40% decrease in the Specific Energy. Much higher throughputs than 0.2 kg/hr are possible in the Dry Twin Screw Granulator if higher screw speeds are used to lower the Barrel Fill Level and prevent Barrel Blocking. Currently the limiting factor preventing the use of higher throughputs and higher screw speeds is that the cooling system cannot mitigate the temperature rise exhibited at these process parameters. If the cooling system could be improved to enable the use of higher throughputs, then according to the trends seen in Figure 7.17, even further decreases in Specific Energy would be possible. This would increase the energy efficiency of the dry TSG process to make it as attractive as the other technologies.

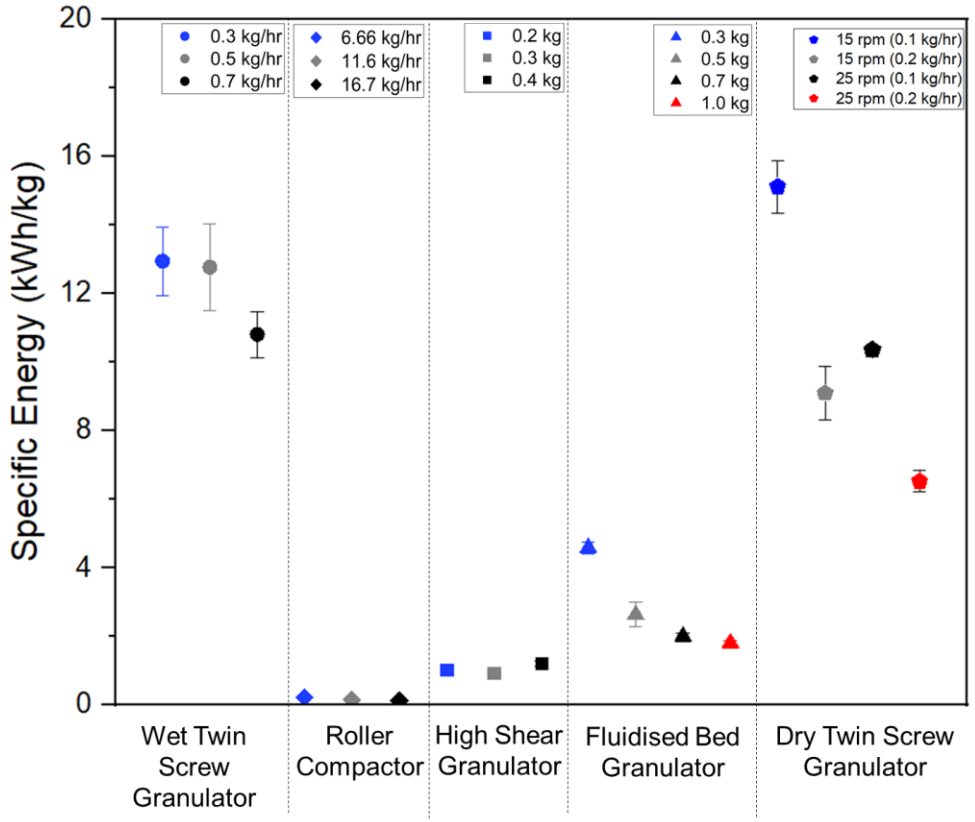

Figure 7.17: Comparing the Specific Energy of the Dry Twin Screw Granulation Process with the established granulation technologies. The Dry TSG displays a high Specific Energy and a poor energy efficiency compared to the other technologies. This is attributed to the low stable throughput of the process which results in a far smaller mass of granules being produced compared to the other technologies leading to a higher Specific Energy. However, the Dry TSG displays rapid decreases in its Specific Energy with increasing throughput from 0.1 to 0.2 kg/hr at both 15 and 25 rpm. This indicates that this process has the potential to reach very low Specific Energy's if the process is run with a more capable cooling system facilitating the running of greater stable throughputs.

7.4.3 Time Efficiency

Finally, Specific Time was used to evaluate the time efficiency of the process with lower Specific Time's indicating a more time efficient process. A lower Specific Time means production facilities can produce more quickly, reducing operating and labour costs. Figure 7.18 shows that the Dry Twin Screw Granulation process is competitive with the Wet Twin Screw Granulation process with regards to Specific Time when looking at the most time efficient condition (25 rpm and 0.2 kg/hr for Dry TSG compared with 0.7 kg/hr for Wet TSG). This is despite the Dry TSG operating at far lower throughputs and therefore producing far less granules than the wet TSG. Similar to the Roller Compaction pathway, this is because the Dry Twin Screw Granulation pathway involves continuous production where only one unit (the granulator itself) is involved in the transition of dry powder to dry granule. Whereas the Wet Twin Screw Granulation pathway requires a drying stage which increases the total process run time. However, the process was not as time efficient as High Shear Granulation, Fluidised Bed Granulation or Roller Compaction. Similarly, to the discussion regarding Specific Energy, this was because these granulators can handle substantially higher throughputs than the Dry Twin Screw Granulation process.

However, like with Specific Energy, the Dry Twin Screw Granulation process displays a sharp decrease in Specific Time (indicating a significant increase in time efficiency) with increasing throughput. At a screw speed of 15 rpm, the specific time decreased from 17.5 hours/kg at 0.1 kg/hr to 9.8 hours/kg at 0.2 kg/hr – a 44% decrease. Improvements to the cooling system to facilitate the use of larger throughputs will lead to further improvements in the time efficiency which will make this technology far more competitive with the other established granulators.

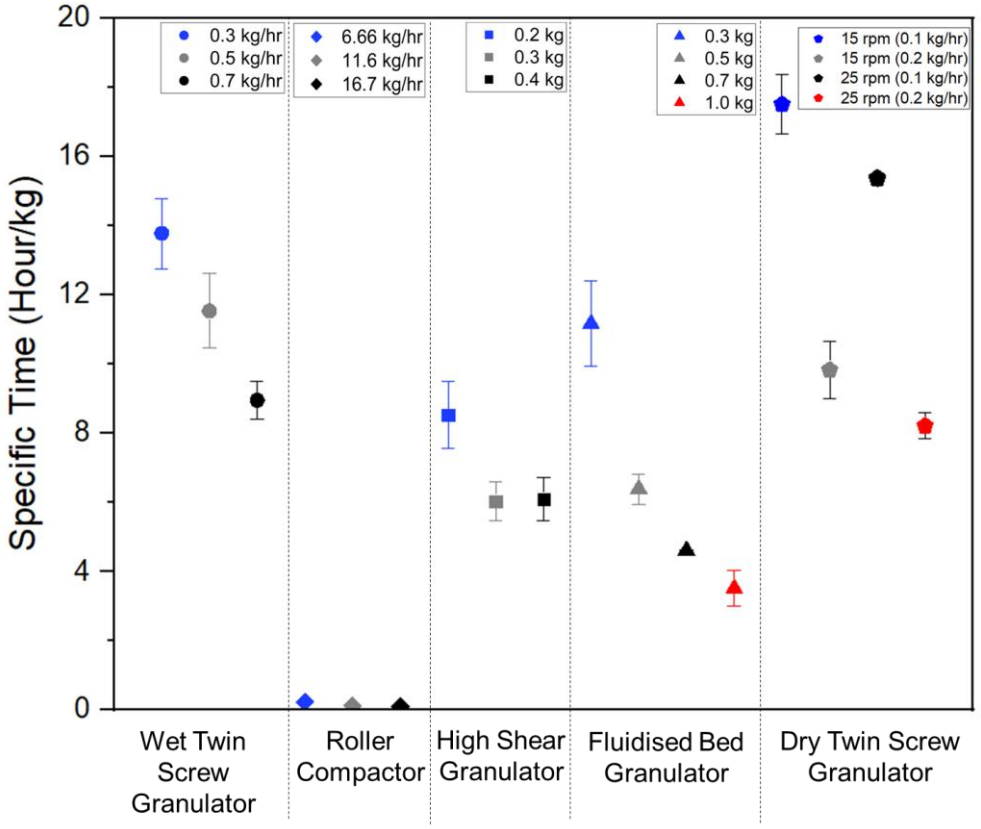

Figure 7.18 Comparing the Time Efficiency of the Dry Twin Screw Granulation Process with the established granulation technologies. The Dry TSG process proved to be competitive with the wet TSG process but was not as time efficient as the remaining granulators. However, as was the case with Specific Energy, increasing Throughput from 0.1 to 0.2 kg/hr at 15 and 25 rpm, resulted in significant reductions in the Specific Time. Once again, this indicates that Dry TSG has the potential to reach very low Specific Time's if the process is run with a more capable cooling system facilitating the running of greater stable throughputs.

7.5 Conclusion

This study has evaluated the feasibility of a dry granulation process in the Twin Screw Granulator for amorphous powder using DE29 as the model material. The process has been found to be feasible with the kneading elements capable of inducing glass transition of the powder leading to agglomeration in the absence of a liquid binder. The region where the process is completely stable is currently constrained to low throughputs and low screw speeds with the major limitation being the limited capabilities of the cooling system available. This knowledge along with modes of failure have been captured in the process

regime maps for each screw configuration. These regime maps will help further develop process understanding of this new technology. The Dry Twin Screw Granulation technology has been compared with the established granulation technologies based on material, energy and time efficiency. While competitive with some of the established granulation technologies, this process is not dominant in any category and still requires further research and development in order to maximise its potential. The key to achieving this dominancy is the use of higher throughputs and screw speeds while keeping the process stable. The use of a high performance cooling system is highly advised for future work to achieve this.

The Dry Twin Screw Granulation process has been found to meet the criteria required for an amorphous powder granulation technology for the future which was mentioned in Section 7.1. It is capable of producing a very high yield (upwards of 90% for granules between 0.5 mm and 4 mm) and it offers continuous operation. The elimination of water from the process has reduced process complexity by reducing the number of key process parameters. It also removes the need for a drying step which will enable the process to achieve high energy efficiencies. This technology warrants greater consideration as a manufacturing route for amorphous powders as food manufacturers aim to make food production cheaper and more sustainable.

8 Conclusion and Future Work

This thesis has focused on enhancing sustainability within the field of granulation. Various avenues have been explored in order to achieve this. These avenues include evaluating the sustainability of existing granulation techniques, identifying optimum operable zones to avoid caking related material loss during production, enhancing granule shelf life during storage and the exploration of energy efficient granulation technologies for the future. The subsequent sections will conclude each research objective stated in the thesis aims and suggest potential future work for each.

8.1 Understanding the sustainability of existing granulation technologies

The first aim of this thesis was to investigate the competing sustainability's of the prominent granulation technologies to identify candidate technologies with a high sustainability. This was successfully achieved in Chapter 4 of this thesis with process sustainability evaluated by considering material efficiency, energy efficiency and time efficiency. Overall, Roller Compaction was found to be a highly sustainable technology, with it possessing the best energy and time efficiency. This work also aimed to identify critical factors that contribute towards determining sustainability. The drying step and mode of operation were two such critical parameters. The drying step was found to be very energy intensive and contributed towards wet granulation technologies being characterized by a higher Specific Energy. Meanwhile, a continuous mode of operation greatly enhanced the time efficiency of a process compared to batch operation. The elimination of the drying step and the continuous mode of operation is what resulted in the high sustainability nature of the Roller Compactor. Of the wet granulation units, the High Shear Granulator was found to be the most energy efficient. Chapter 4 also highlighted the wide range of granule characteristics possible depending on the selected processing route. This was done to emphasize the need to consider granule suitability as well as process sustainability when deciding the optimum manufacturing route. Notably, this study represents the first comprehensive comparison of the sustainability of different granulation technologies, underscoring its novelty and significance in the field.

Chapter 4 evaluated process sustainability of the main granulation technologies using DE29 which was a very moisture and heat sensitive powder. This meant that during the optimisation stage, aggressive processing conditions had to be avoided to prevent caking. For example, in the Twin Screw Granulator, kneading elements were not compatible with DE29 as it led to caking. This meant the Twin Screw Granulator produced a very low yield and performed very poorly in the sustainability metrics. If a less sensitive powder had been used, then perhaps kneading elements could have been included which would have resulted in higher yield and may have changed the sustainability of the Twin Screw Granulator considerably. This makes the results of Chapter 4 only applicable for highly sensitive materials like DE29. Future work could look at evaluating the sustainability of the granulation technologies with

powders of varying sensitivity. Sensitivity can be classified according to the powder's Glass Transition Temperature. This will enable the development of a model where food manufacturers can accurately determine the likely sustainability of different processing routes depending on the sensitivity of the powder they are using.

Future work could also investigate how sustainability metrics change during process scale-up. As a granulator is scaled up, its maximum throughput/batch size increase, leading to substantial changes in the mass of material that can be produced as a technology transitions from laboratory to industrial scale. At the same time, increasing the size of a granulator also raises the energy required for operation. Given the distinct operating mechanisms of the four granulators studied in Chapter 4, it is unclear whether they will exhibit similar scaling behaviour in terms of granular output and energy demand. Therefore, validating the findings of this work using industrial-scale granulators would be valuable in building greater confidence in the conclusions of this chapter.

8.2 Reducing material waste by preventing unwanted over agglomeration

The second aim of this thesis was to develop knowledge on how unwanted, over agglomeration (caking) can be avoided in wet granulation. The High Shear Granulator was chosen for this study because it was the most energy efficient wet granulation technology and is a popular processing route for food powders. It was also a technology that suffered heavily from caking which led to high levels of material loss if unsuitable processing conditions were chosen. Aiming to enhance process sustainability, in Chapter 5, this study successfully developed a regime map which highlights boundary conditions for controlled agglomeration where material waste due to caking can be avoided. This was the first regime map for the High Shear Granulator that included the Glass Transition Temperature (T_g) parameter and represents another significant, novel contribution to the field. The development of the regime map also involved the establishment of a relationship between the liquid content required to granulate the powder and the rate at which binder viscosity increases during wetting. This relationship can be used to optimize the amount of water needed to achieve high yields while avoiding adding excess water to minimize the drying requirement.

The developed regime map currently presents two key regions: a normal operation region where controlled agglomeration is possible and a caking region where process failure becomes inevitable. Future work can build on this foundation by introducing different growth regimes into the normal operation region. Example growth regimes includes Steady Growth or Rapid Growth as outlined by Iveson and Litster [30]. This will involve a detailed measurement of the increase in granule size as a response to changing process parameters to identify critical conditions for different rates of growth. It will also require the direct introduction of a stress parameter onto the y axis to reflect the varying rates of consolidation that are created by the chosen process parameters.

8.3 Reducing material waste during storage by developing humidity resistant granules

The third aim of this study was to reduce granular waste during storage by developing granule structures that were more resistant to humidity induced degradation. Chapter 6 achieved this by first developing a novel, multi-step procedure which facilitated the wet granulation of moisture sensitive amorphous powders without resulting in their structural collapse. This process produced multi-component Layered Granules where moisture insensitive material was selectively placed on the granule surface. The storage properties of these Layered Granules under high humidity were compared with Standard Granules where the components are randomly distributed in the structure. Testing showed that the Layered Granules resulted in far less caking, experienced less colour change and maintained their form better than Standard Granules during storage.

The chapter concluded by proposing a 3-layered granule structure which would not only prevent caking but would mitigate the collapse of moisture sensitive materials in the granule core. This proposal was tested using a tabletted system. Future work could look to produce this 3-layered structure in granule form. This will involve optimising the layered granulation process to ensure as complete a coverage of each layer as possible. If achieved, this will be invaluable to maintaining granular food quality and extending shelf life.

8.4 Developing more sustainable granulation technologies for the future

The last aim of this study was to evaluate whether Dry Twin Screw Granulation was a viable process compared to the more established granulation technologies considered in Chapter 4. Chapter 7 successfully achieved this by granulating DE29 in the TSG without the use of water. The resulting process was found to produce a high granular yield indicating a good material efficiency. Furthermore, its continuous nature and elimination of the drying step indicates that it is capable of achieving high energy and time efficiencies. However, this is heavily reliant on the capability of the cooling system to facilitate the use of higher throughputs. Various different mix behaviours were evidenced by the process depending on the parameters chosen. These behaviours include regions where controlled agglomeration was possible (Operable Region), no granulation occurred (Insufficient Stress Region), screw jamming occurred (Barrel Blocking Region) and a paste was formed (Extrusion Region). These different behaviours were captured to produce the first Dry Twin Screw Granulation Regime Map, highlighting another original contribution to the field of granulation.

This map describes the different process behaviours based on Barrel Fill Level and Peak Shear Rate. While this allows the map to be applied to different Twin Screw Granulators, it is currently only applicable to the DE29 powder at a T_g of 31°C. Future work can further develop this map by evaluating this process for a number of amorphous powders with varying Glass Transition Temperatures. A suitable

material property can then be introduced into the regime map to account for the effect of material property on mix behaviour. One such material property could be the viscosity of the glass transitioned powder flow. The Shear Rate can be multiplied by this viscosity to evolve the term on the x axis of the map to Shear Stress. The introduction of material properties will complete the map and enable its use across different granulators and different materials.

References

[1] S.M. Iveson, J.D. Litster, K. Hapgood, B.J. Ennis, Nucleation, growth and breakage phenomena in agitated wet granulation processes: a review, Powder Technology 117 (2001) 3–39.

[2] T. Schæfer, C. Mathiesen, Melt pelletization in a high shear mixer. IX. Effects of binder particle size, International Journal of Pharmaceutics 139 (1996) 139–148.

[3] K.P. Hapgood, J.D. Litster, R. Smith, Nucleation regime map for liquid bound granules, AIChE Journal 49 (2003) 350–361.

[4] S.A.L. De Koster, K. Pitt, J.D. Litster, R.M. Smith, High-shear granulation: An investigation into the granule consolidation and layering mechanism, Powder Technology 355 (2019) 514–525.

[5] B.J. Ennis, G. Tardos, R. Pfeffer, A microlevel-based characterization of granulation phenomena, Powder Technology 65 (1991) 257–272.

[6] S. Shanmugam, Granulation techniques and technologies: recent progresses, Bioimpacts 5 (2017) 55–63.

[7] M. Singh, S. Shirazian, V. Ranade, G.M. Walker, A. Kumar, Challenges and opportunities in modelling wet granulation in pharmaceutical industry – A critical review, Powder Technology 403 (2022) 117380.

[8] A.K. Vadaga, S.S. Gudla, G.S.K. Nareboina, H. Gubbala, B. Golla, Comprehensive review on modern techniques of granulation in pharmaceutical solid dosage forms, Intelligent Pharmacy 2 (2024) 609–629.

[9] B. Wang, X. Sun, J. Xiang, X. Guo, Z. Cheng, W. Liu, S. Tan, A critical review on granulation of pharmaceuticals and excipients: Principle, analysis and typical applications, Powder Technology 401 (2022) 117329.

[10] T.M. Ho, T. Truong, B.R. Bhandari, Methods to characterize the structure of food powders – a review, Bioscience, Biotechnology, and Biochemistry 81 (2017) 651–671.

[11] Zbigniew H Stachurski, Fundamentals of Amorphous Solids, 1st ed., Wiley-VCH, 2015.

[12] D.L. Sidebottom, Fundamentals of Condensed Matter and Crystalline Physics: An Introduction for Students of Physics and Materials Science, Cambridge University Press, Cambridge, 2012.

[13] N. Castro, V. Durrieu, C. Raynaud, A. Rouilly, Influence of DE-value on the physicochemical properties of maltodextrin for melt extrusion processes, Carbohydrate Polymers 144 (2016) 464–473.

[14] P. Boonyai, B. Bhandari, T. Howes, Stickiness measurement techniques for food powders: a review, Powder Technology 145 (2004) 34–46.

[15] S. Linnenkugel, A.H.J. Paterson, L.M. Huffman, J.E. Bronlund, Prediction of the effect of water on the glass transition temperature of low molecular weight and polysaccharide mixtures, Food Hydrocolloids 128 (2022) 107573.

[16] Bruno C. Hancock, George Zografi, The Relationship Between the Glass Transition Temperature and the Water Content of Amorphous Pharmaceutical Solids, Pharmaceutical Research 11 (1994) 471–477.

[17] Manfred Gordon, James Taylor, Ideal Copolymers and the Second-Order Transitions of Synthetic Rubbers. I. Noncrystalline Copolymers, Rubber Chemistry and Technology 26 (1953) 323–335.

[18] N. Descamps, S. Palzer, Y.H. Roos, J.J. Fitzpatrick, Glass transition and flowability/caking behaviour of maltodextrin DE 21, Journal of Food Engineering 119 (2013) 809–813.

[19] S. Fongin, K. Kawai, N. Harnkarnsujarit, Y. Hagura, Effects of water and maltodextrin on the glass transition temperature of freeze-dried mango pulp and an empirical model to predict plasticizing effect of water on dried fruits, Journal of Food Engineering 210 (2017) 91–97.

[20] A. Stępień, K. Grzyb, Comparison of critical storage parameters of the powders containing soy protein isolate and inulin, based on the concepts: Water activity and Temperature of glass transition, International Journal of Biological Macromolecules 230 (2023) 123174.

[21] M.A. Ruiz-Cabrera, S.J. Schmidt, Determination of glass transition temperatures during cooling and heating of low-moisture amorphous sugar mixtures, Journal of Food Engineering 146 (2015) 36–43.

[22] C.I. Haider, G. Niederreiter, S. Palzer, M.J. Hounslow, A.D. Salman, Unwanted agglomeration of industrial amorphous food powder from a particle perspective, Chemical Engineering Research and Design 132 (2018) 1160–1169.

[23] S. Palzer, The effect of glass transition on the desired and undesired agglomeration of amorphous food powders, Chemical Engineering Science 60 (2005) 3959–3968.

[24] J. Osborne, Bonding Mechanisms Involved in the Roller Compaction of an Amorphous Food Material, Doctor of Philosophy, University of Sheffield, 2013.

[25] I. Siemons, R.G.A. Politiek, R.M. Boom, R.G.M. Van Der Sman, M.A.I. Schutyser, Dextrose equivalence of maltodextrins determines particle morphology development during single sessile droplet drying, Food Research International 131 (2020) 108988.

[26] F. Avaltroni, P. Bouquerand, V. Normand, Maltodextrin molecular weight distribution influence on the glass transition temperature and viscosity in aqueous solutions, Carbohydrate Polymers 58 (2004) 323–334.

[27] P. Dokic, J. Jakovljevic, Lj. Dokic-Baucal, Molecular characteristics of maltodextrins and rheological behaviour of diluted and concentrated solutions, Colloids and Surfaces A: Physicochemical and Engineering Aspects 141 (1998) 435–440.

[28] L. Dokic, J. Jakovljevic, P. Dokic, Relation between Viscous Characteristics and Dextrose Equivalent of Maltodextrins, Starch - Stärke 56 (2004) 520–525.

[29] D. Dopfer, S. Palzer, S. Heinrich, L. Fries, S. Antonyuk, C. Haider, A.D. Salman, Adhesion mechanisms between water soluble particles, Powder Technology 238 (2013) 35–49.

[30] S.M. Iveson, J.D. Litster, Growth regime map for liquid-bound granules, AIChE Journal 44 (1998) 1510–1518.

[31] M. Adepu, S. Hate, A. Bétard, S. Oka, M. Schongut, M. Sen, Y. Sood, D. Wolf, S. Wieland, F. Stepanek, F. Muzzio, B. Glasser, R. Ramachandran, Quantitative validation and analysis of the

regime map approach for the wet granulation of industrially relevant zirconium hydroxide powders, Powder Technology 294 (2016) 177–184.

[32] E. Franceschinis, A.C. Santomaso, L. Benda, B. Perissutti, D. Voinovich, N. Realdon, Influence of process variables on the properties of simvastatin self-emulsifying granules obtained through high shear wet granulation, Powder Technology 274 (2015) 173–179.

[33] P.A.L. Wauters, R. Van De Water, J.D. Litster, G.M.H. Meesters, B. Scarlett, Growth and compaction behaviour of copper concentrate granules in a rotating drum, Powder Technology 124 (2002) 230–237.

[34] P.A.L. Wauters, R.B. Jakobsen, J.D. Litster, G.M.H. Meesters, B. Scarlett, Liquid distribution as a means to describing the granule growth mechanism, Powder Technology 123 (2002) 166–177.

[35] S.M. Iveson, P.A.L. Wauters, S. Forrest, J.D. Litster, G.M.H. Meesters, B. Scarlett, Growth regime map for liquid-bound granules: further development and experimental validation, Powder Technology 117 (2001) 83–97.

[36] A.C. Santomaso, R. Baggio, F. Zorzi, G. Salviulo, N. Realdon, E. Franceschinis, Sugars with different thickening power in high shear granulation, Powder Technology 317 (2017) 391–399.

[37] E.H. Jang, Y.S. Park, M.-S. Kim, D.H. Choi, Model-Based Scale-up Methodologies for Pharmaceutical Granulation, Pharmaceutics 12 (2020) 453.

[38] X. Pepin, S. Blanchon, G. Couarraze, Power consumption profiles in high-shear wet granulation. II: Predicting the overwetting point from a spreading energy, Journal of Pharmaceutical Sciences 90 (2001) 332–339.

[39] G. Betz, P.J. Bürgin, H. Leuenberger, Power consumption measurement and temperature recording during granulation, International Journal of Pharmaceutics 272 (2004) 137–149.

[40] M. Bardin, P.C. Knight, J.P.K. Seville, On control of particle size distribution in granulation using high-shear mixers, Powder Technology 140 (2004) 169–175.

[41] P. Holm, T. Schaefer, H.G. Kristensen, Granulation in high-speed mixers Part VI. Effects of process conditions on power consumption and granule growth, Powder Technology 43 (1985) 225–233.

[42] P. Luukkonen, M. Fransson, I.N. Björn, J. Hautala, B. Lagerholm, S. Folestad, Real-Time Assessment of Granule and Tablet Properties Using In-line Data From a High-shear Granulation Process, Journal of Pharmaceutical Sciences 97 (2008) 950–959.

[43] S. Bandari, D. Nyavanandi, V.R. Kallakunta, K.Y. Janga, S. Sarabu, A. Butreddy, M.A. Repka, Continuous twin screw granulation – An advanced alternative granulation technology for use in the pharmaceutical industry, International Journal of Pharmaceutics 580 (2020) 119215.

[44] L. Kotamarthy, R. Ramachandran, Mechanistic understanding of the effects of process and design parameters on the mixing dynamics in continuous twin-screw granulation, Powder Technology 390 (2021) 73–85.

[45] R.M. Dhenge, J.J. Cartwright, M.J. Hounslow, A.D. Salman, Twin screw wet granulation: Effects of properties of granulation liquid, Powder Technology 229 (2012) 126–136.

[46] R.M. Dhenge, K. Washino, J.J. Cartwright, M.J. Hounslow, A.D. Salman, Twin screw granulation using conveying screws: Effects of viscosity of granulation liquids and flow of powders, Powder Technology 238 (2013) 77–90.

[47] W.-D. Tu, A. Ingram, J. Seville, Regime map development for continuous twin screw granulation, Chemical Engineering Science 87 (2013) 315–326.

[48] S. Pohl, P. Kleinebudde, A review of regime maps for granulation, International Journal of Pharmaceutics 587 (2020) 119660.

[49] A. Ryckaert, F. Stauffer, A. Funke, D. Djuric, V. Vanhoorne, C. Vervaet, T. De Beer, Evaluation of torque as an in-process control for granule size during twin-screw wet granulation, International Journal of Pharmaceutics 602 (2021) 120642.

[50] C. Zheng, N. Govender, L. Zhang, C.-Y. Wu, GPU-enhanced DEM analysis of flow behaviour of irregularly shaped particles in a full-scale twin screw granulator, Particuology 61 (2022) 30–40.

[51] R. Meier, K.-P. Moll, M. Krumme, P. Kleinebudde, Impact of fill-level in twin-screw granulation on critical quality attributes of granules and tablets, European Journal of Pharmaceutics and Biopharmaceutics 115 (2017) 102–112.

[52] Y. Miyazaki, V. Lenhart, P. Kleinebudde, Switch of tablet manufacturing from high shear granulation to twin-screw granulation using quality by design approach, International Journal of Pharmaceutics 579 (2020) 119139.

[53] L. Tan, A.J. Carella, Y. Ren, J.B. Lo, Process optimization for continuous extrusion wet granulation, Pharmaceutical Development and Technology 16 (2011) 302–315.

[54] M. Andrew, Twin-screw dry granulation for producing solid formulations, WO2017185040A1, 2017. https://patents.google.com/patent/WO2017185040A1/en.

[55] V. Kallakunta, H. Patil, R. Tiwari, X. Ye, S. Upadhye, R. Vladyka, S. Sarabu, D. Kim, S. Bandari, M. Repka, Exploratory studies in heat-assisted continuous twin-screw dry granulation- A novel alternative technique to conventional dry granulation, (2019) 380-393.

[56] X. Ye, V. Kallakunta, D.W. Kim, H. Patil, R.V. Tiwari, S.B. Upadhye, R.S. Vladyka, M.A. Repka, Effects of Processing on a Sustained Release Formulation Prepared by Twin-Screw Dry Granulation, Journal of Pharmaceutical Sciences 108 (2019) 2895–2904.

[57] G.M. Walker, C.R. Holland, M.M.N. Ahmad, D.Q.M. Craig, Influence of process parameters on fluidised hot-melt granulation and tablet pressing of pharmaceutical powders, Chemical Engineering Science 60 (2005) 3867–3877.

[58] R. Boerefijn, P.-R. Dontula, R. Kohlus, Chapter 14 Detergent granulation, in: Handbook of Powder Technology, Elsevier, 2007: pp. 673–703.

[59] C. Avilés-Avilés, E. Dumoulin, C. Turchiuli, Fluidised bed agglomeration of particles with different glass transition temperatures, Powder Technology 270 (2015) 445–452.

[60] L. Mielke, T. Hoffmann, M. Henneberg, M. Peglow, A. Bück, E. Tsotsas, Reduction of energy consumption in batch fluidized bed layering granulation processes by temporal separation, Chemical Engineering Research and Design 110 (2016) 2–11.

[61] H. Takasaki, A. Sakurai, T. Katayama, Y. Matsuura, N. Ohyagi, K. Wada, A. Ishikawa, E. Yonemochi, Novel, lean and environment-friendly granulation method: Green fluidized bed granulation (GFBG), International Journal of Pharmaceutics 557 (2019) 18–25.

[62] R. Stevens, Spraying Device And Method For Fluidised Bed Granulation, EP 1 701 798 B1, 2006. https://patents.google.com/patent/EP1701798B1/en.

[63] D. Parikh, Handbook of Pharmaceutical Granulation Technology, 3rd ed., Informa Healthcare, New York, 2009.

[64] J.D. Osborne, T. Althaus, L. Forny, G. Niederreiter, S. Palzer, M.J. Hounslow, A.D. Salman, Investigating the influence of moisture content and pressure on the bonding mechanisms during roller compaction of an amorphous material, Chemical Engineering Science 86 (2013) 61–69.

[65] C.S. Omar, R.M. Dhenge, J.D. Osborne, T.O. Althaus, S. Palzer, M.J. Hounslow, A.D. Salman, Roller compaction: Effect of morphology and amorphous content of lactose powder on product quality, International Journal of Pharmaceutics 496 (2015) 63–74.

[66] R.B. Al-Asady, J.D. Osborne, M.J. Hounslow, A.D. Salman, Roller compactor: The effect of mechanical properties of primary particles, International Journal of Pharmaceutics 496 (2015) 124–136.

[67] L. Fries, J. Dupas, M. Bellamy-Descamps, J. Osborne, A.D. Salman, S. Palzer, Bonding regime map for roller compaction of amorphous particles, Powder Technology 341 (2019) 51–58.

[68] O. Mahmah, M.J. Adams, C.S. Omar, B. Gururajan, A.D. Salman, Roller compaction: Ribbon splitting and sticking, International Journal of Pharmaceutics 559 (2019) 156–172.

[69] L. Briens, R. Logan, The Effect of the Chopper on Granules from Wet High-Shear Granulation Using a PMA-1 Granulator, AAPS PharmSciTech 12 (2011) 1358–1365.

[70] M.F. Saleh, R.M. Dhenge, J.J. Cartwright, M.J. Hounslow, A.D. Salman, Twin screw wet granulation: Effect of process and formulation variables on powder caking during production, International Journal of Pharmaceutics 496 (2015) 571–582.

[71] K.D. Foster, J.E. Bronlund, A.H.J. (Tony) Paterson, Glass transition related cohesion of amorphous sugar powders, Journal of Food Engineering 77 (2006) 997–1006.

[72] U. Zafar, V. Vivacqua, G. Calvert, M. Ghadiri, J.A.S. Cleaver, A review of bulk powder caking, Powder Technology 313 (2017) 389–401.

[73] J. Zang, M. Qing, Y. Chi, Y. Chi, Extending the shelf-life of whole egg powder with different packaging: Based on the multivariate accelerated shelf-life test model, Food Chemistry 460 (2024) 140602.

[74] P. Kumar, H.N. Mishra, Storage stability of mango soy fortified yoghurt powder in two different packaging materials: HDPP and ALP, Journal of Food Engineering 65 (2004) 569–576.

[75] Y. Fu, F. Luo, L. Ma, H. Dai, H. Wang, H. Chen, H. Zhu, Y. Yu, Y. Hou, Y. Zhang, The moisture adsorption, caking, and flowability of silkworm pupae peptide powders: The impacts of anticaking agents, Food Chemistry 419 (2023) 135989.

[76] B. Nurhadi, Y.H. Roos, Influence of anti-caking agent on the water sorption isotherm and flow-ability properties of vacuum dried honey powder, Journal of Food Engineering 210 (2017) 76–82.

[77] JoséM. Aguilera, JoséM. Del Valle, M. Karel, Caking phenomena in amorphous food powders, Trends in Food Science & Technology 6 (1995) 149–155.

[78] Y. Liu, M.R. Thompson, K.P. O'Donnell, Impact of non-binder ingredients and molecular weight of polymer binders on heat assisted twin screw dry granulation, International Journal of Pharmaceutics 536 (2018) 336–344.

[79] Maltodextrin Market Value, Share, Overview, Demand, Drivers, & Global Trends By 2029, Data Bridge Market Research (n.d.). https://www.databridgemarketresearch.com/reports/global-maltodextrin-market (accessed November 23, 2023).

[80] Microtrac, Particle Analyzer | CAMSIZER 3D | MICROTRAC, (n.d.). https://www.microtrac.com/products/particle-size-shape-analysis/dynamic-image-analysis/camsizer-3d/ (accessed February 3, 2025).

[81] A. Ladha-Sabur, S. Bakalis, P.J. Fryer, E. Lopez-Quiroga, Mapping energy consumption in food manufacturing, Trends in Food Science & Technology 86 (2019) 270–280.

[82] O.-R. Arndt, R. Baggio, A.K. Adam, J. Harting, E. Franceschinis, P. Kleinebudde, Impact of Different Dry and Wet Granulation Techniques on Granule and Tablet Properties: A Comparative Study, Journal of Pharmaceutical Sciences 107 (2018) 3143–3152.

[83] H.S. Tan, A.D. Salman, M.J. Hounslow, Kinetics of fluidised bed melt granulation I: The effect of process variables, Chemical Engineering Science 61 (2006) 1585–1601.

[84] P. Geng, X. Chen, S. Pan, H. Zan, J. Ma, D. Liu, C. Liang, Experimental investigation of the particle growth mechanism and influencing factors during granulation process by pyrohydrolysis in fluidized bed, Journal of Environmental Chemical Engineering 11 (2023) 109088.

[85] H.G. Kristensen, T. Schaefer, Granulation: A Review on Pharmaceutical Wet-Granulation, Drug Development and Industrial Pharmacy 13 (1987) 803–872.

[86] K. Terashita, T. Nishimura, S. Natsuyama, Optimization of Operating Conditions in a High-Shear Mixer Using DEM Model: Determination of Optimal Fill Level., Chem. Pharm. Bull. 50 (2002) 1550–1557.

[87] C. Mangwandi, M.J. Adams, M.J. Hounslow, A.D. Salman, Effect of batch size on mechanical properties of granules in high shear granulation, Powder Technology 206 (2011) 44–52.

[88] Y. Miyazaki, T. Uchino, Y. Kagawa, Effect of batch size on the granule properties in planetary centrifugal granulation, Pharmazie (2022) 103–106.

[89] R.M. Dhenge, J.J. Cartwright, D.G. Doughty, M.J. Hounslow, A.D. Salman, Twin screw wet granulation: Effect of powder feed rate, Advanced Powder Technology 22 (2011) 162–166.

[90] S.V. Lute, Continuous Twin Screw Wet Granulation: A Step towards Mechanistic Understanding, Doctor of Philosophy, University of Sheffield, 2018.

[91] A. Kumar, M. Alakarjula, V. Vanhoorne, M. Toiviainen, F. De Leersnyder, J. Vercruysse, M. Juuti, J. Ketolainen, C. Vervaet, J.P. Remon, K.V. Gernaey, T. De Beer, I. Nopens, Linking granulation performance with residence time and granulation liquid distributions in twin-screw granulation: An experimental investigation, European Journal of Pharmaceutical Sciences 90 (2016) 25–37.

[92] S. Yu, G.K. Reynolds, Z. Huang, M. de Matas, A.D. Salman, Granulation of increasingly hydrophobic formulations using a twin screw granulator, International Journal of Pharmaceutics 475 (2014) 82–96.

[93] D. Djuric, B. Vanmelkebeke, P. Kleinebudde, J. Remon, C. Vervaet, Comparison of two twin-screw extruders for continuous granulation, European Journal of Pharmaceutics and Biopharmaceutics 71 (2009) 155–160.

[94] M.A. Järvinen, M. Paavola, S. Poutiainen, P. Itkonen, V. Pasanen, K. Uljas, K. Leiviskä, M. Juuti, J. Ketolainen, K. Järvinen, Comparison of a continuous ring layer wet granulation process with batch high shear and fluidized bed granulation processes, Powder Technology 275 (2015) 113–120.

[95] G. Morin, L. Briens, A Comparison of Granules Produced by High-Shear and Fluidized-Bed Granulation Methods, AAPS PharmSciTech 15 (2014) 1039–1048.

[96] N. Rahmanian, A. Naji, M. Ghadiri, Effects of process parameters on granules properties produced in a high shear granulator, Chemical Engineering Research and Design 89 (2011) 512–518.

[97] N. Rahmanian, M. Ghadiri, X. Jia, F. Stepanek, Characterisation of granule structure and strength made in a high shear granulator, Powder Technology 192 (2009) 184–194.

[98] J. Ji, J. Fitzpatrick, K. Cronin, M.A. Fenelon, S. Miao, The effects of fluidised bed and high shear mixer granulation processes on water adsorption and flow properties of milk protein isolate powder, Journal of Food Engineering 192 (2017) 19–27.

[99] P. Beer, D. Wilson, Z. Huang, M. De Matas, Transfer from High-Shear Batch to Continuous Twin Screw Wet Granulation: A Case Study in Understanding the Relationship Between Process Parameters and Product Quality Attributes, Journal of Pharmaceutical Sciences 103 (2014) 3075–3082.

[100] A. Megarry, A. Taylor, A. Gholami, H. Wikström, P. Tajarobi, Twin-screw granulation and high-shear granulation: The influence of mannitol grade on granule and tablet properties, International Journal of Pharmaceutics 590 (2020) 119890.

[101] K.T. Lee, A. Ingram, N.A. Rowson, Comparison of granule properties produced using Twin Screw Extruder and High Shear Mixer: A step towards understanding the mechanism of twin screw wet granulation, Powder Technology 238 (2013) 91–98.

[102] Y. Miyazaki, V. Lenhart, P. Kleinebudde, Switch of tablet manufacturing from high shear granulation to twin-screw granulation using quality by design approach, International Journal of Pharmaceutics 579 (2020) 119139.

[103] P.K. Le, P. Avontuur, M.J. Hounslow, A.D. Salman, A microscopic study of granulation mechanisms and their effect on granule properties, Powder Technology 206 (2011) 18–24.

[104] M.A. Ansari, F. Stepanek, The effect of granule microstructure on dissolution rate, Powder Technology 181 (2008) 104–114.

[105] M. Leane, K. Pitt, G. Reynolds, The Manufacturing Classification System (MCS) Working Group, A proposal for a drug product Manufacturing Classification System (MCS) for oral solid dosage forms, Pharmaceutical Development and Technology 20 (2015) 12–21.

[106] V. De Simone, D. Caccavo, G. Lamberti, M. d'Amore, A.A. Barba, Wet-granulation process: phenomenological analysis and process parameters optimization, Powder Technology 340 (2018) 411–419.

[107] A.Z. Al Hassn, S. Jeßberger, M.J. Hounslow, A.D. Salman, Multi-stage granulation: An approach to enhance final granule attributes, Chemical Engineering Research and Design 134 (2018) 26–35.

[108] M.X.L. Tan, K.P. Hapgood, Mapping of regimes for the key processes in wet granulation: Foam vs. spray, AIChE Journal 59 (2013) 2328–2338.

[109] J.J. Fitzpatrick, M. Hodnett, M. Twomey, P.S.M. Cerqueira, J. O'Flynn, Y.H. Roos, Glass transition and the flowability and caking of powders containing amorphous lactose, Powder Technology 178 (2007) 119–128.

[110] A. Kumar, J. Dhondt, J. Vercruysse, F. De Leersnyder, V. Vanhoorne, C. Vervaet, J.P. Remon, K.V. Gernaey, T. De Beer, I. Nopens, Development of a process map: A step towards a regime map for steady-state high shear wet twin screw granulation, Powder Technology 300 (2016) 73–82.

[111] S. Palzer, The effect of glass transition on the desired and undesired agglomeration of amorphous food powders, Chemical Engineering Science 60 (2005) 3959–3968.

[112] G.P. Johari, A. Hallbrucker, E. Mayer, The glass–liquid transition of hyperquenched water, Nature 330 (1987) 552–553.

[113] W. Thielicke, R. Sonntag, Particle Image Velocimetry for MATLAB: Accuracy and enhanced algorithms in PIVlab, JORS 9 (2021) 12.

[114] H. Eliasen, H.G. Kristensen, T. Schæfer, Growth mechanisms in melt agglomeration with a low viscosity binder, International Journal of Pharmaceutics 186 (1999) 149–159.

[115] P. Holm, T. Schaefer, H.G. Kristensen, Granulation in high-speed mixers Part V. Power consumption and temperature changes during granulation, Powder Technology 43 (1985) 213–223.

[116] C.-Y. Lin, H.-C. Wang, W.-Y. Hsu, A.-N. Huang, H.-P. Kuo, Stage-wise characterization of the high shear granulation process by impeller torque changing rate, Advanced Powder Technology 30 (2019) 1513–1521.

[117] O. Macho, Ľ. Gabrišová, P. Peciar, M. Juriga, R. Kubinec, P. Rajniak, P. Svačinová, T. Vařilová, Z. Šklubalová, Systematic Study of the Effects of High Shear Granulation Parameters on Process Yield, Granule Size, and Shape by Dynamic Image Analysis, Pharmaceutics 13 (2021) 1894.

[118] Y.H. Karunanayake, L. Brütsch, V. Meunier, A.D. Salman, Sustainability vs suitability in granulation, Chemical Engineering Research and Design 202 (2024) 272–283.

[119] G.K. Reynolds, C.A. Biggs, A.D. Salman, M.J. Hounslow, Non-uniformity of binder distribution in high-shear granulation, Powder Technology 140 (2004) 203–208.

[120] P.C. Knight, T. Instone, J.M.K. Pearson, M.J. Hounslow, An investigation into the kinetics of liquid distribution and growth in high shear mixer agglomeration, Powder Technology 97 (1998) 246–257.

[121] R. Wang, R.W. Hartel, Effects of moisture content and saccharide distribution on the stickiness of syrups, Journal of Food Engineering 284 (2020) 110067.

[122] C.M. Nowakowski, R.W. Hartel, Moisture Sorption of Amorphous Sugar Products, Journal of Food Science 67 (2002) 1419–1425.

[123] S.R.L. Werner, J.R. Jones, A.H.J. Paterson, Stickiness of maltodextrins using probe tack test during in-situ drying, Journal of Food Engineering 80 (2007) 859–868.

[124] R.G.M. Van Der Sman, J. Ubbink, M. Dupas-Langlet, M. Kristiawan, I. Siemons, Scaling relations in rheology of concentrated starches and maltodextrins, Food Hydrocolloids 124 (2022) 107306.

[125] R. Plank, B. Diehl, H. Grinstead, J. Zega, Quantifying liquid coverage and powder flux in high-shear granulators, Powder Technology 134 (2003) 223–234.

[126] E.L. Chan, G.K. Reynolds, B. Gururajan, M.J. Hounslow, A.D. Salman, Blade–granule bed stress in a cylindrical high shear granulator: I—Online measurement and characterisation, Chemical Engineering Science 86 (2013) 38–49.

[127] T.M. Chitu, D. Oulahna, M. Hemati, Wet granulation in laboratory scale high shear mixers: Effect of binder properties, Powder Technology 206 (2011) 25–33.

[128] M. Cavinato, E. Franceschinis, S. Cavallari, N. Realdon, A. Santomaso, Relationship between particle shape and some process variables in high shear wet granulation using binders of different viscosity, Chemical Engineering Journal 164 (2010) 292–298.

[129] Y. Roos, M. Karel, Phase Transitions of Mixtures of Amorphous Polysaccharides and Sugars, Biotechnology Progress 7 (1991) 49–53.

[130] L. Kotamarthy, C. Sampat, R. Ramachandran, Development of a Granule Growth Regime Map for Twin Screw Wet Granulation Process via Data Imputation Techniques, Pharmaceutics 14 (2022) 2211.

[131] U. Zafar, V. Vivacqua, G. Calvert, M. Ghadiri, J.A.S. Cleaver, A review of bulk powder caking, Powder Technology 313 (2017) 389–401.

[132] J. Petit, F. Michaux, C. Jacquot, E. Chávez Montes, J. Dupas, V. Girard, A. Gianfrancesco, J. Scher, C. Gaiani, Storage-induced caking of cocoa powder, Journal of Food Engineering 199 (2017) 42–53.

[133] M. Carpin, H. Bertelsen, J.K. Bech, R. Jeantet, J. Risbo, P. Schuck, Caking of lactose: A critical review, Trends in Food Science & Technology 53 (2016) 1–12.

[134] S. Shanmugam, Granulation techniques and technologies: recent progresses, Bioimpacts 5 (2017) 55–63.

[135] N. Özkan, N. Walisinghe, X.D. Chen, Characterization of stickiness and cake formation in whole and skim milk powders, Journal of Food Engineering 55 (2002) 293–303.

[136] J.J. Fitzpatrick, N. Descamps, K. O'Meara, C. Jones, D. Walsh, M. Spitere, Comparing the caking behaviours of skim milk powder, amorphous maltodextrin and crystalline common salt, Powder Technology 204 (2010) 131–137.

[137] Y.H. Karunanayake, L. Brütsch, V. Meunier, A.D. Salman, Sustainability vs suitability in granulation, Chemical Engineering Research and Design 202 (2024) 272–283.

[138] S. Fongin, A.E. Alvino Granados, N. Harnkarnsujarit, Y. Hagura, K. Kawai, Effects of maltodextrin and pulp on the water sorption, glass transition, and caking properties of freeze-dried mango powder, Journal of Food Engineering 247 (2019) 95–103.

[139] J.J. Fitzpatrick, J. O'Connor, M. Cudmore, D. Dos Santos, Caking behaviour of food powder binary mixes containing sticky and non-sticky powders, Journal of Food Engineering 204 (2017) 73–79.

[140] W. Wang, W. Zhou, Characterization of spray-dried soy sauce powders using maltodextrins as carrier, Journal of Food Engineering 109 (2012) 399–405.

[141] A.C. Santomaso, R. Baggio, F. Zorzi, G. Salviulo, N. Realdon, E. Franceschinis, Sugars with different thickening power in high shear granulation, Powder Technology 317 (2017) 391–399.

[142] N. Rahmanian, M. Ghadiri, X. Jia, Seeded granulation, Powder Technology 206 (2011) 53–62.

[143] M. Carpin, H. Bertelsen, A. Dalberg, J.K. Bech, J. Risbo, P. Schuck, R. Jeantet, How does particle size influence caking in lactose powder?, Journal of Food Engineering 209 (2017) 61–67.

[144] N. Castro, V. Durrieu, C. Raynaud, A. Rouilly, Influence of DE-value on the physicochemical properties of maltodextrin for melt extrusion processes, Carbohydrate Polymers 144 (2016) 464–473.

[145] Y.-J. Wang, L. Wang, Structures and Properties of Commercial Maltodextrins from Corn, Potato, and Rice Starches, Starch/Stärke 52 (2000) 296–304.

[146] I. Siemons, R.G.A. Politiek, R.M. Boom, R.G.M. Van Der Sman, M.A.I. Schutyser, Dextrose equivalence of maltodextrins determines particle morphology development during single sessile droplet drying, Food Research International 131 (2020) 108988.

[147] Jam Pier Cruz-Tirado, Juliana Martins, Bruna Olmos, Rodrigo Condotta, Louise Kurozawa, Impact of glass transition on chemical properties, caking and flowability of soymilk powder during storage, Powder Technology 386 (2021) 20–29.

[148] V.V. Kenekar, S.B. Ghugare, V. Patil-Shinde, Multi-objective optimization of high-shear wet granulation process for better granule properties and fluidized bed drying characteristics, Powder Technology 420 (2023) 118373.

[149] T. Kitagawa, T. Ito, N. Takatsu, E. Yamazoe, K. Tahara, Granulation of ibuprofen/isonicotinamide co-crystals by continuous spray granulator (CTS-SGR), Advanced Powder Technology 34 (2023) 104042.

[150] L. Shi, Y. Feng, C.C. Sun, Massing in high shear wet granulation can simultaneously improve powder flow and deteriorate powder compaction: A double-edged sword, European Journal of Pharmaceutical Sciences 43 (2011) 50–56.

[151] M.D. Tousey, The Granulation Process 101, Pharmaceutical Technology 2002 (2002) 8–13.

[152] E. Jannat, A.A. Arif, M. Hasan, A. Bin, H.A. Rashid, Granulation techniques & its updated modules, The Pharma Innovation Journal 5 (2016) 134–141.

[153] L. Meeus, Direct Compression Versus Granulation, Pharmaceutical Technology Europe 23 (2011).

[154] P. Kleinebudde, Roll compaction/dry granulation: pharmaceutical applications, European Journal of Pharmaceutics and Biopharmaceutics 58 (2004) 317–326.

[155] C. Vervaet, J.P. Remon, Continuous granulation in the pharmaceutical industry, Chemical Engineering Science 60 (2005) 3949–3957.

[156] S. Inghelbrecht, J.P. Remon, Reducing dust and improving granule and tablet quality in the roller compaction process, International Journal of Pharmaceutics 171 (1998) 195–206.

[157] Y. Liu, M.R. Thompson, K.P. O'Donnell, S. Ali, Heat assisted twin screw dry granulation, AIChE Journal 63 (2017) 4748–4760.

[158] S. Lute, R. Dhenge, A. Salman, Twin Screw Granulation: An Investigation of the Effect of Barrel Fill Level, Pharmaceutics 10 (2018) 67.

[159] D. Djuric, P. Kleinebudde, Impact of screw elements on continuous granulation with a twin-screw extruder, Journal of Pharmaceutical Sciences 97 (2008) 4934–4942.

[160] M. Peeters, A.A. Barrera Jiménez, K. Matsunami, M. Ghijs, E. Dos Santos Schultz, M. Roudgar, T. Vigh, F. Stauffer, I. Nopens, T. De Beer, Analysis of the effect of formulation properties and process parameters on granule formation in twin-screw wet granulation, International Journal of Pharmaceutics 650 (2024) 123671.

[161] R.M. Dhenge, R.S. Fyles, J.J. Cartwright, D.G. Doughty, M.J. Hounslow, A.D. Salman, Twin screw wet granulation: Granule properties, Chemical Engineering Journal 164 (2010) 322–329.

[162] J. Matić, M. Stanković-Brandl, H. Bauer, J. Lovey, S. Martel, C. Herkenne, A. Paudel, J. Khinast, Pharmaceutical hot melt extrusion process development using QbD and digital twins, International Journal of Pharmaceutics 631 (2023) 122469.

Appendix

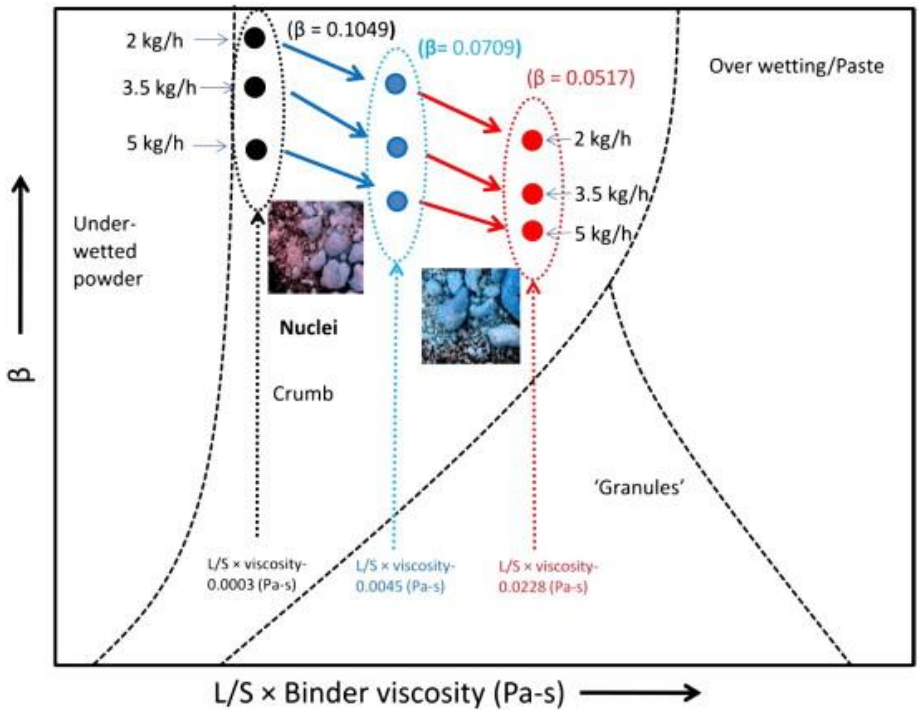

Figure 1A: Twin Screw Granulation regime map for a conveying element only screw configuration. Highlights 4 possible mix regimes depending on the Deformation value (β) and the multiple of L/S ratio and Binder Viscosity [46].

Tables A1-A3 outline the procedure used to develop the radar chart presented in Figure 4.16.

Table A1: Displays the sustainability and granule suitability metrics for the most energy efficient condition for each technology. These energy efficient conditions are as follows: Fluidised Bed Granulator (1 kg), High Shear Granulator (0.3 kg), Roller Compactor (16.7 kg/hr) and Twin Screw Granulator (0.7 kg/hr). The green highlighted cell indicates the highest value for each metric between these 4 conditions.

	Yield (%)	Specific Energy (kWh/kg)	Specific Time (hr/kg)	Flowability (ffc)	Friability (%)	Dissolution Time (s)
Fluidised Bed Granulator (1 kg)	78.2	1.81	3.52	4.61	41.15	10.6
High Shear Granulator (0.3 kg)	66.6	0.95	6.05	11.76	1.61	83.65
Roller Compactor (16.7 kg/hr)	61.7	0.14	0.1	9.05	10.68	55.08
Twin Screw Granulator (0.7 kg/hr)	20.6	10.81	8.96	5.14	24.07	47

Table A2: The next step involved dividing the experimental data values for each metric by the highest value of that metric (as highlighted by the green cells in Table A1). Looking at Yield for example, the Yield of each chosen granulator condition is as follows: FBG (1 kg) – 78%, HSG (0.3 kg) – 67%, RC (16.7 kg/hr) – 62% and TSG (0.7 kg/hr) – 21%. Dividing each value by the highest yield (78%), gives a rating of 1 for the FBG, 0.85 for the HSG, 0.79 for the RC and 0.26 for the TSG. This produces the results shown in Table A2.

	Yield	Specific Energy	Specific Time	Flowability	Friability	Dissolution Time
Fluidised Bed Granulator (1 kg)	1.00	0.17	0.39	0.39	1.00	0.13
High Shear Granulator (0.3 kg)	0.85	0.09	0.68	1.00	0.04	1.00
Roller Compactor (16.7 kg/hr)	0.79	0.01	0.01	0.77	0.26	0.66
Twin Screw Granulator (0.7 kg/hr)	0.26	1.00	1.00	0.44	0.58	0.56

Table A3: Next, metrics where a high value is undesirable are identified. A high Specific Energy and Specific Time are always undesirable as they indicate a less energy and time efficient process. For the given case study (the production of a strong and quickly dissolving granular product), a high friability and dissolution time is also undesirable. These metrics have been highlighted in red below. For these identified metrics, the values shown in Table A2 are subtracted from a value of 1. In this manner, coefficients are developed for each technology which ranks how desirable their performance in each metric is. A ranking closer to 1 indicates optimal performance while a ranking closer to 0 indicates poor performance.

	Yield	Specific Energy	Specific Time	Flowability	Friability	Dissolution Time
Fluidised Bed Granulator (1 kg)	1.00	0.83	0.61	0.39	0.00	0.87
High Shear Granulator (0.3 kg)	0.85	0.91	0.32	1.00	0.96	0.00
Roller Compactor (16.7 kg/hr)	0.79	0.99	0.99	0.77	0.74	0.34
Twin Screw Granulator (0.7 kg/hr)	0.26	0.00	0.00	0.44	0.42	0.44

Tables A4-A6 outline the procedure used to develop Technology Coefficients used in the Priority Scoring System presented in Table 4.1. Table A7-A10 outline how these Technology Coefficients are used alongside the Priority Weightings to determine the overall process rating for a technology.

Table A4: Displays the sustainability and granule suitability metrics for the most energy efficient condition for each technology. These energy efficient conditions are as follows: Fluidised Bed Granulator (1 kg), High Shear Granulator (0.3 kg), Roller Compactor (16.7 kg/hr) and Twin Screw Granulator (0.7 kg/hr). The green highlighted cell indicates the highest value for each metric that was observed between the four technology.

	Yield (%)	Specific Energy (kWh/kg)	Specific Time (hr/kg)	Flowability (ffc)	Friability (%)	Dissolution Time (s)
Fluidised Bed Granulator (1 kg)	78.2	1.81	3.52	4.61	41.15	10.6
High Shear Granulator (0.3 kg)	66.6	0.95	6.05	11.76	1.61	83.65
Roller Compactor (16.7 kg/hr)	61.7	0.14	0.1	9.05	10.68	55.08
Twin Screw Granulator (0.7 kg/hr)	20.6	10.81	8.96	5.14	24.07	47

Table A5: The next step involves producing technology coefficients for each metric which can be used to represent the performance of that technology in that metric. This is done by dividing the experimental data values for each metric by the highest value of that metric (as highlighted by the green cells in Table A4). Looking at Yield for example, the Yield of each chosen granulator condition is as follows: FBG (1 kg) – 78%, HSG (0.3 kg) – 67%, RC (16.7 kg/hr) – 62% and TSG (0.7 kg/hr) – 21%. Dividing each value by the highest yield (78%), gives a Yield Technology Coefficient of 1 for the FBG, 0.85 for the HSG, 0.79 for the RC and 0.26 for the TSG. This produces the results shown in Table A5.

	Yield	Specific Energy	Specific Time	Flowability	Friability	Dissolution Time
Fluidised Bed Granulator (1 kg)	1.00	0.17	0.39	0.39	1.00	0.13
High Shear Granulator (0.3 kg)	0.85	0.09	0.68	1.00	0.04	1.00
Roller Compactor (16.7 kg/hr)	0.79	0.01	0.01	0.77	0.26	0.66
Twin Screw Granulator (0.7 kg/hr)	0.26	1.00	1.00	0.44	0.58	0.56

Table A6: Next, metrics where a high value is undesirable are identified. A high Specific Energy and Specific Time are always undesirable as they indicate a less energy and time efficient process. For the given case study (the production of a strong and quickly dissolving granular product), a high friability and dissolution time is also undesirable. These metrics have been highlighted in red below. For these identified metrics, the technology coefficients developed for them in Table A5 are multiplied by -1 to reflect the fact that a high coefficient is undesirable and detracts from process viability.

	Yield	Specific Energy	Specific Time	Flowability	Friability	Dissolution Time
Fluidised Bed Granulator (1 kg)	1.00	-0.17	-0.39	0.39	-1.00	-0.13
High Shear Granulator (0.3 kg)	0.85	-0.09	-0.68	1.00	-0.04	-1.00
Roller Compactor (16.7 kg/hr)	0.79	-0.01	-0.01	0.77	-0.26	-0.66
Twin Screw Granulator (0.7 kg/hr)	0.26	-1.00	-1.00	0.44	-0.58	-0.56

Table A7: Evaluating process suitability for the Fluidised Bed Granulator based on the presented Priority Weighting assigned by the user as explained in Table 4.1. Technology coefficients for the FBG are selected from Table A6. Multiplying the Priority Weighting with the Technology Coefficient produces a Parameter Rating for that technology in each metric. Summing the Parameter Ratings produces an overall process rating for the technology which accounts for the significant of each metric and the performance of the technology in that metric.

Parameter	Priority Weighting	Technology Coefficient	Parameter Rating
Yield	0.25	1.00	0.250
Specific Energy	0.3	-0.17	-0.050
Specific Time	0.05	-0.39	-0.020
Flowability	0.2	0.39	0.078
Friability	0.1	-1.00	-0.100
Dissolution Time	0.1	-0.13	-0.013
Total Process Rating			0.146

Table A8: Evaluating process suitability for the High Shear Granulator based on the presented Priority Weighting assigned by the user as explained in Table 4.1. Technology coefficients for the HSG are selected from Table A6. Multiplying the Priority Weighting with the Technology Coefficient produces a Parameter Rating for that technology in each metric. Summing the Parameter Ratings produces an overall process rating for the technology which accounts for the significant of each metric and the performance of the technology in that metric.

Parameter	Priority Weighting	Technology Coefficient	Parameter Rating
Yield	0.25	0.85	0.213
Specific Energy	0.3	-0.09	-0.026
Specific Time	0.05	-0.68	-0.034
Flowability	0.2	1.00	0.200
Friability	0.1	-0.04	-0.004
Dissolution Time	0.1	-1.00	-0.100
Total Process Rating			0.249

Table A9: Evaluating process suitability for the Roller Compactor based on the presented Priority Weighting assigned by the user as explained in Table 4.1. Technology coefficients for the RC are selected from Table A6. Multiplying the Priority Weighting with the Technology Coefficient produces a Parameter Rating for that technology in each metric. Summing the Parameter Ratings produces an overall process rating for the technology which accounts for the significant of each metric and the performance of the technology in that metric.

Parameter	Priority Weighting	Technology Coefficient	Parameter Rating
Yield	0.25	0.79	0.197
Specific Energy	0.3	-0.01	-0.004
Specific Time	0.05	-0.01	-0.001
Flowability	0.2	0.77	0.154
Friability	0.1	-0.26	-0.026
Dissolution Time	0.1	-0.66	-0.066
Total Process Rating			0.255

Table A10: Evaluating process suitability for the Twin Screw Granulator based on the presented Priority Weighting assigned by the user as explained in Table 4.1. Technology coefficients for the TSG are selected from Table A6. Multiplying the Priority Weighting with the Technology Coefficient produces a Parameter Rating for that technology in each metric. Summing the Parameter Ratings produces an overall process rating for the technology which accounts for the significant of each metric and the performance of the technology in that metric.

Parameter	Priority Weighting	Technology Coefficient	Parameter Rating
Yield	0.25	0.26	0.066
Specific Energy	0.3	-1.00	-0.300
Specific Time	0.05	-1.00	-0.050
Flowability	0.2	0.44	0.087
Friability	0.1	-0.58	-0.058
Dissolution Time	0.1	-0.56	-0.056
Total Process Rating			-0.311

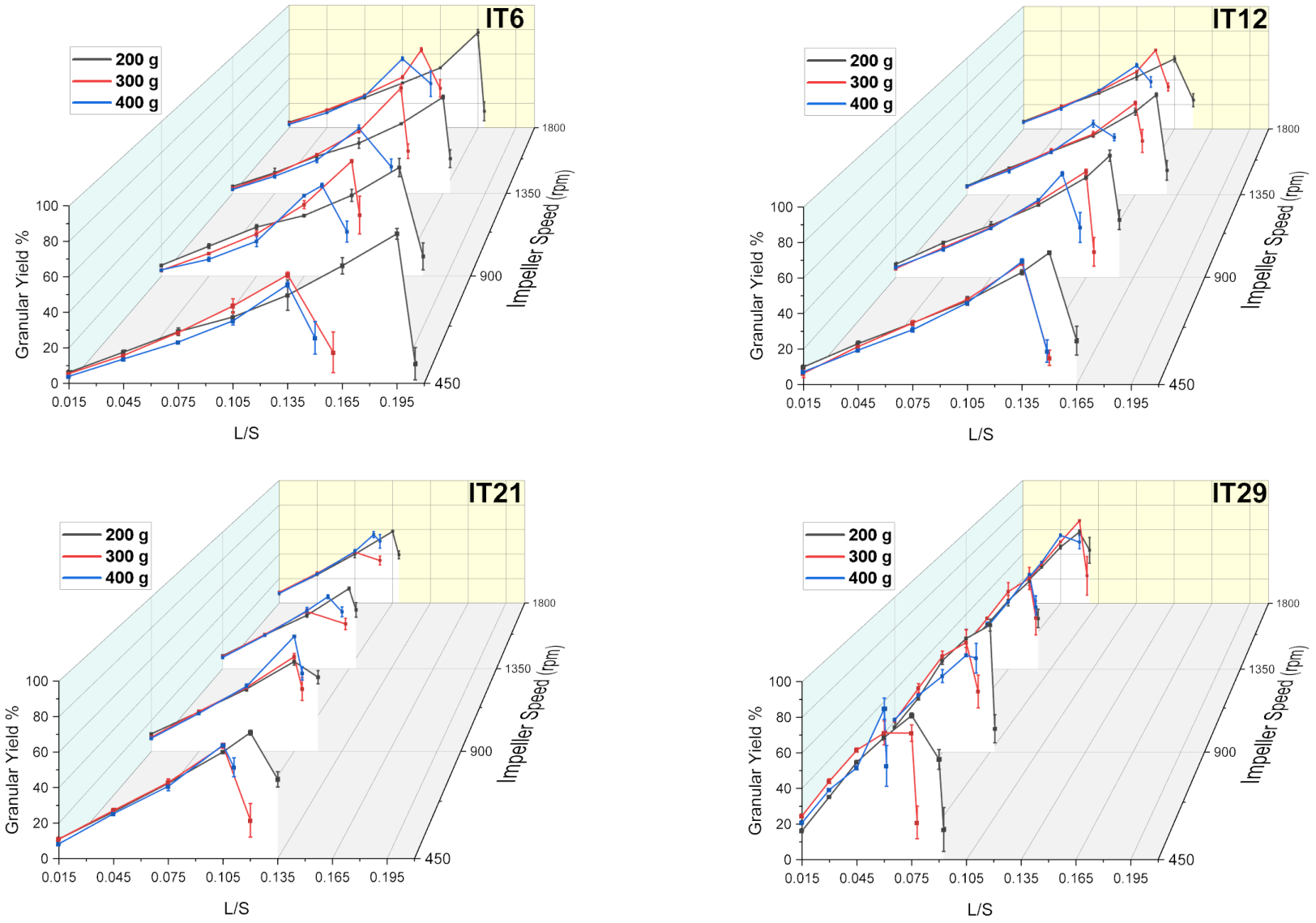

Figure 2A: Change in granular yield with increasing L/S, impeller speed and batch size This is the same data presented in Figure 7, with the trend line now representing batch size to show its effect on the granular yield.

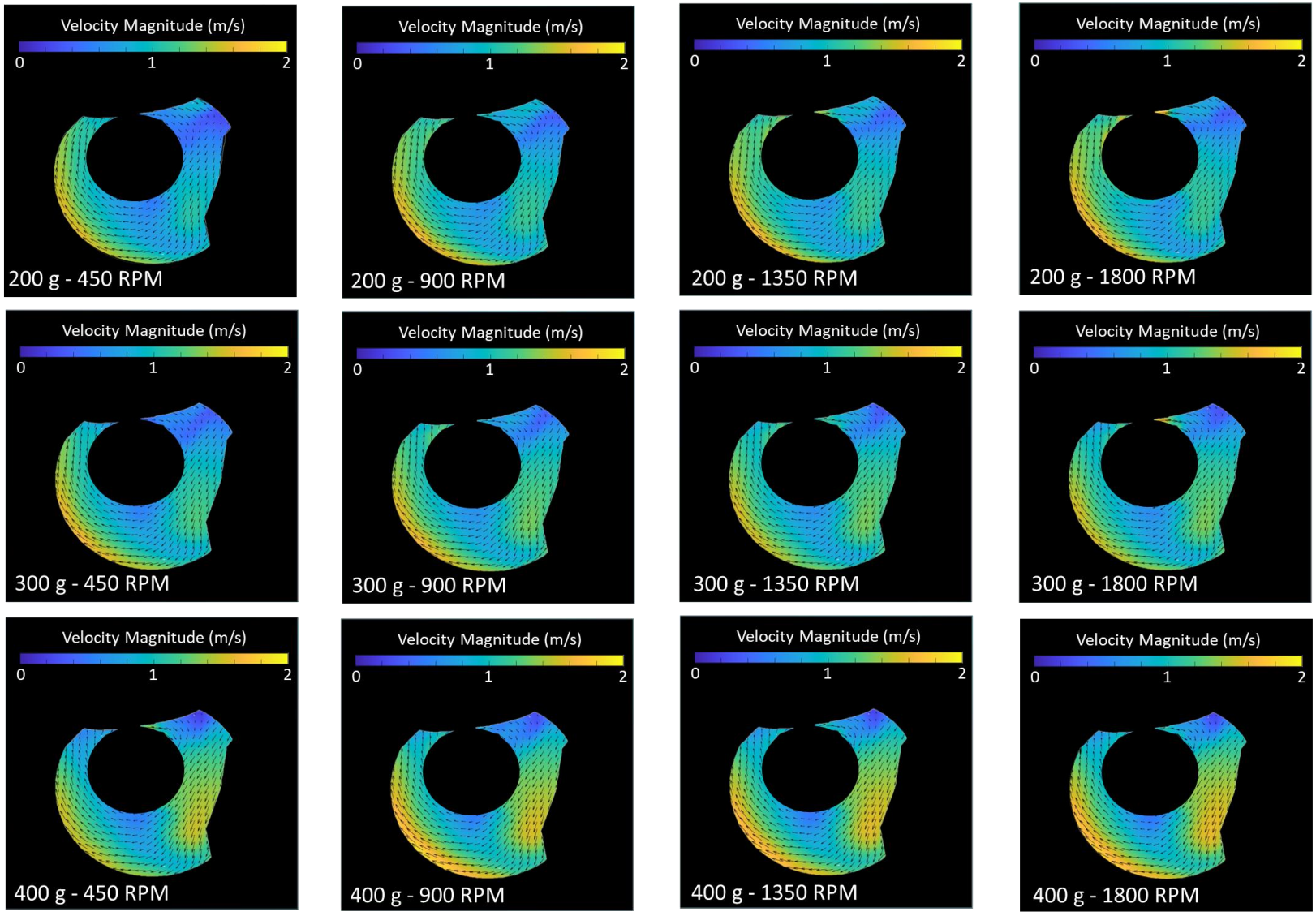

Figure 3A: Powder bed surface velocities generated at different batch sizes and impeller speeds in the Eirich Granulator for the work done in Chapter 5

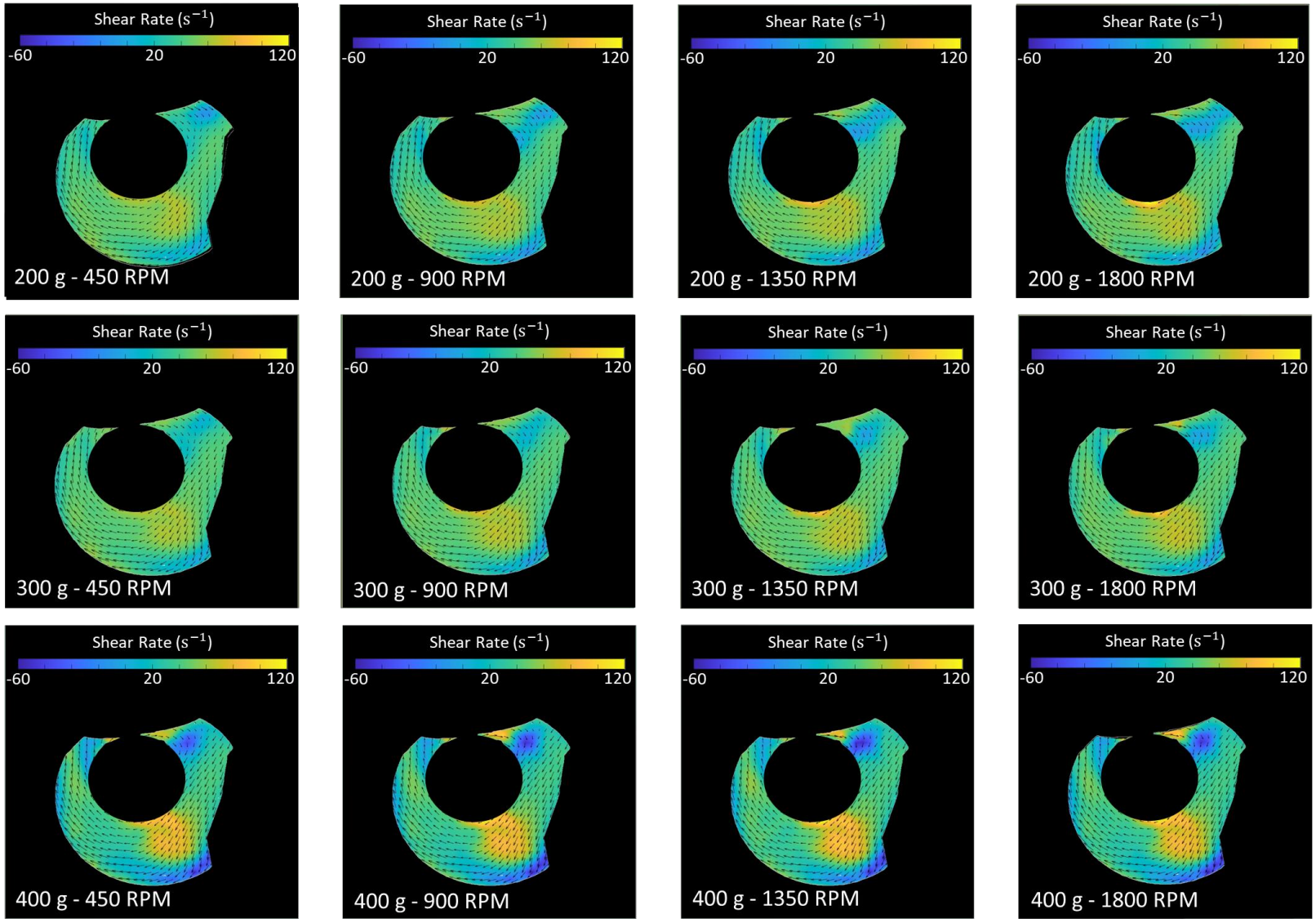

Figure 4A: Powder bed shear rates generated at different batch sizes and impeller speeds in the Eirich Granulator for the work done in Chapter 5